Development and characterisation of biosynthetic hydrogels for wound management applications

A thesis presented for the degree of

Doctor of Philosophy

by

Abhishek Gupta

D-Pharm, B. Sc., M. Sc., MPhil., PGCert (HE), FHEA

A Thesis Submitted in partial fulfilment of the requirement of the University of Wolverhampton for the degree of doctor of Philosophy.

29th April 2020

This work or any part thereof has not previously been presented in any form to the University for the purpose of assessment (unless otherwise indicated). Save for any express acknowledgement, references and/or bibliographies cited in the work, I confirm that the intellectual content of the work is the result of my own efforts and no other person.

Signature: Abhishek Gupta

Date: 29th April 2020

List of Abbreviations

$AgNO_3$	Silver nitrate
AgNP	Silver nanoparticles
AgZ	Silver zeolite
AMPS	2-acrylamido-2-methylpropane sulfonic acid
ANOVA	Analysis of variance
ASTM	American Society for Testing and Materials
ATCC	American type culture collection
BC	Bacterial cellulose
βCD	beta cyclodextrin
bcs	Bacterial cellulose synthase operon
cAgNP	Curcumin reduced silver nanoparticles
CD	Cyclodextrin
CMC	Carboxymethyl cellulose
CUR	Curcumin
DLS	Dynamic light scattering
DMEM	Dulbecco's modified Eagle's medium
DMSO	Dimethyl sulfoxide
DNA	Deoxyribonucleic acid
DPPH	2,2-diphenyl-1-picrylhydrazyl
DSC	Differential scanning calorimetry
DTG	Derivative thermgravimetry
EDX	Energy dispersive X-ray analysis
EE	Encapsulation efficiency
EGF	Epidermal growth factor
FDA	Food and Drug Administration

FGF	Fibroblast growth factor
FTIR	Fourier transform infrared
Gram –ve	Gram negative
Gram +ve	Gram positive
G. xylinus	*Gluconoacetobacter xylinus*
HB-EGF	Heparin binding epidermal growth factor
HEK	Human embryonic kidney epithelium
HMBC	Heteronuclear multiple bond correlation
HPβCD	Hydroxypropyl-β-cyclodextrin
HS medium	Hestrin and Shramm medium
HSQC	Heteronuclear single quantum correlation
IC	Inclusion complex
ICP	Inductively coupled plasma spectroscopy
IL	Interleukin
KGF	Keratinocyte growth factor
LCST	Lower critical solution temperature
MBC	Minimum bactericidal concentration
M_c	Moisture content
MDR	Microbial drug resistance
MIC	Minimum inhibitory concentration
MLC	Minimum lethal concentration
MRSA	Methicillin resistant *Staphaloccus aureus*
MTT	(3-(4,5-dimethylthiazol-2-yl)-2,5-diphenyl tetrazolium bromide)
NMR	Nuclear magnetic resonance spectroscopy
P. aeruginosa	*Pseudomonas aeruginosa*
PBS	Phosphate-buffered saline
PDGF	Platelet derived growth factor

PDI	Poly dispersity index
PEG	Poly(ethylene glycol)
PGA	Poly-γ-glutamic acid
PNIPAM	Poly(n-isopropylacrylamide)
PVA	Poly(vinyl alcohol)
PVP	Poly(N-vinyl-2-pyrrolidone)
ROESY	Rotating frame nuclear Overhauser spectroscopy
S. aureus	*Staphylococcus aureus*
SBMA	Poly(sulfobetaine methacrylate)
SEM	Scanning electron microscopy
TEM	Transmission electron microscopy
TGA	Thermal gravimetric analysis
TGF	Transforming growth factor
TIME	Tissue, infection, moisture, edge advancement
TNF-α	Tumor necrosis factor-alpha
TSA	Tryptone soy agar
TSB	Tryptone soy broth
UDP	Uridine diphosphate
UDPG	Uridine-5’-phosphate-α-D-glucose
VEGF	Vascular endothelial growth factor
VPT	Volume phase transition
VRE	Vancomycin resistant enterococci
WVTR	Water vapour transmission rate
XRD	X-ray diffractometric analysis

Abstract

Wounds that remain in the inflammatory phase for a prolonged period of time are likely to be colonised and infected by a range of commensal and pathogenic microorganisms. Treatment associated with these types of wounds mainly focuses on controlling infection and providing an optimum environment capable of facilitating re-epithelialisation, thus promoting wound healing. Hydrogels have attracted vast interest as moist wound-responsive dressing materials. Hydrogels facilitate wound healing due to unique properties and 3D network structures which allows encapsulation of healing agents. In the current study, biosynthetic bacterial cellulose hydrogels synthesised by *Gluconacetobacter xylinus* (ATCC 23770) and subsequently loaded with antimicrobial healing agents, were characterised for their wound healing properties. Loading parameters were optimised based on experimental findings. Natural bioactive materials with wound healing properties such as curcumin are attracting interest due to the emergence of resistant bacterial strains. The hydrophobicity of curcumin has been counteracted by using solubility enhancing cyclodextrins. In this study, water soluble curcumin:hydroxypropyl-β-cyclodextrin supramolecular inclusion complex was produced by a solvent evaporation method. The ratios of solvents to solubilise curcumin and hydroxypropyl-β-cyclodextrin were tested for the production of the inclusion complex with optimum encapsulation efficacy. The results confirmed that hydroxypropyl-β-cyclodextrin enhanced the aqueous solubility of curcumin and allowed loading into bacterial cellulose to produce antimicrobial hydrogels. Silver is a broad spectrum natural antimicrobial agent with wide applications extending to proprietary wound dressings. Based on the broad spectrum antimicrobial properties of silver, silver nitrate-loaded and silver zeolite-loaded bacterial cellulose hydrogels were produced. Recently silver

nanoparticles have also attracted attention in wound management. A novel green synthesis of nanoparticles was accomplished in this study using a natural reducing agent, curcumin which is a natural polyphenolic compound, well known as a wound healing agent. In addition to physicochemical properties, these hydrogels were characterised (*in vitro*) for wound management applications. The results indicate that both silver nitrate and silver zeolite-loaded biosynthetic hydrogels possess antimicrobial activity against both *Staphylococcus aureus* and *Pseudomonas aeruginosa*. Furthermore, the curcumin:hydroxypropyl-β-cyclodextrin-loaded bacterial cellulose hydrogels possess unique properties including haemocompatability, cytocompatability, anti-staphylococcal and antioxidant abilities. In addition to high cytocompatibility, curcumin reduced silver nanoparticles-loaded bacterial cellulose hydrogels dressings exhibited antimicrobial activity against representative wound infecting pathogenic microbes *Pseudomonas aeruginosa* and *Staphylococcus aureus*. In conclusion, the results presented support the potential use of all the investigated bacterial cellulose hydrogels for wound management applications as dressings.

Table of Contents

List of Tables Page

List of Figures

Acknowledgements

I sincerely thank my supervisor Prof Izabela Radecka for her understanding and careful supervision of my project and to my co-supervisors, Prof Marek Kowalczuk, and Dr Hazel Gibson. I would like to thank my co-supervisors, Dr Claire Martin and Prof Stephen Britland for invaluable contribution at the start of this project.

I would like to thank the staff at the Centre of Polymer and Carbon Materials, Polish Academy of Sciences, Zabrze, Poland for collaboration and help in this project. I would like to thank Sophie Briffa at the University of Birmingham for letting me use their equipment and the valuable support.

I am grateful to the School of Pharmacy at the University of Wolverhampton for their support for the project. Special thanks to Dr Colin Brown for his support and encouragement for my research. I would also like to thank Dr Keith Jones, Dr Joanne Skidmore, David Luckhurst, Keith Holding, Surila Darbar, Clare Murcott, David Townrow, Karen Hollyhead, Andrew Brook, Balbir Singh Bains, Nadia Ahmad and Dr Angela Williams in the Faculty of Science and Engineering. I would like to extend thanks to my fellow researchers who rendered me advice whenever needed.

I would like to take an opportunity to thank my father, Mr Krishan Kumar Gupta and my mother, Mrs Veena Gupta who encouraged me in my studies and gave me both the freedom and support that I needed. They trusted in me enough to let me choose my own goals and I hope that I have lived up to their expectations. I would like to thank my son, Krish Gupta and daughter, Anjali Gupta for their endless love and patience during my research. Thanks to Neeru Gusain for her best wishes to make my research study a success. My sincere thanks to Brahma Kumari, sister Saroj Kohli, Brahma Kumar, brother Sham Kohli and Mr Vijay Mann.

Chapter 1

Introduction

1.1 Microbial Drug Resistance (MDR)

Uncontrolled pathogenic microbial colonisation has posed challenges in regular treatment leading to disease, disability and even death. Oral, systemic and topical administration of antimicrobial agents, including antibiotics, is the common practice to tackle this challenge. Antibiotics are the class of antimicrobials produced by microorganisms that are capable of inhibiting the growth of other microbes. Nowadays, antibiotics are also produced by synthetic alteration to accomplish similar tasks [Radecka *et al.,* 2015]. Based on their action, antibiotics can be bacteriostatic (inhibit cell growth) or bactericidal (kill the cells). With several antibiotics having been developed and used to control unwanted bacterial colonisation. The widespread use of antibiotics for both clinical and nonclinical settings has resulted in increased levels of antibiotics in the environment. A study undertaken on the antibiotic consumption in 76 countries between years 2000 to 2015 revealed 65 % increase in the use of antibiotics in clinical practice, agriculture and live-stock farming [Klein *et al.,* 2018]. Orally administered antibiotics are not completely metabolised in human and animal body and up to 90 % could be excreted in the environment through urine and faeces [Du and Liu, 2012; Hiller *et al.,* 2019]. As a result of ubiquitous occurrence of these antibiotics, bacteria developed resistance and now several multi-resistant strains (superbugs) like methicillin-resistant *Staphylococcus aureus* (MRSA), vancomycin-intermediate *Staphylococcus aureus* (VISA) and carbapenem-resistant *Mycobacterium tuberculosis* have emerged [Hiller *et al.,* 2019]. Increasing numbers of antimicrobial resistant strains compounded with slow development of new antimicrobial agents has raised serious concerns [Schulz *et al.,* 2019]. In Europe alone, more than 25000 patients die annually from bacterial infections due to reduced effectiveness of existing antimicrobials [Radecka *et al.,* 2015].

1.1.1. Gram positive (+ve) and Gram negative (–ve) bacteria

Different types of bacteria display varied sensitivities to different antimicrobial agents. In order to understand the varied sensitivities and the mode of action of antimicrobial agents, it is imperative to understand different types of bacteria. Based on the difference in the structure of the cell wall outside the plasma membrane, bacteria are broadly classified as Gram +ve and Gram –ve. The inner cytoplasmic membrane of both Gram +ve and Gram –ve bacteria are similar; it's the outer cell envelopes that vary in these bacterial groups. In most Gram +ve bacteria, there is a relatively thick continuous cell wall composed of peptidoglycans (20 to 80 nm) with covalently attached teichoic acid. Teichoic acids are highly negatively charged polyol phosphate polymers only found in certain Gram +ve bacteria (like *Staphylococcus*, *Streptococci* spp.) and are absent in Gram –ve bacteria. Contrary to this, Gram –ve bacteria have a thinner (5 to 10 nm) peptidoglycan layer with no teichoic acid. The peptidoglycan layer in Gram –ve bacteria is less crosslinked as compared to the one in Gram +ve bacteria. Also, in Gram –ve bacteria, there is an additional outer membrane (7.5 to 10 nm thick) outside the peptidoglycan layer, which is anchored noncovalently to lipoprotein molecules. This outer membrane has channel proteins, mainly porin, that control the passage of hydrophilic molecules and there exists the hydrophobic pathway that is responsible for limiting the penetration of certain antimicrobial agents. The outer membrane has a coating of lipopolysaccharides (LPS) with negatively charged phosphate groups. These LPS are pyrogenic and play a vital role in pathogenesis of Gram –ve bacterial infections [Li *et al.,* 2017, Salton and Kim, 1996]. These surface structural differences in these groups contribute to varied sensitivity to different antimicrobial agents.

1.1.2. Types of antimicrobial agents

An antimicrobial is an agent that either destroys pathogens or inhibit their growth in order to avoid potential damage to the host. When an antimicrobial agent inhibits bacterial cell growth, it is classed as a bacteriostatic agent and when it kills the bacterial cells, it is classified as a bactericidal agent [Radecka *et al.,* 2015].

After the success of Ehrlich in developing Arsphenamine as an antimicrobial drug, many more compounds with antimicrobial properties were discovered. The discovery of *penicillin* as the first antibiotic revolutionised the field and many new antibiotics were discovered and developed. Most bactericidal antibiotics kill bacterial cells by interfering with the vital cellular processes. This could be by inhibiting nucleic acids, translation or cell wall disruption [Radecka *et al.,* 2015]. Due to the emerging antibiotic resistance, new antimicrobial agents with non-antibiotic origin have also been explored and used to control infections [Kateel *et al*., 2018; Cao *et al*., 2019]. Various botanical and zoological natural compounds, metal complexes, nanotechnological materials and synthetic polymers endowed with distinct and multifaceted antimicrobial properties to which many opportunistic pathogens are not resistant have been searched as antimicrobial agents. Below is the list of major classes of antimicrobial agents with a brief overview on their mode of action (**Table 1.1**):

Table 1.1. Different major group of antimicrobial agents with examples and mode of action.

Antimicrobial agents group	Class of antimicrobial drug	Example of drugs	Mode of action	Primary target	Target organisms	References
Antibiotic	β-lactams • Penicillins • Cephalosporins • Carbapenems • Carbacephems	• Amoxicillin • Cefotaxime • Meropenem • Lorabid	Inhibition of bacterial cell wall synthesis	Penicillin binding protein	Gram +ve and Gram –ve bacteria	Radecka *et al*., 2015; Ullah and Ali., 2017; Wong *et a*l., 2012
	Tetracyclines	• Doxycyclin	Inhibition of bacterial protein synthesis	30S ribosome	Aerobic Gram +ve and Gram –ve bacteria	Radecka *et al*., 2015; Ullah and Ali., 2017
	Quinolones	• Ciprofloxacin	Inhibition of bacterial DNA replication and transcription	Topoisomerase II and IV	Aerobic Gram +ve and Gram –ve bacteria; some anaerobic Gram –ve bacteria	Radecka *et al*., 2015; Ullah and Ali., 2017
	Macrolides	• Erythromycin	Inhibition of bacterial protein synthesis	50S ribosome	Aerobic and anaerobic Gram +ve and Gram –ve bacteria	Radecka *et al*., 2015; Ullah and Ali., 2017
	Sulphonamides	• Sulfanilamide	Antimetabolite in folic acid synthesis	Competitive inhibitor of dihydropteroate synthase	Gram +ve and Gram –ve bacteria	Ullah and Ali., 2017; Wong *et a*l., 2012
	Glycopeptides/ glycolipopeptides	• Vancomycin	Inhibition of bacterial cell wall synthesis	Peptidoglycan units	Gram +ve bacteria	Radecka *et al*., 2015; Wong *et a*l., 2012
	Aminoglycosides	• Gentamicin	Inhibition of bacterial cell wall synthesis	30S ribosome	Aerobic Gram +ve and Gram –ve bacteria	Radecka *et al*., 2015; Ullah and Ali., 2017
	Lipopeptides	• Polymixin B	Inhibition of bacterial cell wall synthesis	Cell membrane	Gram +ve and Gram –ve bacteria	Radecka *et al*., 2015; Wong *et a*l., 2012
	Streptogramins	• Dalfopristin, quinopristin	Inhibition of bacterial protein synthesis	50S ribosome	Aerobic and anaerobic Gram +ve and Gram –ve bacteria	Radecka *et al*., 2015; Ullah and Ali, 2017
	Phenicols	• Chloramphenicol	Inhibition of bacterial protein synthesis	50S ribosome	Some Gram +ve and Gram –ve bacteria	Radecka *et al*., 2015

	Others like Ansamycins, oxazolidinones	• Rifamycin, linezolid	Inhibition of bacterial RNA synthesis, Inhibition of bacterial protein synthesis	DNA-dependent RNA polymerase; 50S ribosome		Ullah and Ali, 2017
Non-antibiotic	Plant-based antimicrobials	• Curcumin	Inhibition of cell division	FtsZ protein	Gram +ve and some Gram –ve bacteria	da Silva *et al*., 2018
	Animal-based antimicrobials	• Honey	Multifacted: Enzymatic production of hydrogen peroxide; osmotic effect; pH; enzymatic activity	Hydrolyses linkages in peptidoglycan of bacterial cell wall	Gram +ve and Gram –ve bacteria	Khan *et al*., 2018; Kateel *et al.,* 2018
	Antimicrobial metal: • Metal ions • Metal nanoparticles	• Silver (Ag) • Ag nanoparticles	Multifacted: Destabilisation of bacterial cell membrane; interaction with nucleic acids and enzymes; production of ROS	Cell membrane; enzymes; nucleic acids	Aerobic and anaerobic Gram +ve and Gram –ve bacteria	Cao *et al*., 2019
	Antimicrobial peptides (AMPs)	• Omiganan • Human cathelicidin peptide LL37	Disruption of bacterial cell wall, inhibit intracellular functions	Cell membrane; enzymes; proteins; nucleic acids	Gram +ve and Gram –ve bacteria	Zhang and Galo, 2016; Cao *et al*., 2019
	Antimicrobial enzymes • Proteolytic • Polysaccharide -degrading	• Subtilisins • Lysozyme	Hydrolyse adhesins; rupture cell wall	Cell membrane	Gram +ve and Gram –ve bacteria	Cao *et al*., 2019
	Synthetic polymers	• Polyionenes	Cell membrane disruption	Cell membrane	Gram +ve and Gram –ve bacteria	Lou *et al*., 2018

1.1.3. Tackling microbial drug resistance (MDR)

Undoubtedly, the discovery of antibiotics was the important achievement in modern medicine to control infections. The majority of existing antibiotics work mainly by targeting the bacterial cell wall, DNA replication and translational processes [Ruddaraju *et al.,* 2019]. However, the emergence of microbial drug resistance strains has severely affected the treatment of bacterial infections. Drug resistance could be developed by various ways like intrinsic resistance for a particular antibiotic or multiple antibiotics. This information gets transferred by genetic elements like bacterial naked DNA and plasmids and results in the development of single or multiple drug resistant strains. Also, the sequential mutations in microbial chromosomes DNA can cause drug resistance. These mutated chromosomal genes can also transfer from one bacterium to another through the uptake of naked DNA (*transformation*) [Radecka *et al.,* 2015]. Once the bacterial resistance is developed, the normal type gets eradicated by drugs but the drug resistant strains can survive and spread the resistance genes.

Microbial resistance has developed for nearly all the conventional antibiotics produced during the Golden era (1940s to 1970s). Only three new classes of antibiotics have been marketed since then, with none for Gram –ve bacteria [Coates and Hu, 2015]. In light of these issues, the use of non-antibiotic therapies, combination therapy of antibiotic-antibiotic and antibiotic-non-antibiotic have been developed. The non-antibiotic antimicrobials, like metals (silver) and natural and biological products (Curcumin), attributed to their multifaceted mode of action are inhibiting antibacterial drug resistance and used to control infections [Cao *et al.,* 2019]. Moreover, the dynamic advancement of nanotechnology in recent years

provided the opportunities to fabricate metal nanoparticles (silver nanoparticles) for the targeted drug delivery for appropriate time at the right place, in the right concentrations. Unlike the use of chemical reducing and capping agents for metal nanoparticle production, the benefit of medicinal plants in phyto-nanotechnology has drawn significant research interest. It involves the production of nanoparticles using natural compounds such as aloe vera, neem extract and lemonglass (Verma and Mehata, 2016). Curcumin is another natural plant product that has attracted wide research interest as a reducing and capping agent for nanoparticle synthesis. These Green synthesised antimicrobial metal nanoparticles are reported to inhibit bacterial strategies of drug resistance mechanisms [Ruddaraju *et al.,* 2019], thus enabling the control of infections without the risk of developing drug resistance.

1.2. Wounds and Wound management

A wound is an injury that disrupts the integrity of the epidermis as a physical barrier, thereby interrupting its normal anatomical structure and physiology [Han, 2016]. Dermal injury can be caused by acute trauma or surgical event. The resultant damage can affect local epidermal tissue, the vascular network and, depending on the nature and depth of the wound, dermal intricate structure may also get damaged. In the case of surgical incisions, as the tissue loss is minimal and the healing process is rapid, unless there is an underlying pathological condition hindering the healing process. In the case of acute trauma associated with substantial dermal matrix loss, allowing the defect to be filled with granulation tissue is the primary approach followed for the repair process. The reparative process is protracted when the defect area is large, due to increased demand for production of dermal matrix forming cells for healing [Martin, 2013a].

1.2.1. The Wound Healing Process

Wound healing is a continuous process that follows a complex series of cellular and biochemical cascades occurring in orderly, sequential but overlapping phases to repair and regenerate the damaged tissue [Martin *et al.,* 2013]. The healing process occurs in the following four stages (**Figure 1.1**): exudative, inflammatory, proliferative and regenerative. Various growth factors, cytokines, chemokines and other biomolecules are involved in this process [Tejiram *et al.,* 2016; Dealey, 2012; Paul and Sharma, 2015] and their role in wound healing are summarised in **Table 1.2**. The exudative stage, also called coagulation and haemostasis, consists of stopping blood loss and preventing excessive bleeding (**Figure 1.1a**). Although the act of bleeding is beneficial; washing the damaged tissue and reducing microbial invasion, it is controlled by haemostatic reflex vasoconstriction (local and systemic) and by the formation of insoluble fibrin plug, to prevent excessive blood loss. As blood interacts with exposed collagen and other components of the extracellular matrix, activated platelets release clotting factors and aggregate into a plug-like matrix, thus controlling blood loss [Wang *et al.,* 2018]. Once haemostasis has been achieved, the inflammatory (or resorptive) stage begins with an increased infiltration of phagocytes (neutrophils and macrophages) (**Figure 1.1b**). The presence of neutrophils is time restricted to the early stages of healing, whereas macrophages persist through all phases from exudative to regenerative [Lucas *et al.,* 2010]. Within 24-36 hours post-injury, neutrophils migrate into the wound site and initiate phagocytic activity of macrophages by releasing proteolytic enzymes, chromatin, protease 'traps' and free-radical reactive oxygen species (ROS), with concurrent localised inflammation, heat and redness. The combined activity of neutrophils and macrophages helps to clear damaged and/or necrotic tissues, particulate contaminants and microorganisms from

the wound site [Tymen *et al.,* 2013; Velnar *et al.,* 2009; Singh *et al.,* 2017a]. To enable the healing process to progress, neutrophils are removed from the wound site by apoptosis, phagocytosis (by macrophages), and disposal from the surface by sloughing or autolytic debridement. Modified monocyte macrophages arrive at the wound site 48-72 hours post-injury and phenotypically change into reparative tissue macrophages [Lucas *et al.,* 2010; Qing, 2017; Koh and DiPietro, 2011] that both promote and resolve inflammation as well as removing apoptotic cells (by phagocytosis) [Velnar *et al.,* 2009; Singh *et al.,* 2017a]. Macrophages stimulate angiogenesis and granulation tissue formation in the later stages [Häkkinen *et al.,* 2015]. Infected wounds typically become halted in the inflammatory stage and hence, fail to follow the normal healing process [Kasuya and Tokura, 2014]. Wound debridement, which involves the removal of non-viable, hyperkeratotic tissue and microorganisms, is a vital stage of the healing process [Koehler *et al.,* 2018].

Once autolytic debridement is successfully achieved and the immune response has resolved, wound healing progresses into the proliferation stage, which is the phase of tissue formation (**Figure 1.1c**). During this stage, tissue repair starts and wound closure is initiated. The wound site is filled with granulation tissue and epithelialisation from the wound edges takes place. The epithelial cells around the wound edges divide mitotically and migrate until a continuous sheet of cells is formed. Collagen (type III) formation by fibroblasts acts as a provisional matrix and provides strength to the newly formed granulation tissue, which is responsible for scar formation [Martin *et al.,* 2013; Morton and Phillips, 2016]. To ensure the supply of oxygen and nutrients to newly formed tissue, angiogenesis also occurs at this stage, with a microvascular network of new blood capillaries forming from the surrounding viable blood vessels [Singh et al., 2017a; Schreml *et al.,* 2010].

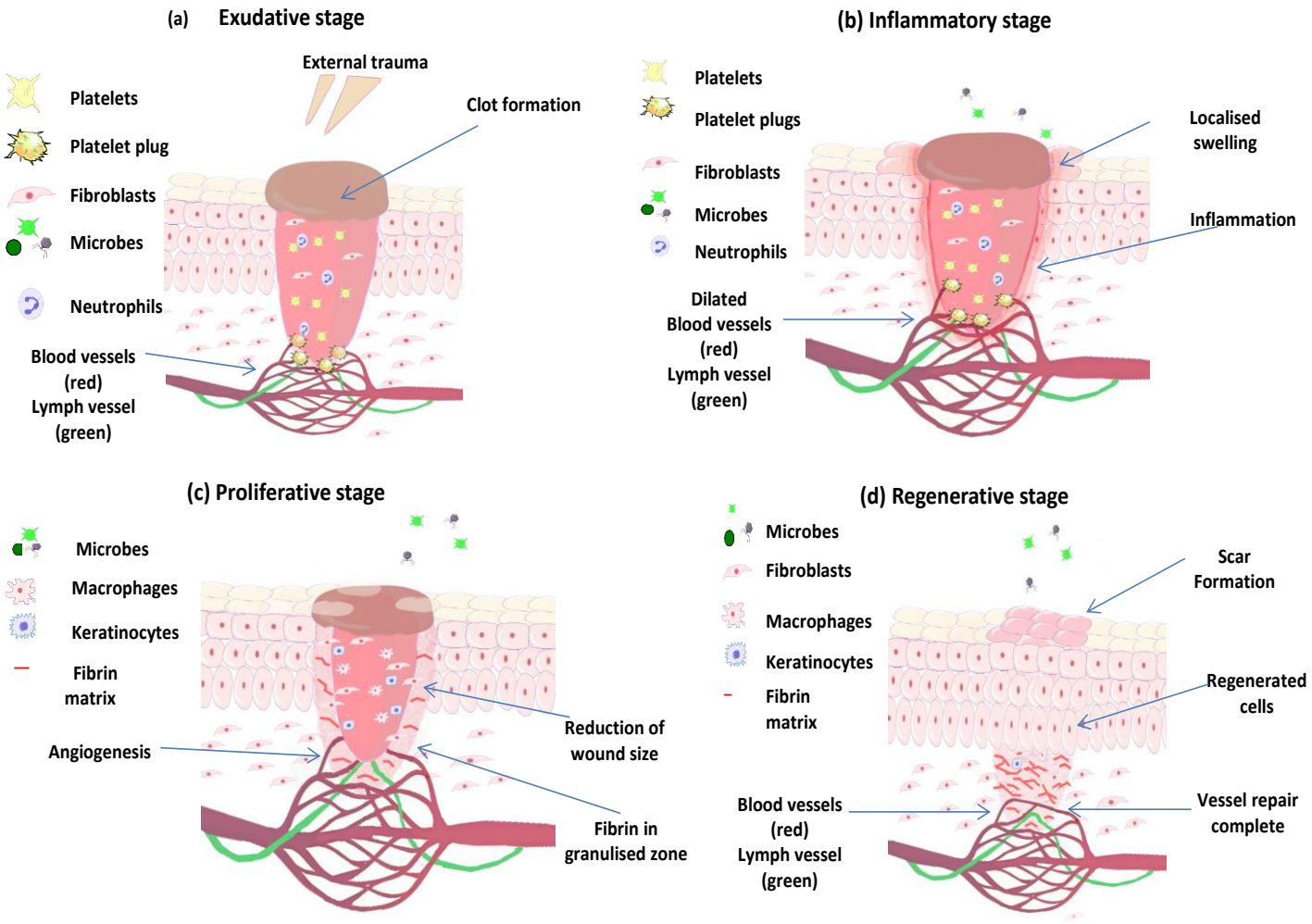

Figure 1.1. Illustration of the stages of wound healing, **(a)** Exudative stage with the formation of blood clot **(b)** Inflammatory stage, marked with oedema, pain and inflammation **(c)** Proliferation stage with granulation tissue formation and **(d)** Regenerative stage, characterised by scar tissue formation.

The final stage of wound healing is regeneration where normal dermal architecture is restored and scar tissue tensile strength increased (**Figure 1.1d**). Inflammatory cells clear from the regenerated area whilst collagen undergoes remodelling to increase the tensile strength of the tissue [Martin *et al.,* 2013].

Table 1.2. Important mediators in wound healing process, with their respective receptors, cell sources, targets and roles in wound healing.

Factor	Family	Receptors	Cells	Function	Level in acute wounds	Level in chronic wounds	Reference
PDGF	PDGF-BB **Additional:** PDGF-AA PDGF-AB PDGF-CC PDGF-DD)	Tyrosine kinase: α-receptor β -receptor	Platelets Fibroblasts Endothelial cells Macrophages Keratinocytes	Chemotaxis Proliferation of fibroblasts Promote blood vessel maturation Matrix deposition Reepithelialisation	Increased levels	Decreased levels	Singh *et al.,* 2017a; Barrientos *et al.,* 2008; Yang *et al.,* 2017
FGF	FGF-2 or bFGF **Additional:** FGF-7 FGF-10 KGF Total: 23 members	Tyrosine kinase: FGFR 1-4	Keratinocytes Mast Cells Fibroblasts Endothelial cells	Angiogenesis Formation of granulation tissue Reepithelialisation	Increased levels	Decreased levels	Singh *et al.,* 2017a; Barrientos *et al.,* 2008; Yoo *et al.,* 2018; Joao *et al.,* 2016
EGF	EGF TGF-α HB-EGF **Additional:** Amphiregulin Epiregulin Betacellulin Neuregulins	Tyrosine kinase: EGFR HER2 HER3 HER4	Platelets Macrophages Fibroblasts	Formation of granulation tissue Reepithelialisation Increases tensile strength in wound	Increased levels	Decreased levels	Singh *et al.,* 2017a; Barrientos *et al.,* 2008; Yoo *et al.,* 2018; Joao *et al.,* 2016; Ramanathan *et al.,* 2017
VEGF	VEGF-A **Additional:** VEGF-B VEGF-C VEGF-D	Tyrosine kinase: VEGFR-1 VEGFR-2 VEGFR-3	Platelets Endothelial cells Macrophages Lymphocytes Neutrophils Keratinocytes	Vasculogenesis Angiogenesis	Increased levels	Decreased levels	Singh *et al.,* 2017a; Barrientos *et al.,* 2008; Yang *et al.,* 2017; Joao *et al.,* 2016 Ramanathan *et al.,* 2017 Ram *et al.,* 2015

	VEGF-E PLGF						
TGF-β	TGF-β1 **Additional:** TGF-β2 TGF-β3	Serine-threonine kinases: TGFβRI TGFβRII	Platelets Macrophages Fibroblasts Keratinocytes	Angiogenesis Chemotaxis Reepithelialisation Anabolism of ECM Collagen production by stimulating fibroblasts Cellular proliferation and differentiation	Increased levels	Decreased levels	Singh *et al.,* 2017a; Barrientos *et al.,* 2008; Ramanathan *et al.,* 2017; Ram *et al.,* 2015
Proinflammatory cytokines	IL-1 IL-6 **Additional:** TNF-α IL-8 IL-11 IL-27	ICAM-1 IL-6Rα	Monocytes Neutrophils Macrophages Keratinocytes	Chemotaxis Inflammation (except IL-27) Reepithelialisation Collagen synthesis Synthesis and breakdown of ECM Regulation of immune response	Increased levels at initial healing stages	Persistent Increased levels	Singh *et al.,* 2017a; Barrientos *et al.,* 2008; Ram *et al.,* 2015

Abbreviations: PDGF: Platelet-Derived Growth Factor, FGF: Fibroblast Growth Factor, KGF: Keratinocyte Growth Factor, EGF: Epidermal Growth Factor; TGF-α: Transforming Growth Factor-alpha; HB-EGF: Heparin binding EGF, VEGF: (Vascular Endothelial Growth Factor), PLGF: Placenta Growth Factor, TGF-β: (Transforming Growth Factor- β); IL: (Interleukin); TNF-α: Tumor Necrosis Factor-alpha

1.2.2. Types of wounds

Healthy wound healing follows the sequential stages, but completeness and length of time for wound healing depends on several factors, including, but not limited to, general health, underlying long-term disease states such as diabetes, an impaired (HIV) or altered immune response (patients undergoing immunosuppression therapy) and/or a high level of microbial burden on and around the wound [Kiritsi and Nystrom, 2018; Guo and DiPietro, 2010]. These factors dictate whether the wound is acute or chronic. The principles, processes and stages of acute and chronic wound healing are different. Acute wounds like abrasions, minor cuts and burns, bites, lacerations have high mitogenic activity, high levels of growth factors (**Table 1.2**) and low cytokines [Tort *et al.,* 2019; Okur *et al.,* 2020]. Moreover, a well organised extra cellular matrix (ECM), timely controlled angiogenesis and generally low microbial burden support the healing process. These wounds are characterised with short inflammatory stage with the normal progression through different stages of healing, hence they generally heal within 8-12 weeks [Demidova-Rice *et al.,* 2012]. Contrary to this, chronic wounds like diabetic foot ulcers, pressure ulcers, venous leg ulcers, arterial ulcers are difficult to heal. Even though the underlying pathologies of different types of chronic wounds vary, they share common features like low mitogenic activity, low levels of growth factors (**Table 1.2**), low responsive cell population resulting in limited proliferation and migration, impaired angiogenesis and persistent infections [Demidova-Rice *et al.,* 2012]. Chronic wounds can develop from a combination of poor debridement, inadequate vascularisation and microbial invasion, that both delay proliferation and tissue regeneration. These wounds are characterised by prolonged inflammatory stage, hence the wound healing generally exceeds 12 weeks to full resolution [Tort *et al.,* 2019; Saghazadeh *et al.,* 2018;

Flanagan 2013]. These non-healing chronic wounds require long-term care and impose substantial socio-economic burden on the patient and healthcare services [Pal *et al*., 2018].

1.2.3. Cost and Social implications

A retrospective cohort analysis revealed that during 2012/2013, the total annual health economic burden spent by the National Health Service (NHS) in the UK on wound management was nearly £5.3 billion, which equated to approximately 4% of the annual public health expenditure in the UK in 2013 (£125.5 billion), spent on wound management alone [Guest *et al.,* 2017]. During this year, wound care was provided to an estimated 2.2 million patients and the outcome of the treatment revealed that 39% of wounds didn't heal during the duration of the study. Since many chronic non-healing wounds do not respond to the standard care, the cost of management for these wounds was substantially greater (£3.2 billion) than acute wounds (£2.1 billion) [Guest *et al.,* 2017]. While chronic non-healing wounds occur in all age groups, these are prevalent in the elderly population. Moreover, obese community and diabetic patients are more at risk. Globally, the population is ageing rapidly; obesity and diabetic cases are also increasing, which is leading to the staggering increase in the number of chronic wounds. Studies suggested an estimated annual increase of 6-7% in the number of venous and pressure ulcers and around 9% increase in cases of diabetic ulcers, which would put extra financial strain on health services [Krzyszczyk *et al.,* 2018].

1.2.4. Strategies of treatment

Clinical treatment of wounds is decided based on the type of wound. To ensure healing, tissue, infection, moisture imbalance and edge advancement (TIME) guidelines must be followed [Powers *et al.,* 2016]. Wound sites free from devitalised tissue, controlled infection, appropriate moist environment and local and systematic factors like sufficient oxygen and nutrient supply for wound edge closure are proven to facilitate healing [Powers *et al.,* 2016]. Acute wounds heal in an orderly and timely way however, the treatment strategy is decided based on the site, size and depth of wounds. Clean, surgical wounds require minimal interventions and can be closed by a variety of techniques, including adhesive strips, sutures or skin adhesives (closure by primary intention). In the case of acute traumatic injury, surgical debridement and antimicrobial therapy, in order to remove the devitalised tissue and contaminating foreign material from the wound site, may prove beneficial for the natural progression of the healing stages. Moreover, the selection of appropriate dressing, ensuring protection and optimum moisture at the wound site, is imperative [Martin, 2013; Okur *et al.,* 2020].

Contrary to this, chronic wounds cause significant morbidity and mortality and treatment cost of these wounds is significantly higher. Chronic wounds are commonly characterised by the presence of dead necrotic tissue and high microbial bioburden. The wound site requires appropriate treatment strategy following TIME guidelines. Different approaches like surgical, mechanical, autolytic, enzymatic or biological interventions can be taken to ensure that the wound site is clean and free from devitalised tissue [Powers *et al*., 2016; Manna and Morrison, 2020]. Infection is a common challenge, which could potentially impair healing leading to the chronic situation. To ensure the control of infection, suitable cleaning agents (medical

grade), topical antimicrobials for controlling the superficial infections and systemic antibiotics for systemic infection could prove beneficial. Optimum moisture at the wound site has been proven to facilitate healing [Powers *et al*., 2016; Winter, 1962]. Appropriate protective dressings capable of maintaining optimum moisture is essential to ensure healing. Advancement of wound edges to ensure closure involves local and systemic factors. Sufficient vascularisation, adequate oxygen and nutrient supply facilitate reepithelialisation, leading to wound closure. Therefore, the underlying pathophysiology of vascular insufficiency and oxygen deprivation must be investigated. Moreover, various interventions like cultured epidermal allografts, biological dressings with growth factors and hyperbaric oxygen may prove beneficial. Moreover, balanced dietary intake is equally vital [Powers *et al.,* 2016]. If the wounds fail to heal after taking all the above measures, advanced technologies with disease-specific medical management could be considered.

Despite an increased understanding about the pathophysiology of chronic wounds and emergence of new therapies, treatment of these wounds is still a growing challenge. Wound dressings play a vital role in the healing process, as they provide protection and maintain the moisture level at the wound site, hence vast research efforts have been put to produce a variety of dressings. Regardless of a plethora of materials and proprietary dressings, there is still an urgent need for an effective approach to tackle this challenge and hydrogels are a vital candidate as an advanced wound dressing to encounter this problem.

1.3. Wound Dressings

Correct care and management of wounds, whether acute or chronic, is vital. As dressings play an essential role in the wound treatment, the correct selection of

dressing is imperative. Historically, dressings were designed to protect the wound site from external environment but the increased understanding of various wound types resulted in the rapid evolution of dressings [Moura *et al.,* 2013; Ovington, 2007]. These dressings can be broadly classified as follows:

1.3.1. Conventional dressings

Conventional dressings were designed to provide protection to the wounds from external trauma and contamination and are capable of creating a dry environment at the wound site. Common examples of these dressings are: gauze, tulle and cotton wool [Dhivya *et al.,* 2015]. Gauze dressings, which could be woven (100 % cotton yarn) or non-woven (rayon or synthetic fibre blends), are primarily protective dressings. These dressings are undoubtedly inexpensive and capable of minimising trauma at the wound site from external knocks. Moreover, these are able to provide some protection against external contaminants and absorb wound exudate. However, woven gauze dressings have a major drawback of shedding or leaving fibres at the time of removal, which can contaminate the healing wound. Also, owing to the wound drainage, these dressings being absorptive, get moistened and sticky (in the case of exudative wounds), hence may require frequent change, which could be painful [Dhivya *et al.,* 2015; Jones 2006; Daunton *et al.,* 2012]. Tulle dressings, are another type of conventional dressing which are generally recommended for clean and dry acute wounds. Paraffin impregnated Bactigras® (Smith & Nephew) is an example of these dressings offering low-adhesion and soothing effects at the wound site.

Such dressings undoubtedly are inexpensive and provide some protection, but being passive, cannot respond to changing wound conditions or deliver medicaments in a

controlled or sustained manner to enhance the healing process. For wounds that follow the normal healing process, conventional, barrier-type dressings may be effective; conversely, chronic wounds are difficult to treat hence, correct clinical management becomes imperative to minimise complications [Han, 2016; Arroyo *et al.,* 2015].

Ideal dressings not only cover and protect the affected area, but can also create an optimal moist environment at the wound site and facilitate healing [Jayakumar *et al.,* 2011; Selig *et al.,* 2012; Chen *et al.,* 2013; Morgado *et al.,* 2014, Vowden & Vowden, 2017]. Advanced wound management strategies involve non-invasive monitoring of healing, pain management and the controlled release of agents capable of promoting regeneration, repair and scar minimisation [Andreu *et al.,* 2015].

1.3.2. Advanced dressings

The concept of moist healing, as proposed by George Winter, revolutionised the field of wound management, and the focus of wound dressing changed from conventional dry passive products, to responsive moisture-promoting materials [Winter, 1962; Kokabi *et al.,* 2007; Dealey, 2012a]. Dressing types used to achieve a moist wound healing environment include films, hydrocolloids, foams and hydrogels (**Table 1.3**).

Table 1.3. List of commercially available dressings based on the concept of moist wound healing environment.

Type of dressing	Characteristics	Cautions	Proprietary products	Reference
Film dressings	• Polyurethane films with an adhesive to hold the dressing • Create moist healing environment • Elastic, durable and conformable • Waterproof and transparent • Semi-permeable to water vapour and gases • Impermeable to bacteria • Impervious to liquids such as wound fluid • No secondary dressing required	• Being non-absorbent, limited use for highly exuding wounds • Being adhesive, newly formed epithelium could be disrupted during removal • Frequently develop leakage channels	Opsite® Films (Smith & Nephew) Tegaderm™ (3M™, UK Plc.) Mepitel® Film (Mölnlycke Health Care Limited)	Arroyo *et al.,* 2015; Vowden and Vowden, 2017
Hydrocolloid dressings	• Moist wound dressing • Capable of absorbing wound exudate • Usually made of polyurethane film with an adhesive mass • Adhesive mass is often composed of gelatin, pectin and sodium CMC which swells on absorbing exudate • Impermeable to water and gases	• Not indicated for infected or heavy exudating wounds • Being opaque difficult to follow the healing process without prior removal • May produce a distinct odour at wound site	DuoDERM® (ConvaTec Inc,) 3M™ Tegaderm™ hydrocolloid dressing (3M™, UK Plc.) Replicare® (Smith and Nephew)	Martin *et al.,* 2010; Skorkowska *et al*. 2013; Brolmaann *et al.,* 2013; Powers *et al.,* 2013
Foam dressings	• Bilaminate (or trilaminate) moist wound dressing with varying thickness • Excellent absorption capacity • Can expand and conform to wound shape • Easy to remove • Can be loaded with antimicrobials and other active agents	• Not suitable for low exudating wounds • Frequent change may be required for heavy exudating wounds • May cause maceration on saturation with exudate	Mepilex® and Mepilex Ag® (Molnlycke Health Care) Allevyn (Smith and Nephew) Aquacel® (ConvaTec Inc.) Cutimed® Siltec B (BSN medical Inc.) Biatain® Silicone Ag (Coloplast Ltd.)	Powers *et al.,* 2016; Santamaria *et al*. 2013; Song *et al*. 2017
Hydrogel dressings	• Insoluble aqueous gels as moist wound dressing • Moisture retention and donation properties • Usually non-adhesive so easy to remove • Can be loaded with antimicrobials and several active wound healing agents • Can be smart and stimuli responsive • Can be injected • Can be crosslinked *In situ*	• Some hydrogels are mechanically weak in swollen state but mechanical properties can be enhanced by copolymerisation with appropriate polymer(s). • May cause maceration after accumulation of exudate • May require secondary dressing	Purilon® Gel (Coloplast Ltd) Derma-Gel (Medline Ind. Inc.) Intrasite® Gel (Smith & Nephew)	Song *et al.,* 2017; Cirillo *et al.,* 2017; Tyeb *et al.,* 2018

In addition to the above examples of commercially available dressings, there is a plethora of wound dressing products available on the market today, aiming at promoting wound healing, including Adaptic Touch® (a non-adhesive silicone

dressing by Systagenix Wound Management Limited), ALGICELL® and Algosteril® (an alginate dressing by Derma Sciences Inc. and calcium alginate dressing by Smith & Nephew, UK respectively), Altrazeal™ (by ULURU Inc., a white wound filler powder dressing that transforms into a malleable protective dressing on contact with the exudate that fills the wound,), BIOSTEP™ (by Smith & Nephew, UK, a collagen matrix dressing that optimises wound closure by deactivating excess matrix matalloproteinases) and Drawtex® (hydroconductive dressing by Beier Drawtex Healthcare, featuring LevaFiber™ technology works by capillary, hydroconductive and electrostatic action).

In addition to these dressings, hydrogel dressings are one of the most versatile advanced form of moist wound dressings [Varghese *et al.,* 2012] that are commercially available in different forms. AmeriGel® (Amerx Health Care Corp., a hydrogel dressing with moisture sustaining properties), ActiGuard™ (by Dynarex Inc., a hydrogel sheet dressing that is permeable to air and water vapours enhancing wound breathe) and Intrasite® gel (Smith & Nephew Inc., an amorphous hydrogel dressing that helps in optimising wound environment for re-epithelialisation), are some of the proprietary hydrogel dressings.

1.4. Hydrogel Dressings

Hydrogels are composed of water insoluble, cross-linked polymers with a high affinity for aqueous media. These three dimensional polymeric gels have a hydrophilic, porous structure that permits a massive degree of water absorption, several times greater than the original dry weight [Capanema *et al.,* 2018; Fan *et al.,* 2016]. The hydrophilic properties of hydrogels are related to the cross-linking density

of polar functional groups such as amide, amino, carboxyl and hydroxyl in the polymer structure [Miguel *et al.,* 2014; Zhu and Bratlie*,* 2018; Mukherjee *et al.,* 2018; Kaith *et al.,* 2015; Pal *et al.,* 2009]. Hydrogels offer the unique properties of high water content (up to 99.5%), non-adhesive nature, malleability and a resemblance to living tissues in terms of their biocompatibility [Moura *et al.,* 2013; Tyeb *et al.,* 2018; Capanema *et al.,* 2018; Li *et al.,* 2011; Caló *et al.,* 2015]; all combine to make them an ideal dressing candidate. Moreover, hydrogels display the property of swelling and de-swelling reversibly in aqueous solutions, hence their application in a range of sectors include regenerative medicine, drug delivery and wound management.

Hydrogels help promote wound healing [Wu *et al.,* 2018] *via* their moisture exchanging activities that develops an optimum microclimate between the wound bed and the dressing [Miguel *et al.,* 2014; Singh and Dhiman 2015]. Due to their high moisture content, these dressings also provide a cooling, soothing effect; reducing the pain associated with dressing changes [Gonzalez *et al.,* 2014]. In addition, the limited adhesion of hydrogels means that they can be easily removed from the wound, without causing further trauma to the healing tissue [Madaghiele *et al.,* 2014]. The transparent nature of some hydrogel dressings also allows clinical assessment of the healing process, without the need to remove the dressing.

Hydrogels can be formulated to behave in a stimuli responsive manner [Wu *et al.,* 2018] so that when loaded with a drug or active biomolecule they are able to control diffusion and release, thus making them truly interactive dressings [Guaresti *et al.,* 2018; Sood *et al.,* 2016]. Moreover, hydrogels have been successfully used as a matrix for the fabrication of dressings for the sustained delivery of essential growth factors (**Table 1.2**) and healing agents to facilitate wound healing [Yang *et al.,* 2017; Yoo *et al.,* 2018] (**Figure 1.2**). All these properties resulted into several proprietary

hydrogel wound dressings used in clinical practice for wound management all over the globe. Due to their unique properties, hydrogel dressings are indicated for use in variety of wounds such as, but not limited to, dry wounds with necrotic tissue, burn wounds, diabetic foot ulcers, pressure ulcers, chronic leg ulcers and low to moderately exudating wounds **[**Skórkowska *et al* 2013; Aguiar *et al.,* 2017; Fleck *et al.,* 2016; Solway *et al.,* 2010]**.** In spite of the various hydrogel dressing products already in the market, there is still an ongoing research in the area with the aim to further improve the hydrogel dressings covering patient comfort, clinical efficacy and multiple aspects of wound healing.

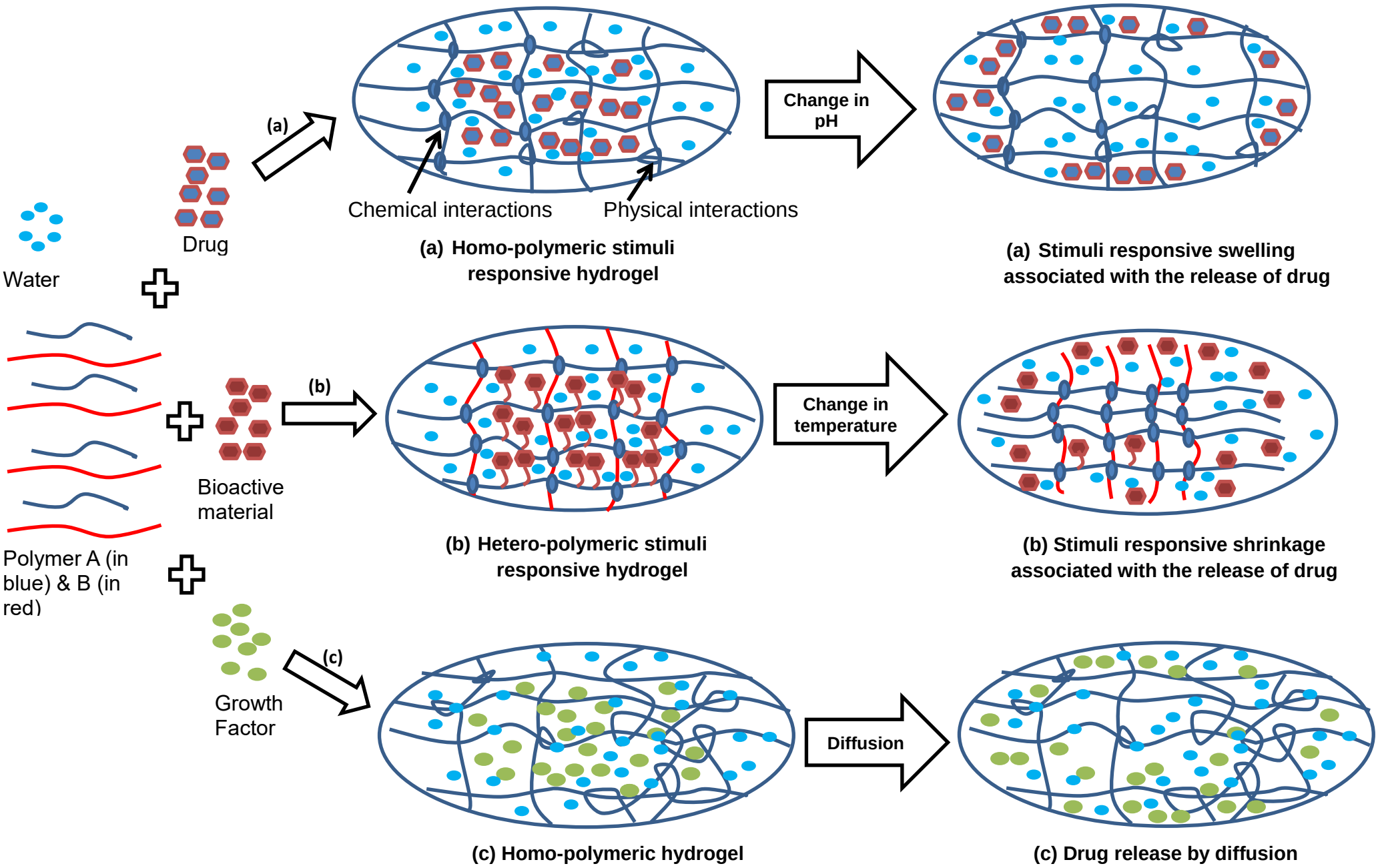

Figure 1.2. Schematic illustration of **(a)** Drug loaded homo-polymeric pH responsive hydrogel **(b)** Hetero-polymeric bioactive material loaded temperature responsive hydrogel **(c)** Growth factor loaded homo-polymeric hydrogel, with their release trends.

1.4.1. Preparation of Hydrogels

Hydrogels can be prepared from various natural and synthetic polymers, using a range of different compositions as well as physical and chemical cross-linking techniques. The crosslinks in hydrogels can be due to covalent bonds, ionic interactions and chain entanglements, leading to a variety of physical configurations, chemical arrangements and interactions. Interestingly, it is the very nature of the cross-linkage that determines much of the hydrogel's physicochemical properties and hence, eventual applications.

1.4.1.1. Physically crosslinked hydrogels are formed by the physical linking of polymer chains *via* molecular entanglement, ionic interactions, hydrogen bonding or hydrophobic association [Ahmed, 2015]. Several thermodynamic changes (*e.g.* heating or cooling of polymer solutions, freeze-thawing, lowering pH, selection of anionic and cationic polymers) can result in physical crosslinking between polymeric chains [Mukherjee *et al.,* 2018; Wathoni *et al.,* 2016; Kenawy *et al.,* 2014; Ullah *et al.,* 2015]. Preparation of these hydrogels involves relatively mild conditions and simple purification procedures as no toxic chemical crosslinking agents are required during their synthesis; offering them exceptional biological nontoxic, biocompatible properties, thus making them ideal matrix material for the delivery of therapeutic agents at the wound site [Fan *et al.,* 2016; Chaturvedi *et al*., 2016].

1.4.1.1.1. *Ionic interactions*:

These hydrogels are formed between ionic polymers crosslinked with multivalent, counter charged species. Polyanionic polymers that are complexed with polycationic polymers form hydrogels by a process of polyelectroyte complexation, which is also referred to as complex coacervation [Hennink and van Nostrum, 2012]. Alginate

hydrogel dressings using divalent calcium cations ($CaCl_2$) are commonly synthesised by this technique [Rezvanian *et al.,* 2017; Pereira *et al.,* 2013].

1.4.1.1.2. *Crystallisation*:

Hydrogels for wound management applications can also be synthesised by freeze-thawing. During freeze-thawing of an aqueous polymeric solution, water freezes causing phase separation, which leads to the formation of microcrystals [Holloway *et al.,* 2013; Ahmed *et al.,* 2017]. Repeated freeze-thaw cycles facilitate reinforcing existing crystals within the structure and offers higher crystallinity and added stability upon swelling [Chaturvedi *et al.,* 2016; Zhang *et al.,* 2013]. Physically crosslinked biocompatible and elastic hydrogels using PVA/PEG polymers [Ahmed *et al.,* 2017] and PVA/sodium alginate [Kamoun *et al.,* 2015], fabricated by consecutive freeze-thaw cycles as a potential wound dressing formulation, are examples of this type of gelation.

1.4.1.1.3. *Hydrogen bonding between chains*:

This class of hydrogels can be produced by lowering the pH of aqueous polymer solutions, when carboxylic groups are present on the chains. At acidic pH, aqueous polymer solubility is reduced, which promotes hydrogen bonding and the formation of hydrogels [Gulrez *et al*., 2011]. However, these physical networks can easily disperse with the influx of water; therefore, in addition to these, other types of crosslinking can be considered to hold the hydrogel constituents [Hoare and Kohane 2008]. Hydrogels with pH sensitive gelation (around pH 6.5) of chitosan can be produced by these physical interactions [Liu *et al.,* 2016].

1.4.1.1.4. *Amphiphilic block copolymers*:

These physical hydrogels are made from two chemically different homopolymer blocks, one of which is hydrophobic and the other is hydrophilic. These copolymers self-assemble in aqueous media forming hydrogels due to thermodynamic incompatibility between the blocks [Kaditi *et al.,* 2011; Tsai *et al.,* 2015]. Moreover, drugs like antimicrobials can be incorporated in these copolymers and sustained release can be achieved for wound management applications [Zhang *et al.,* 2012; Haas *et al.,* 2013]. Thermoresponsive poly(Ɛ-caprolactone)-poly(ethylene glycol) block copolymer hydrogels with potential wound dressing applications are a good example of this category [Haas *et al.,* 2013; Boffito *et al.,* 2014; Li and Tan, 2014].

1.4.1.1.5. *Protein interactions*:

With the advancement in biotechnology, hydrogel synthesis by engineering of recombinant proteins has become possible. This new development in the field of material chemistry pioneered by Tirrell and Cappello [Cappello *et al.,* 1990; Tirrell *et al.,* 1991] allows the control of the structural and functional design of protein block, thus preparing the physically crosslinked hydrogels with desirable biological, physical and mechanical properties. These biopolymeric protein based hydrogels primarily assemble by protein-protein interactions or aggregation of polypeptides by phase (temperature) transitions [Li *et al.,* 2016]. It can be foreseen that these hydrogels hold a strong potential in wound management. Fabrication of protein engineered bioactive collagen-mimetic protein ($eCol_{GFPGER}$) with PEG based matrix hydrogel dressings with a potential of wound healing in humans is an innovative approach in the field of wound management [Cereceres *et al.,* 2015].

1.4.1.2. Chemical crosslinked hydrogels are formed by covalent linkages resulting in high mechanical strength networks. These can be synthesised by chain growth polymerisation, addition and condensation polymerisation and high energy irradiations (gamma ray or electron beam).

1.4.1.2.1. Crosslinking by chain growth polymerisation:

It includes three stages: initiation, propagation and termination. Generation of free radical sites by a suitable reaction initiator initiates the polymerisation process, followed by chain elongation by the addition of low molecular weight monomeric building blocks. The elongated polymer chains are randomly crosslinked by the cross-linking agent, leading to the hydrogel formation [Maitra and Shukla, 2014]. Hydrogel of 2-acrylamido-2-methylpropane sulfonic acid sodium salt (AMPS-Na^+) using potassium persulfate as a free radical initiator and ethylene glycol dimethacrylate as a crosslinking agent can be synthesised by redox initiation via free radical polymerisation for wound dressing applications [Witthayaprapakorn and Molloy 2012]. Chemically crosslinked hydrogel of AMPS with AMPS-Na^+ prepared by using 4,4-azo-bis(4-cyanopentanoic acid) as photo-initiator and N,N'-methylene-bisacrylamide as a cross-linking agent demonstrated optimum water absorption and retention properties for wound management applications. Moreover, their flexible and transparent nature with good skin adhesion properties advocates their potential biomedical applications [Witthayaprapakorn, 2011].

1.4.1.2.2. Crosslinking by chemical reactions of complementary groups:

Hydrophilic polymers have functional groups like COOH, OH and NH_2, which can be utilised for the hydrogel formation. These pendant functional groups with complementary reactivity (amine-carboxylic acid or isocyanate-OH/NH_2 reaction or

Schiff base formation) can establish covalent linkages between polymer chains, leading to the hydrogel formation using crosslinking agents [Chen *et al.,* 2017; Gupta *et al.,* 2014; Akhtar *et al.,* 2016]. Antibacterial alginate-chitosan hydrogel wound dressings can be synthesised by the Schiff based reaction between aldehyde group of oxidised alginate and amino group of carboxymethyl chitosan [Chen *et al.,* 2017]. Injectable *in situ* chitosan-hyaluronic acid hydrogels [Li and Tan 2014] for wound applications are another example, with gelation attributed to Schiff base reaction between amino group of carboxymethyl chitosan and aldehyde group of aldehydic hyaluronic acid. Being injectable, these hydrogel dressings hold an added advantage of easy and comfortable application with high conformability without wrinkles, which could lead to improved patient compliance.

1.4.1.2.3. Crosslinking by using high energy radiations:

Cross-linking by radiations is widely used to polymerise unsaturated compounds for hydrogel synthesis, since it is devoid of the use of toxic chemical crosslinking agents [Hennink and van Nostrum, 2012], and is a cost effective technique as separate sterilisation of hydrogel formulation can be avoided. On exposure to high energy radiations, radicals are formed on polymer chains in an aqueous solution, which initiates free radical polymerisation. Recombination of these radicals on different polymer chains lead to the formation of covalent crosslinked hydrogels [Fan *et al.,* 2016; Hennink and van Nostrum, 2012]. Silver nanoparticles loaded AMPS-Na^+ hydrogels [Boonkaew *et al.,* 2014], PVA/gum acacia [Juby *et al.,* 2012] and nanosilver/gelatin/carboxymethyl chitosan hydrogels synthesised by gamma (cobalt-60) irradiation technique are examples of potential antimicrobial hydrogel wound dressings [Zhou *et al.,* 2012].

1.4.1.2.4. Crosslinking by thiol-ene click reaction:

The reaction of thiols (nucleophile) to electron-rich alkenes leading to the production of thioether polymer networks is another method of choice for hydrogel preparation, owing to their biological inertness, rapid reaction rate and controlled release properties. Dictated by the functional groups and reaction conditions, the reaction mechanism could be thiol-Michael click reaction or radical-mediated thiol-ene reaction [Kharkar *et al.,* 2016]. Synthesis of gelatin/poly(ethylene glycol) hydrogels for the delivery of immunomodulatory molecules like cytokines and growth factors through mesenchymal stem cells (MSC) carriers [Xu *et al.,* 2013], epidermal growth factors loaded heparin-based hydrogels [Goh *et al.,* 2016], and poly(urethane-acrylate) based antimicrobial hydrogel wound dressings [Gharibi *et al.,* 2018] for wound management applications are good examples of thiol-ene reactions.

1.4.2. Hydrogel dressing products:

There are many different types of wounds with a multitude of different symptoms, including necrotic, sloughy, granulating and epithelialising that vary in size, shape and thickness. Understanding the purpose and principle of dressing formulations for these differing applications helps to match the correct dressing and wound combination.

Hydrogel dressings are indicated for the treatment of a variety of wound types, with precise selection of formulation ultimately based on clinical application:

1.4.2.1. Amorphous hydrogels:

Lacking a fixed shape, these hydrogels can be evenly applied over the wound using an applicator and being amorphous, these would mould into the shape of wound

defect easily. These are specifically indicated in the treatment of uneven or cavity wounds that cannot be easily covered with fixed, definite shape dressings. Examples of commercially available products include: 1) Aquasite®, an amorphous, glycerine-based hydrogel dressing [Derma Sciences Inc.], and 2) Intrasite® gel, a partially hydrated, amorphous propylene glycol hydrogel [Smith & Nephew, UK].

1.4.2.2. Impregnated hydrogel gauze dressings:

Used for partial or full thickness wounds where sterile packing of the wound bed is required, these formulations combine the advantages of hydrogels with non-woven dressings. Impregnated gauze dressings are saturated and/or permeated with an amorphous hydrogel and are commercially available as gauze pads, non-woven sponges and strips of different sizes. Commercially available products under this category are: 1) Aquasite® impregnated gauze dressing, a 100% cotton gauze pads incorporated with a hydrogel [Derma Sciences Inc.], and 2) Intrasite® conformable, hydrogel impregnated gauze dressings [Smith & Nephew, UK]. These dressings are available in various sizes and are indicated for use in necrotic, sloughy and granulating full thickness wounds [Wound Care, 2020].

1.4.2.3. Sheet hydrogel dressings:

Consisting purely of hydrogel, these dressings can be cut into the required size and shape to fit the wound. Hydrogel sheet dressings are indicated for the treatment of deep cavity and partial thickness wounds (*e.g.* ulcers, including venous and arterial, pressure sores, skin donor sites, surgical incisions, 1st and 2nd degree burns). Aquasite® hydrogel sheet dressing, glycerine based hydrogel formulations [Derma Science Inc.] and Flexigel® sheet, polyacrylamide based hydrogel sheet dressings [Smith & Nephew, UK] are commercial products available in different sizes (e.g.

2”x2” and 4”x4”) and can be easily cut to fit wound. These act as advanced wound dressing by keeping the wound bed moist, thus offering a soothing effect and facilitate wound healing as well as providing a physical barrier between wound and external environment. Moreover, being transparent, these sheet dressings allow easy monitoring of healing process [Smith & Nephew, 2020].

1.4.3. Polymers suitable for hydrogel wound dressings:

Some polymers, due to their physicochemical and biocompatible properties, are extensively used in biomedical applications. Most commonly used polymers used for fabricating hydrogels for wound dressing applications are discussed below. Moreover, other commonly used polymers with wound dressing applications are listed in **Table 1.4**.

1.4.3.1. Poly(vinyl alcohol) (PVA)

PVA is a polyhydroxy synthetic polymer with hydrophilic and biodegradable characters. Being biocompatible, transparent and capable of maintaining a moist environment, it has attracted application in different biomedical sectors, including wound care [Chhatri *et al.,* 2011; Oliveira *et al.,* 2016; Jiang *et al.,* 2011]. PVA makes gels when mixed with an appropriate amount of water and these gels possess tissue-mimicking properties [Jiang *et al.,* 2011]. The elasticity of these hydrogels can be improved by preparing blend hydrogels of PVA with other polymers [Kamoun *et al.,* 2015]. PVA chains can be crosslinked to produce PVA hydrogels by a variety of techniques, including freeze-thawing cycle, electron beam irradiation and using cross linkers like glutaraldehyde [Kokabi *et al.,* 2007]. As PVA doesn’t have inherent antimicrobial properties, PVA based hydrogels can be loaded with antimicrobial

agents for wound management applications [Kamoun *et al.,* 2015; Koehler *et al.,* 2018].

1.4.3.2. Poly(N-vinyl-2-pyrrolidone) (PVP):

PVP, a well-known water soluble synthetic polymer, due to its biocompatible and biodegradable nature, has attracted several biomedical applications including wound management. Due to its low cytotoxicity and good water vapour transmission rate (WVTR), it has been considered as a hydrogel membrane in the wound care sector as a skin substitute [Kamoun *et al.,* 2017]. Nu-Gel® (Systagenix) and Neoheal® (Kikgel) are PVP based proprietary hydrogel products indicated for use in first and second degree burns, severe sun burns, partial thickness wounds, ulcerations and bedsore. PVP undergoes crosslinking under ionising radiation, resulting in transparent hydrogels, but these hydrogels have poor mechanical properties with limited swelling. It's swelling behaviour and mechanical properties can be enhanced by blending it with other polymers, such as polysaccharides [Wang *et al.,* 2007; Singh and Pal, 2011; Singh and Singh 2012; Plungpongpan *et al.,* 2013; Archana *et al.,* 2013]. The use of ionising radiations is considered to be a favourable tool, wherever feasible, for hydrogel formation (and sterilisation) due to easy process control, minimal wastage, low cost and no chemical crosslinkers requirement [Sing and Pal, 2011; Raafat *et al.,* 2012].

1.4.3.3. Poly(ethylene glycol) (PEG):

PEG is a polyether which attracted a wide interest in the biomedical applications, including wound management, due to its transparent, non-toxic, non-immunogenic, biocompatible and biodegradable properties [Koehler *et al.,* 2017; Xu *et al.,* 2018]. PEG fumarate [Koosehgol *et al.,* 2017] and PEG acrylates like PEG diacrylate

(PEGDA) [Goh *et al.,* 2016; Nalampang *et al.,* 2013], PEG dimethyacrylate (PEGDMA) [Pacelli *et al.,* 2015] and PEG methyl ether methacrylate (PEGMEMA) are some of the commonly used acrylates in hydrogel formation for biomedical applications. Due to its featured biological properties, PEG has been used in proprietary products like Aquaflo™ (Covidien), Neoheal® (Kikgel) and AmeriGel® (Amerx Health Care Corp.) hydrogel wound dressings.

1.4.3.4. Poly(n-isopropylacrylamide) (PNIPAM):

PNIPAM is a temperature responsive smart polymer with amide and propyl moieties in its monomeric structure responsible for its temperature dependent volume phase transition (VPT at 34ºC). Its lower critical solution temperature (LCST) is slightly lower (32ºC) than VPT temperature. Being nontoxic, biocompatible [Capella *et al.,* 2019] and with phase transition close to the human body it has attracted wide biomedical applications [Nistor *et al.,* 2011; Shepherd *et al.,* 2011; Zubik *et al.,* 2017].

1.4.3.5. Alginate:

Alginate, a natural polysaccharide derived from marine brown algae and some soil bacteria has attracted wide biomedical application, including wound management, due to its hydrophilic, biocompatible and non-toxic nature [Rezvanian *et al.,* 2017; Hoefer *et al.,* 2015; Malagurski *et al.,* 2018; Kondaveeti *et al.,* 2018; Catanzano *et al.,* 2015]. Its exceptional wound healing properties like enhancing cell migration, angiogenesis and collagen I production, resulted in its use for fabricating commercially available hydrogel dressings like Purilon® Gel (Coloplast Ltd.) and Nu-Gel™ Hydrogel with Alginate (Systagenix Wound Management Ltd.) [Koehler *et al.,* 2018]. Alginate has an ability to form hydrogels by addition of divalent cations like

Ca^{2+}, which bind to guluronate blocks of alginate chains, enabling ionic cross-linking between guluronate block of adjacent alginate chains in the so called egg-box cross-linking model leading to gel formation [Wu *et al.,* 2018a; Kurczewska *et al.,* 2017; Lee *et al.,* 2012]. In case of loss of the divalent cationic cross-linker, the alginate dressing can easily degrade but this issue is commonly overcome by cross-linking (ionic or covalent) alginate with other polymers like PVA, gelatine and chitosan. [Moura *et al.,* 2013].

1.4.3.6. Bacterial Cellulose (BC):

BC, a biosynthetic cellulose is produced by several bacteria. BC being hydrophilic, highly pure, biocompatible, nonpyrogenic [Andrade *et al.,* 2011, Pértile *et al.,* 2012, Pandey *et al.,* 2017] and transparent material has resulted in its use for fabrication of proprietary (XCell®, Bioprocess®, Dermafill™, Gengiflex® and Biofill®) wound dressings with the clinical rationale being to facilitate autolytic debridement. The hydrophilicity and relatively high swelling ratio of BC [Nakayama *et al.,* 2004; Maneerung *et al.,* 2008] allows it to establish a moist microenvironment at the wound interface in addition to maintaining water vapour transmission rate (WVTR) and a constant temperature. Hydrophilicity also enables reversible swelling and de-swelling of the hydrogel, which can be exploited in the fluid management of heavily exuding wounds. In addition, BC hydrogel dressings can protect tissues forming over and around the wound site, as well as promote angiogenesis [Maneerung *et al.,* 2008]. Whilst not inherently antimicrobial itself, BC's unique 3-D nanofibrillar network is highly porous and amenable to high loading and controlled release of a range of antimicrobial agents [Fu *et al.,* 2013; Shah *et al.,* 2013; Wu *et al.,* 2014]. Further details on BC are presented in Chapter 2.

1.4.3.7. Chitosan:

Chitosan is a linear natural cationic polysaccharide derived by alkaline N-deacetylation of chitin, obtained from exoskeleton of crustaceans like crab, lobster and shrimp [Matica *et al.,* 2019; Kumari *et al.,* 2017; Mozalewska *et al.,* 2017]. Due to its biocompatibility, haemocompatibility, biodegradable nature and featured haemostatic, antimicrobial (bacteriostatic and fungistatic), antioxidant and wound healing properties [Matica *et al.,* 2019; Chen *et al.,* 2013; Behera *et al.,* 2017], it is considered fit as wound dressing material. In clinical trials, chitosan treated wounds have been reported to demonstrate faster healing in comparison to chitosan-free dressings [Koehler *et al.,* 2018]. Owing to its wound healing properties (cell proliferation, collagen and hyaluronic acid formation), chitosan has found its application in proprietary products like KytoCel® (Aspen Medical) and Chitoderm® plus (Trusetal Verbandstoffwerk GMBH) [Koehler *et al.,* 2018]. Chitosan can be used to produce membrane, sponge, scaffold and it also has hydrogel forming ability. However, a hydrogel formulation would be the most suitable form as it is able to protect, interact, contract the wound and facilitate wound healing by developing an optimum moist healing environment [Wang *et al.,* 2012]. Chitosan can get deformed easily through external stress, but this challenge can be overcome by blending it with suitable polymers to enhance its mechanical properties for fabricating wound dressing [Chen *et al.,* 2013].

1.4.3.8. Carboxymethyl cellulose (CMC):

CMC is a semi-synthetic, water-soluble ether derivative of cellulose in which H atoms from the hydroxyl groups are replaced with carboxymethyl [Reeves *et al.,* 2010]. CMC can be crosslinked using radiation technique, to make biocompatible

and biodegradable hydrogel with high water uptake capacity [Park *et al.,* 2017; Capanema *et al.,* 2018; Rakhshaei and Namazi*,* 2017]. Its unique properties resulted in its use in proprietary hydrogel dressing products like FlexiGel™ and Regranex® gel (Smith & Nephew, UK) and Purilon Gel®, a sodium carboxymethyl cellulose (NaCMC) based hydrogel dressing (Coloplast).

1.4.3.9. **Starch**:

Starch is one of the most abundant natural polysaccharides composed of two different polymers, namely amylose (about 30 %) and amylopectin (70 %) [Pal *et al.,* 2006]. Being economical, non-toxic, biocompatible and biodegradable, native starch has a potential as a wound management material, but its highly hydrophilic nature and relatively poor mechanical properties have limited its application [Jiang *et al*., 2020]. These problems can be overcome by either combining it with other polymers to make blend hydrogels [Jiang *et al*., 2020; Pal *et al.,* 2006] or by chemically modifying native starch to improve its properties for biomedical applications. Oxidised starch [Kamoun 2016; Hadisi *et al.,* 2018] and hydroxyethyl starch (HES) [Lee *et al.,* 2012a] are the common forms of modified starch used in the preparation of wound dressing. Starch has no inherent antimicrobial activity but can be functionalised with antimicrobial agents for wound management applications [Naseri-Nosar and Ziora, 2018].

1.4.3.10. **Natural gums**:

Natural bioactive plant-based gum polysaccharides made up of sugars like mannose, arabinose, dextrose, rhamnose and xylose have gained research attention in wound care section as a biomaterial for the preparation of wound dressings [Padil *et al.,* 2018; Mohammadinejad *et al.,* 2019]. Owing to their low cost, renewable,

biodegradable, biocompatible and tunable properties, the natural gums like guar gum (**Table 1.4**), gum arabic, tragacanth gum, gum tamarind and xanthan gum have been tested to fabricate wound dressings [Ahmad *et al.,* 2019]. Recently, many new gums have been introduced and functionally characterised. Natural gums carry components and are proven to accelerate wound healing process, e.g. tragacanth gums has inherent wound healing properties and effective in proliferation and remodelling phase of healing [Singh *et al.,* 2017]. These polysaccharide gums when blended with other polymers allows the production of composite hydrogel matrix with tailored porosity and sustained release of drugs [Singh and Dhiman, 2016; Juby *et al.,* 2012]. Of note, nanosilver-containing composite of gum acacia/PVA hydrogel is an example of antimicrobial hydrogel dressings with potential wound dressing applications [Juby *et al.,* 2012].

Table 1.4. Other natural and synthetic polymeric material used individually or in combination with other polymers for the production of hydrogel wound dressings.

	Source	Properties	Model/Case Study	Results	Commercial products	References
Collagen	Bovine; Porcine; Avian; Rodent; Marine	Natural polymer, nontoxic, biocompatible, biodegradable, haemostatic, support fibroblast growth, creates wound healing environment, stimulate macrophages and fibroblast, promote cell attachment and proliferation, cellular migration and tissue development.	Wounds in diabetic mice [Moura *et al.,* 2014] Burn wounds in male rats [Oryan *et al.,* 2018]	Promotes wound healing and epithelialisation	Woun'Dres® (Coloplast) Regenecare® (MPM Medical Inc.)	Xie *et al.,* 2018; Moura *et al.,* 2014; Oryan *et al.,* 2018
Gelatin	Partial denaturation of bovine or porcine collagen	Natural polymer, Type A and B gelatine, elastic, biocompatible, biodegradable, activate microphages, haemostatic, high water absorption capacity, forms thermally-reversible hydrogels	Wounds in diabetic mice [Yoon *et al.,* 2016]	Chemokine-loaded gelatin hydrogel dressings promoted healing, enhanced re-epithelialisation, neovascularisation	HyStem®-C (BioTime Inc.) Extracel-HP ™ (Glycosan Biosystems)	Saarai *et al.,* 2012; Yoon *et al.,* 2016; Wang and Wei, 2017
Hyaluronic acid	Bacterial fermentation; Extraction from animal tissues	Poly anionic biological macromolecule, biocompatible, biodegradable, non-immunogenic, non-thrombogenic, hydrophilic, antioxidant activity by reacting with oxygen-derived free radicals, wound healing activity by stimulating inflammatory signals and facilitate cell motility and proliferation.	Wounds in diabetic mice [da Silva *et al.,* 2017]	HA hydrogels accelerated wound closure and wound healing. When incorporated with stem cells increased neoepidermis thickness observed	Restore® Hydrogels (Hollister woundcare) Regenecare® HA HyStem™ (BioTime Inc.)	Luo *et al.,* 2018; da Silva *et al.,* 2017; Zhao *et al.,* 2015
Dextran	*Leuconostoc spp.* *Weissella spp.* *Lactobacilli*	Bacterial polysaccharide, biocompatible, biodegradable, hydrophilic, stimulate wound healing, enhance angiogenesis, promote reepithelialisation	Burn wounds in mice [Sun *et al.,* 2011] Wounds in mice [Alibolandi *et al.,* 2017]	Promotes wound healing, enables neovascularisation, promotes angiogenesis, accelerates epithelial maturation, dermal differentiation and skin regeneration Dextran hydrogels accelerate wound healing which was further improved by loading hydrogels with curcumin nanomicelles		Hwang *et al.,* 2010; Alibolandi *et al.,* 2017; Sun *et al.,* 2011

Glucan	Cell wall of bacteria, yeasts, algae, lichens, plants (oats and barley)	Polysaccharide, biocompatible, biodegradable, antibacterial, antiviral, anti-inflammatory, exhibits wound healing activity, immune enhancing ability, enhances tensile strength of scar tissue	26 patients (human subjects) with Hard-to-heal wounds like leg ulcers, diabetic foot ulcers and pressure ulcers [King *et al.,* 2017] Wounds in diabetic mice [Grip *et al.,* 2018]	Beta-glucan based Woulgan was very easy to apply and remove, capable of restarting healing process in a range of stalled wounds with wound size reduction	Woulgan® [Biotec Betaglucans]	Grip *et al.,* 2018; King *et al.,* 2017; Park *et al.,* 2018
Guar Gum	*Cyamopsis tetragonolobus*	High molecular weight non-ionic natural hetero-polysaccharide, low cost, hydrophilic, nontoxic, biodegradable, biocompatible, FDA approved			ActivHeal® (Advanced Medical Solutions Ltd.) 3M™ Tegaderm™ Hydrogel Wound Filler (3M Health Care)	Kaith *et al.,* 2015; Singh *et al.,* 2014; Kono *et al.,* 2014
Polyurethanes	Synthetic polymers with repetitive urethane groups produced by condensation and polymerisation methods	Biocompatible, nontoxic, good strength, good toughness, tear resistance , abrasion resistance, non-allergenic, favours epithelialisation, allows oxygen permeability	81 patients (human subjects) with acute and chronic wounds [Zoellner *et al.,* 2007] Wounds in rat model [Bankoti *et al.,* 2017]	Enhanced granulation and epithelialisation, reduction in wound surface slough, pain relief, wound size reduction Enhanced wound healing, increased neovascularization; higher re-epithelialisation, increased collagen synthesis	Hydrosorb® (Hartmann) Hydrosorb® Comfort (Hartmann)	Ghadi *et al.,* 2016; Zoellner *et al.,* 2007; Bankoti *et al.,* 2017
Poly(acrylic acid)	Synthetic polymer produced by polymerisation of acrylic acid	Biocompatible, biodegradable, hydrophilic, pH responsive polymer so can be utilised in producing smart hydrogels,anti-bacterial	Wounds in Swiss mice [Champeau *et al.,* 2018]	Nitric oxide controlled release PAA hydrogels lead to increased angiogenesis, organised collagen and accelerated wound contraction		Ijaz *et al.,* 2018; Champeau *et al.,* 2018; Jankaew *et al.,* 2015
2-acrylamido-2-methylpropane sulfonic acid (AMPS)	Commercially available or by Ritter reaction of acrylonitrile-isobutylene with sulphuric acid	Hydrophilic, non-toxic, biocompatible, thermal stability, pH independent swelling stability, good coherency with good skin adhesion, easy to remove from wound surface, high oxygen permeability, flexible	Porcine burn model [Boonkaew *et al.,* 2014]	Silver nanoparticle loaded AMPs hydrogels efficiently prevented bacterial colonisation of wound during healing process		Witthayaprapakorn 2011; Boonkaew *et al.,* 2014; Boonkaew *et al.,* 2014a

1.5. Characterisation of hydrogel dressings

1.5.1. Biocompatibility

Biocompatibility is “the ability of a material to perform with an appropriate host response in a specific application” [Williams, 1986]. It refers to the immune tolerance of a material in contact with living cells [Balan and Verestiuc, 2014]. As the wound dressing is intended to be in direct contact with the host cells, it must be safe and compatible (local and systemic) with no adverse effects with the living cells and tissues. Hence, it is fundamental for the hydrogels dressing and its degradation products to be non-toxic, cytocompatible and non-pyrogenic. The hydrogel should fulfil the bio-safety (noncytotoxic, nonmutagenic, noncarcinogenic) and bio-functionality (suitable for the intended purpose) aspects to be classified as biocompatible.

The selection of base material (monomers or polymers), cross linkers (if any), organic solvents, manufacturing and purification process dictates the suitability of the final hydrogel product for its wound management application as a dressing. Natural or synthetic monomers or polymers used in the hydrogel production should be biocompatible. The examples of such materials with proven biocompatible nature include bacterial cellulose, chitosan, collagen, gelatin, polyurethanes [section 1.4.3]. Moreover, the use of cross-linkers, initiators and other additives employed in the polymerisation process may raise cytotoxicity concerns, hence special attention should be given on the correct selection of such material. Extensive washing of the final hydrogel can reduce potential toxicity in the case of leachable or unreacted moieties [Das, 2013].

The tissue compatibility of the final hydrogel can be evaluated by testing the immunological response of the live host cells when the hydrogel material is placed in contact. This can be determined by *in vitro* (cell culture tests) and *in vivo* (animal studies) models [Das, 2013].

1.5.2. Haemocompatibility

Haemocompatibility is the tolerance of blood to the device, material or surface that comes in contact with the blood [Balan and Verestiuc, 2014]. As the wound dressing could potentially come in contact with blood so haemocompatibility is another fundamental characteristic for a hydrogel dressing. The interactions of blood with the material involves several factors like charge, surface chemistry and wettability [Chen *et al.,* 2011]. When the hydrogel dressing is applied at the wound site, blood can respond to the material of the hydrogel in different ways. These can be studied by assessing thrombosis, coagulation, platelet function, haemolysis and complement systems in blood [Balan and Verestiuc, 2014]. Based on the response of the hydrogel dressing, it would be classed as haemocompatible or non-haemocomatible.

American Society for Testing and Materials (ASTM) has set a protocol to assess the haemolytic properties of the material used in fabrication of medical devices with potential contact with blood. Based on the percentage haemolysis caused by the material when in contact with blood, it is classified as non-haemolytic (0-2 % haemolysis), slightly haemolytic (2-5% haemolysis) and haemolytic (>5 % haemolysis) [ASTM F756 - 17]. In the current project, haemocompatibility screening of the hydrogel dressings was evaluated by determining the haemolytic behaviour.

1.5.3. Morphology

Polymer chains in hydrogels are physically or chemically cross-linked to each other imparting the characteristic morphology to the hydrogel. The morphology of the hydrogel dictates its area of potential application. The morphological structure and physicochemical properties of the hydrogel may change temporarily or permanently with the altered parameters like change in composition, preparation method, external conditions like temperature, pH and electric signals [Das, 2013]. For the wound management application, change in structural morphology could alter loading and release profile, swelling ratio, WVTR and gas permeability [Mousavi *et al.,* 2019, Pan *et al.,* 2019]. Understanding of the structural architecture like pore morphology and pore size distribution is therefore vital and can be evaluated using stereo microscope, atomic force microscopy (AFM) and scanning electron microscope (SEM).

1.5.4. Water vapour transmission rate (WVTR)

Skin has a property of fluid conservation by controlling the rate of evaporation in order to maintain homeostasis. Normal skin loses water around 200 g/m^2/day [Pan *et al.,* 2019]. If the integrity of the skin is disturbed, as in the case of injury or burns, the fluid conservation functionality of normal skin is destroyed and it leads to increased rate of evaporation, which can be up to 25 times greater than the normal skin [Morgado *et al.,* 2015; Pan *et al.,* 2019]. If the water loss by evaporation from the wound site is not controlled, it may lead to wound surface dehydration, which may affect wound repair. Therefore, in order to maintain the moist wound environment, it is essential to maintain optimum moisture at the wound site.

Different WVTR values have been quoted in literature for an effective wound dressing. Though there is no exact value for WVTR for an ideal wound dressing, the value between 2000-2500 g/m^2/day [Morgado *et al.,* 2015] is considered to be effective to maintain optimum moisture required for wound healing. The wound dressing with the WVTR within this range is considered to be capable of controlling excessive water loss in order to avoid dehydration. Moreover, being capable of maintaining optimum water loss, it would tackle the exudate retention at the wound site, which if not controlled may lead to maceration of the healthy surrounding tissue [Queen *et al.,* 1987; Morgado *et al.,* 2015]. Hydrogels offer a double benefit as moist wound dressings as they are capable of controlling the excessive WVTR from the wound and at the same time transmit the water held in their network to keep the wound area moist [Jadhav *et al.,* 2012].

1.5.5. Optical transmission

The assessment of the wound site is important to assess patients' response to the treatment. Conventional wound dressings, including gauze dressings, are not ideal when it comes to monitoring the wound healing as these dressings have to be removed in order to assess the healing process. Periodic removal of the dressing can be traumatic for healing wounds. With the rapid advancement in the field of biomedical materials, new wound dressings have been produced from both natural and synthetic sources that are transparent in nature [Saito *et al.,* 2012]. Attributed to the high water content, hydrogels are usually clear and transparent hence, considered as a good candidate capable of delivering this property [Vowden and Vowden, 2017; Koehler *et al.,* 2018]. These transparent advanced dressings enable the non-invasive monitoring of the healing wound without the need for the removal of the dressing.

1.5.6. Moisture content

George Winter in 1960s established that the optimum moisture at the wound site increases reepithelialisation and promotes healing [Winter 1962]. This research revolutionised the field of wound management and the focus of wound dressings changed from conventional dry passive products, to responsive moisture-promoting materials [Abdelrahman and Newton 2011; Winter 1962]. Following these research findings, a wide range of dressings based on the moist healing concept were developed with a range of different material compositions.

Wound dressings with high moisture content offers several benefits including, but not limited to, high malleability, easy and pain free removal of the dressing, cooling and soothing effect resulting in a sensation of pain reduction with a capability of developing a moist microclimate that has been proven to enhance epithelialisation [Vowden and Vowden 2017; Winter 1962; Di *et al.,* 2017; Tyeb *et al.,* 2018]. Hydrogels are one of the most promising candidates amongst the category of advanced moist wound dressings. Hydrogels are composed of over 90% water [Koehler *et al.,* 2018] which is responsible for their soft and malleable texture. Hydrogels facilitate healing by donating moisture in the case of dry necrotic wounds and absorbing excessive exudate in the case of exudative wounds. This feature makes them capable of creating the moist micro-climate between the wound bed and the dressing at the wound site and reduces pain as a result of the cooling effect [Koehler *et al.,* 2018].

1.5.7. Swelling characteristic

The fluid absorbing and retaining capability of a dressing is an important property determining its suitability for wound management application. The ideal dressing

should have excellent fluid absorption and retention capabilities without degradation [Mousavi *et al*. 2019]. Hydrogels have an ability to absorb water and they get swollen as they have excellent water retention ability. They become soft and elastic after water absorption. The swollen, elastic hydrogels offer flexibility, which matches the flexibility of human tissue, leading to patient comfort when applied as wound dressing [El-Sherbiny and Yacoub, 2013].

Despite having intrinsic water content in the swollen state, hydrogels are usually able to take additional fluid from exudating wounds. At the same time, they are able to donate moisture to the dehydrated wound. This feature makes hydrogels a very useful tool as wound dressings.

1.6. Cyclodextrins for biomedical applications

Some healing agents are hydrophobic in nature and their delivery in a hydrophilic environment (wound dressing hydrogel) can be achieved by using solubility enhancing drug carriers like cyclodextrins (CDs). Cyclodextrins, a family of cyclic truncated-cone shaped oligosaccharide, offers a heterogeneous environment *i.e.* hydrophilic outer surface and hydrophobic inner cavity [Sun *et al.,* 2014]. In view of their biocompatibility and solubility enhancing properties, there are more than 30 proprietary pharmaceutical products containing CDs. Cyclodextrin monograms (e.g. αCD and βCD) can be found in several Pharmacopoeias like the US Pharmacopeia, European Pharmacopeia and the Japanese Pharmacopeia [Loftsson *et al*., 2005]. In addition to the solubility enhancement of the active compound, the inclusion of drug in the hydrophobic cavity of CDs, leading to the inclusion complex (IC) formation, offers protection with regards to increased shelf-life, avoiding incompatibility between

active compounds in the same formulation, offering stability against oxidation, hydrolysis and photolysis. Moreover, it offers release modulating properties in the formulation [Rakmai *et al.,* 2017; Jeong *et al.,* 2018].

Cyclodextrins (CDs) are naturally occurring cyclic oligosaccharides obtained from starch by enzymatic cyclisation using enzymes called cycloglycosyl transferase and are recognised as pharmaceutical excipients [Del Valle, 2004; Jambhekar and Breen 2016]. There are three commonly used native cyclodextrins: α-cyclodextrin, β-cyclodextrin and γ- cyclodextrin with six, seven and eight D-glucopyranose units linked by α-1,4 glycosidic bonds respectively. These linkages of glucopyranose units result in truncated cone structures (**Figure 1.3**).

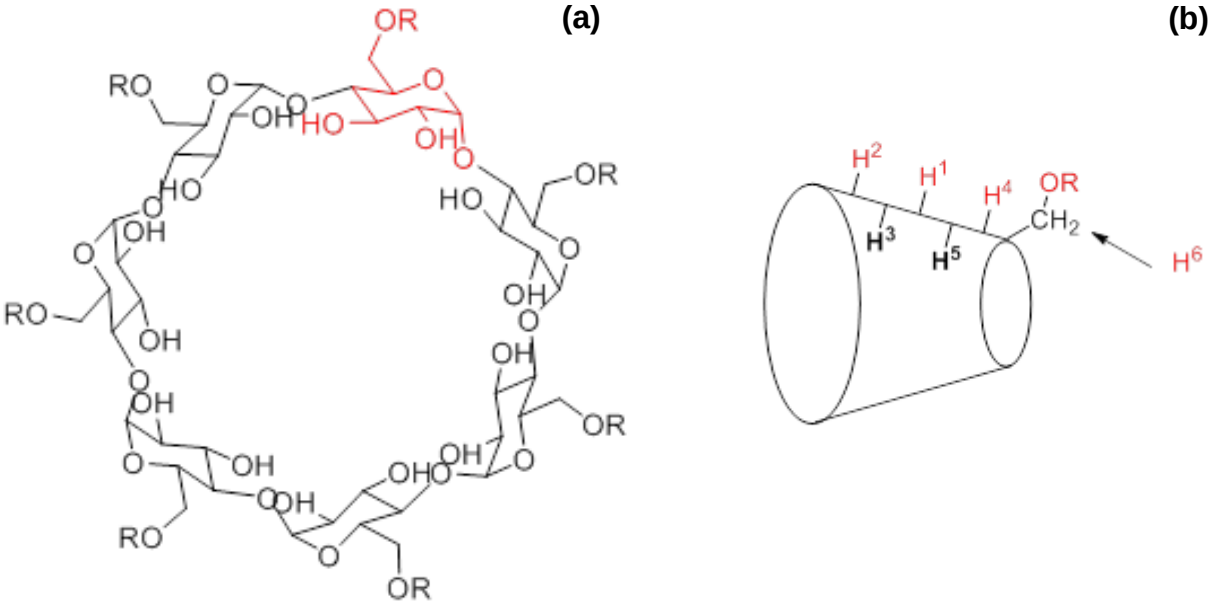

Figure 1.3. (a) Chemical structure and **(b)** a truncated cone schematic of cyclodextrin.

The primary and secondary hydroxyl groups located at the edges are responsible for the hydrophilic exterior surface of CDs. The skeletal carbons (C_3 and C_5) and endocyclic acetal oxygen of glucose residues are oriented inside, which imparts a hydrophobic character to the interior CD cavity [Dufour *et al.,* 2015]. The polarity of

the CD cavity has been reported to be similar to an aqueous ethanolic solution [Jambhekar and Breen 2016]. Apart from naturally occurring CDs, several chemically modified derivatives have been synthesised to improve the properties (aqueous solubility and toxicological profiles) of native CDs [Jambhekar and Breen 2016; Kurkov and Loftsson 2013]. Although a native βCD is hydrophilic, its aqueous solubility is limited (18.5 mg/mL). Substitution of the hydroxyl groups in CDs leading to the production of CD derivatives results in improvement in the aqueous solubility. There are a vast number of potential derivatives of CDs and hydroxypropyl betacyclodextrin (HPβCD) is one of the most important chemically modified CD with enhanced aqueous solubility (> 600 mg/mL for 0.65 substitution) [Loftsson *et al*., 2005]. HPβCD can be industrially produced under base catalysis from a controlled reaction of propylene oxide and βCD [Roquette, 2006] and is available in both oral and parenteral grade.

There are several studies reported on the enhancement of aqueous solubility of lipophilic compounds by their inclusion in the CD cavity [Wathoni *et al.,* 2017; Paramera *et al.,* 2011; Yallapu *et al.,* 2010; Mohan *et al.,* 2012]. This can be achieved by several techniques like co-precipitation, hot melt extrusion, solvent evaporation, freeze drying, spray drying, slurry mixing and dry mixing [Del Valle, 2004].

CD containing hydrogels can be produced in different ways; loading the pre-formulated CD-drug IC during or after crosslinking, grafted on the hydrogels [Lee *et al.,* 2012a] or cross-linking with diglycidyl-ethers [Jeong *et al.,* 2018]. The first approach is simple, but it may have a limitation of unmodulated drug release. In contrast, the release can be controlled with the other approaches [Jeong *et al.,* 2018; Hoare and Kohane 2008; Pinho *et al.,* 2014]. Modern therapies where more than one

medication with different hydrophilic/hydrophobic nature may benefit, development of CD-based hydrogel with dual drug delivery of hydrophobic drug (attributed to CDs) and hydrophilic compound (selecting polymers with hydrophilic active substance like chitosan), has opened a new scope. The efficacy of these CD-based hydrogels has demonstrated enhanced therapeutic capacity for wound dressing applications [Jeong *et al.,* 2018; Lee *et al.,* 2012a; Pinho *et al.,* 2014].

Chapter 2.
Bacterial cellulose

2.1. Introduction

Cellulose is one of the most abundant renewable biopolymer resources extensively available in nature. Cellulose is the main structural component of the cell wall of plants and the major constituent of cotton (90 %), flax (80 %), jute (65 %) and wood (50 %). Apart from plants, cellulose is produced by several algae and fungi. Many bacteria are also capable of producing cellulose by consuming carbohydrate sources like glucose and this form of cellulose is called bacterial cellulose (BC) (**Figure 2.1**) [Gopi *et al.,* 2019]. Cellulose from animal sources in not uncommon and tunicin, a cell wall (tunic) component of marine animals (Tunicates), is a good example [Almeida *et al.,* 2020].

Cellulose is a long linear organic homopolysaccharide made up of repeating units of glucose. The repeating units are composed of two anhydroglucose rings with oxygen covalently bonded to C1 of one glucose and C4 of the adjacent glucose leading to β (1-4) glycosidic linkages with the molecular formula $(C_6H_{10}O_5)_n$. Cellulose has a high degree of polymerisation, *n*, ranging between 10,000 to 15,000 [Gopi *et al.,* 2019; Sharma *et al.,* 2019]. Plant cellulose is derived from glucose that is produced by carbon dioxide fixation during photosynthesis. A similar process is followed by marine algae for cellulose synthesis. Some fungi and bacteria lack the photosynthesis capacity and produce cellulose from various carbon sources like glucose, mannitol and sucrose [Mohammadkazemi *et al.,* 2015].

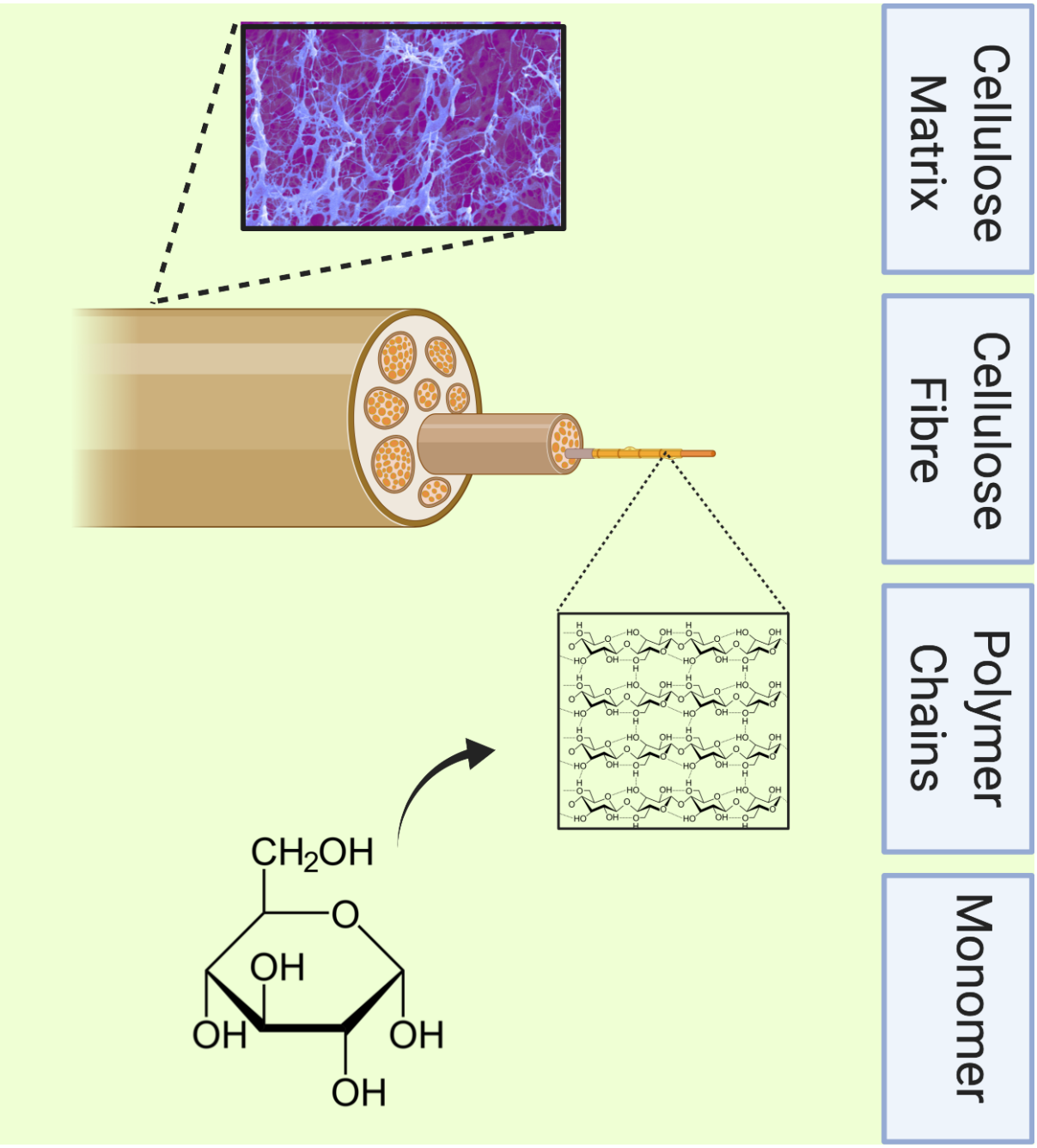

Figure 2.1. Illustration of structural organisation of bacterial.

2.2. Microbial synthesis of bacterial cellulose

The production of cellulose by bacteria, specifically *Acetobacter xylinum,* was first reported by Brown in 1886 [Wang *et al.,* 2019]. Several other Gram-negative bacterial species like *Azotobacter*, *Agrobacterium*, *Alcaligenes*, *Salmonella*, as well as Gram-positive bacteria such as *Sarcina*, have since been reported to produce BC.

Among the aforementioned bacteria, *Gluconoacetobacter xylinus*, formerly called *Acetobacter xylinum* and due to further taxonomical changes reclassified and now known as *Komagataeibacter xylinus* [Gorgieva and Trček, 2019], (would be referred to as *Gluconoacetobacter xylinus* through the text in this study) is most commonly used for the synthesis of BC, due to its high productivity [Mohammadkazemi *et al.,* 2015; Wang *et al.,* 2019]. Bacterial cellulose biosynthesised by different bacteria vary in morphology and properties.

G. xylinus, a Gram-negative rod-shaped obligate aerobe classified into *α-Proteobacteria*, in the presence of oxygen, is capable of transforming glucose and other organic substances to an ultra-pure form of BC [Chawla *et al.,* 2009]. It has been reported in literature that one bacterium can convert 108 glucose molecules into cellulose per hour [Wang *et al.,* 2019]. It is capable of producing BC at pH between 3-7 and temperatures between 25 ºC to 30 ºC in a precisely regulated manner [Esa *et al.,* 2014].

The genomic sequence of *G. xylinus* revealed that there are four BC synthase operons (bcs). Out of these, only *bcsI* is structurally complete, comprising of *bcsA*, *bcsB*, *bcsC* and *bcsD*. *G. xylinus* has a complete glycolytic pathway as it possesses a phosphofructosekinase (pfk)-encoding gene. Glucose-6-phosphate, a glycolytic intermediate is the origin of substrate synthesis in BC production. It is isomerised by an enzyme, phosphoglucomutase to glucose-1-phosphate, which under the action of UDP-glucosepyrophosphorylase (UGPase) forms uridine-5'-phosphate-α-D-glucose (UDPG). Cellulose is finally synthesised by BC synthase (bcs) complex which spans the outer and cytoplasmic membrane [Liu *et al.,* 2018]. Cellulose synthase complexes are linearly arranged and associated with pores present on the surface of

the bacterium. Bacteria secrete glucan chains, which assemble into protofibrils and further assemble to form nanofibrils cellulose ribbons (**Figure 2.2**) [Klemm *et al.,* 2001; Chawla *et al.,* 2009; Esa *et al.,* 2014].

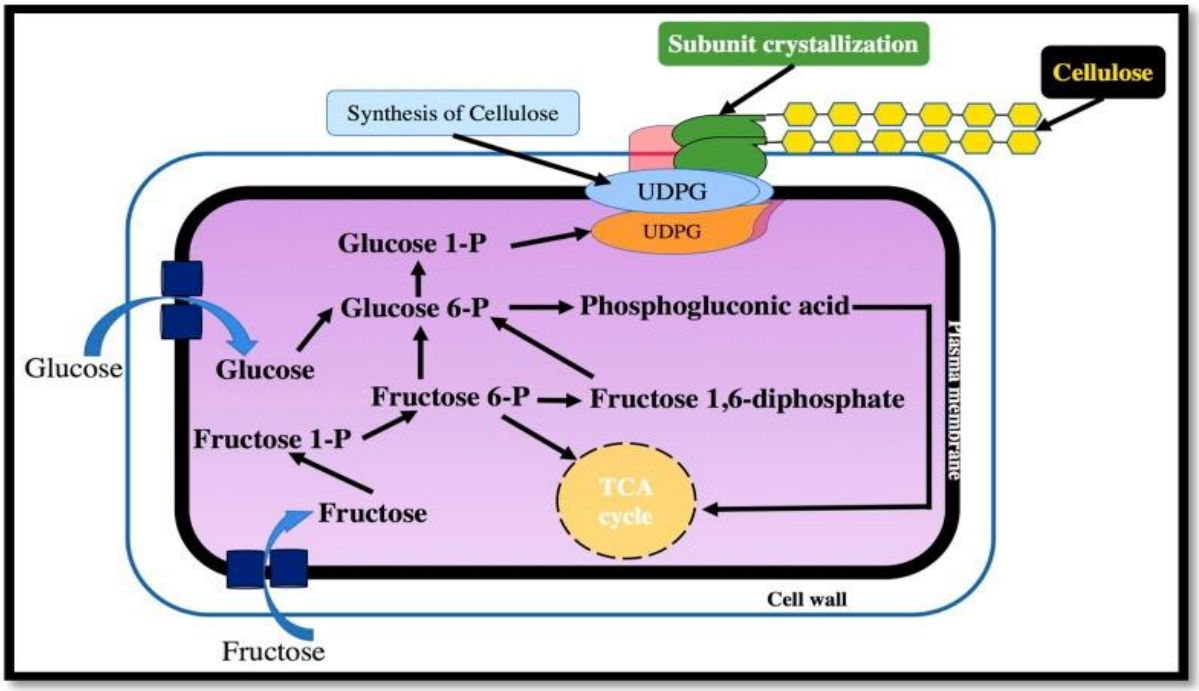

Figure 2.2. Biosynthetic pathway of cellulose in the bacterial cells (adapted from Moniri *et al.,* 2017).

G. xylinus produces two forms of cellulose: cellulose I, which is a ribbon like polymer, and cellulose II, which is a thermodynamically stable amorphous polymeric form (**Figure 2.3**). Most of the unique properties of bacterial cellulose are attributed to its nanofibrillar structure [Chawla *et al.,* 2009].

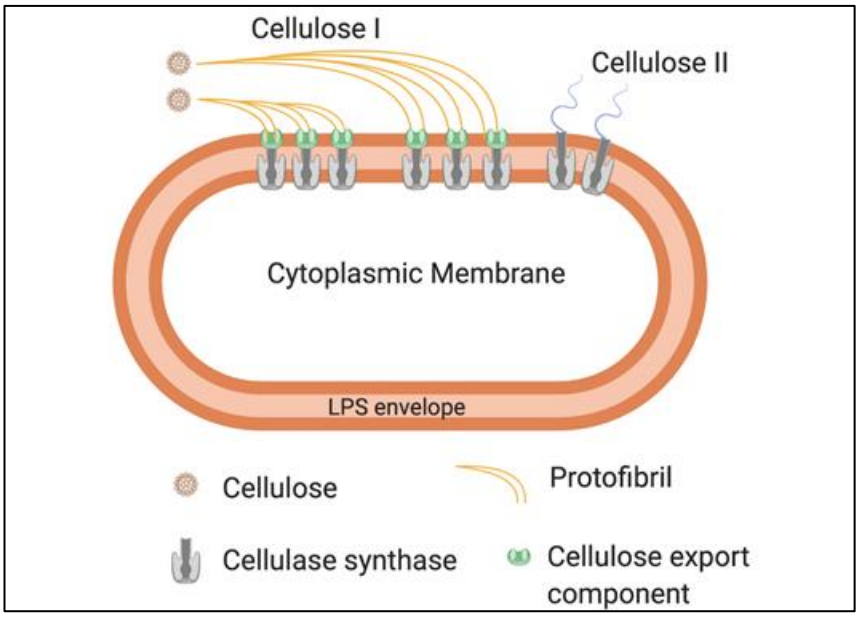

Figure 2.3. Illustration of production of cellulose microfibrils by *G. xylinus*.

Under static conditions, *G. xylinus* produces cellulose as pellicles at the air-liquid interface. This cellulose synthesis process helps these aerobes to arrive at the oxygen-rich surface and the BC pellicles hold the bacteria in the aerobic environment and protect bacterial cells from ultraviolet light [Klemm *et al.,* 2001].

2.3. Difference between plant cellulose and bacterial cellulose

Although plant cellulose and bacterial cellulose are both natural and have the similar molecular formula, they differ significantly in purity, structural and physicochemical properties (**Table 2.1**) [Portela *et al.,* 2019]. Plant cellulose is mainly found in the cell wall and is associated with other non-cellulosic bye products. In the majority of plants, cell wall has lignin (10-25 % of dry weight) that acts as a binder between cellulose (35-50 % of dry weight) and hemicellulose (20-35 % of dry weight) [Sharma *et al.,* 2019]. The purification process of BC is simpler than plant cellulose [Pang *et al.,* 2020]. Even though plant cellulose is chemically equivalent to BC but BC is a purer form, hence has found proprietary applications not only in the food industry but also in the biomedical field, including wound management and tissue regeneration [Liu *et al.,* 2018; Portela *et al.,* 2019; Gorgieva and Trček, 2019].

Table 2.1. Differences between bacterial cellulose and plant cellulose.

Properties	Bacterial Cellulose	Plant Cellulose	References
Raw material	Carbon source like glucose	CO_2 and H_2O	Klemm *et al*., 2001; Mohammadkazemi *et al.,* 2015
Fibre thickness	20-100 nm	In micrometer scale	Chawla *et al.,* 2009
Impurities	None	Lignin, hemicellulose, pectin	Portela *et al.,* 2019; Liu *et al.,* 2018
Purity	> 99 %	< 80 %	Klemm *et al*., 2005; Wang *et al.,* 2019
Water holding capacity	> 96 %	25-35 %	Rebelo *et al*., 2018; Wang *et al.,* 2019
Crystallinity	High (up to 96 %)	Low (up to 85 %)	Klemm *et al*., 2001; Wang *et al.,* 2019
In-situ state	Mouldable *in-situ* and available in wet state	Not mouldable *in-situ* and not available in the initial wet state	Klemm *et al.,* 2001
Mechanical strength in wet state	Higher	Lower	Klemm *et al*., 2001; Keshk, 2014
Intracellular cavity	Absent	Present	Kurosumi *et al.,* 2009
Intermediates in the biosynthesis process	Uridine Diphosphoglucose (UDPG)	Guanidine Diphosphoglucose (GDPG)	Keshk, 2014

2.4. Production and purification of bacterial cellulose

2.4.1. Static and agitated production

Fermentation production of BC can be performed using various carbon sources, nitrogen sources and at different pH. BC production between 25 ºC to 30 ºC using the Hestrin and Shramm medium [Hestrin and Shramm, 1954] which is composed of glucose, peptone, yeast extract, disodium phosphate, citric acid and pH adjusted to 6.0 is widely used. A number of methods have been reported for BC production, including static cultivation and agitated cultivation method. BC produced by these different methods vary in physicochemical properties and application. Growth of

bacteria under static conditions produces BC pellicles floating at the air-liquid interface. A shallow tray, flask or beaker is filled with the broth medium, inoculated and incubated for 5 to 14 days under sterile static conditions. BC pellicle is produced during the incubation period, which floats on the surface of the medium. The BC production in the static cultivation is directly proportional to the surface area of the air/liquid interface. Moreover, the shape of the pellicles can also be dictated by the shape of the container used for cultivation process. Furthermore, the thickness of the pellicles can also be dictated by varying duration of incubation. This type of BC pellicles has found several biomedical applications including as wound dressings [Ul-Islam *et al.,* 2015].

Agitated cultivation method is a convenient method for scale-up production of BC. Contrary to the static cultivation methods, in this method the inoculated culture media is constantly rotated and BC is produced as irregular forms like spheres, pellets or fibrous suspension [Esa *et al.,* 2014]. BC produced under agitated conditions has a lower degree of polymerisation, lower crystallinity and mechanical strength compared to pellicles produced under static conditions.

2.4.2. Purification procedures

Unlike plant cellulose, as the bacterial cellulose is not bound to bye-products hence its purification process is different from plant cellulose. Once the BC is produced, its purification is aimed at removing the bacteria trapped in the BC network structure and the removal of proteins and nucleic acids from yeast extract or bacteria during incubation process. These impurities along with the residual media imparts a slimy yellowish brown colour to BC.

Alkali is the most commonly used chemical for this purpose. Various concentrations of NaOH (0.4 %, 1 %, 2.5 %), KOH or Na_2CO_3 are used for this purpose [Embuscado *et al.,* 1996; Mohammadkazemi *et al.,* 2015; Gea *et al.,* 2011; Moniri *et al.,* 2017]. It has been reported that NaOH concentration above 6 % can cause the transformation of cellulose I to cellulose II hence most of the protocols use the concentration below 6 % [Gea *et al.,* 2011]. Duration of NaOH treatment varies from 15 min to 24 h at different temperature ranges (80 ºC to 100 ºC) and subsequent washing or boiling of BC pellicles in water until purified completely [Moniri *et al.,* 2017].

Some protocols follow the two-step purification, which involves an alkaline treatment followed by bleaching with NaOCl (2.5 %). The argument for this treatment is to get rid of the impurities like proteins and nucleic acids which couldn't be completely removed by NaOH treatment for long term storage of BC without any colour change [Gea *et al.,* 2011].

2.5. Factors affecting bacterial cellulose production

The cultivation of *G. xylinus* for BC production has received vast research interest. Several attempts were made to understand the factors affecting BC production. BC is produced by very few genera of bacteria, but due to the production of large quantities of cellulose, *G. xylinus* is the most investigated strain for BC production (details in section 2.2) [Masaoka *et al.,* 1993; Keshk, 2014]. BC production has been found to be dependent on several factors:

2.5.1. Influence of cultivation method

BC can be produced under different cultivation conditions like static, agitated and a combination of static and agitated cultures in a horizontal fermenter [Krystynowicz *et al.,* 2002; Shi *et al.,* 2014]. The choice of the cultivation technique depends on desired physical and mechanical properties and the final application. BC produced under static conditions appears as pellicles whereas under agitated conditions, it is produced as pellets, spheres or irregular masses (see section 2.4.1 for more details). Using the horizontal fermenters BC membranes or tubes can be produced [Krystynowicz *et al.,* 2002]. Due to varied cultivation conditions, the yield and the properties like morphology, crystallinity, Young's modulus, tensile strength and water holding capacity of BC produced by these methods vary [Krystynowicz *et al.,* 2002; Chawla *et al.,* 2009; Wang *et al.,* 2019].

2.5.2. Influence of composition of culture medium

It has been experimentally proved that the carbon and nitrogen source have direct impact on the BC yield [Costa *et al*., 2017]. Generally, glucose is used as a carbon source for BC production however, BC can be produced by several other carbon sources like 5 or 6 carbon chain monosaccharides (fructose, galactose, xylose), oligosaccharides (lactose, maltose, sucrose), starch, alcohol (ethanol, glycerol, ethylene glycol), organic acids (citric acid, malic acid, succinic acid) [Masaoka *et al.,* 1993, Keshk, 2014]. *G xylinus* is known to oxidise glucose to gluconic acid, which lowers the pH of the culture medium and inhibits bacterial growth and cellulose production [Oikawa *et al.,* 1995]. Initial glucose concentration in the culture medium is an important factor in BC production, as the by-product gluconic acid formed during BC production decreases the yield of cellulose production [Chawla *et al.,*

2009; Keshk, 2014]. Masaoka *et al.,* 1993 reported their findings on using varied initial glucose concentrations 0.6, 1.2, 2.4 and 4.8 g/flask for BC production and discovered 100 %, 100 %, 68 % and 28 % yield of cellulose respectively. These results indicated that the yield of cellulose to the amount of glucose consumed decreased with an increase in initial concentration of glucose used for cultivation. Higher cellulose production at the first two initial glucose concentrations was attributed to the trace production of gluconic acid, which increased with further glucose concentration increase [Masaoka *et al.,* 1993]. The effect of gluconic acid on BC production could be encountered by adding lignosulphonate in the culture medium. The antioxidant and polyphenolic compounds in lignosulphonate have been proven to inhibit gluconic acid formation, hence increase the BC yield [Keshk and Sameshima, 2006].

When other carbon sources like arabitol were used for cultivation, the BC production was more than 6 times as compared to glucose. The final pH of the culture medium when arabitol was used as a carbon source did not decrease to the acidic pH range and no gluconic acid was found [Oikawa *et al.,* 1995]. The use of fructose and glycerol as carbon sources have been reported to give nearly the same yield as glucose. Galactose, xylose and arabinose gave lower yield, mostly due to the slower growth rate [Masaoka *et al.,* 1993, Keshk, 2014]. The yield of BC was less than half as compared to glucose when sucrose was used. This is primarily due to the low activity of sucrose in *G xylinus* [Keshk, 2014].

In addition to the carbon source, nitrogen is another vital media component for BC production. Yeast extract is commonly used in the culture medium as a nitrogen source, but other nitrogen sources like corn steep liquor, polypeptones and chitosan have also been found to give higher BC production. Furthermore, many organic

acids (like lactic acid, malic acid, acetic acid, fumaric acid, succinic acid), inorganic salts (like $FeSO_4$. $7H_20$, $CaCl_2$. $2H_20$, $CuSO_4$. $5H_20$), vitamins (like folic acid, biotin, riboflavin, nicotinamide) and polymers (like agar, xanthan, acetane) have been reported to increase BC production [Dobre *et al.,* 2008].

2.5.3. Influence of cultivation conditions

It has been demonstrated that BC yield depends not only on the constituents in the culture medium but also on cultivation conditions like temperature, pH, aeration degree of the medium and surface area of the cultivation system.

The optimum temperature for the cultivation of *G xylinus* for BC production is 28 ºC to 30 ºC as in this range the enzymes work at optimum performance [Zakaria and Nazeri, 2012]. In a study, different incubation temperatures ranging between 5 ºC to 40 ºC for BC production were investigated and it emerged that 28 ºC served as the most favourable temperature for the growth of *G. xylinus* for BC production. The authors reported that, at this temperature, bacteria get sufficient energy which enhances the cellulose biosynthesis pathways for BC production [Zahan *et al.,* 2015]. In another study, the highest BC production was observed at the temperature range of 29.5 ºC to 30.5 ºC and 30 ºC has been reported as the optimum temperature for BC production by *G. xylinus* [Zakaria and Nazeri, 2012]. Most researchers use 30 ºC as the optimum temperature where the enzymes perform well, leading to the highest BC production [Raghunathan, 2013].

pH is another parameter dictating *G. xylinus* growth and BC production. *G. xylinus* is an acidophilic bacterium that is capable of growing in a low pH environment. It can survive at a pH as low as 3.5 [Zahan *et al.,* 2015a] but at pH below 4.0, reduction in BC yield has been observed. It has been reported that the optimum pH for BC

production is between 4.0 to 6.0 [Masaoka *et al.,* 1993]. Along with gluconic acid, *G. xylinus* can secrete acetic acid during cell growth which gets released in the culture medium and decreases the pH in the culture medium [Kongruang, 2008]. The decrease in pH (below pH 4) can inhibit bacterial growth and lower BC production [Zahan, 2015a]. Zakaria and Nazeri (2012) examined the BC production at various pH values ranging between 4.5 to 8.5 and found an increased yield of BC in the pH range of 5.25 to 5.75. Few researchers have reported the high BC yield at pH 7.0 [Raghunathan, 2013] but culture medium pH between 5.0 to 6.0 is commonly used for BC production.

Dissolved oxygen in the culture medium has been reported to have an effect on BC production. During BC production under static conditions, the carbon source is readily available to bacteria, but oxygen can be a limiting factor which can have a negative effect on BC production [Chawla *et al.,* 2009]. Several attempts have been made to ensure sufficient transfer of oxygen to bacteria during BC production by keeping the lids of the flasks loose [Lestari *et al.,* 2014], using the loop airlift reactor [Chao *et al.,* 2001] and using silicon membrane (100 µm thick) in the vessel to supply oxygen from the bottom of the vessel [Yoshino *et al.,* 1996]. These reports suggested increased BC production with better access of oxygen during the cultivation process.

2.6. Properties of bacterial cellulose

BC is well known for its biomedical applications due to its unique properties. BC has a 3-D nanofibrillar structure with pores. Its unique network structure allows impregnation and controlled release of several healing agents [Zmejkoski *et al.,* 2018]. Moreover, the ability of BC to participate in the development of new

composite materials is attributed to its morphological properties. Biocompatibility is an essential property for a material to be considered for the biomedical applications. Being non-toxic and non-pyrogenic, BC when tested for cytocompatiblity and haemocompatiblity for biomedical use, demonstrated promising results. Different mammalian cells when cultured (*in vitro*) on BC membranes demonstrated high viability with no significant difference in morphological and cellular functions [Zhu *et al.,* 2014; Jiji *et al.,* 2019]. Likewise, when tested *in vivo* for its biocompatibility, BC demonstrated no inflammatory reaction, absence of foreign body reaction and angiogenesis was evident around the BC implant in a rat model [Helenius *et al.,* 2006]. Along with cytocompatible nature, BC is found to be haemocompatible [Leitão *et al.,* 2013], advocating its biomedical applications including as a wound dressing.

The 3-D fibrillary structure of BC enables it to hold a high water content (up to 99 %), which offers elasticity without losing mechanical strength even in the hydrated state [Schumann *et al.,* 2009; Costa *et al.,* 2017]. These properties make BC resemble the natural tissue [Costa *et al.,* 2017] and support its application in several biomedical sectors. BC hydrogels have water in bonded and unbonded free state (**Figure 2.4**).

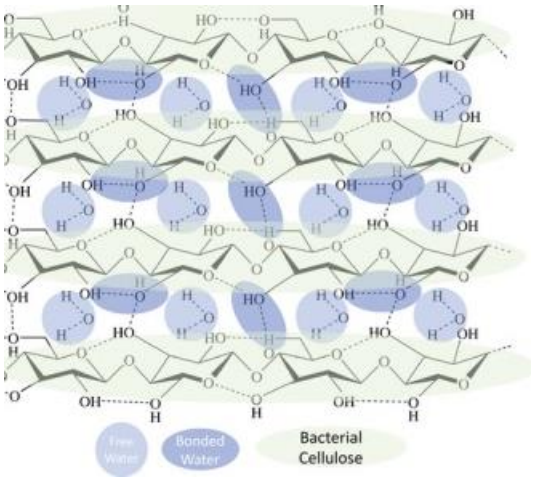

Figure 2.4. Illustration of BC hydrogel with bonded and unbonded water (adapted from Portela *et al*., 2019).

The unbound water can penetrate or exit the BC network structure, imparting the ability to BC hydrogels to maintain a hydrated environment, which could prove beneficial in wound healing [Portela *et al*., 2019]. Moreover, the shape of the BC pellicles can be tailored according to the desirable application and this feature opens its use in a wide range of sectors like wound management, acoustics, textile and the fashion industry [Nishi *et al.,* 1990; Chan *et al.,* 2018]. Other properties including thermally stability, high crystallinity, biodegradability and transparent nature make BC a preferred choice over plant cellulose for a broad spectrum of practical applications [Moniri *et al.,* 2017; Ullah *et al.,* 2019].

2.7. Applications of bacterial cellulose

Attributed to its physicochemical properties and high purity, BC has found its application in several sectors including food industry, pharmaceutical and medical applications, textile and paper industries.

2.7.1. BC in Food industry

In view of its highly pure, safe to consume and non-pyrogenic nature, BC is widely used in the food industry. BC has long been used in the Philippines as a food (Nata) additive in nata-de-pina and nata-de-coco [Azeredo *et al.,* 2019]. BC is a type of dietary fibre which has many advantages compared to other dietary fibre sources and has been approved by USA Food and Drug Administration (FDA) and classified as a “generally recognised as safe” for human consumption [Shi *et al.,* 2014]. BC has several potential food applications as a thickening agent, stabilising agent, gelling agent and suspending agent. BC can be used to produce low-calorie food and this has been demonstrated in a study where 10 % BC as an additive to Chinese-style meatball offered the desirable quality and proposed as a replacement

for the fat in emulsified meat product [Lin and Lin, 2004]. Moreover, attempts have been made to assess the potential of BC as a cryoprotectant for probiotic lactic acid bacteria [Jagannath *et al.,* 2010].

2.7.2. BC in Shoe and Textile industry

For decades, continuous attempts have been made for the development of analogues of leather. One such attempt has led to the production of malleable, breathable and water impermeable BC nanocomposite material with satisfactory performance for the shoe and textile industry. These newly developed BC-nanocomposites are proposed to offer a suitable alternative to leather and synthetic cellulosic fibres [Fernandes *et al.,* 2019].

In an ongoing attempt to explore natural and sustainable materials for the textile and fashion industry, BC has been identified as an innovative textile material. Fabrication of textiles by tailor-shaped cultivation technique is a good example of use of BC in the fashion and textile industry. Chan *et al.,* (2018), demonstrated this technique with self-synthesising properties and zero textile material waste with no cutting process for textile manufacturing. Further research needs to be undertaken to address the challenges for the wide application of BC in this sector.

2.7.3. BC in Wound management

In advanced wound management, the use of moist wound dressings is the first-line therapy. BC being a hydrogel has attracted wide research interest as wound dressing. Attributed to its physicochemical properties, BC based hydrogel dressings are capable of creating the ideal milieu for wound healing. Hydrophilicity,

biocompatible, non-pyrogenic, high wet strength and transparency are amongst the few of the desirable properties that resulted in the use of BC in fabrication of proprietary wound dressings like XCell®, Bioprocess®, Dermafill™, Gengiflex® and Biofill® [Martínez Ávila *et al.,* 2014; de Oliveira Barud *et al.,* 2016]. The primary focus of BC based dressings is autolytic debridement to facilitate wound healing [Sulaeva *et al.,* 2020]. The application of BC dressings has been demonstrated to facilitate wound healing by shortening the time for healing and wound closure [de Oliveira Barud *et al.,* 2016]. BC has no inherent antimicrobial properties [Jiji *et al.,* 2019] but its fine network fibrous architecture allows impregnation of different antimicrobial and healing agents for wound management [Maneerung *et al.,* 2008; Sulaeva *et al.,* 2020; Pang *et al.,* 2020]. Similar attempts have been successfully made in the current study to produce hydrogels for wound management as dressings.

To enhance the properties of BC as wound dressing, several composite dressings of BC with other materials like collagen, gelatine, alginate etc. have also been developed [Fu *et al.,* 2013]. These composite dressings have modified and added benefit of the other candidates used in the development of dressings. Apart from wound management, BC has many other biomedical applications, some of which are summarised in table 2.2.

2.7.4. BC in other sectors

BC has found application in several other sectors. Due to its high Young's modulus, BC has been reported to be an ideal material as an electroacoustic transducer for loudspeakers and headsets [Nishi *et al.,* 1990]. Tympanic membrane perforations can lead to hearing loss. BC has been reported as a promising treatment for tympanic membrane repair closure in a randomised controlled trial in patients with

tympanic membrane perforations in Brazil [Silveira *et al.,* 2016; de Oliveira Barud *et al.,* 2016], BC has other interesting applications in sectors like ophthalmology as artificial cornea and as contact lens, neural implants for nervous tissue regeneration [de Oliveira Barud *et al.,* 2016] and a biofabricated patient-specific auricular implants with desirable mechanical properties for ear cartilage replacement [Nimeskern *et al.,* 2013].

Regardless of the listed applications, BC has other applications like in paper industry, pharmaceutical tablet modification, biosensors and diagnostics for bioanalysis [Gao *et al.,* 2011; Keshk 2014; Moniri *et al.,* 2017] and holds vast potential with plenty more applications to be explored.

Table 2.2. Application of bacterial cellulose and its derivatives in other biomedical sectors.

Sector	Application	Properties	Reference
Biomedical sector	Artificial skin	BC has been considered as a valuable candidate as a temporary skin substitute. BC membrane has been developed and commercialised as an artificial skin, in Brazil. BC has been tested in patients suffering from skin burns, ulcers and facial dermabrasion	Keshk, 2014; Fontana *et al.,* 1990; Fu *et al.,* 2009
	Drug delivery	BC has attracted research interest as a carrier and drug delivery system for topical release of drugs. BC has found application as controlled release system of antimicrobials.	Barud *et al.,* 2016; Moniri *et al.,* 2017
	Bone regeneration	Owing to the slow degradation and biocompatibility, BC has attracted applications as a composite synthetic bone repair material in bone tissue engineering. To enhance its properties for bone repair, it is impregnated with other bone repair components like hydroxyapatite, growth factors, bone marrow mesenchymal stem cells etc.	Pang *et al.,* 2020
	Cardiovascular system	High mechanical strength in wet state, smooth surface and processing properties of BC allowed the production of vitalising BC tubes (patented BASYC®-tubes) with varied dimeters which have potential application as vascular conduits. BC tubes have been demonstrated to have successfully replaced carotid artery in *in vivo* models (rats, sheep, pigs). These tubes are an innovation approach for tackling reconstructive problems linked with extended vascular diseases.	Klemm *et al.,* 2001; Schumann *et al.,* 2009; Barud *et al.,* 2016
	Dental implant	BC based Gengiflex® and Gore-Tex® membranes have been proven to help periodontal tissue improvement. Gengiflex® has been demonstrated to support recovery of periodontal tissue in osseous deficiency around a $TiAl_6V_4$ dental implant.	Moniri *et al.,* 2017; Gorgieeva and Trcek, 2019; Novaes and Novaes, 1993

2.8. Aim of the current study

The aim of the work is the production and characterisation of biosynthetic hydrogels with antimicrobial properties as wound dressings. Natural bioactive materials with healing properties will be selected and loaded in a biosynthetic matrix to produce hydrogel dressings. Moreover, metal nanoparticles will be synthesised following the green chemistry approach using a natural healing agent and loaded to produce biosynthetic hydrogels as potential wound dressings.

2.9. Objectives set to achieve the aim of the study

1. Production of bacterial cellulose pellicles as the hydrogel wound dressing matrix
2. Characterisation of bacterial cellulose hydrogels for potential wound management applications
3. Production and characterisation of silver-loaded bacterial cellulose hydrogels as wound dressings
4. Production of water soluble curcumin by encapsulation in cyclodextrins
5. Production and characterisation of curcumin:hydroxypropyl-β-cyclodextrin-loaded bacterial cellulose hydrogels as wound dressings
6. Production of silver nanoparticles using Green chemistry approach by using curcumin:hydroxypropyl-β-cyclodextrin
7. Production and characterisation of silver nanoparticles-loaded bacterial cellulose hydrogels as wound dressings.

Chapter 3
Materials and Methods

3.1. Materials

3.1.1. Microbial strains, cell lines and blood

Gluconoacetobacter xylinus (ATCC 23770), *Pseudomonas aeruginosa* (NCIMB 8295) and *Staphylococcus aureus* (NCIMB 6571) were obtained from the University of Wolverhampton culture collection. All three microorganisms were maintained at -20 °C in a lyophilised form. Stock culture of *G. xylinus* was resuscitated on sterile mannitol agar, the components of the medium are in **Table 3.1** and incubated for 48 h at 30 °C. Stock cultures of *P. aeruginosa* and *S. aureus* were resuscitated on sterile tryptone soy agar (TSA) (**Table 3.1**), prepared according to the manufacturer's protocol and sterilised by autoclaving (Priorclave, England) at 121 °C for at least 30 min using saturated steam under at least 15 psi pressure, prior to use, and incubated for 48 h at 37 °C.

HEK293 (Human Embryonic Kidney epithelium), A549 lung adenocarcinoma, U251MG glioblastoma (referred as U251 throughout this research project), MSTO mesothelioma and Panc 1 pancreatic ductal adenocarcinoma were purchased from ATCC (UK).

Defibrinated horse whole blood was purchased from TCS Biosciences Ltd (UK) and stored at 4 °C.

3.1.2. Microbiological and cell culture media

Overnight broth cultures for microbes were aseptically prepared in suitable broth using the stock plates prior to experimental use. For BC production, Hestrin and Schramm (HS) medium (**Table 3.1**) was prepared following the standard protocol

[Hestrin and Schramm, 1954] and for antimicrobial studies, Tryptone soya broth (TSB) (**Table 3.1**) was used for *P. aeruginosa* and *S. aureus*.

Table 3.1. Composition of HS medium, TSA and TSB.

Composition of HS medium			**Composition of TSA**			**Composition of TSB**		
Chemicals	**Quantity (g/L)**	**Company**	**Chemicals**	**Quantity (g/L)**	**Company**	**Chemicals**	**Quantity (g/L)**	**Company**
Dextrose	20	Lab M, UK	**Soy Peptone**	5	Sigma-Aldrich, UK	**Soy Peptone**	3	Sigma-Aldrich, UK
Yeast extract	5	Lab M, UK	**Casein peptone**	15	Sigma-Aldrich, UK	**Casein peptone**	17	Sigma-Aldrich, UK
Bacteriological Peptone	5	Lab M, UK	**NaCl**	5	Sigma-Aldrich, UK	**K_2HPO_4**	2.5	Sigma-Aldrich, UK
Citric acid	1.15	Sigma Aldrich, UK	**Agar**	15	Sigma-Aldrich, UK	**D-Glucose**	2.5	Sigma-Aldrich, UK
Disodium Phosphate	2.7	Sigma Aldrich, UK				**NaCl**	5	Sigma-Aldrich, UK
Agar number 2 (for Mannitol agar)	15	Lab M, UK						

All media were sterilised prior to experimental use. Final pH of HS media adjusted at 6.0 and for TSA and TSB, 7.3 ± 0.2 (at 25 ºC).

For cytocompatibility studies, mammalian cells were grown in Dulbecco's Modified Eagle's Medium (DMEM), the components of the cell culture medium are in **Table 3.2**. In this report, DMEM and complete DMEM are used interchangeably throughout the text. The medium was filter sterilised using the filter unit (Fischerbrand, Filter Unit, Fischer Scientific, USA).

Table 3.2. Composition of complete DMEM media (pH adjusted to 7.3).

Chemical	Quantity	Company
DMEM containing 4.5 g/L glucose	Made up to 1 L	Gibco, UK
Fetal Bovine Serum	100 mL (10 %)	Gibco, UK
L-Glutamine	10 mL (2 mM)	Gibco, UK
Antibiotic Antimycotic containing: **Penicillin: 10,000 units/mL,** **Streptomycin: 10,000 µg/mL,** **Amphotericin B: 25 µg/mL**	10 mL (1 %)	Gibco, UK
Sodium bicarbonate	3.7 g/L	Sigma-Aldrich, UK

3.1.3. Materials and chemicals

Cellulose (microcrystalline form) was purchased from Sigma- Aldrich (UK). Zeolites (13X) were purchased from Laporte Inorganics (UK) and AgZ were purchased from Sigma- Aldrich (UK). Silver nitrate ($AgNO_3$) was from Fisher Scientific (UK) and sodium hydroxide from Acros Organics (Belgium). Ringer solution (1/4 strength) tablets were purchased from Lab M (UK) and prepared by dissolving one tablet in 500 mL of de-ionised water with constant magnetic stirring prior to sterilisation. Carbon-coated 300 mesh copper grids were purchased from Agar Scientific (UK).

Hydroxypropyl-β-cyclodextrin (parenteral grade) was kindly provided by Roquette (France) and curcumin was purchased from Alfa Aesar (UK). Acetone was purchased from Fischer Scientific (UK). Deuterium oxide (D_2O) was purchased from Goss Scientific (UK). Thiazolyl Blue Tetrazolium Bromide (MTT), sodium bicarbonate and 2,2-diphenyl-1-picrylhydrazyl (DPPH) were purchased from Sigma-Aldrich (UK). Dimethyl sulfoxide (DMSO), spectrophotometric grade, was purchased from Alfa Aesar (UK). NaCl (5.8 g/L) and glycine (7.6 g/L) were used for preparing Sorensen's glycine buffer and purchased from Sigma-Aldrich, UK. Trypsin was purchased from

Lonza (Belgium). Sodium chloride 0.9 % (w/v) (normal saline, intravenous infusion) was purchased from Baxter, UK.

Sterile 24-well tissue culture plates were purchased from Sarstedt (UK).

3.2. Methods

3.2.1. Production and purification of bacterial cellulose hydrogels

Once HS medium was prepared, pH was adjusted to 6.0 using glacial acetic acid and autoclaved (Priorclave, England) before use. The starter culture was prepared by inoculating a mucoid colony of *G. xylinus* in 100 mL autoclaved HS media. This was cultivated aerobically in a rotary shaker (Innova® 43, USA) at 30 °C for 72 h at 180 rpm.

After the incubation period, 10 % of *G. xylinus* starter culture was transferred to each 500 mL sterile conical flask containing 200 mL freshly prepared sterile HS culture medium. BC hydrogels were biosynthesised at 30 °C in an incubator (Laboratory Thermal Equipment LTD, UK), under static conditions. After 14 days, biosynthetic BC pellicles floated on top of the HS growth medium. After harvesting, these pellicles were purified by heating in 1% w/v sodium hydroxide at 80 °C for 15 min to remove the bacterial cells and medium components. BC pellicles were further boiled in deionised water until a neutral pH (pH 7) was achieved and at this point BC became clear and transparent. Some purified BC pellicles were lyophilised (Christ β 1,8-LSC plus, Martin Christ GmbH, Osterode am Harz, Germany) for further experimental purposes.

3.2.2. Production of silver-loaded bacterial cellulose hydrogels

The combination of silver and BC is not extensively reported in the literature. In the current study, two different forms of silver ($AgNO_3$ and AgZ) were used to produce hydrogel dressings with antimicrobial properties. Also, the effect of silver ion donor type on Ag^+ release and antimicrobial performance of the hydrogel dressings was explored. The proportion of Ag^+ in both formulations, i.e. $AgNO_3$ and AgZ, was kept equivalent.

3.2.2.1. Loading silver nitrate in bacterial cellulose to produce hydrogel dressings

The silver content in $AgNO_3$ (Fisher Scientific, UK) used in this investigation was 63.5% w/w. Purified wet BC pellicles were padded dry and loaded with aqueous $AgNO_3$ (0.55% w/v) by overnight incubation with constant agitation (180 rpm) (Innova® 43, USA) at 37 °C.

3.2.2.2. Loading silver zeolite in bacterial cellulose to produce hydrogel dressings

The silver content in the commercially available AgZ (Sigma-Aldrich, UK) used in the current study was 35% w/w. The AgZ pellets were fine ground using the pestle and mortar. After purification, BC pellicles were padded dry on filter paper and loaded with ground AgZ by overnight immersion in 1% w/v aqueous AgZ suspension at 37 °C under static conditions. It was subsequently noticed that some AgZ settled at the bottom of the vessel during loading, so the above procedure was repeated by immersing freshly purified padded dry BC in an aqueous AgZ suspension at 37 °C under constant agitation (180 rpm) (Innova® 43, USA) overnight.

3.2.3. Production of curcumin:hydroxypropyl-β-cyclodextrin-loaded bacterial cellulose hydrogels

Before the production of inclusion complex of CUR with HPβCD, native βCD was used and the inclusion complex formation was performed by different methods as described below.

3.2.3.1. Preparation of curcumin:cyclodextrin inclusion complex

Inclusion of CUR was first tested using native βCD as a carrier. CUR:βCD inclusion complex was synthesised by three different methods i.e. solvent evaporation, freeze drying and co-precipitation methods.

3.2.3.1.1. Solvent evaporation method: Inclusion complex of CUR with βCD was prepared by the solvent evaporation method at the molar ratio of 1:1, following the protocol reported by Yallapu *et al.,* (2010) with appropriate modifications. Curcumin (0.72 g) was dissolved in acetone (15 mL) and βCD (2.2 g) was dissolved in deionised water (160 mL). CUR solution was added dropwise to the aqueous βCD solution under constant stirring in a Schott bottle covered with aluminium foil to maintain dark conditions. Stirring was performed in a fume hood (BioMAT 2, CAS, UK) at room temperature for up to 72 h by replacing the lids of Schott bottles with perforated aluminium foil to allow acetone to slowly evaporate. Samples were then centrifuged (Eppendorf AG Centrifuge 5804 R, Germany) at 3000 rpm for 10 min and the supernatant containing water soluble inclusion complex of CUR:βCD was collected. The resultant inclusion complex was filtered through a 0.45 µm filter (MILLEX® HA, Merck Millipore) to remove any free CUR. The aqueous solution of CUR:βCD inclusion complex was then frozen at -20 °C overnight and lyophilised

(Christ β 1,8-LSC plus, Martin Christ GmbH, Osterode am Harz, Germany) to obtain solid powders and CUR content determined.

3.2.3.1.2. Freeze drying method: Inclusion complex of CUR with βCD was prepared at the molar ratio of 1:1, following the protocol reported by Mohan *et al.,* 2012, with slight modification. Curcumin (0.72 g) was added to an aqueous solution of βCD (2.2 g) dissolved in deionised water (160 mL) in a closed Schott bottle, covered with aluminium foil to protect from light, and then shaken in an orbital shaker (Innova® 43, USA) for 7 days at 180 rpm at 37 °C. Samples were then centrifuged (Eppendorf AG Centrifuge 5804 R, Germany) at 3000 rpm for 10 min and the supernatant containing water soluble inclusion complex of CUR:βCD was collected. The resultant inclusion complex was filtered through a 0.45 µm filter (MILLEX® HA, Merck Millipore) and frozen at -20 °C overnight followed by lyophilisation (Christ β 1,8-LSC plus, Martin Christ GmbH, Osterode am Harz, Germany). CUR content in the powder samples was determined.

3.2.3.1.3. Co-precipitation method: Inclusion complex of CUR with βCD was prepared at the molar ratio of 1:1, following the protocol reported by Marcolino *et al.,* (2011), with slight modification. An aqueous solution of βCD (2.2 g) was transferred to a round bottom flask and stirred at 60 °C. CUR (0.72 g) was dissolved in a minimum volume of ethanol (10 mL) at 60 °C and added dropwise to βCD solution under constant stirring. The mixture was refluxed with constant stirring at 70 °C for 4 h. Ethanol was removed by rotary evaporation followed by cooling at 25 °C. It was stored overnight at 4 °C and filtered. The product was dried in a vacuum oven (Townson + Mercer, Cheshire, UK) at 50 °C and CUR content measured.

3.2.3.2. Preparation of curcumin:hydroxypropyl-β-cyclodextrin inclusion complex

After evaluation of CUR content in CUR:βCD inclusion complex samples prepared by solvent evaporation, freeze drying and co-precipitation methods, the study was extended to produce curcumin inclusion complex using HPβCD as an aqueous solubility enhancing carrier. Based on the findings of CUR:βCD experiments, solvent evaporation method was adopted as a standard protocol for the production of CUR:HPβCD inclusion complex. Inclusion complex of CUR with HPβCD was synthesised by the solvent evaporation method at the molar ratio of 1:1, following the protocol report by Yallapu *et al*., (2010), with appropriate modifications. In the current study, an attempt was made to prepare CUR:HPβCD inclusion complex by varying the volume ratio of solvents and evaluating the effect on encapsulation efficacy.

Briefly, CUR (0.79 g) was dissolved in acetone (5 mL) and HPβCD (3.0 g) was dissolved in deionised water (45 mL). CUR solution was added dropwise to the aqueous HPβCD solution under constant stirring in a Schott bottle covered with aluminium foil to maintain dark conditions. As the volume ratio of acetone to water was 10 %, this sample was designated as IC 10. Similarly, using the same amounts of material (CUR 0.79 g and 3.0 g HPβCD) while varying the solvent volume ratio, IC 25 (CUR in 12.5 mL acetone and HPβCD in 37.5 mL water), IC 50 (CUR in 25 mL acetone: HPβCD in 25 mL water), IC 75 (CUR in 37.5 mL acetone: HPβCD in 12.5 mL water) and IC 90 (CUR in 45 mL acetone: HPβCD in 5 mL water) were prepared (**Table. 3.3**). Stirring was performed in a fume hood (BioMAT 2, CAS, UK) at room temperature for up to 72 h by replacing the lids of Schott bottles with perforated aluminium foil to allow acetone to slowly evaporate. Samples were then centrifuged (Eppendorf AG Centrifuge 5804 R, Germany) at 3000 rpm for 10 min and the

supernatant containing water soluble inclusion complex of CUR:HPβCD was collected. The resultant inclusion complex was filtered through a 0.45 µm filter (MILLEX® HA, Merck Millipore) to remove any free CUR. The aqueous solution of ICs were then frozen at -20 °C overnight and lyophilised (Christ β 1,8-LSC plus, Martin Christ GmbH, Osterode am Harz, Germany) to obtain solid powders which were stored in dark for further experimental use.

Table 3.3. Summary of the preparation of CUR:HPβCD inclusion complexes by varying the volume ratio of solvent.

Inclusion complex	Mass of CUR (g)	Mass of HPβCD (g)	Volume of acetone to dissolve CUR (mL)	Volume of water to dissolve HPβCD (mL)
IC 10	0.79	3.00	5.00	45.00
IC 25	0.79	3.00	12.50	37.50
IC 50	0.79	3.00	25.00	25.00
IC 75	0.79	3.00	37.50	12.50
IC 90	0.79	3.00	45.00	5.00

3.2.3.3. Loading curcumin:hydroxypropyl-β-cyclodextrin in bacterial cellulose to produce hydrogel dressings

Based on the experimental findings, HPβCD was chosen as a standard solubility enhancing carrier for CUR encapsulation. It is important to note that due to the highest encapsulation efficacy, IC 75 (CUR:HPβCD inclusion complex) was selected for loading and further characterisation. Purified BC pellicles were padded dry using filter paper and loaded with IC 75 by immersing in 2 % (w/v) aqueous solution of CUR:HPβCD overnight under constant agitation (180 rpm) (Innova® 43, USA) at 37 °C. Sterile conditions were maintained throughout the loading process.

3.2.4. Production of curcumin reduced silver nanopartilces (cAgNP)-loaded bacterial cellulose hydrogels

3.2.4.1. Preparation of curcumin reduced silver nanoparticles (cAgNP)

A novel green chemistry approach was developed for cAgNP synthesis by reducing $AgNO_3$ (Fisher Scientific, UK) with an aqueous solution of CUR:HPβCD (IC 75). CUR:HPβCD (0.19 g) solution was prepared by dissolving in deionised water (18 mL). CUR:HPβCD aqueous solution was added drop-wise with constant stirring to 1 mM $AgNO_3$ aqueous solution (42 mL) under boiling condition in a conical flasks. The mixed solutions were boiled for 3 h for reduction of Ag ions followed by cooling at room temperature for 30 min. The flask was covered with aluminium foil to maintain dark conditions throughout the reduction process to avoid any photochemical reactions.

3.2.4.2. Loading cAgNP in bacterial cellulose to produce hydrogel dressings

BC pellicles after purification were padded dry on sterilised filter paper and loaded with cAgNP by immersing in aqueous colloidal cAgNP overnight under agitated conditions (180 rpm) at 4 ºC. Sterilised conditions were maintained throughout the loading process.

3.3. Characterisation studies:

With the aim of wound management applications, hydrogels with different antimicrobial agents (AgZ, $AgNO_3$, CUR:HPβCD, cAgNP) were produced and characterised in the current study. The formation of antimicrobial healing agents like CUR:HPβCD inclusion complex was evaluated by additional characterisation studies like solubility study, encapsulation study, X-ray diffraction analysis (XRD), nuclear

magnetic resonance (NMR) and thermal analysis prior to loading in the BC matrix to obtain the hydrogel dressings. Likewise, the properties of cAgNP produced by the novel approach was underpinned by studies like transmission electron microscopy (TEM), zeta potential and dynamic light scattering (DLS) before loading in BC. BC hydrogel dressings produced after loading with the healing agents were characterised to underpin and evaluate their properties for the potential wound dressing applications.

3.3.1. Solubility study

The formation of the inclusion complex was confirmed by testing its physicochemical properties. CUR, HPβCD and CUR:HPβCD (10 mg each) were weighed and added to deionised water (10 mL) in separate universal tubes. These were stirred for 1 h at room temperature (22 °C) followed by filtration using 0.45 µm filter (MILLEX® HA, Merck Millipore). An aliquot was taken for UV-Visible spectrophotometric scan (WPA Biowave II, England) between 350-650 nm.

3.3.2. Determination of curcumin content and Encapsulation Efficiency (EE)

CUR content in the inclusion complex was quantified by using UV-Visible spectroscopy (WPA Biowave II, England) at a wavelength of 430 nm. The wavelength of 430 nm is the λ_{max} of CUR without any interference absorbance from HPβCD [Jantarat *et al.,* 2014]. CUR:HPβCD (1 mg) was dissolved in dimethyl sulfoxide (DMSO) (5 mL) and gently shaken in an orbital shaker (Innova® 43, USA) at 150 rpm at 37 °C for 1 h to extract CUR. The solution was filtered through 0.45 µm filter (MILLEX® HA, Merck Millipore) and CUR content was determined by UV-Visible spectroscopy (WPA Biowave II, England) at 430 nm. A standard calibration plot of

CUR in DMSO was produced as a reference. The Encapsulation Efficiency (%) was determined using the formula:

$$\% EE = \frac{mass\ of\ encapsulated\ curcumin}{mass\ of\ curcumin\ initially\ used} \times 100 \quad (1)$$

3.3.3. Nuclear Magnetic Resonance (NMR)

NMR is a powerful structural elucidation analytical tool in which radio frequency waves induce transitions between magnetic energy levels of nuclei of a molecule. The NMR analysis was undertaken to confirm the formation of inclusion complex of CUR:HPβCD. The NMR experiments including ^{1}H, proton-decoupled ^{13}C, homonuclear correlation spectroscopy (COSY), heteronuclear single quantum correlation (HSQC), heteronuclear multiple bond correlation (HMBC), and rotating-frame nuclear Overhauser spectroscopy (ROESY) were performed on a 400 MHz JEOL NMR spectrometer JNM-ECZ400R/M1 (Japan). The sample consisted of 10-20 mg of the inclusion complex dissolved in deuterium oxide. All spectra were internally referenced to residual solvent [Gottlieb *et al*., 1997]. ^{1}H spectra were acquired with a 45° pulse and inter-pulse delay of 5 seconds across 16 transients with acquisition time of 2.18628 seconds and pulse width of 6.48 µs; ^{13}C NMR spectra were recorded with a 30° pulse and inter pulse delay of 5 seconds across 4097 transients with acquisition time of 1.03809 seconds, and pulse width of 10.338 µs; HSQC spectra were recorded using a matrix consisting of 256 × 819 points across eight scans with a relaxation delay of 3 seconds; HMBC spectra were recorded using a matrix consisting of 512 × 1638 points across eight scans with a relaxation delay of 3 seconds; COSY spectra were recorded by using a matrix of 1024 × 1024 points across 1 scan with a relaxation delay of 3 seconds; ROESY

spectra were recorded in a phase sensitive mode with 1024 points in the *x* direction and 256 points in the *y* direction and acquired with 4 scans and relaxation delay of 1.5 seconds. Mixing time value was 0.25 seconds.

3.3.4. X-ray Diffractometric Analysis (XRD)

XRD is an analytical tool used in the identification of crystalline phases by their diffraction patterns. A structure in which atoms are arranged in a regular pattern is a crystalline phase, whereas the pattern is irregular in the amorphous phase. Crystalline phase is represented by sharp and narrow diffraction peaks on the spectrum, while the amorphous phase is represented by broad peaks [Patel and Parsania, 2018].

The X-ray diffraction patterns of CUR, HPβCD and CUR:HPβCD were obtained by an X-ray diffractometer (Empyrean, PANalytical, Netherlands) with Cu radiation source. The X-ray diffractometer was set at a voltage of 40 kV and current of 40 mA.

3.3.5. Thermal Gravimetric Analysis (TGA)

When matter is heated it undergoes certain physical and chemical changes. These changes are characteristic of the material being examined. The evaluation of the thermal properties of lyophilised BC, CUR, HPβCD and CUR:HPβCD and physical mixture of CUR and HPβCD was undertaken using a Mettler Toledo Thermogravimetric Analyzer, TGA/DSC 1 STAR® System, UK. Samples were subjected to TGA from 25 °C to 800 °C at 10 °C/min under constant flow of nitrogen (60 mL per min). Differential thermogravimetry (DTG) curve was also studied as a first derivative of TGA curve.

3.3.6. Differential Scanning Calorimetry (DSC)

DSC scans of CUR, HPβCD, CUR:HPβCD and physical mixture of CUR and HPβCD were performed using DSC Q2000 (TA instruments, New Castle, USA). The scans were collected using aluminum pans (TA instruments) with a nitrogen flow rate of 50 mL/min and temperature ramp rate of 20 °C/min.

3.3.7. Dynamic Light Scattering (DLS) and Zeta potential

DLS is a non-invasive analytical technique for determination of the size and size distribution of particles in the submicron region. The Brownian motion of dispersed particles is used to determine the hydrodynamic diameter using the Stokes-Einstein relationship. DLS measurements for cAgNP samples were performed on a Malvern Zetasizer (nano ZS), UK. Five consecutive measurements were carried out at 25 °C with samples equilibrated for 2 min before the measurements were started. The results were averaged to calculate the mean size.

The same instrument was used to obtain the Zeta potential values. Zeta potential measurement is the surface charge analysis of nanoparticles in a colloidal solution. The same samples were used for size measurements, equilibrated for 2 min before measurements were started. The results were obtained at 25 °C. Five consecutive measurements were taken and averaged to calculate the Zeta potential.

3.3.8. Transmission Electron Microscopy (TEM)

TEM is a powerful microscopic tool, where a high energy electron beam is shone through the sample and attributing to the short wavelength of electrons, highly detailed TEM images can be obtained. The shape, size and distribution of cAgNP produced using CUR:HPβCD was investigated by TEM. Briefly, a drop of aqueous

colloidal cAgNP was casted on a carbon-coated 300 mesh copper grid (agar scientific), left for 30 min, rinsed off and allowed to dry at room temperature in a covered container. TEM imaging was performed using JEOL 1400 electron microscope, operated at 80 keV. Images were captured at a different range of magnifications. A 100 cAgNP were randomly selected and measured using ImageJ to obtain the size distribution.

3.3.9. Morphological study by Scanning Electron Microscopy (SEM)

SEM makes use of electrons to form the image of the object. A focused electron beam generates a variety of signals at the surface of the specimen, which ultimately produces an image. The samples were freeze dried for 48 h (Christ β 1,8-LSC plus, Martin Christ GmbH, Osterode am Harz, Germany) and coated with an ultrafine gold coating using SC500 fine coater (Emscope, Kent, UK) and placed on a carbon stub for SEM imaging. The morphology of BC before and after purification was studied. Similarly, the shape and morphology of solid samples of CUR, HPβCD, CUR:HPβCD and lyophilised samples of AgZ-loaded BC under static and agitated conditions, $AgNO_3$-loaded BC, CUR:HPβCD-loaded BC and cAgNP-loaded BC were studied using Zeiss EvoVR 50 EP, SEM (Carl Zeiss AG, Oberkochen, Germany).

3.3.10. Energy Dispersive X-ray (EDX) analysis

EDX is a surface analytical technique for identification and quantification of elemental composition in a sample using an electron beam. Lyophilised AgZ-loaded BC, $AgNO_3$-loaded BC and cAgNP-loaded BC hydrogel samples were analysed by EDX (Zeiss Evo 50 EP, SEM) coupled with X-Max^N 50 Silicon Drift Detector (Oxford Instruments). The analysis was performed by Oxford Instruments INCA Energy Dispersive Spectroscopy Nanoanalysis software using the Point & ID function, to

confirm the presence of silver. Prior to analysis, each sample was placed on a carbon stub and sprayed with compressed air to remove any traces of dust, which can affect analysis.

3.3.11. Fourier Transform Infrared (FTIR) spectroscopy

Purified lyophilised BC was analysed in a transmission mode using FTIR spectroscopy (Bruker, Alpha, Platinum-ATR). The loading stage of the spectrophotometer was cleaned with acetone. Small BC sample was used to cover the disc hole on the diamond attenuated total reflector and scanned. Subsequent to BC analysis, pure cellulose, lyophilised AgZ-loaded BC (agitated), $AgNO_3$-loaded BC were also investigated by FTIR. The scanning range used was 400-4000 cm^{-1} with 16 scans settings for each sample run. Correspondingly, FTIR of CUR, HPβCD, CUR:HPβCD and lyophilised CUR:HPβCD-loaded BC was recorded in a similar way. A background scan was run prior to the scan of samples to obtain spectra.

3.3.12. Swelling ratio

Before the antimicrobial agents were loaded in the BC, the swelling behaviour of BC was investigated. This was underpinned using BC pellicles (9.25 ± 0.25 cm diameter) that were padded dry on sterile filter paper and the weight (W_x) recorded. Padded dry pellicles were soaked in 200 mL de-ionised water at 37 ºC for 24 h under static conditions. After 24 h, the pellicles were withdrawn from water and the swollen BC gently wiped with filter paper prior to reweighing (W_s). The swelling ratio (conducted in triplicate) was calculated as follows:

$$Swelling\ ratio = \frac{(W_s - W_x)}{W_x} \quad (2)$$

Where W_s = swollen rehydrated BC; W_x = padded dry BC.

3.3.13. Moisture content (M_c)

The wet mass (W_w) of BC (neat BC hydrogels) and 1% AgZ-loaded BC, 0.55 % $AgNO_3$-loaded BC, (2 % w/v) CUR:HPβCD-loaded BC and cAgNP-loaded BC was determined before lyophilisation and the dry mass (W_d) was recorded after 72 h of lyophilisation. M_C (%) was calculated using a formula:

$$\% M_c = \frac{(W_W - W_d)}{W_w} \times 100 \quad (3)$$

Where W_w = Wet BC samples; W_d = lyophilised BC samples

3.3.14. Optical Transmission

The quantitative optical transmission (%) of hydrogels was determined using LI-250A Light meter (LI-COR® Biosciences). BC pellicles were padded dry and rehydrated with deionised water (neat BC) and optical transmission (% T) of light was recorded. This was repeated with the test hydrogels of padded dry BC rehydrated with 2 % (w/v) aqueous solution of CUR:HPβCD (test hydrogels). Readings were taken for petri dish with deionised water (control), neat BC pellicles in petri dish and test BC pellicles. Four readings from different sections of each neat and test BC pellicles were recorded and averages used to examine the % T by comparison to the control (100 %T).

3.3.15. Transparency test

Monitoring the healing process without the need of removing dressing could help minimise trauma to the granulating tissue. With the aim of wound dressing application, the transparency level of PBS-loaded BC, AgZ-loaded BC, $AgNO_3$-loaded BC, CUR:HPβCD-loaded BC and cAgNP-loaded-BC hydrogels was assessed by simulation. The hydrogel samples were transferred on the laminated paper with text typed in different colours. The clarity of text beneath each hydrogel was examined to determine if it would permit observation and assessment simulating to wound monitoring context.

3.3.16. Release studies:

3.3.16.1. Silver release study:

Similar sized discs of AgZ-loaded BC, $AgNO_3$-loaded BC and a negative control of BC loaded with zeolite (BC-Z) (all 7.0 mm diameter) were cut using a corer. BC-Z, AgZ-loaded BC and $AgNO_3$-loaded BC discs were transferred into individual wells of a 24-well tissue culture flat bottom plate, and 1 mL of freshly prepared sterile TSB (release media) was added. Discs were then incubated under static conditions at 37 ºC for 96 h, and a 1 mL aliquot of release media withdrawn every 24 h; an equal volume (1 mL) of fresh sterile TSB was added at each time point to maintain sink conditions. Silver release was subsequently assessed by Inductively Coupled Plasma (ICP) spectrometry (Agilent Technologies 5100 ICP-OES, Agilent Technologies Inc., Santa Clara, CA). The kinetics of Ag^+ release from $AgNO_3$-loaded BC and AgZ-loaded BC were analysed by fitting the ICP data to zero order, first order, Higuichi and Korsmeyer–Peppas equations (for equations see Table T1 in the supporting information) [Costa and Lobo, 2001].

3.3.16.2. Curcumin release study

Small (≈8.0 mm diameter) sized discs of purified BC were cut using a biopsy punch and padded dry on filter paper. These discs were loaded with 2 % (w/v) aqueous solution of CUR:HPβCD by incubating overnight at 37 °C in glass Bijoux bottles, under constant agitation (Innova® 43, USA).

These discs were transferred to individual Bijoux tube containing 1 mL 0.9 % saline (pH 5.5) and incubated under static conditions at 35 °C. At set intervals, discs were moved to a new set of bijoux tubes with fresh 1 mL saline and incubated under same conditions. This was repeated over 48 h and CUR release was spectroscopically (WPA Biowave II, England) assessed at 430 nm for each time interval.

The standard calibration curve of CUR in 0.9 % saline (pH 5.5) was produced as a reference. Briefly, the stock solution (1000 µg/mL) of CUR was prepared by taking CUR (10 mg) and dissolving in ethanol:saline (70:30 % v/v) and making up to 10 mL. A standard solution (30 µg/mL) was prepared by taking 150 µL of stock solution and making up to 5.0 mL using saline. Using this standard solution, other standards were prepared in saline and the standards were read at 430 nm (WPA Biowave II, England) using saline as blank.

3.3.17. Antimicrobial study (disc diffusion assay)

The antimicrobial activity of AgZ-loaded BC (loaded under both static and constantly agitated conditions) and $AgNO_3$-loaded BC was investigated against *P. aeruginosa* (Gram –ve) and *S. aureus* (Gram +ve), using the disc diffusion assay; purified BC and BC-Z (loaded under constant agitation) were used as controls. Discs of AgZ-

loaded BC, $AgNO_3$-loaded BC, BC-Z and BC (7.0 mm diameter) were aseptically placed on TSA plates seeded with overnight cultures of *P. aeruginosa* or *S. aureus* and following incubation at 37 ºC for 24 h, the zone of inhibition (ZOI) was measured along X, Y and Z axes and average taken. This approach of measuring the ZOI was adopted as a standard procedure throughout this project. Individual discs (same discs) were subsequently transferred onto freshly seeded plates (*P. aeruginosa* or *S. aureus*) to ensure consistent, reproducible microbial growth and incubated again under the same conditions for a further 24 h. Results are statistically analysed and presented for ZOI at 24, 48, 72 and 96 h.

The antimicrobial activity of BC loaded with 2 % (w/v) aqueous CUR:HPβCD was also investigated against *S. aureus*, using the disc diffusion assay; purified BC and HPβCD-loaded BC were used as controls. Discs of BC, HPβCD-loaded BC and CUR:HPβCD-loaded BC (8.0 mm diameter) were aseptically cut and placed on TSA plates spread with overnight culture of *S. aureus* and following incubation at 37 °C for 24 h, the zone of inhibition (ZOI) was measured. Results are presented for ZOI (mm) at 24 h and statistically analysed by one-way Analysis of variance (ANOVA) with a Tukey's multi comparisons test using GraphPad Prism (version 7.02).

Furthermore, the antimicrobial activity of cAgNP-loaded BC was investigated against *P. aeruginosa* and *S. aureus* bacteria. PBS-loaded BC and HPβCD-loaded BC were used as controls. Discs (8.0 mm) of PBS-loaded BC, HPβCD-loaded BC and cAgNP-loaded BC were placed aseptically on TSA plates spread with an overnight culture of *P. aeruginosa* or *S. aureus* and incubated at 37 ºC for 24 h and zone of inhibition (ZOI) were measured. Data is presented as mean ± standard deviation (SD) and

analysed statistically by two-way ANOVA with a Tukey's multi comparisons test using GraphPad Prism (version 7.02).

3.3.18. *In vitro* tests hydrogels

3.3.18.1. Haemocompatibility

Non-haemocompatible material on contact with blood can cause serious health problems. In the current study, with the intended wound management applications, the haemocompatibility of NS-loaded BC, AgZ-loaded BC, $AgNO_3$-loaded BC, CUR:HPβCD-loaded BC and cAgNP-loaded BC hydrogels was evaluated *in vitro,* by assessing haemolytic potential of hydrogels. Defibrinated horse whole blood (purchased from TCS Biosciences Ltd) was washed twice with commercially available sterile normal saline (pH 5.5) (Baxter, UK) and centrifuged (Eppendorf AG Centrifuge 5804 R, Germany) at 3000 rpm for 10 min before re-suspending in saline solution. Padded dry BC was soaked in NS. 2 % (w/v) CUR:HPβCD was prepared in saline and loaded in padded dry BC pellicles. Using the biopsy punch, NS-loaded BC, AgZ-loaded BC, $AgNO_3$-loaded BC, CUR:HPβCD-loaded BC discs and cAgNP-loaded BC hydrogels (8.0 mm) were cut and incubated with 1.9 mL saline-suspended horse blood cells in test Eppendorfs under sterile conditions. Positive (+ve) controls were distilled water suspended blood cells and negative (-ve) controls were blood cells suspended in saline. Eppendorfs were incubated at 4 °C for 2 h with gentle inversion after every 15 min. Post-incubation, BC discs were removed under sterile condition followed by each sample being centrifuged (VWR Micro Star 17, Germany) at 3000 rpm for 10 min and supernatant decanted. Absorbance was recorded at 540 nm (WPA Biowave II, England) and percentage (%) haemolysis was determined as follows:

$$\%\ Haemolysis = \frac{(Abs\ of\ sample) - (Abs\ of - ve\ control)}{(Abs\ of + ve\ control) - (Abs\ of - ve\ control)} \times 100 \quad (4)$$

3.3.18.2. Cytocompatibility (*In vitro* cell viability)

Cytocompatibility is a vital parameter in material selection for its potential wound management application as a dressing. The preliminary study to investigate the cytotoxicity of BC was undertaken using complete Dulbecco's Modified Eagle's Medium (DMEM) (**Table 3.2**) conditioned with freeze dried (FD) BC pellicle (9.25 ± 0.25cm) overnight at 37°C under constant agitation (180 rpm) (Innova® 43, USA). HEK293 cells (10,000 cells per well) were seeded onto sterile 96 well plates prior to incubation with 200 µl BC-conditioned media at 37°C for 24 h in 5% CO_2; cell viability was assessed at 595 nm using the standard 3-(4,5-dimethylthiazol-2-yl)-2,5-diphenyltetrazolium bromide (MTT) assay by adding 5 mg/mL MTT solution (Sigma, UK) in all the wells and incubated for 2 h, followed by solubilising the formazan crystals with DMSO and Sorensen's glycine buffer (pH 10.5). Procedure was conducted aseptically in triplicate.

To evaluate the effect of the CUR:HPβCD-loaded BC on cell viability, the previously reported study was extended on 4 human cancer cell lines from different tissues, namely, A549 (human lung adenocarcinoma), MSTO (human mesothelioma), Panc1 (human pancreatic ductal adenocarcinoma) and U251 (human glioblastoma). Instead of testing the cytocompatibility using conditioned medium, as adopted in the preliminary study, BC discs (8.0 mm) (control) and CUR:HPβCD-loaded BC discs (8.0 mm) were suspended in wells of the cell culture plate using inserts. Moreover, the cytocompatibility of AgZ-loaded BC, $AgNO_3$-loaded BC and cAgNP-loaded BC was evaluated following the same procedure using Panc 1, U251 and MSTO.

All cell lines were cultured in complete DMEM medium and incubated at 37 °C in a humidity incubator with 5 % CO_2. The cytocompatibility of free CUR:HPβCD and CUR:HPβCD-loaded BC was investigated. Four different concentrations of CUR:HPβCD (1 %, 1.25 %, 1.5 %, 2 % w/v) were prepared in DMEM. BC pellicles were padded dried and either rehydrated with DMEM (control) or the respective concentrations of CUR:HPβCD in DMEM (test) in an orbital shaker (Innova® 43, USA) at 37 °C at 150 rpm (Innova® 43, USA) for overnight. Discs (8.0 mm diameter) were cut from the control and test pellicles using a corer for the experimental purposes and suspended in the wells using inserts throughout the duration of the experiment. The whole procedure was conducted aseptically. Similar procedure was followed by making appropriate modifications, to underpin the cytocompatibility of AgZ-loaded BC, $AgNO_3$-loaded BC and cAgNP-loaded BC. BC pellicles (test) after pad drying were rehydrated with 1 % aqueous AgZ or 0.55 % aqueous $AgNO_3$ or cAgNP overnight under agitated conditions at 4 ºC. In order to supplement water (instead of DMEM) used for sample preparation; PBS-loaded BC was used as a control. The sample (control and test) discs (8.0 mm) were adjusted to 37 ºC before use.

Briefly, 25,000 cells per well were seeded in 24 well plates for 24 h at 37 °C in 5% CO_2 incubator. The cells were then exposed to either free antimicrobial agent, 1 % aqueous AgZ, 0.55 % aqueous $AgNO_3$, CUR:HPβCD in DMEM (different concentrations), cAgNP produced in deionised water (equivalent amount) or AgZ-loaded BC, $AgNO_3$-loaded BC, CUR:HPβCD-loaded BC (different concentrations) or cAgNP-loaded BC discs (8.0 mm) for 24 h to investigate the effect on cell viability. Cells without BC discs (in DMEM or PBS supplemented DMEM) and DMEM-loaded

BC discs (for CUR:HPβCD) or PBS-loaded BC discs (for rest of the healing agents) were used as controls.

After incubation, the morphology of cells, confluence of the cell monolayer and cell viability was observed microscopically using an inverted light microscope (Nikon, Japan). The effect of free AgZ, $AgNO_3$, CUR:HPβCD, cAgNP and AgZ-loaded BC, $AgNO_3$-loaded BC, CUR:HPβCD-loaded BC or cAgNP-loaded BC discs on cell viability was evaluated by standard MTT cytotoxicity assay. The cell viability was calculated using the mean absorbance measured at 540 nm and the results were statistically analysed by ANOVA with a Tukey's multi comparisons test using GraphPad Prism (version 7.02).

3.3.19. Anti-oxidant activity by DPPH assay

2,2-diphenyl-1-picrylhydrazyl (DPPH) is a colorimetric radical scavenging assay for the determination of antioxidant properties of material. In the current study, DPPH assay was performed according the protocol reported by [Takao *et al.,* 1994] with appropriate modification. Briefly, test solutions of varying concentrations of CUR:HPβCD in methanol were prepared and methanol was used in preparing a blank. The assay mixture with 1 mL DPPH (80 µg/mL) methanolic solution and 1 mL solutions of various concentrations of the material (including a blank) after mixing were incubated in dark for 30 min at room temperature. Absorbance was measured spectrophotometrically (WPA Biowave II, England) at 517 nm. The free radical scavenging capacity was calculated as percent antioxidant effect (% E) using the following equation. Different sample concentrations were used to produce a curve for calculating IC_{50} values, the amount of sample required to obtain 50 % of the free radical inhibition [Chen *et al.,* 2013a].

The antioxidant potential of AgZ, $AgNO_3$ and cAgNP was also evaluated using DPPH radical scavenging assay. The assay mixture with 1 ml DPPH (80 µg/mL) methanolic solution and 1 ml of test AgZ, $AgNO_3$ and colloidal cAgNP (including the blank) after mixing were incubated under same conditions before recording the absorbance.

$$\%E = \frac{Abs_{control} - Abs_{sample}}{Abs_{control}} \times 100 \quad (5)$$

3.3.20. Water vapour transmission rate (WVTR)

The WVTR of neat BC and 2 % CUR:HPβCD-loaded BC hydrogel dressings was measured using the cup test method according to the American Society for Testing and Materials (ASTM) standard [ASTM E96 / E96M-16; Hu *et al.,* 2019]. In the current study, to achieve controlled conditions with minimum variations in set parameters during the entire length of the experiment, hypoxia incubator (Optronix, Oxford, UK) was used. An incubator temperature of 35 ± 0.1 °C and 60 ± 1 % relative humidity [RH] was maintained using compressed air during the entire period of the experiment. There was no attempt to artificially adjust air flow in the chamber as the influence of local air velocity was not examined in this study. A digital balance (ON BALANCE™, Myco MZ-100-BK) was placed inside the chamber for weighing the assemblies. The selected temperature (35 °C) corresponds to the temperature of the wound site, as reported by Lamke *et al.,* (1977).

Purified BC pellicles were padded dry and rehydrated either with deionised water (neat BC) or 2 % (w/v) CUR:HPβCD aqueous solution (test hydrogels) under constant agitation at 37 °C overnight in an orbital shaker (Innova® 43, USA).

Thickness of the rehydrated BC pellicles was measured using a Vernier calliper (Whitworth Digital calliper). Four readings for each pellicle were taken and average thickness calculated. Neat BC and/or CUR:HPβCD-loaded BC hydrogels (2.44 cm exposed diameter) were secured onto glass vessels containing 7.5 mL distilled water. The assemblies were kept in the chamber in upright position. WVTR was determined (in triplicates) by weighing the complete beaker assembly inside the chamber at set time intervals and calculated as [Balakrishnan *et al.,* 2005]:

$$WVTR = \frac{slope \text{ x } 24}{test\ area\ in\ m^2}\ g/m^2/day \qquad (6)$$

3.4. Statistical analysis

All the statistical analysis was carried out using Microsoft Excel 2016 and GraphPad Prism, version 7.02. One-way and two-way Analysis of Variance (ANOVA) using the Tukey's multiple comparison test for non-parametric analysis to determine the difference between individual groups in a data set was used. A comparison is statistically significant if the P value is ≤ 0.05.

Chapter 4
Results

Part I:

Introduction

This section of the thesis is focused on the findings of the production and characterisation of bacterial cellulose pellicles and silver-loaded bacterial cellulose hydrogels for potential wound management applications. The findings were published in Gupta *et al*., 2016 and Gupta *et al*., 2017.

4.1. Bacterial cellulose (BC)

4.1.1. Production and purification of BC hydrogel pellicles

G. xylinus produced pellicles of cellulose in 2 weeks of growth at 30 ºC under static conditions. During the production, BC pellicles appeared as a thin film on the air-liquid interface of the medium at day 4. These pellicles gradually increased in thickness by 14 days and at this stage, the pellicles were harvested. BC pellicles harvested from HS media were opaque with extensive brown mottling due to residual media, entrapped bacterial cells and other fermentation debris (**Figure 4.1a**). After washing once in hot 1% w/v sodium hydroxide, followed by repeated washing in deionised water, entrapped bacterial cells and excess media were successfully removed. The hydrogel pellicles after purification became clear and transparent (**Figure 4.1b**).

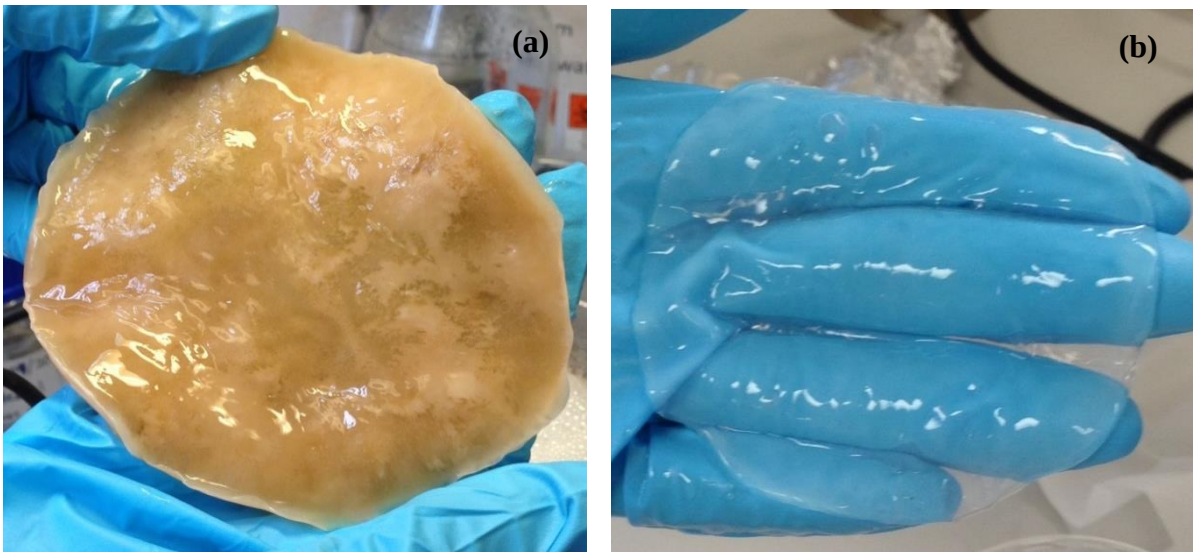

Figure 4.1. Photographs of **(a)** untreated BC; **(b)** purified BC.

4.2. Production of silver-loaded BC hydrogels

4.2.1. Production of AgZ-loaded bacterial cellulose hydrogels: static versus agitated conditions

Visual inspection of AgZ-loaded BC under static conditions revealed inconsistent loading (**Figure 4.2a**), where some areas of the BC displayed a higher AgZ content and others very little. AgZ-loaded BC under constant agitation appeared to have a more even distribution of AgZ and hence, more consistent loading (**Figure 4.2b**). Based on these findings, loading under agitated conditions was set as a standard procedure.

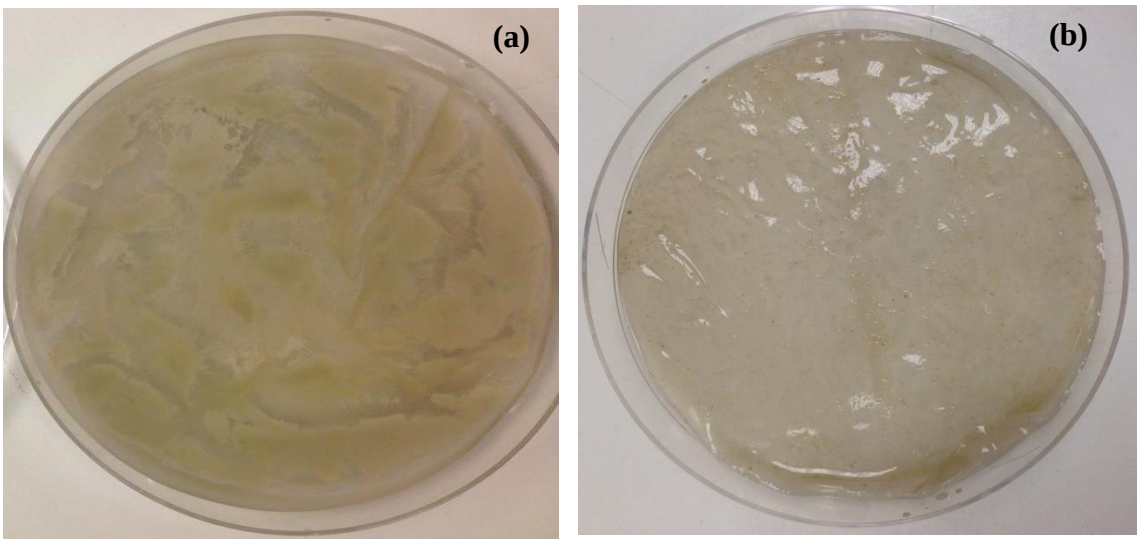

Figure 4.2. Photographs of **(a)** AgZ-loaded BC under static conditions; **(b)** AgZ-loaded BC under constant agitation.

4.2.3. Characterisation of silver-loaded BC

4.2.3.1. Scanning electron microscopy (SEM)

SEM was carried out on lyophilised BC samples of untreated, purified and silver-loaded BC. Moreover, morphology of AgZ and $AgNO_3$ was investigated in dry state before loading. Individual *G. xylinus* produces ribbons of cellulose that become entangled with each other, thus creating a dense network structure. Untreated BC pellicles revealed the presence of bacteria and other fermentation debris entrapped within the cellulose network (**Figures 4.3a**), but once purified, no bacteria were visible (**Figure 4.3b**). The process of washing in hot NaOH followed by boiling in deionised water resulted in the removal of bacteria and extraneous material revealing a network of microscopic fibres (**Figure 4.3b**). BC pellicles are interwoven thick mats of cellulose fibres, that following freeze drying, have a dense, fibrous network with voids (**Figure 4.3b**). It emerged that the fine ribbons (30-105 nm thickness) (**Fig. 4.3c**) of cellulose entangle with each other forming the network structure interspersed with voids. Morphological studies of lyophilised purified BC revealed two types of pores in the BC network structure; nano pores with pore size as low as 27 nm (**Fig. 4.3d**) and some large superficial pores with diameter value of up to 10 µm (**Fig. 4.3e**). It may be noted that these pores may further expand on hydration with water.

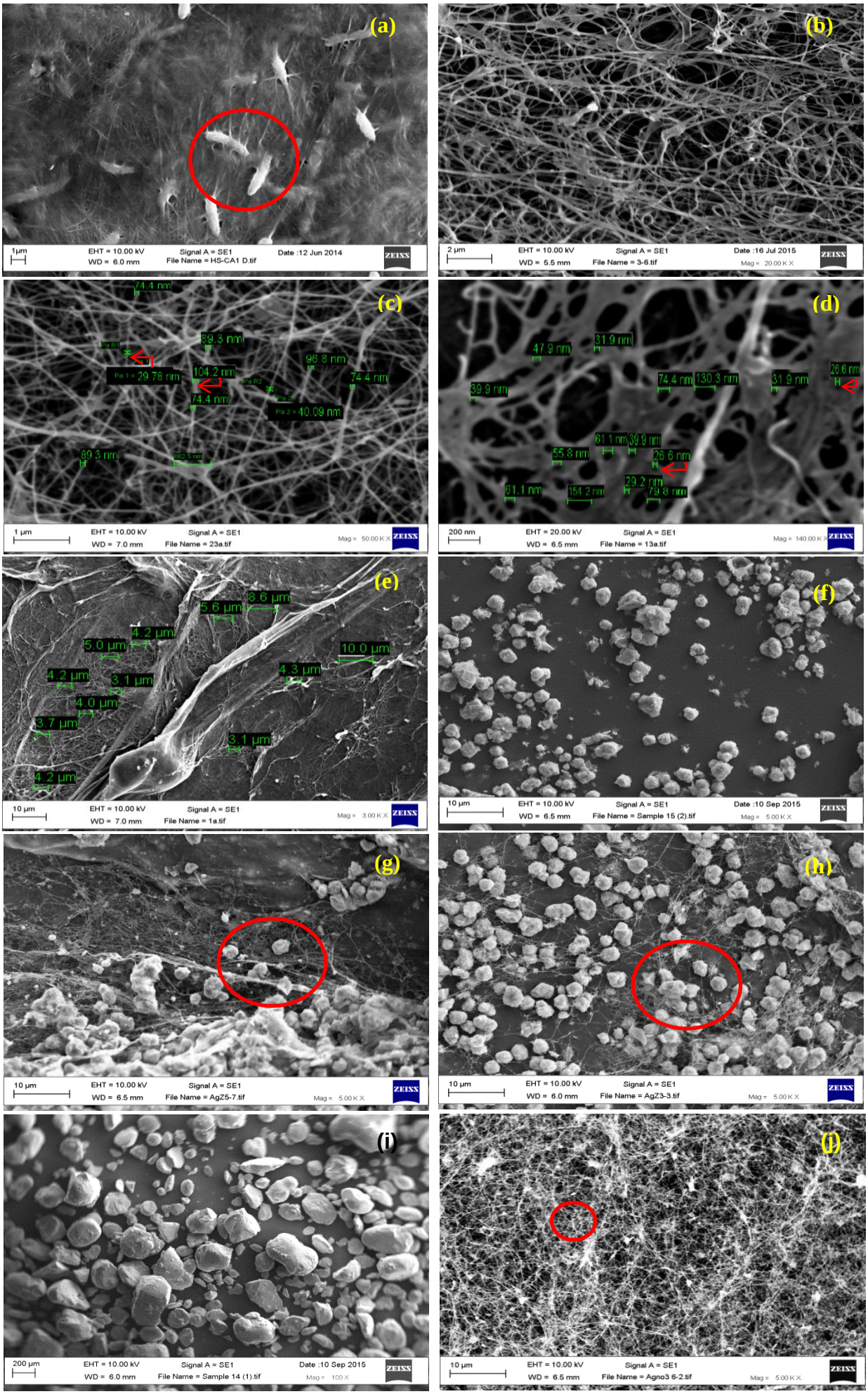

Figure 4.3. SEM photomicrographs of **(a)** untreated BC, entrapped residual *G. xylinus* highlighted; **(b)** purified BC revealing fibre network structure; **(c)** BC morphology with fibre thickness **(d & e)** BC morphology with pore size distribution; **(f)** morphology of ground AgZ; **(g)** AgZ-loaded BC under static condition; **(h)** AgZ-loaded BC under constant agitation; **(i)** morphology of $AgNO_3$; **(j)** $AgNO_3$-loaded BC under constant agitation.

SEM results revealed that ground AgZ has round to irregular structure (**Fig. 4.3f**) and $AgNO_3$ has irregular shape (**Fig. 4.3i**). Freeze dried AgZ-loaded BC (**Figure 4.3g&h**) and $AgNO_3$-loaded BC (**Figure 4.3j**) revealed AgZ and silver microcrystals got entrapped within the dense cellulose network. After loading with AgZ under constant agitation, AgZ-loaded BC displayed more consistent, uniform loading (**Figure 4.3h**) compared to that prepared under static conditions (**Figure 4.3g**). Clusters of encapsulated AgZ particles ranged from 2.0 to 20.0 µm, with single AgZ particles (0.5–5.0 µm) also encapsulated within the BC (**Figure 4.3g&h**). Conversely, crystals of $AgNO_3$ entrapped within the BC fibres had an average range of 0.08–3.5 µm (**Figure 4.3j**). In summary, the three-dimensional cellulose network consists of a large number of voids that become pores for sequestration of encapsulated silver microcrystals or AgZ when rehydrated.

4.2.3.2. Energy Dispersive X-ray analysis (EDX)

The purification process of BC was also confirmed by EDX spectra, which indicated the removal of extraneous material from the BC (**Figure 4.4a&b**). In addition to carbon (C) and oxygen (O), untreated BC had elemental traces like nitrogen (N), sodium (Na), phosphorus (P), sulphur (S) and potassium (K), which confirmed the presence of entrapped bacterial and extraneous components from the medium (**Figure 4.4a**). Once purified in hot NaOH and subsequent repeated boiling in deionised water, all trace elements from entrapped bacterial and medium were successfully removed resulting in purified BC (**Figure 4.4b**). The presence of silver in both AgZ-loaded BC and $AgNO_3$-loaded BC was confirmed by EDX spectra (**Figure 4.4c&d**). Additionally, the presence of aluminium, silicon as well as

elemental traces of calcium, sodium, magnesium and iron was also evident on EDX spectra of AgZ-loaded BC (**Figure 4.4c**).

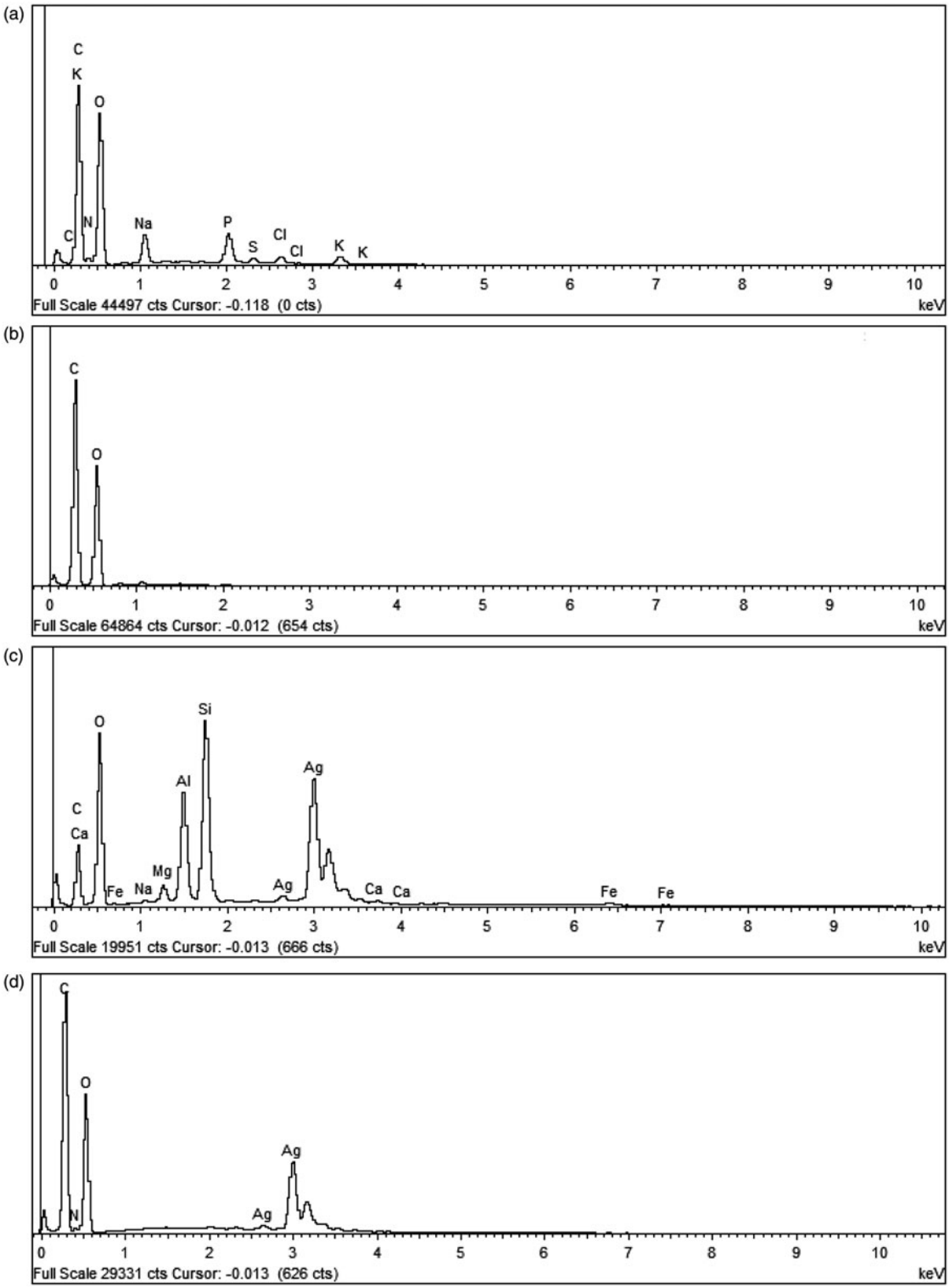

Figure 4.4. EDX spectra of **(a)** untreated BC; **(b)** purified BC; **(c)** AgZ-loaded BC; **(d)** $AgNO_3$-loaded BC.

4.2.3.3. Fourier transform infrared (FTIR)

The FTIR spectra of a commercially available cellulose sample, purified BC, $AgNO_3$-loaded BC and AgZ-loaded BC are shown in **Figure 4.5**. Similarity in peak characteristics are shown in the spectra for the commercially available cellulose and purified BC at band regions of 3330 cm^{-1}, 2894 cm^{-1}, 1641 cm^{-1}, 1370 cm^{-1}, 1159 cm^{-1} and 1056 cm^{-1} (**Figure 4.5a&b**); these peaks were also observed in both the $AgNO_3$-loaded BC and AgZ-loaded BC spectra (**Figure 4.5c&d**). The characteristic peaks for $AgNO_3$ (733 cm^{-1}, 803 cm^{-1} and 1300 cm^{-1}) (**Figure 4.5c**) and AgZ (434 cm^{-1} and 980 cm^{-1}) (**Figure 4.5d**) were also observed in the spectra, thereby confirming the encapsulation of $AgNO_3$ or AgZ within the BC network.

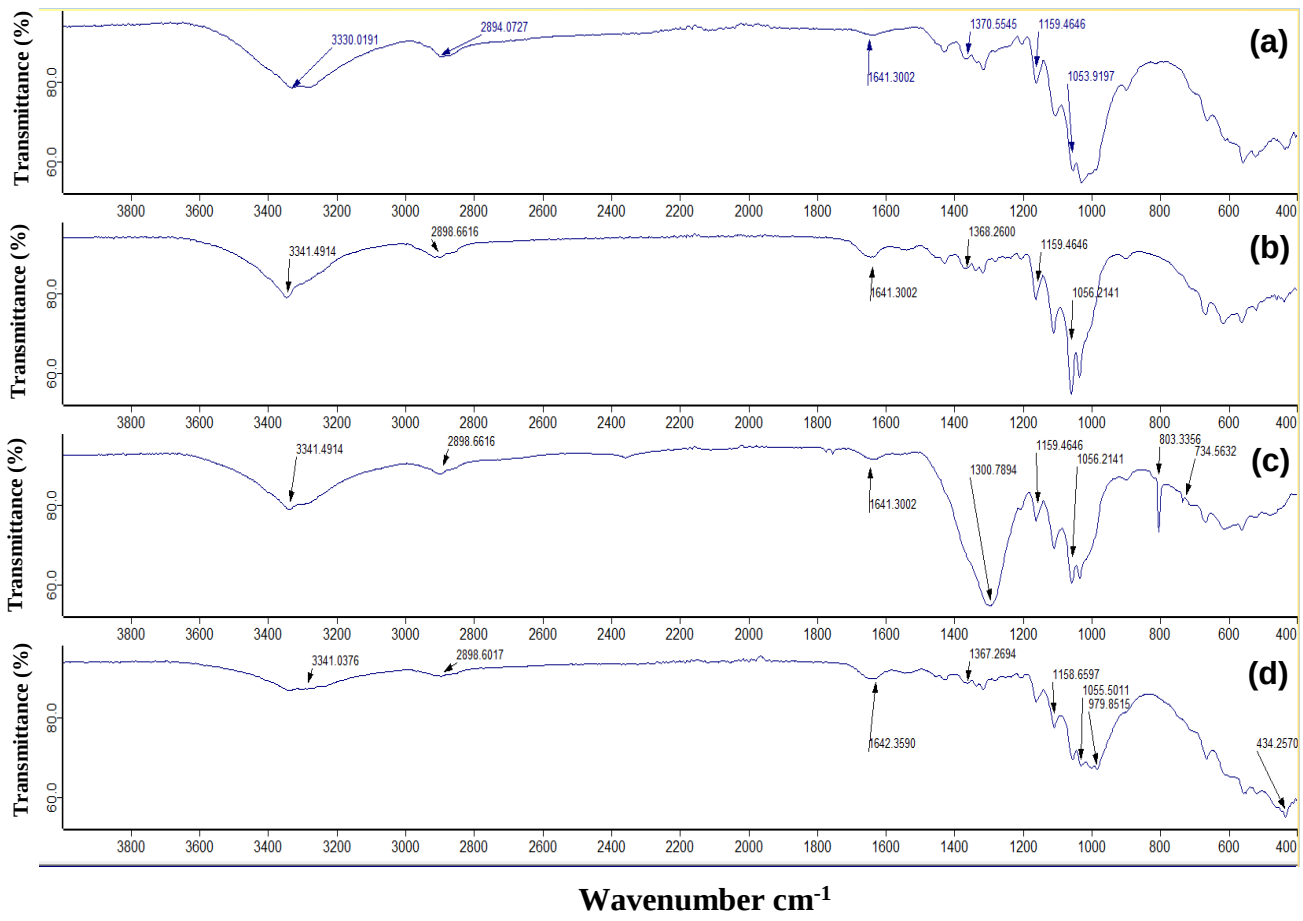

Figure 4.5. FTIR spectra from 400 to 4000 cm-1 for **(a)** commercially available cellulose; **(b)** purified BC; **(c)** $AgNO_3$-loaded BC; **(d)** AgZ-loaded BC.

4.2.3.4. Swelling ratio

The absorption of surrounding fluids is a vital characteristic of hydrogels for potential application in the management of exudating wounds. After immersion in deionised water, padded dry BC pellicles imbibed an amount of water up to several times its original dehydrated weight, with a swelling ratio of 12.08 ± 0.96 (n=3) after 24 h.

4.2.3.5. Moisture content

BC hydrogels have been reported to have high water content and in the current study, the water content of BC, $AgNO_3$-loaded BC and AgZ-loaded BC hydrogels was determined. The results revealed that BC imbibed > 99.55 ± 0.044 % (v/w) (n = 3) water. Moreover, the results revealed that 0.55 % $AgNO_3$-loaded BC (n = 3) and 1 % AgZ-loaded BC (n = 3) imbibed 99.16 ± 0.20 % and 98.06 ± 0.16 % water respectively.

4.2.3.6. Transparency test

In this study, the transparency property of BC, $AgNO_3$-loaded-BC and AgZ-loaded-BC was evaluated by reading the text in different colours on white laminated paper sheet through the test hydrogels. The results demonstrate the neat BC rehydrated with deionised water allows reading the text without the need for removal of the dressing (**Figure 4.6a**). When the study was performed using 0.55 % $AgNO_3$-loaded BC hydrogels the text could be easily read through these hydrogels as well (**Figure 4.6b**). The clarity of letters through the hydrogels (neat BC and $AgNO_3$-loaded BC) supported high transparency through both the hydrogels (**Figure 4.6a&b**). The test results for 1 % AgZ-loaded BC revealed that transparency through these hydrogels was very limited (**Figure 4.6c**).

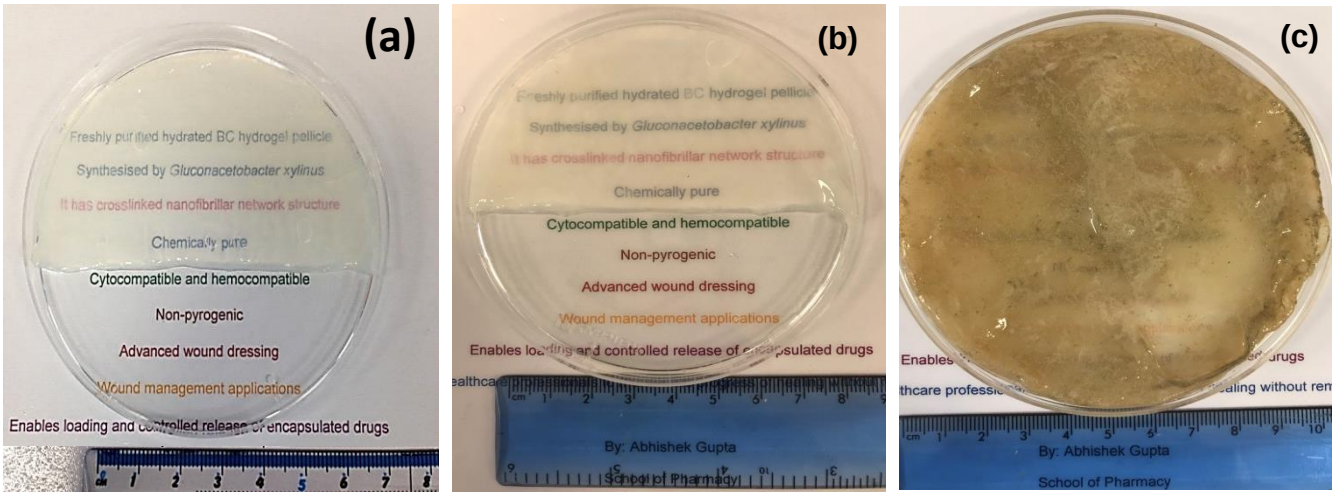

Figure 4.6: Visual appearance of text through **(a)** BC rehydrated with deionised water; **(b)** 0.55 % $AgNO_3$-loaded BC; **(c)** 1 % AgZ-loaded BC.

4.2.3.7. Silver release

Ag^+ release from BC hydrogels, as determined by ICP analysis, is presented in **Figure 4.7**. Results indicate that Ag^+ release was greater after 24 h from AgZ-loaded BC (60.65 ± 4.18 ppm) as compared to $AgNO_3$-loaded BC (36.76 ± 1.68 ppm). Silver release from $AgNO_3$-loaded BC plateaued after 72 h whereas from AgZ-loaded BC release was steady and controlled (**Figure 4.7**). Overall, AgZ-loaded BC released more silver (137.60 ± 16.17 ppm) over the 96 h compared to BC-$AgNO_3$ (64.53 ± 6.47 ppm).

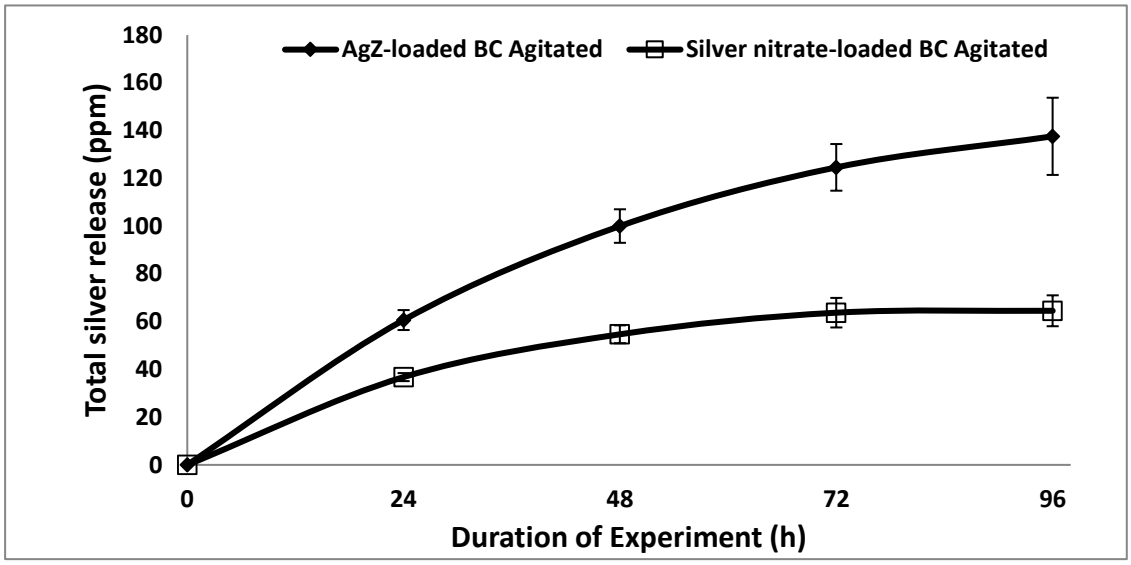

Figure 4.7. Silver release (ppm) over 96 h from $AgNO_3$-loaded BC and AgZ-loaded BC (n = 4; error bars = SD).

Mathematical modelling of silver release

When silver release was analysed with zero order, first order, Higuchi and Korsmeyer–Peppas equations, results confirm that AgZ-loaded BC and $AgNO_3$-loaded BC adhere to the Korsmeyer–Peppas model (**Table 4.1**). With a correlation coefficient of >0.97 (R^2 ≥ 0.99 for both BC-AgZ and BC-$AgNO_3$) and release exponent between 0.45 and 0.89 (AgZ-loaded BC = 0.73; BC-$AgNO_3$-loaded BC = 0.56), which indicates that Ag^+ release is non-Fickian (anomalous transport) [Costa and Lobo, 2001; Dash et al., 2010]. Interestingly, Ag^+ release from AgZ-loaded BC also follows the Higuichi model with a correlation coefficient of >0.97 (R^2 = 0.99), i.e. diffusional release [Costa and Lobo, 2001]. The additional diffusional release of Ag^+ from AgZ at the surface of the BC may be due to ion exchange with cations present in the TSB media. The correlation coefficients for zero and first order models were both <0.97 (**Table 4.1**).

Table 4.1. Mathematical modelling of Ag^{+} release kinetics from $AgNO_3$-loaded-BC and AgZ-loaded BC hydrogels.

	Correlation coefficient (R^2)			
	Zero order	**First order**	**Higuichi**	**Korsmeyer-Peppas**
AgZ-loaded BC	0.93	0.92	0.99	>0.99
$AgNO_3$-loaded BC	0.84	0.69	0.98	0.99

4.2.3.8. Antimicrobial activity by disc diffusion assay

Pure BC and Zeolite-loaded BC exhibited no antimicrobial activity. There was a difference in antimicrobial activity for AgZ-loaded BC via static and agitation methods (**Figure 4.8a&b**). The antimicrobial activity of AgZ-BC loaded under constant agitation was significantly better against *P. aeruginosa* (AgZ-loaded BC (static): 8.29 mm (at 96 h) ≤ ZOI ≤ 14.15 mm (at 48 h); AgZ-loaded BC (agitated): 16.10 mm (at 24 h) ≤ ZOI ≤ 17.96 mm (at 48 h); $p < 0.05$). However, this was not observed in the case of *S. aureus* when comparing the antimicrobial activity of AgZ-loaded BC under static or agitated condition (AgZ-loaded BC (static): 7.94 mm (at 96 h) ≤ ZOI ≤ 10.31 mm (24 h); AgZ-loaded BC (agitated): 7.71 mm (96 h) ≤ ZOI ≤ 10.06 mm (24 h); $p > 0.05$).

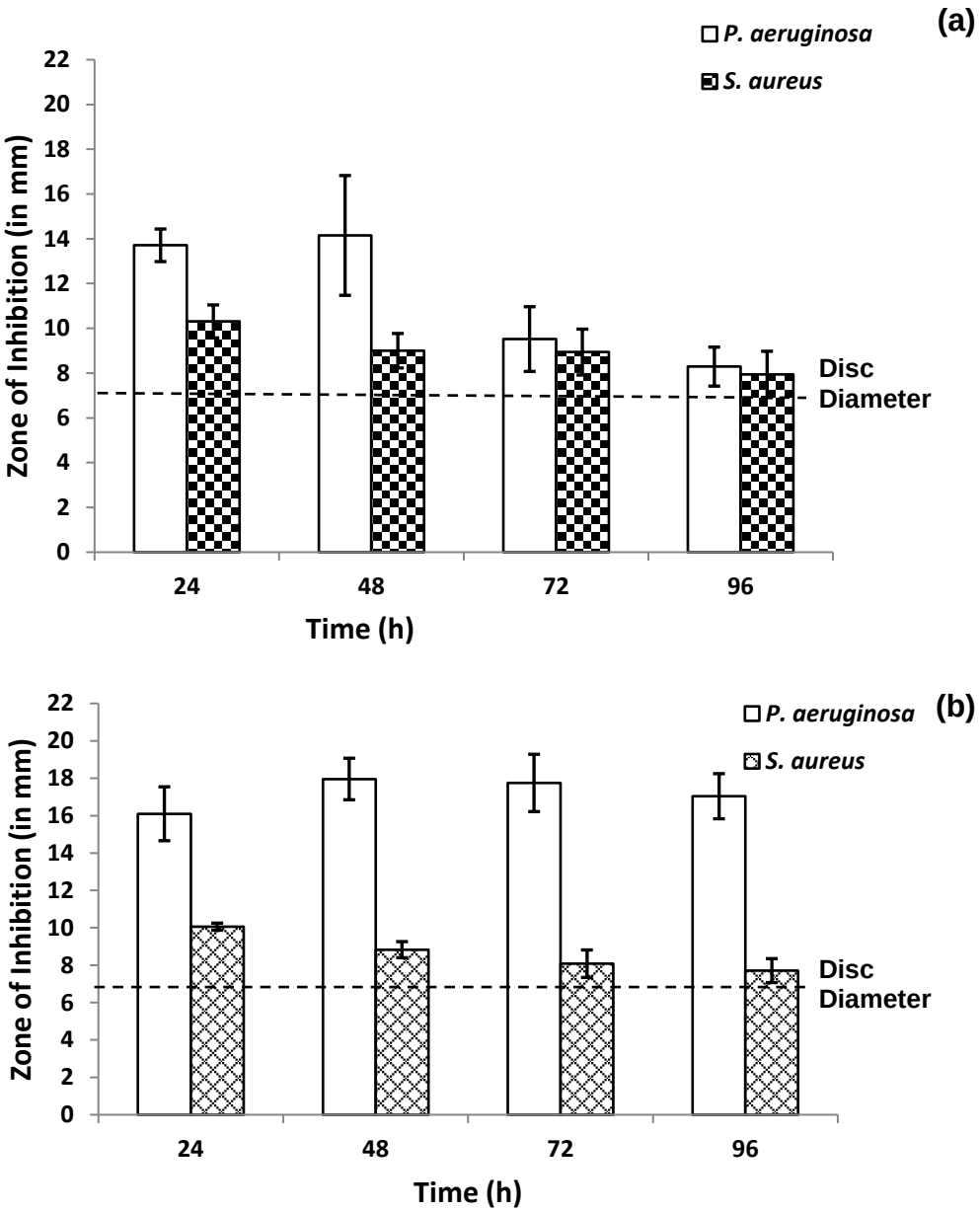

Figure 4.8. Antimicrobial activity assessed by ZOI during the disc diffusion assay for AgZ-loaded BC under **(a)** static and **(b)** constant agitated conditions against *P. aeruginosa* and *S. aureus* (n = 6; error bars = SD).

The disc diffusion assay for antimicrobial activity indicated that both AgZ-loaded BC and $AgNO_3$-loaded BC exhibited higher antimicrobial activity against *P. aeruginosa* compared to *S. aureus* (**Figure 4.9a&b**). Statistical analysis using ANOVA suggests that there is a significant difference between the ZOI of *P. aeruginosa* and *S. aureus* ($p < 0.05$) when treated with AgZ-loaded BC. This is also the case for both strains ($p < 0.05$) when treated with $AgNO_3$-loaded BC.

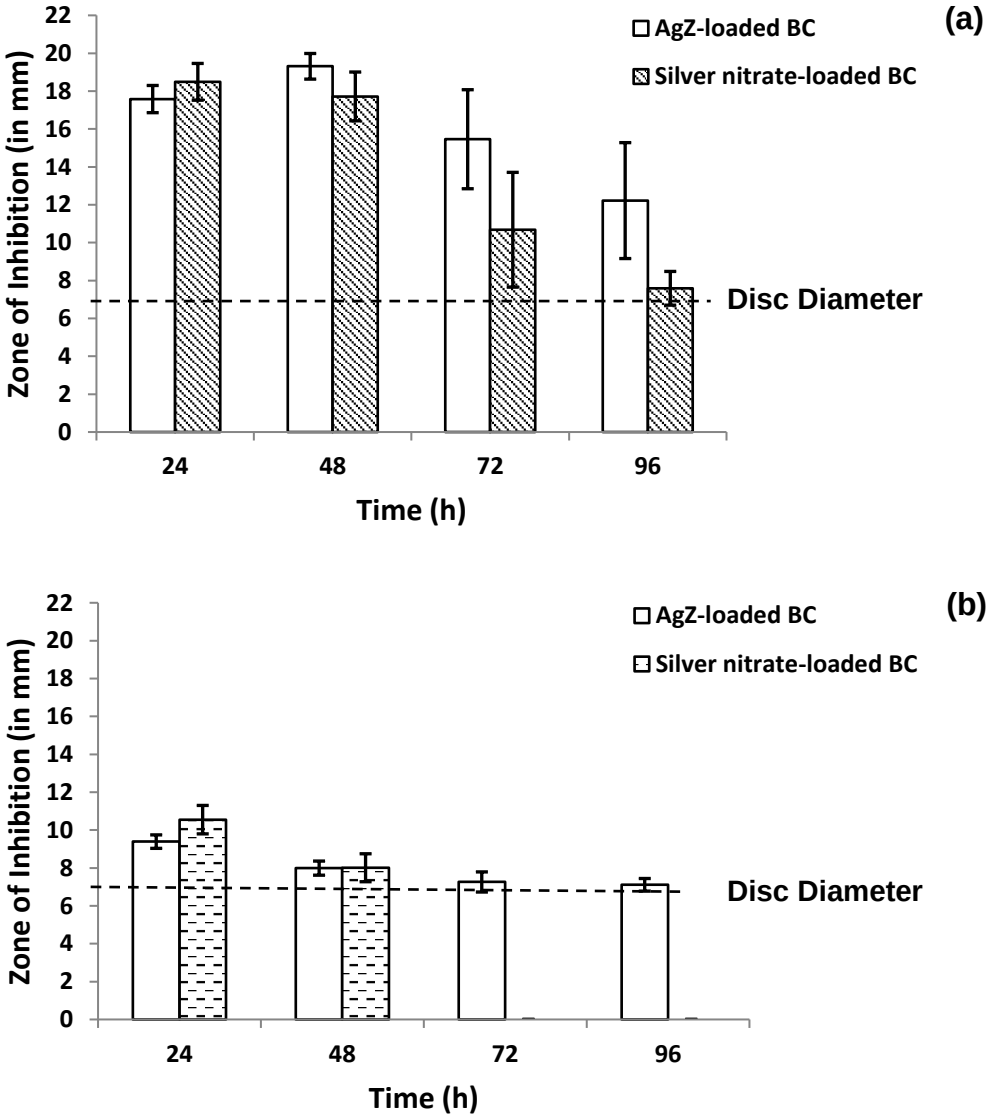

Figure 4.9. Antimicrobial activity assessed by ZOI during the disc diffusion assay for AgZ-loaded BC and $AgNO_3$-loaded BC against **(a)** *P. aeruginosa* and **(b)** *S. aureus* constant agitated conditions against and (n = 9; error bars = SD).

The disc diffusion assay results indicated that $AgNO_3$-loaded BC had higher antimicrobial activity against *P. aeruginosa* up to 24 h when compared to AgZ-loaded BC, but the difference in the activity was not significantly different ($p > 0.05$). After 24 h, the antimicrobial activity of $AgNO_3$-loaded BC reduced and AgZ-loaded BC exhibited higher activity against *P. aeruginosa* (**Figure 4.9a & 4.10**). Antimicrobial activity against *S. aureus* also had the same trend at 24 h with $AgNO_3$-loaded BC exhibiting larger ZOI compared to AgZ-loaded BC. At 48 h, there was no significant difference between $AgNO_3$-loaded BC and AgZ-loaded against *S. aureus*; following incubation at 72 and 96 h, $AgNO_3$-loaded BC had highly reduced antimicrobial activity against *S. aureus* (ZOI = 0 mm), whereas AgZ-loaded BC still exhibited some antimicrobial activity at 72 h (ZOI = 7.26 ± 0.53 mm), which was further reduced at 96 h (ZOI = 7.11 ± 0.33 mm) (**Figure 4.9b & 4.10**). The difference in activity of AgZ-loaded BC and $AgNO_3$-loaded BC against *P. aeruginosa* (Gram negative) and *S. aureus* (Gram positive) bacteria may be due to their structural differences (see chapter “Discussion” for details).

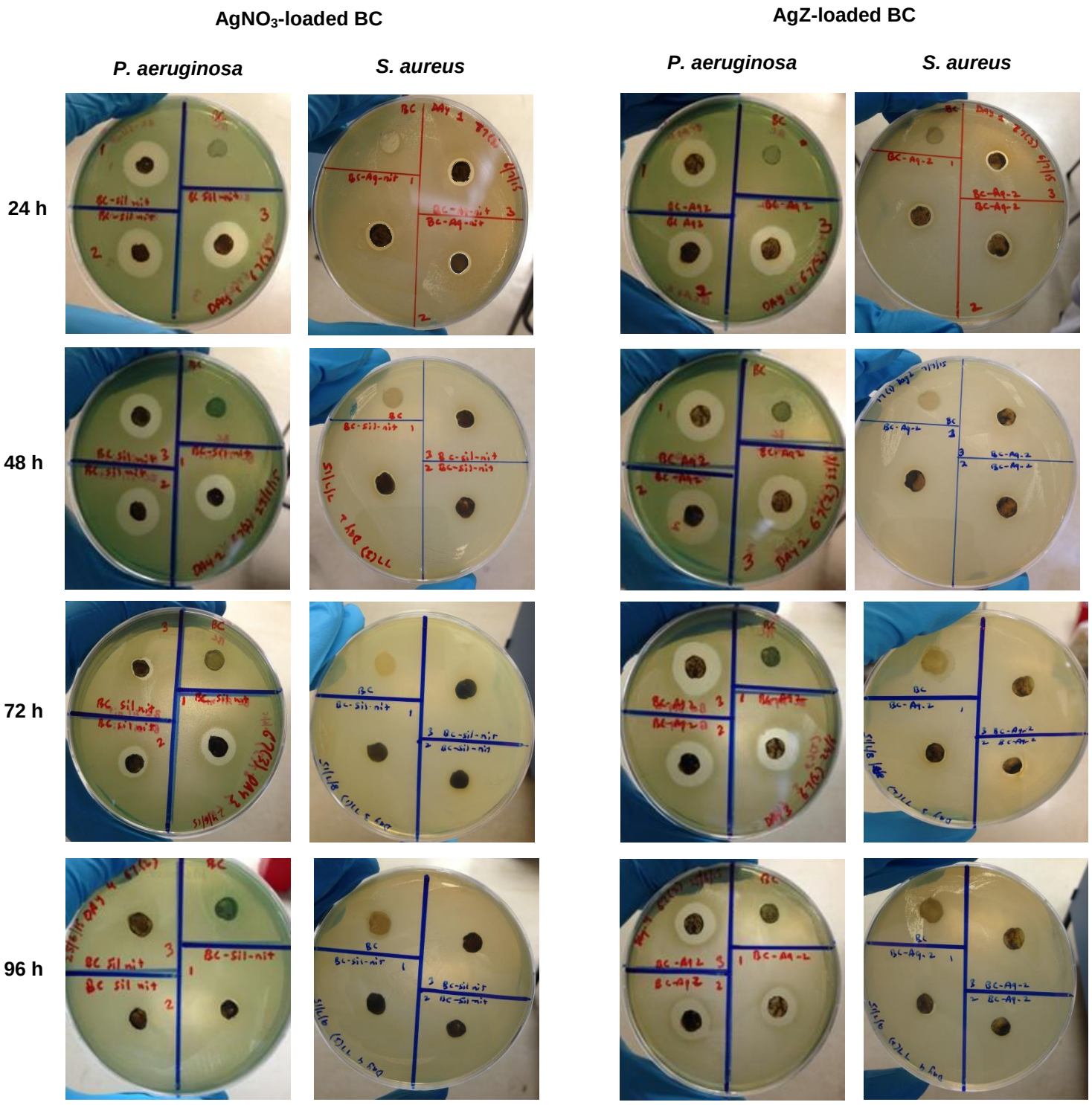

Figure 4.10. Disc diffusion assay showing antimicrobial activity as ZOI of $AgNO_3$-loaded BC and AgZ-loaded BC over 96 h against *P. aeruginosa* and *S. aureus*.

4.2.3.9. Haemocompatibility

When materials come in contact with blood, they may cause haemolysis of the blood cells; thus, assessment of haemolytic properties becomes vital for materials with potential biomedical applications. According to the ASTM F756 standards, haemolytic indices, the test samples can be: (a) haemolytic materials with haemolysis >5 % (b) slightly haemolytic with haemolysis between 2-5 % and (c) non-haemolytic materials having haemolysis below 2 % [Kamoun *et al*., 2015; Mohamad *et al*., 2016]. The *in vitro* blood compatibility results revealed that BC hydrogels are haemocompatible with % haemolysis < 0.1 % (n=9), which is well below the acceptable limit for haemolysis. $AgNO_3$-loaded BC and AgZ-loaded BC demonstrated high % haemolysis (n = 9); hence, based on the ASTM standards, these hydrogels would be classed as haemolytic.

4.2.3.10. Cytocompatibility

A preliminary cytocompatibility of BC was undertaken using the DMEM medium conditioned with BC. HEK 293 cells were incubated in the conditioned medium to determine the cell viability. The cytotoxicity of BC against HEK 293 epithelial cell line, as determined by the MTT assay confirmed that biosynthetic BC is cytocompatible with cell viability > 98.5 % (n = 9).

After testing the cytocompatibility of purified BC using the conditioned medium, the study was extended to evaluate the cytotoxicity of 1 % aqueous AgZ and 0.55 % aqueous $AgNO_3$ in free state and loaded in BC (8.0 mm discs) against Panc1, U251 and MSTO mammalian cell lines. It emerged that 0.55 % $AgNO_3$-loaded BC has variable cytotoxic effect on the tested cell lines (**Figure 4.11a&b**). Furthermore, the cytocompatibility of free $AgNO_3$ versus $AgNO_3$-loaded BC demonstrated that free

$AgNO_3$ had higher cytotoxic effect, resulting in lower cell viability compared to $AgNO_3$-loaded in BC on U251 (p = 0.0286) and MSTO (p = 0.0152) (**Fig. 4.11a&b**). No significant difference was seen with Panc1 cell line (p = 0.1801) (**Figure 4.11a**).

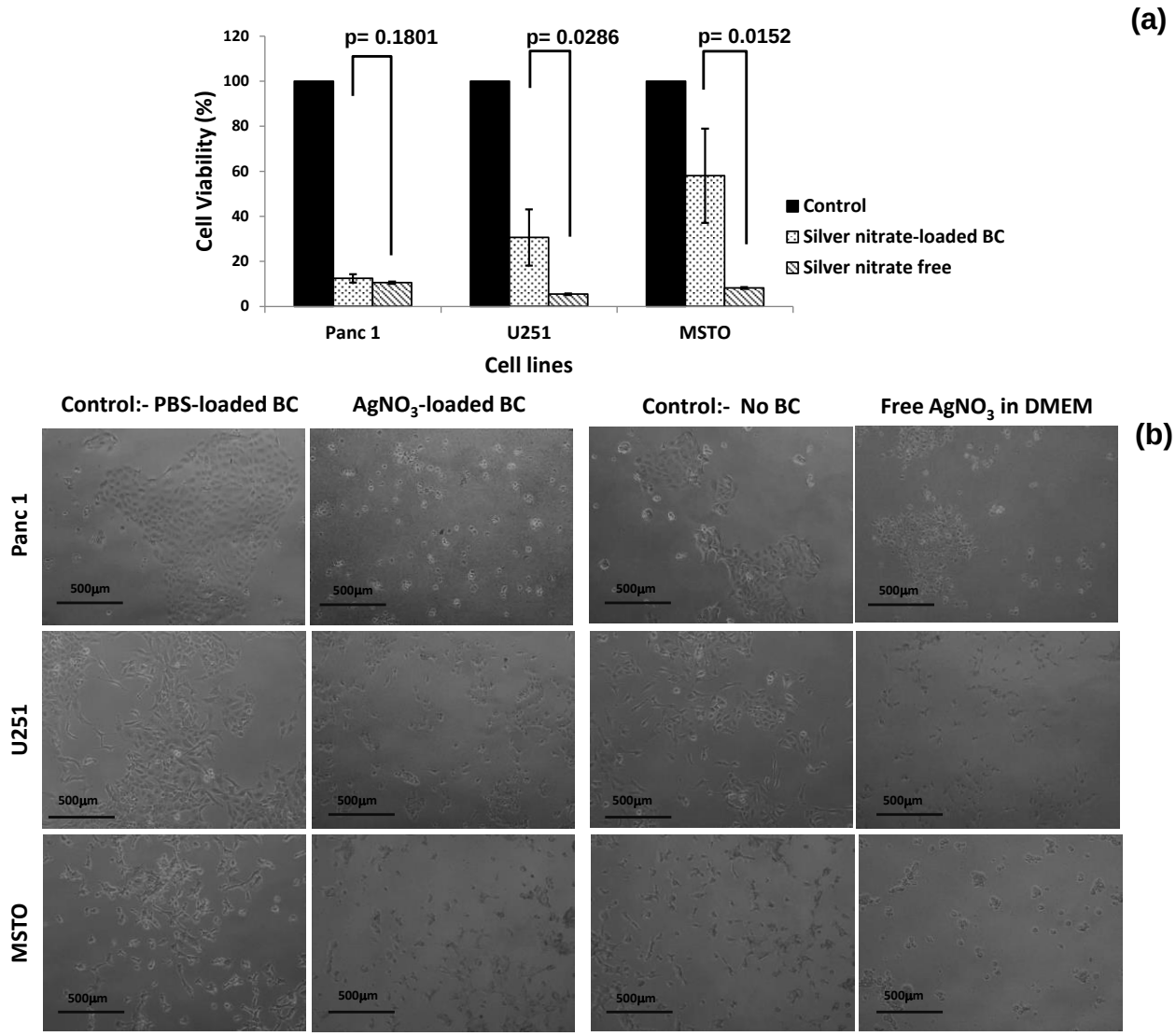

Figure. 4.11. Cytocompatibility test results. **(a)** Bar graph showing the cell viability (%) after 24 h exposure to $AgNO_3$-loaded BC and free $AgNO_3$ (equivalent amount) (n = 3); **(b)** Representative photomicrographs of cells captured at 10x magnification after exposure for 24 h to $AgNO_3$-loaded BC and free $AgNO_3$.

The results of cytocompatibility study for AgZ-loaded BC also revealed variable cytotoxic effect on the tested cell lines. Panc1 demonstrated lower cell viability as compared to U251 and MSTO (**Figure 4.12a&b**). Free AgZ (equivalent amount) demonstrated higher cytotoxicity on all the tested cell lines resulting in lower cell viability.

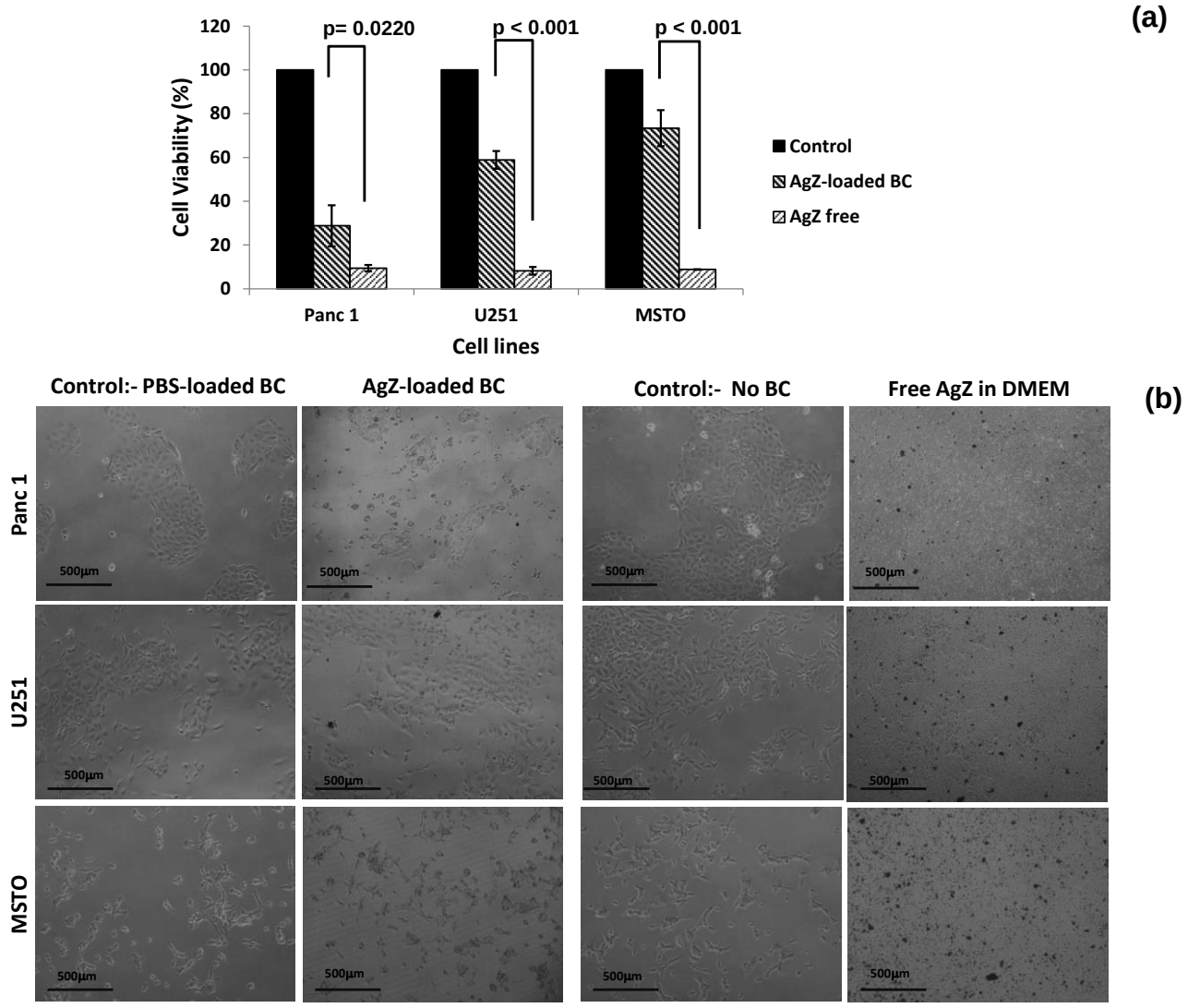

Figure. 4.12. Cytocompatibility test results. **(a)** Bar graph showing the cell viability (%) after 24 h exposure to AgZ-loaded BC and free AgZ (equivalent amount) (n = 3); **(b)** Representative photomicrographs of cells captured at 10x magnification after exposure for 24 h to AgZ-loaded BC and free AgZ.

When comparing the cytocompatibility of $AgNO_3$ and AgZ (free and loaded in BC), AgZ demonstrated higher cell viability for the tested cell lines (except Panc1,free drug) as compared to $AgNO_3$ (**Table 4.2**), (**Figure 4.11a&b** & **Figure 4.12a&b**).

Table 4.2. MTT assay test results summary for $AgNO_3$ and AgZ (free and loaded in BC) against three mammalian cell lines.

	Cell Viability (%)		
	Panc1	**U251**	**MSTO**
$AgNO_3$-loaded BC	12.40 ± 1.86	30.578 ± 12.47	58.01 ± 20.93
$AgNO_3$ (free, equivalent amount)	10.53 ± 0.51	5.41 ± 0.37	8.14 ± 0.41
AgZ-loaded BC	28.80 ± 9.38	58.87 ± 4.10	73.36 ± 8.25
AgZ (free, equivalent amount)	9.38 ± 1.46	8.17 ± 1.76	8.82 ± 0.14

4.2.3.11. Antioxidant activity

With the aim of wound dressing application for chronic wounds, the antioxidant potential of $AgNO_3$-loaded BC and AgZ-loaded BC (n = 3) was evaluated using DPPH assay. The results revealed that $AgNO_3$ and AgZ (n = 6) does not have free radical scavenging properties. These results suggest that BC hydrogels loaded with $AgNO_3$ or AgZ would not have intrinsic ability of reducing the oxidative stress at the wound site as they do not have significant potential of scavenging the free radical.

Part II

Introduction

This section of the thesis is focused on the solubility enhancement of curcumin by encapsulation in cyclodextrins. Moreover, the production and characterisation of CUR:HPβCD-loaded bacterial cellulose hydrogels for the potential wound management applications has been presented. The findings were published in Gupta *et al*., 2019.

4.3. Preparation of CUR:βCD inclusion complex

CUR:βCD (yellow powder) was produced from CUR (dark yellow powder) and native βCD (white powder) by solvent evaporation, freeze drying and co-precipitation methods. The CUR contents by all these methods varied (**Table 4.3**). As the CUR content in the samples was either low (solvent evaporation and freeze drying method) or free CUR was present in the final sample (co-precipitation method), the study was extended by replacing βCD with HPβCD to produce CUR:HPβCD inclusion complex (see section 4.4).

Table 4.3. Summary table of curcumin content and encapsulation efficacy (%) of curcumin in native βCD by different methods (n = 3).

Inclusion complexation method	CUR:βCD mole ratio	% Encapsulation
Solvent evaporation	1:1	3.39 ± 0.44
Freeze drying	1:1	2.19 ± 0.45
Co-precipitation	1:1	88.79 ± 4.51

4.4. CUR:HPβCD-loaded BC hydrogels

4.4.1. Preparation of CUR:HPβCD inclusion complex

Due to low encapsulation of CUR in βCD, hydroxypropyl derivative of native βCD with enhanced aqueous solubility was tested for encapsulation. Moreover, based on the findings of CUR:βCD experiments, solvent evaporation method was adopted as a standard procedure for encapsulation. CUR:HPβCD was produced from the CUR and HPβCD (white powder) by solvent extraction method. The novel approach taken in this study to produce IC 10, IC 25, IC 50, IC 75 and IC 90, supramolecular inclusion complexes revealed that varied solvent volume ratios have an influence on CUR content encapsulated in HPβCD. The EE (%) results of IC 10, IC 25, IC 50, IC 75 and IC 90 (n=3) revealed varied encapsulation efficacy (**Table 4.4**). These results suggested that IC 75 produced by CUR dissolved in 37.5 mL acetone and HPβCD dissolved in 12.5 mL water for the inclusion complex production gave the highest % EE, hence it was selected as a standard procedure for the preparation of inclusion complex for further experimental investigations. It is important to note that all the characterisations for CUR:HPβCD were done using IC 75. CUR content determined in IC 75 samples was in the range of 3.28±0.38 % (n=4).

Table 4.4. Summary table of encapsulation efficacy (%) of CUR:HPβCD by varying the volume ratio of solvents (n = 3).

Inclusion complex	Encapsulation efficacy (%)
IC 10	3.64 ± 0.16 %
IC 25	3.84 ± 0.37 %
IC 50	7.37 ± 1.24 %
IC 75	18.26 ± 1.02 %
IC 90	16.34 ± 0.75 %

4.4.2. Production of CUR:HPβCD-loaded-BC hydrogels

IC 75 was loaded in padded dry BC to produce hydrogels for wound management applications. Visual inspection of purified BC hydrogel pellicles loaded with 2 % (w/v) CUR:HPβCD revealed highly consistent loading (Figure 4.13b). After loading of the inclusion complex, the colour of BC hydrogels changed from clear to orange yellow (Figure 4.13a-b).

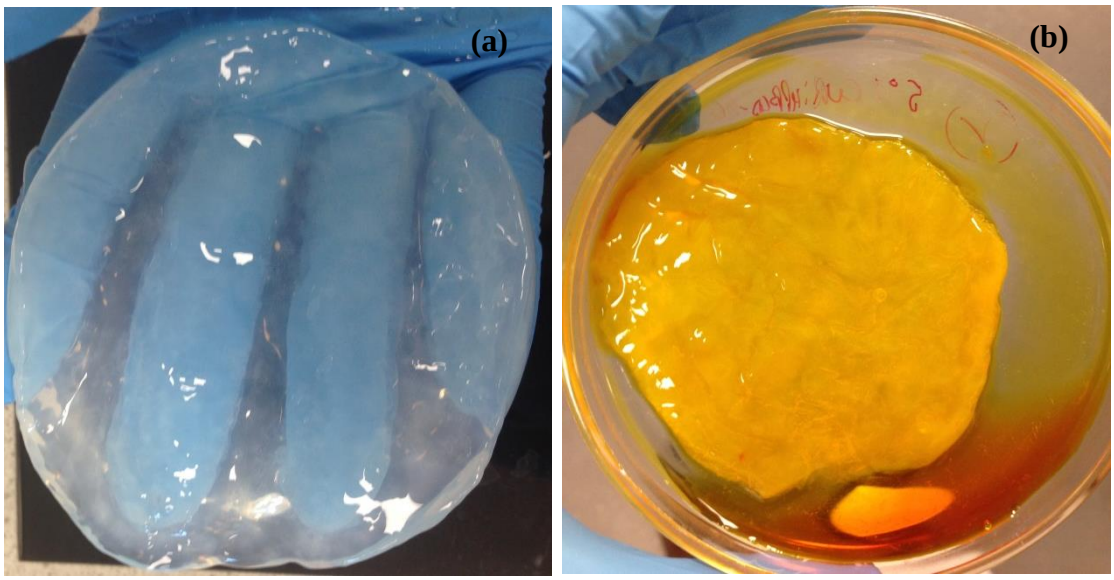

Figure 4.13. Visual appearance of **(a)** BC hydrogel pellicle after purification; **(b)** CUR:HPβCD-loaded-BC hydrogel pellicle.

4.4.3. Characterisation studies

4.4.3.1. Solubility in water: CUR versus CUR:HPβCD inclusion complex

CUR exhibits the maximum absorbance at ≈430 nm [Manolova *et al*., 2014; Zhao *et al*., 2018]. In the current study, the inclusion of CUR in HPβCD enhanced its aqueous solubility, which was evident in the spectral scan (**Figure. 4.14**). The UV-Visible spectrum of aqueous filtrate of CUR didn't exhibit significant absorption in the specified spectral range. Moreover, the aqueous solution of HPβCD didn't show significant absorbance in the selected range. In case of the CUR:HPβCD, there was

strong absorbance recorded around 430 nm due to enhanced aqueous solubility of CUR.

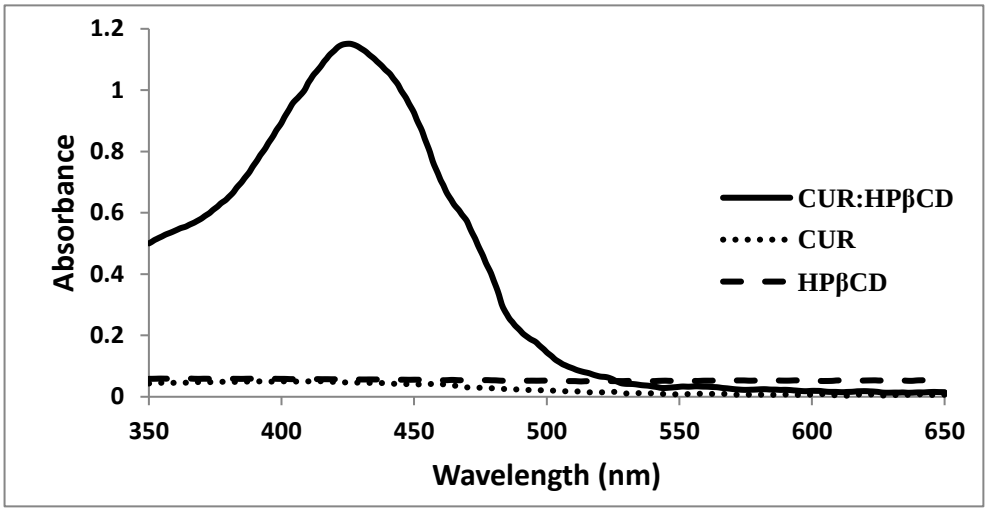

Figure 4.14: UV-Visible absorption spectra of CUR, HPβCD and CUR:HPβCD dissolved in water after 1 h stirring at room temperature followed by filtration through 0.45 µm filter.

4.4.3.2. Scanning electron microscopy (SEM)

BC appears as a dense interwoven fibre network (**Figure 4.3b**). SEM results revealed that the shape of CUR and HPβCD changed from round to irregular shape to plate like structures in CUR:HPβCD (**Figure 4.15a-c**). When padded dry BC was rehydrated by immersion in aqueous solution of CUR:HPβCD, the voids allowed penetration of the inclusion complex, which then got physically entrapped in the BC fibre network (**Figure 4.15d**). This resulted in the production of CUR:HPβCD-loaded BC hydrogels.

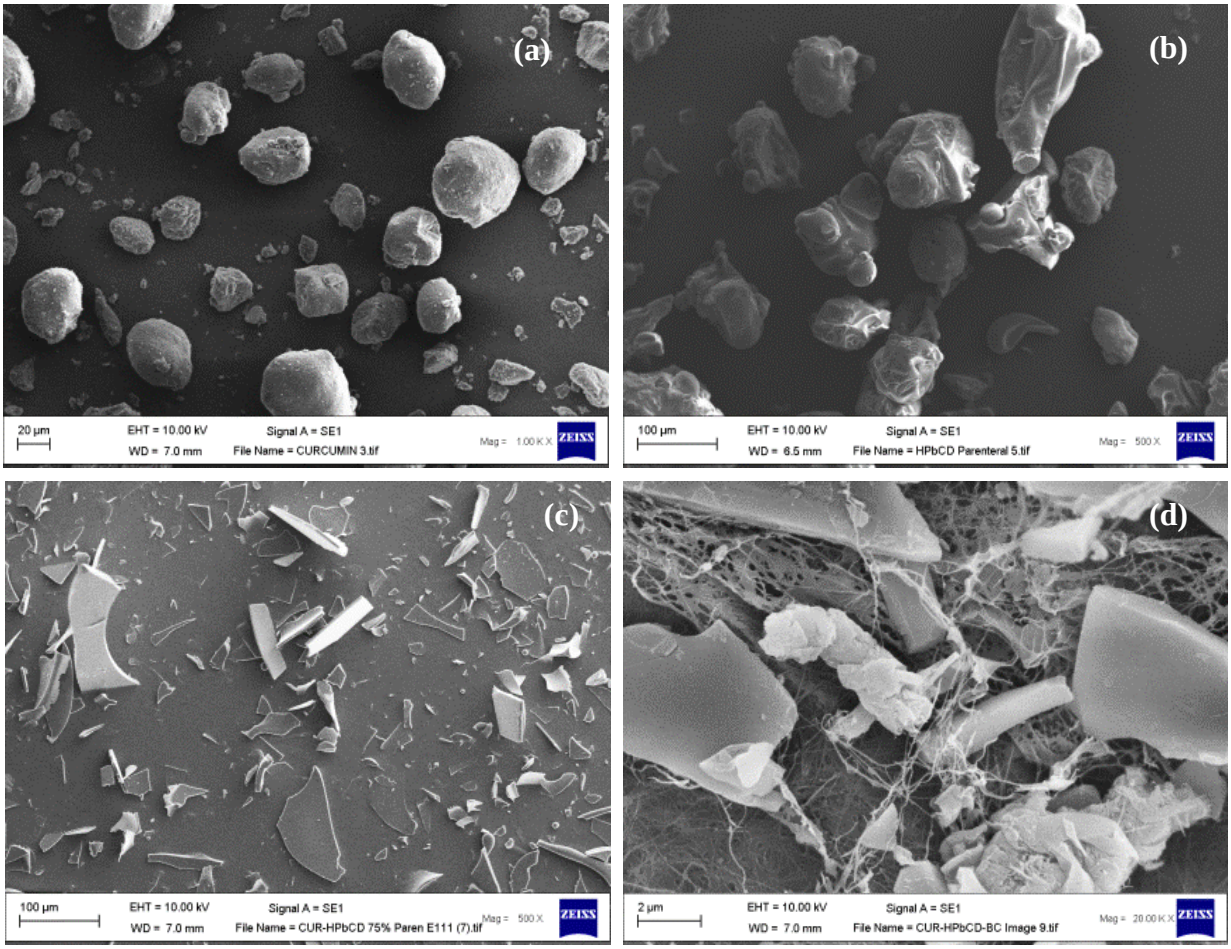

Figure 4.15: SEM images of **(a)** CUR; **(b)** HPβCD; **(c)** CUR:HPβCD; **(d)** CUR:HPβCD-loaded in BC.

4.4.3.3. Fourier Transform Infrared (FTIR)

FTIR spectral results of CUR, HPβCD, CUR:HPβCD, purified BC and CUR:HPβCD-loaded-BC are illustrated in **Figure 4.16**. The characteristic sharp peak at 3504 cm^{-1}; 1619 cm^{-1}; 1591 cm^{-1} and 1497 cm^{-1} were observed in CUR spectrum (**Figure 4.16a**). For HPβCD the characteristic broad peak at 3340 cm^{-1}; 2927 cm^{-1}; 1156 cm^{-1}; 1084 cm^{-1}; 1024 cm^{-1} were recorded (**Figure 4.16b**). In CUR:HPβCD, the prominent peaks at 3504 cm^{-1} and 1619 cm^{-1} appeared to be masked (**Figure 4.16c**).

BC has characteristic peaks at around 3341 cm^{-1}, 2899 cm^{-1}, 1640 cm^{-1}, 1370 cm^{-1}, 1159 cm^{-1}, 1057 cm^{-1} (**Figure 4.16d & 4.5b**). These peaks appeared in

CUR:HPβCD-loaded BC spectrum (**Figure 4.16e**). Furthermore, the characteristic peaks of the inclusion complex were also observed in the spectrum (**Figure 4.16e**).

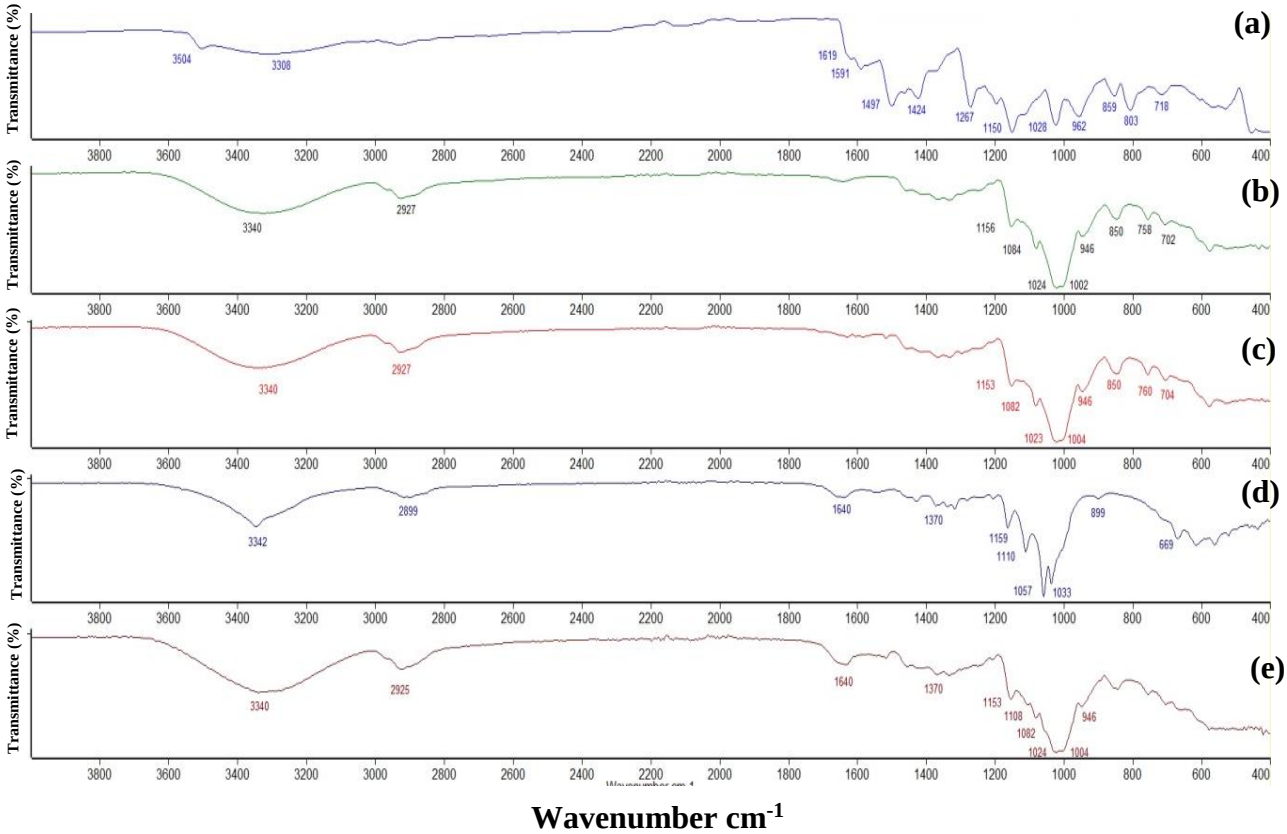

Figure 4.16: FTIR spectra from 400-4000cm^{-1} for **(a)** CUR; **(b)** HPβCD; **(c)** CUR:HPβCD; **(d)** bacterial cellulose; **(e)** CUR:HPβCD-loaded-BC.

4.4.3.4. X-ray Diffractometric analysis (XRD)

The XRD spectra of CUR, HPβCD and lyophilised CUR:HPβCD are shown in **Figure 4.17**. Results revealed that CUR exists in a crystalline form, which is indicated by the characteristic peaks (**Figure 4.17a**), whereas HPβCD is amorphous (**Figure 4.17b**) in nature. After complexation with HPβCD, there was no noticeable evidence of crystallinity of CUR in the inclusion complex (**Figure 4.17c**).

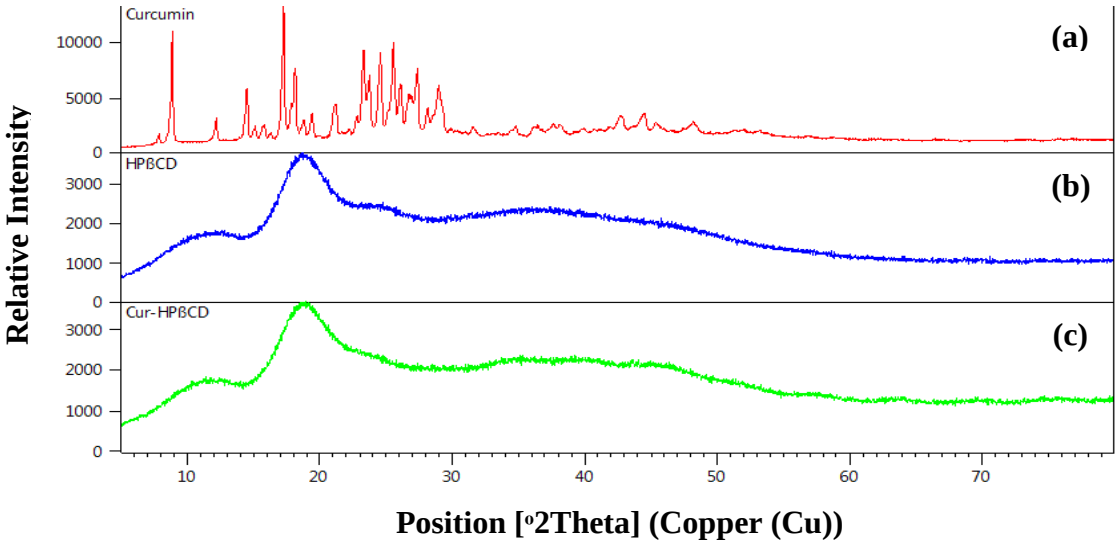

Figure 4.17: XRD results of **(a)** CUR; **(b)** HPβCD; **(c)** CUR:HPβCD.

4.4.3.5. Nuclear Magnetic Resonance spectroscopy (NMR)

NMR spectroscopy was used to investigate the success of the formation of the inclusion complex between hydroxypropyl-β-cyclodextrin and curcumin (sample IC 75). The ^{1}H and ^{13}C NMR data of the CUR:HPβCD was assigned using a combination of previously reported proton NMR data [Hsu *et al*., 2013] and 2D NMR techniques (COSY, HSQC and HMBC) (see Figure S1-S4 in the supporting information).

Evidence for the formation of the CUR:HPβCD inclusion complex can be chiefly observed through both ^{1}H and ROESY NMR. Comparison between the ^{1}H NMR spectra of HPβCD and CUR:HPβCD shows a distinctive shift in the proton resonances of the internally facing protons, H^{3} and H^{5} of HPβCD, upon inclusion of CUR, indicating a change in the local magnetic environment; the resonances of the externally facing protons remained unchanged (**Figure 4.18a&b**; see **Scheme S5a-c** for structural assignments in the supporting information).

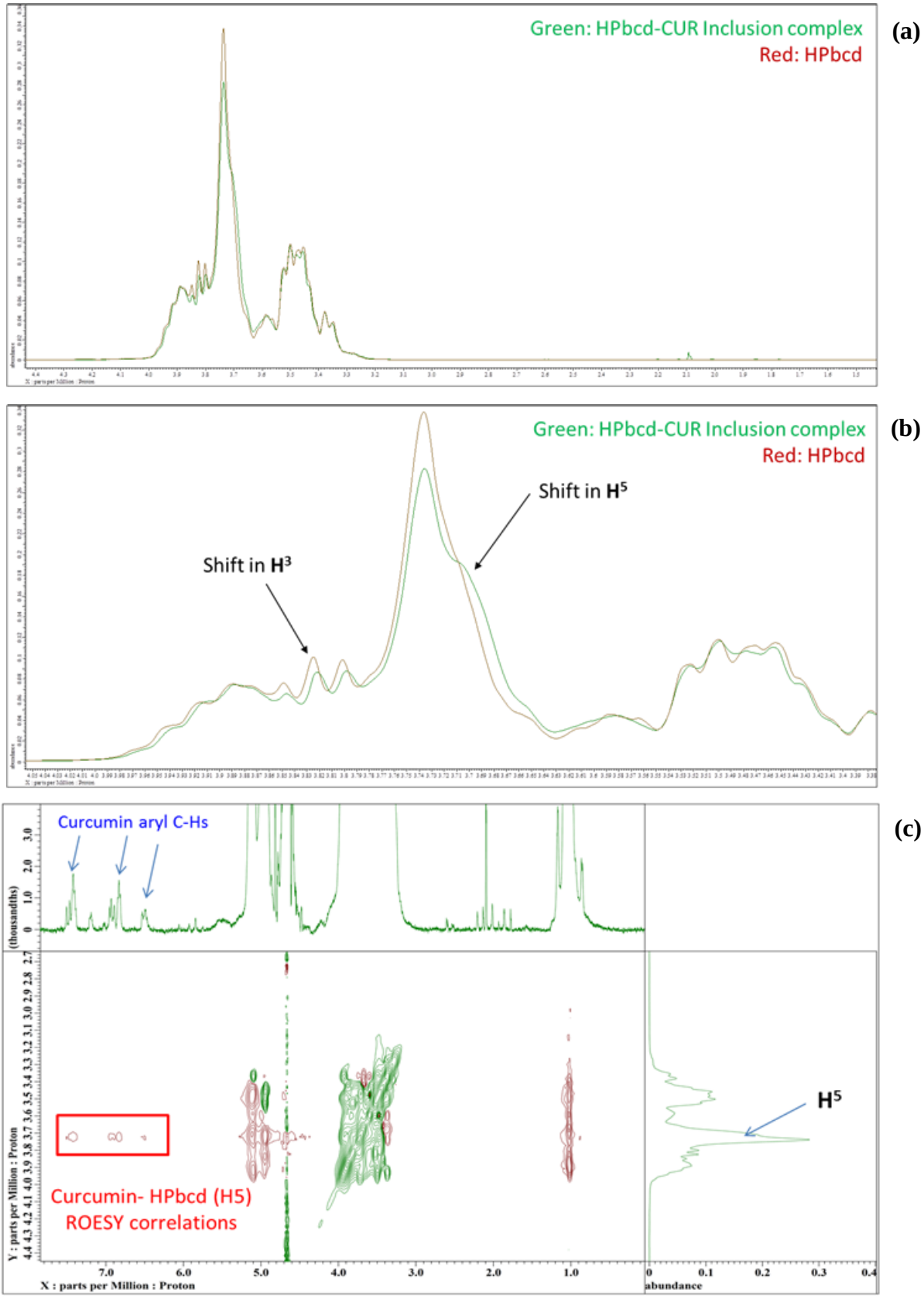

Figure 4.18: (a), **(b)** Overlay and expansion overlay of ^{1}H spectra of HPβCD and the CUR:HPβCD inclusion complex in D_2O respectively; **(c)** Expansion of the ROESY spectrum of the CUR:HPβCD inclusion complex in D_2O indicating correlation cross peaks between HPβCD and CUR.

Further conclusive evidence for the formation of CUR:HPβCD was subsequently obtained by ROESY NMR analysis; a ROESY correlation between H^5 of HPβCD and CUR aryl protons spectrum clearly indicates a through space interaction indicative of an inclusion complex (**Figure 4.18c**).

4.4.3.6. Thermal Analysis (TGA and DSC)

The TGA curve of freeze dried BC (**Figure 4.19**) showed a distinct percentage weight loss between 100-200°C and ≈350°C. The initial weight reduction of 5-8% may be due to the BC losing surface water, whilst the second weight loss (over 60%) was associated with the thermal degradation of BC.

The thermal analytical techniques like TGA and DSC are widely used in pre-formulation studies. Thermal behaviour of CUR, HPβCD, CUR:HPβCD was investigated and compared to CUR and HPβCD physical mixture, to understand the solid-state characterisation and thermal stability of the inclusion complex during production and storage. Thermogravimetric data revealed that thermal degradation of CUR starts at around 220 °C, which is ≈ 40 °C above its melting point. It loses around 54 % mass between 300-420 °C. HPβCD mass loss of nearly 6 % at around 91 °C, attributed to the loss of water and major mass loss (>70 %) peaks at 344 °C due to the decomposition of the molecule (**Figure 4.20a-b**). These weight losses were visible in both the physical mixture and CUR:HPβCD inclusion complex. On further examination, it was noticed that the inclusion complex displayed higher thermal stability (**Figure 4.20a&b**). The thermokinetic data did not show decomposition at normal working temperatures. The data from the current study revealed that the inclusion complex is also thermally stable at such temperatures.

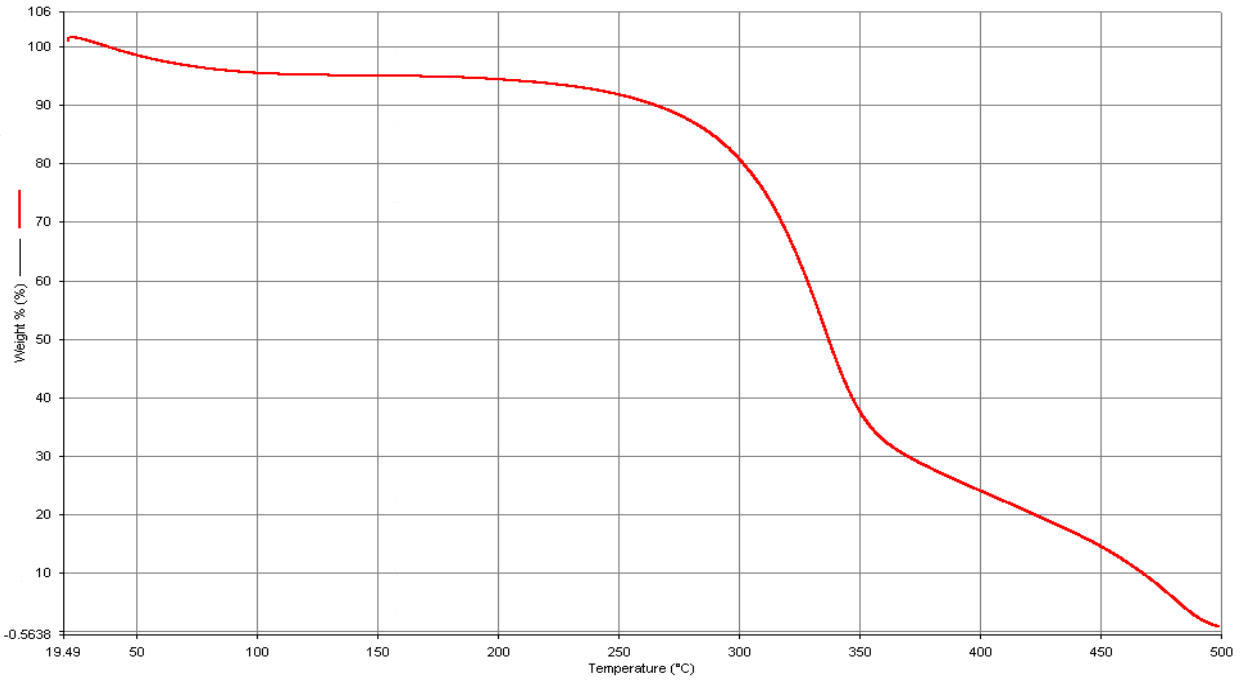

Figure 4.19: TGA curve of freeze dried BC.

DSC analysis was performed to further corroborate the results obtained from TGA. DSC results of CUR revealed an enthalpy change with a sharp endotherm in the region of 179 °C (**Figure 4.20c**). In the case of HPβCD, there was observed two endotherms around 259 °C and 291 °C, followed by its decomposition (Fig. 6c). In the case of physical mixture, the characteristic endotherms of CUR appeared at 179 °C. Moreover, endotherm peaks attributed to HPβCD were also visible. However, shift in peak positions was observed (**Figure 4.20c**). The thermogram of CUR:HPβCD revealed that the melting endotherm peak for CUR in the inclusion complex disappeared. Moreover, the shift in endotherm peaks in CUR:HPβCD inclusion complex was observed (**Figure 4.20c**).

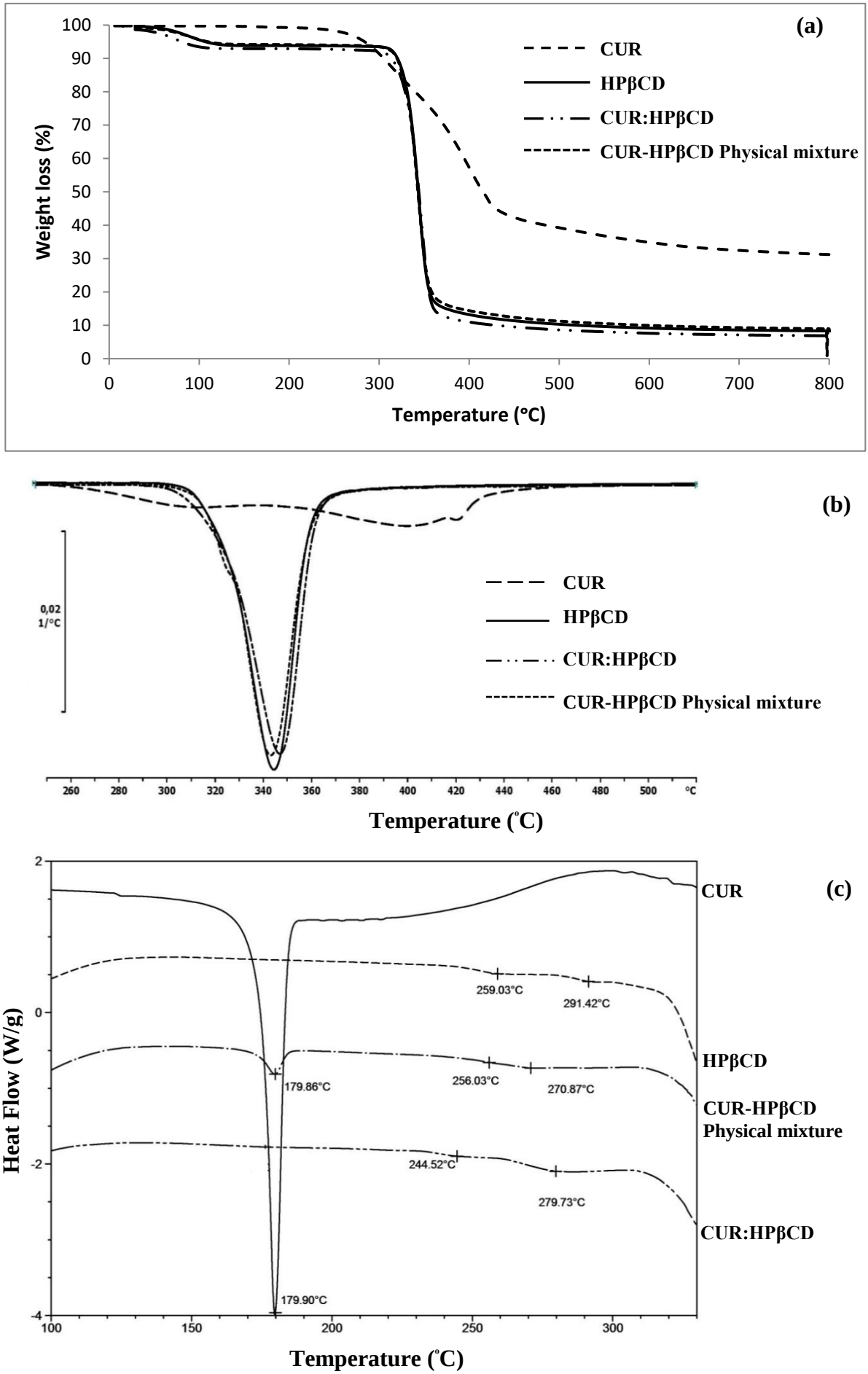

Figure 4.20: (a) TGA curves; **(b)** DTG curves; **(c)** DSC spectra of CUR, HPβCD, CUR, HPβCD Physical mixture and CUR:HPβCD.

4.4.3.7. Moisture content (M_c)

BC hydrogels have high water content, which was determined in Part I. Moisture content of BC was determined again in this part of experiment and the results of the moisture content determination study revealed neat BC hydrogels imbibed > 99.5 % (n=4) water. Moreover, the results revealed that BC loaded with 2 % (w/v) CUR:HPβCD imbibed 97.63±0.057 % (n=4) water.

4.4.3.8. Optical Transmission and Transparency test

The appearance of the wound site is vital to assess patients' response to the treatment. In the current study, neat BC hydrogels demonstrated the % Transmission of 85.72 ± 1.57 % (n=3). Although, the light transmittance of CUR:HPβCD-loaded BC hydrogel dressings was reduced, this is sufficiently high (66.13 ± 2.36 %) (n=3).

On further evaluation, the clarity of letters through the hydrogels supported high transparency through both the neat and CUR:HPβCD-loaded-BC hydrogels (**Figure 4.21**). These results support the capability of CUR:HPβCD-loaded BC hydrogel dressings for non-invasive clinical wound monitoring.

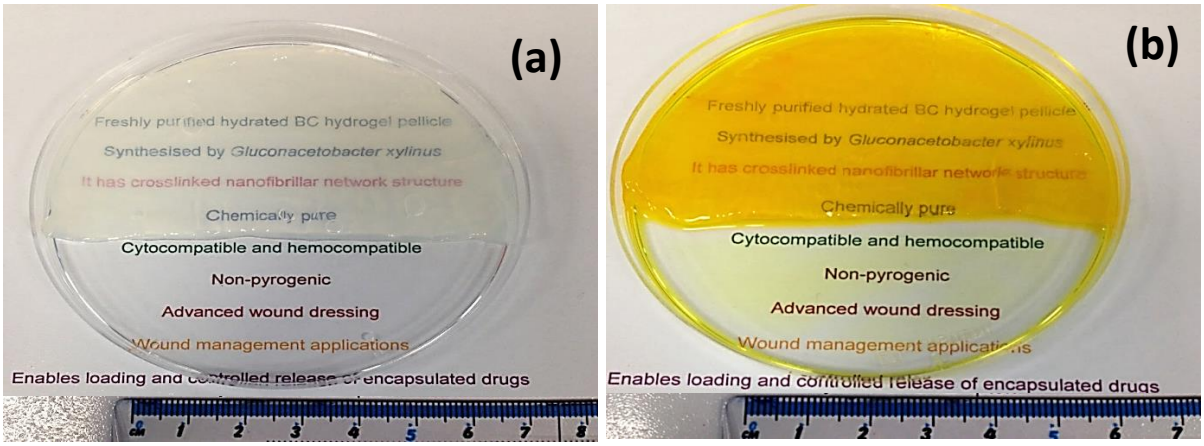

Figure 4.21: Visual appearance of text through **(a)** neat BC sheet; **(b)** 2% CUR:HPβCD-loaded BC.

4.4.3.9. Water Vapour Transmission Rate (WVTR)

In the current study, WVTR was evaluated as the gradient of weight loss from the samples versus time. The thickness of rehydrated hydrogels (neat and test) was in the range of 1.5-2.5 mm. WVTR values for neat BC were in the range of 2526.32-3137.68 g/m^2/24 h (n=3) and for 2 % CUR:HPβCD-loaded BC were 2258.53-2460.63 g/m^2/24 h (n=3).

4.4.3.10. Biocompatibility studies (Haemocompatibility and Cytocompatibility)

The *in vitro* blood compatibility results revealed that the test hydrogels are haemocompatible with % haemolysis <0.20 % (n=9), which is well below the acceptable limit for haemolysis. These results confirmed that CUR:HPβCD-loaded BC hydrogels are non-haemolytic material and suitable for wound management applications.

In the current study, the cytotoxicity as determined by MTT assay demonstrated that the CUR:HPβCD-loaded BC hydrogels have varied compatibility with the tested cell lines (**Figure 4.22a**). Despite the varied response, all cell lines demonstrated cell viability when exposed to CUR:HPβCD or CUR:HPβCD-loaded-BC hydrogels (**Figure 4.22a-c**). Furthermore, the cytocompatibility of CUR:HPβCD-loaded-BC hydrogels with that of free CUR:HPβCD (equivalent amount) was compared. The results showed that there was no significant difference ($p>0.05$) between the free CUR:HPβCD or the 2 % CUR:HPβCD-loaded-BC hydrogels.

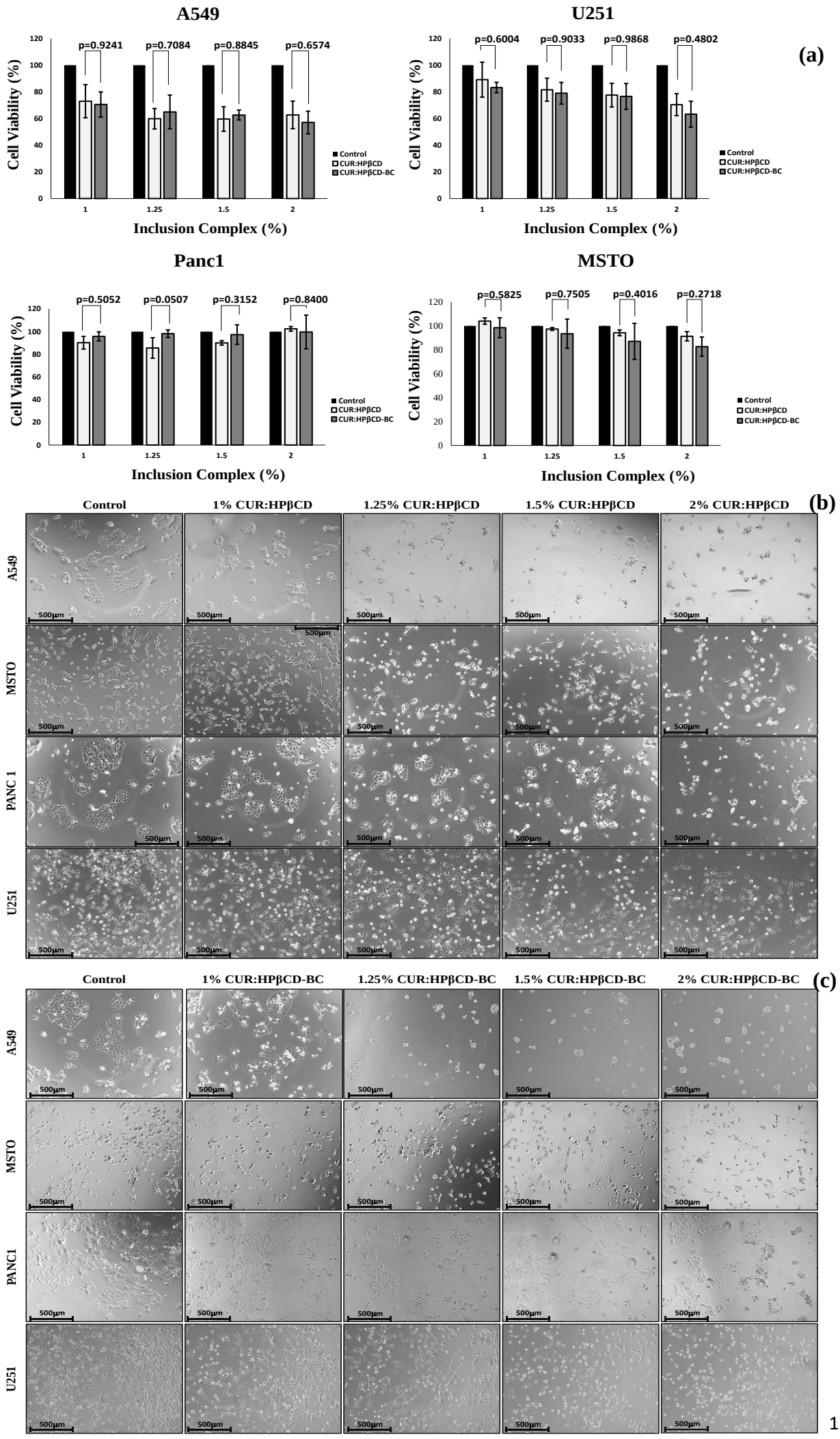

Figure 4.22: Cytocompatibility test results. **(a)** Bar graphs showing viability of different cells after 24 h exposure to free CUR:HPβCD and CUR:HPβCD-loaded-BC. Representative optical photomicrographs of cells captured at 10X magnification after exposure for 24 h to **(b)** free CUR:HPβCD; **(c)** CUR:HPβCD-loaded-BC.

4.4.3.11. CUR release and Antimicrobial study

CUR release from CUR:HPβCD-loaded BC hydrogels, as determined by UV-Visible spectroscopy, is presented in **Figure 4.23**. Results indicate that 76.99 ± 4.46 % release (n=6) was achieved after 6 h from CUR:HPβCD-loaded BC hydrogels. The release was slow after this duration and reached 79.36 ± 4.71 % at 24 h. The maximum release achieved at 48 h was 82.19 ± 4.75 %.

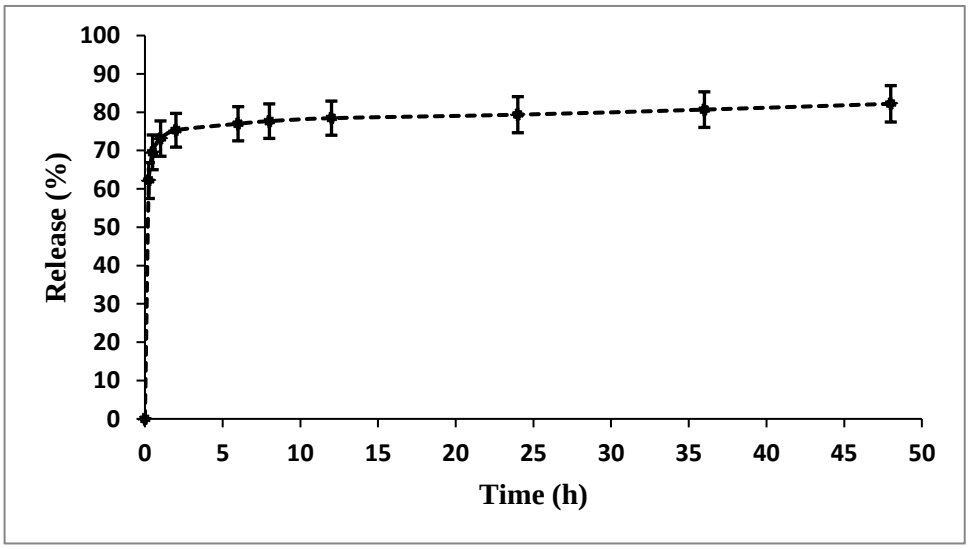

Figure 4.23: Release profile over 48 h from CUR:HPβCD-loaded-BC hydrogels (n=6; error bars = SD).

After the release profile was evaluated, the disc diffusion assay was undertaken to assess the antimicrobial activity of CUR:HPβCD-loaded BC hydrogels. The results revealed no anti-microbial activity against *S. aureus* (Gram positive) for neat BC and HPβCD-loaded BC However, CUR:HPβCD-loaded BC hydrogels demonstrated significant ($p<0.01$) antimicrobial activity (**Figure 4.24**) (ZOI= 11.08 ± 0.90 mm) (n=12) compared to neat BC and HPβCD-loaded BC.

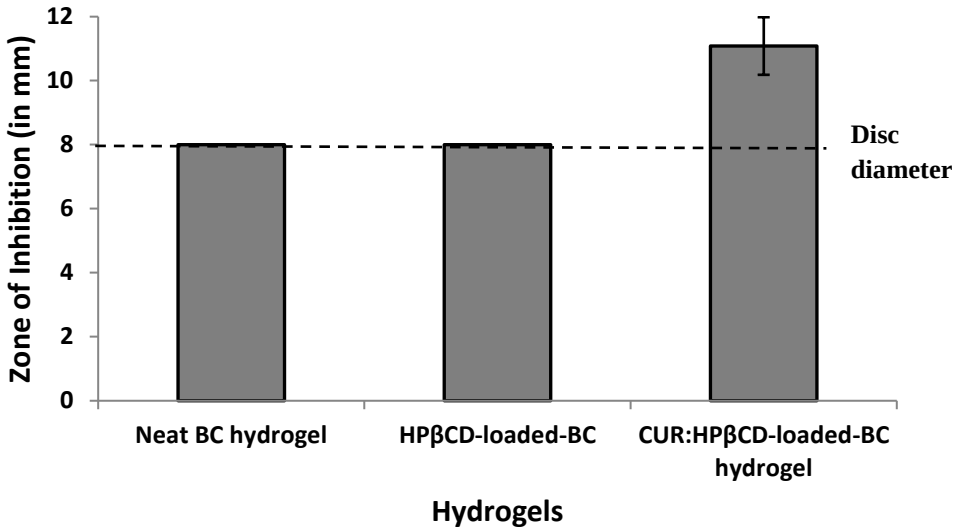

Figure 4.24: Antimicrobial activity assessed by ZOI during the disc diffusion assay for neat BC hydrogel, HPβCD-loaded-BC and CUR:HPβCD-loaded-BC hydrogels against *S. aureus* (n=12; error bars = SD).

4.4.3.12. Anti-oxidant activity by DPPH assay

It was found that HPβCD does not have antioxidant activity. The percent antioxidant effect for supramolecular CUR:HPβCD against DPPH determined in the current study ranged from 12.06 ± 0.014 - 79.75 ± 0.001 % in the range of 125-2000 µg/mL and the IC_{50} was found to be 1087.49 ± 6.47 µg/mL (n=3). These findings confirmed that the antioxidant activity of CUR stays preserved even after its encapsulation in HPβCD cavity in the CUR:HPβCD inclusion complex.

Part III

Introduction

This section of the thesis is focused on the synthesis of silver nanoparticles following the Green chemistry approach. Herein, the production of curcumin reduced silver nanoparticles using the aqueous solution of CUR:HPβCD inclusion complex has been presented. The findings on the production and characterisation of cAgNP-loaded bacterial cellulose for wound dressing applications have been presented. The findings were published as Gupta *et al*., 2020.

4.5. cAgNP-loaded BC hydrogels

4.5.1. Preparation of cAgNP

Most of the AgNP synthesis methods involve the use of organic solvents and toxic reducing agents with the potential threat to the environment and cytotoxic effect on mammalian cell lines. The method presented herein involved bio-reduction of $AgNO_3$ with aqueous CUR:HPβCD, resulting in nanoparticle formation. The colour changed from colourless to pale yellow at the start of CUR:HPβCD addition, which intensified with increased dosage and subsequently changed to yellow-brown with time, suggesting the production of nanoparticles.

4.5.2. Production of cAgNP-loaded BC hydrogels

When the purified padded dry BC was rehydrated with the aqueous colloidal cAgNP, the pellicles re-swelled and the colour changed to yellow-brown. These cAgNP-loaded BC hydrogels were stored at 4 ºC throughout the experimental procedure.

4.5.3. Characterisation of cAgNP and cAgNP-loaded BC hydrogels

The formation of colloidal cAgNP produced was confirmed by testing its properties like size distribution and charge. After loading aqueous colloidal cAgNP in the padded dry BC, the physicochemical and *in vitro* haemocompatibility and cytocompatibility hydrogels were investigated.

4.5.3.1. Particle size distribution and surface charge by TEM, DLS and Zeta potential

The size and morphology of cAgNP produced using CUR:HPβCD were studied from the TEM images (**Figure 4.25a-c**). TEM imaging showed that the morphology of the nanoparticles was mainly spherical in shape with smooth edges. The majority of bioreduced cAgNP were in the diameter range of 20-55 nm (80 %) and the average size of 42.71 ± 17.97 nm. (**Figure 4.25a-c**). It emerged from the results that nanoparticles were homogeneously surrounded by a thin layer of capping material.

DLS measurements identified nanoparticles with the hydrodynamic diameter in the range of 182.10 ± 8.83 nm (**Figure 4.25d**) and the Poly Dispersity Index (PDI) value of 0.196 ± 0.009. Zeta potential studies revealed a negative charge on the synthesised nanoparticles with the magnitude of -20.1 ± 0.702 mV.

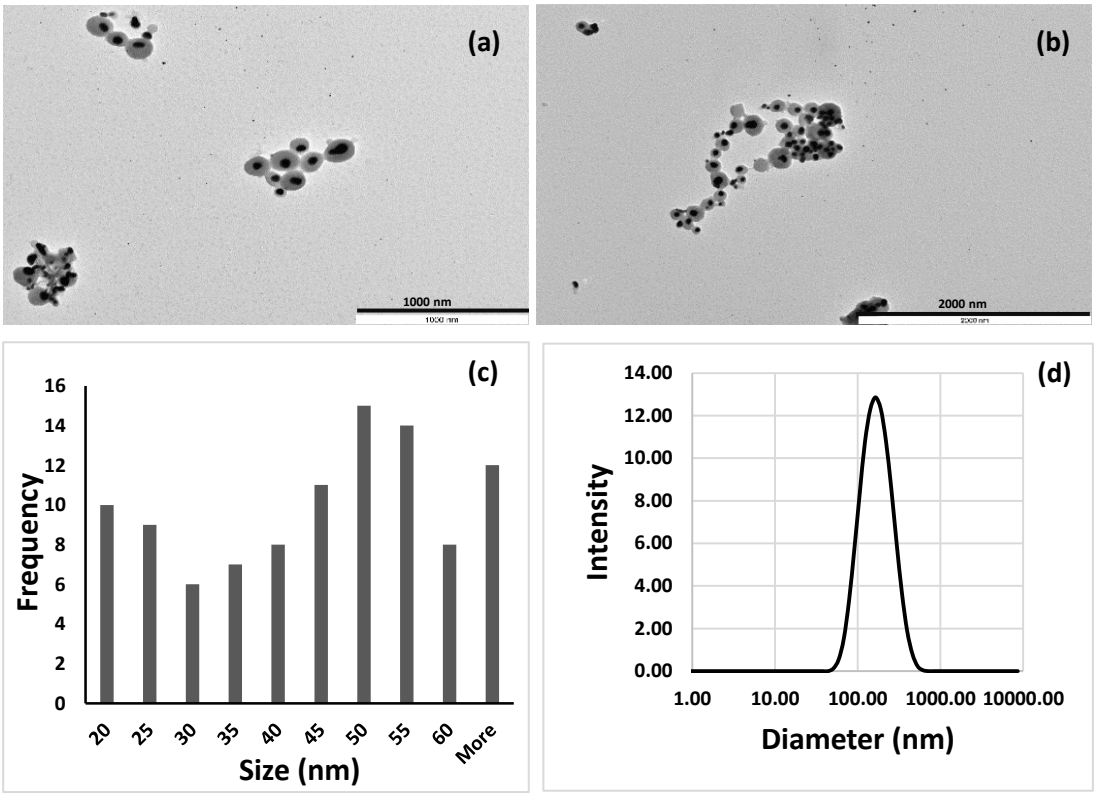

Figure. 4.25. Characterisation of cAgNP produced using CUR:HPβCD, **(a-b)** TEM photomicrographs; **(c)** size distribution as measured by TEM analysis and calculated with 100 nanoparticles; **(d)** DLS data of cAgNP with size distribution.

4.5.3.2. Scanning electron microscopy (SEM)

BC has a fine fibre network structure with voids (**Figure 4.3b**). SEM of lyophilised cAgNP-loaded BC revealed that cAgNP penetrated through the voids during rehydration of padded dry BC pellicles and got physically trapped in the fibre network structure (**Figure 4.26a**). Also, it emerged that along with bioreduced cAgNP, there was free CUR:HPβCD trapped in the BC.

Morphology and size of nanoparticles was also determined in the SEM photomicrographs (**Figure 4.26b**). The average diameter was in the range of 37.2 - 65.1 nm and most of the nanoparticles appeared spherical. These results are in accordance with TEM results discussed in section above.

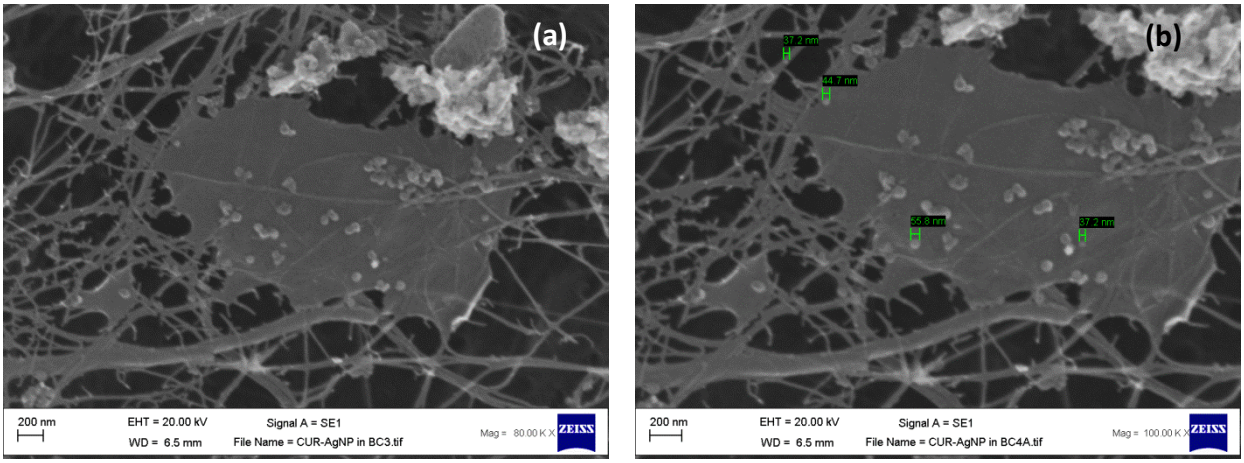

Figure. 4.26. SEM photomicrograph images of **(a)** and **(b)** cAgNP loaded in BC fibre network.

4.5.3.3. Energy dispersive X-ray (EDX) analysis

The elemental analysis was carried out by EDX studies. The results confirmed that BC (neat) is composed mainly of carbon and oxygen (**Figure 4.4b**). In addition to carbon and oxygen, detection of silver in the EDX spectra of cAgNP-loaded BC (test) confirmed nanoparticle loading in the test samples (**Figure 4.27**).

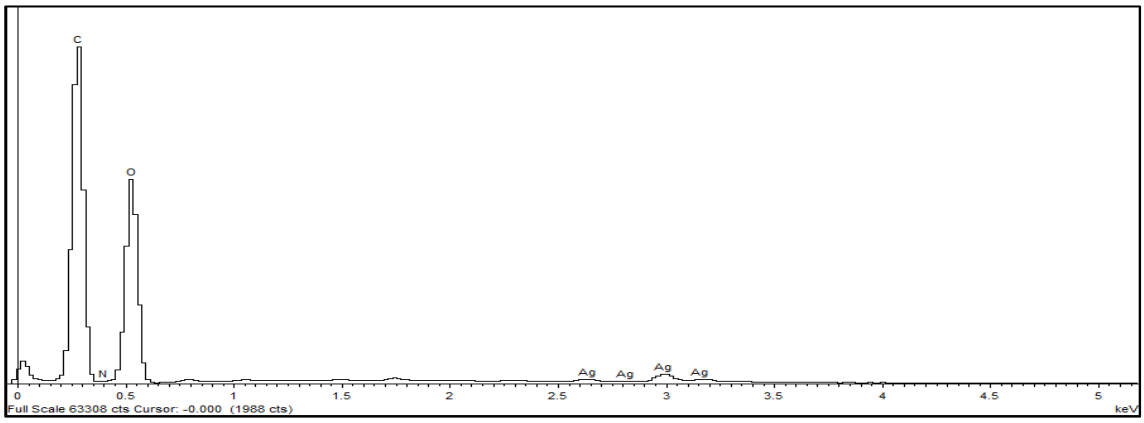

Figure. 4.27. EDX spectrum of cAgNP-loaded BC.

4.5.3.4. Moisture content (M_c)

In this part of the study, the moisture content of neat BC and cAgNP-loaded BC hydrogels was evaluated. The results confirmed that neat BC pellicles imbibed 99.68 ± 0.09 % (v/w) (n = 3) water. Moreover, the study on cAgNP-loaded BC revealed that the moisture content in these hydrogels was 98.86 ± 0.04 % (n = 3).

4.5.3.5. Cytocompatibility (*In vitro* study)

The cytocompatible nature of BC is presented earlier in this report (section 4.2.3.10). In this part of the current study, the cytocompatibility of cAgNP-loaded BC hydrogels was evaluated using three different mammalian cell lines. The cytotoxicity as determined by MTT assay revealed that cAgNP-loaded BC is cytocompatible, as all the tested cell lines demonstrated good survival rate (**Figure 4.28a**).

Furthermore, we compared the cytocompatibility of free cAgNP to cAgNP-loaded BC on U251, MSTO and Panc 1 cell lines. The results demonstrated that free cAgNP had cytotoxic effect on all the tested cell lines resulting in lower cell viability compared to cAgNP-loaded in BC ($p < 0.001$) (**Figure 4.28a&b**).

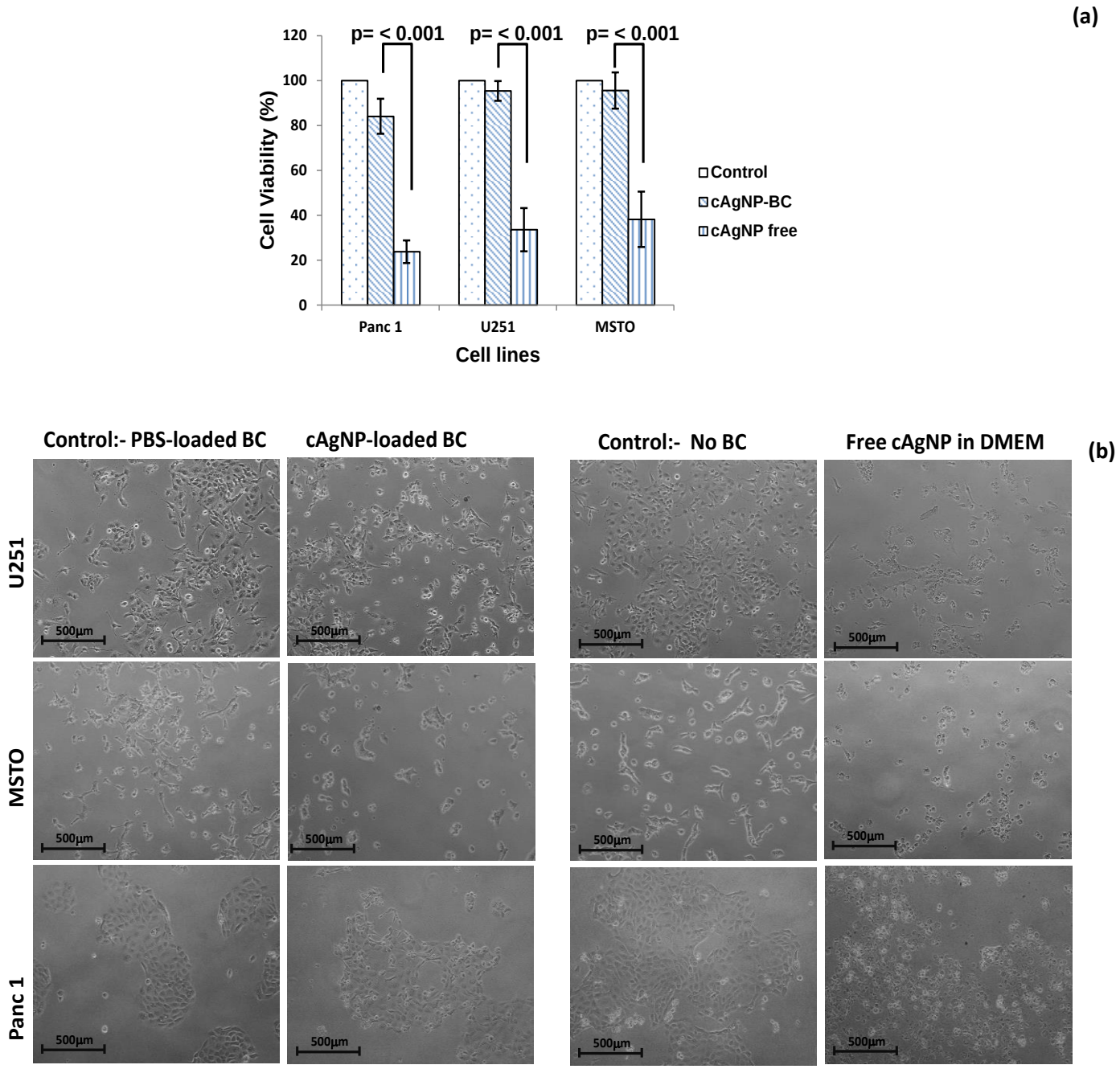

Figure. 4.28. Cytocompatibility test results. **(a)** Bar graph showing the cell viability (%) after 24 h exposure to cAgNP-loaded BC and free cAgNP (equivalent amount) (n = 8); **(b)** Representative photomicrographs of cells captured at 10x magnification after exposure for 24 h to cAgNP-loaded BC and free cAgNP.

4.5.3.6. Haemocompatibility

Haemocompatibility is an important property for biomedical applications of a material. In the current study, cAgNPs were prepared in deionised water hence, the hypothesis was drawn that cAgNP-loaded BC hydrogels may have haemolytic properties. The test results revealed that cAgNP-loaded BC hydrogels have a percentage haemolysis of 6.85 ± 1.12 % (n = 6). According to the ASTM F756 standards haemolytic indices, this range is over the threshold value of 5 %; hence, cAgNP-loaded BC hydrogels would be classified as a haemolytic material.

4.5.3.7. Antimicrobial study

In the current study, PBS-loaded BC, HPβCD-loaded BC and cAgNP-loaded BC hydrogels were tested against *P. aeruginosa* and *S. aureus* using the disc diffusion assay at 24 h. PBS-loaded BC and HPβCD-loaded BC did not exhibit antimicrobial activity; however, cAgNP-loaded BC demonstrated significant antimicrobial activity ($p < 0.001$) against both of the tested microbial strains (**Figure 4.29**).

These results confirm the broad spectrum antimicrobial activity of cAgNP-loaded in BC. Moreover, it emerged that cAgNP-loaded BC have stronger antimicrobial activity (**Figure 4.29**) against *P. aeruginosa* as compared to *S. aureus* ($p < 0.001$).

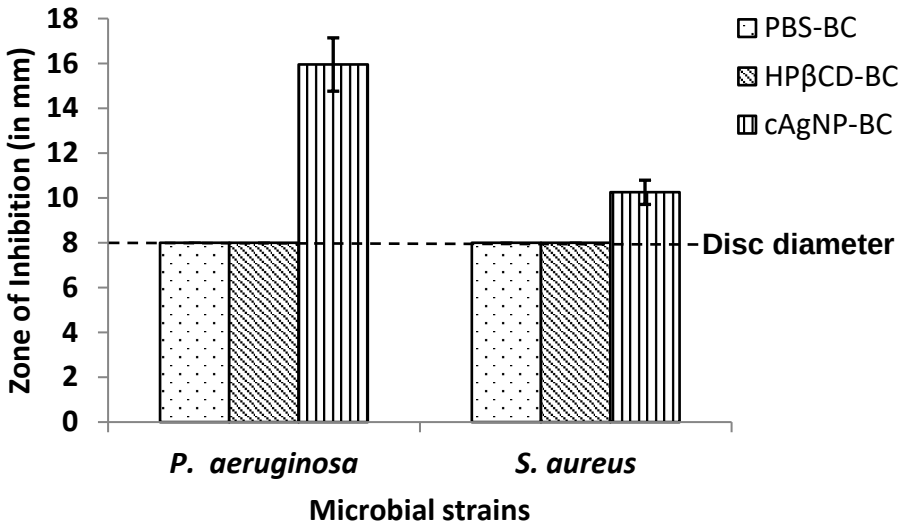

Figure. 4.29. Antimicrobial activity assessed by ZOI measurements during the disc diffusion assay for PBS-loaded BC, HPβCD-loaded BC and cAgNP-loaded BC against *P. aeruginosa*, *S. aureus* and *C.auris* at 24 h (n = 10; error bars = SD).

4.5.3.8. Anti-oxidant activity of cAgNP by DPPH assay

In the current study, the test results confirmed that silver nitrate and HPβCD does not have antioxidant activity. cAgNP were successfully prepared using CUR:HPβCD as reducing and stabilising agent. The percent antioxidant effect (% E) for aqueous cAgNP colloidal suspension against DPPH was determined to be 76.65 ± 3.21 % (n = 6).

4.5.3.9. Transparency test

The transparent nature of BC has already been presented **(Figure 4.6a**) and in this part of the study, PBS-loaded BC hydrogels reconfirmed these findings (**Figure 4.30a**). In this study, the transparency property of cAgNP-loaded BC was evaluated by reading the text in different colours on white laminated paper sheet through the test hydrogels. The results (**Figure 4.30b**) demonstrate

cAgNP-loaded BC hydrogels allow monitoring the wound without the need for removal of the dressing. This transparency testing is a simulation study and in order to confirm the results, clinical validation would be required and could be evaluated using *in vivo* animal models.

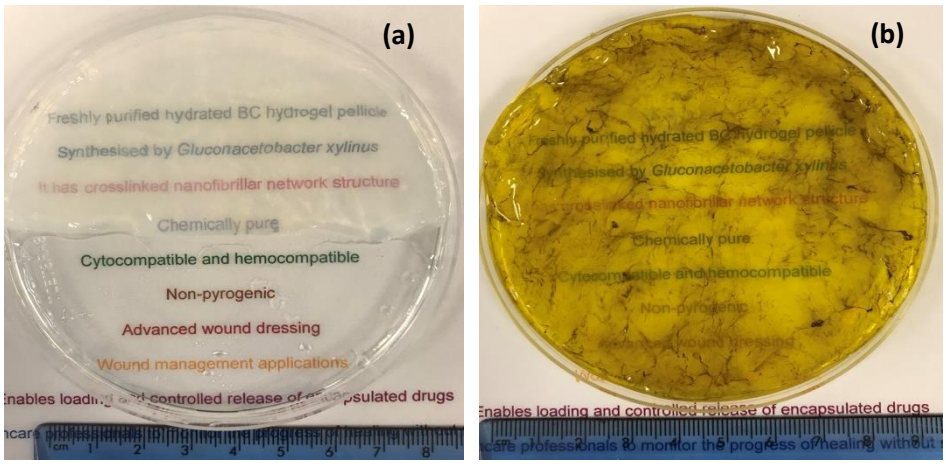

Figure. 4.30. Photomicrographs with the visual appearance of **(a)** BC loaded with PBS; **(b)** cAgNP-loaded BC hydrogel pellicle.

Chapter 5
Discussion

5.1. Discussion- Introduction

Wound healing is a complex and dynamic physiological process involving four different phases [Martin *et al.,* 2013] (**Figure 1.1**). On infliction of a wound, an immune response is initiated to close the wounded area to protect from infection [Tort *et al*., 2019]. Several mediators [Tejiram *et al.,* 2016; Dealey, 2012; Paul and Sharma, 2015; Singh *et al.,* 2017a; Ramanathan *et al.,* 2017] play a crucial role in this process (**Table 1.2**). Wound healing facets require controlled inflammation, low levels of reactive oxygen species (ROS) and controlled infections [Tort *et al*., 2019; Mohanty and Sahoo, 2017; Akbik *et al*., 2014]. Various antibiotic and non-antibiotic based antimicrobial agents (**Table 1.1**) are used to tackle the infected wounds, but the emergence of antibiotic resistant strains and biofilms still pose a great deal of challenge in the wound care sector [Radecka *et al.,* 2015; Cao *et al.,* 2019].

The conventional wound management approach that mainly aims to form a barrier from the external environment and keeps the wound dry, fails to facilitate healing in such non-healing chronic wounds [Arroyo *et al.,* 2015]. Advanced wound management, based on the concept of moist healing, is the treatment of choice for such wounds [Winter, 1962]. Out of the different types of such moist advanced dressings (**Table 1.3**), hydrogels have gained high research and clinical attention [Varghese *et al.,* 2012]. Various natural (e.g. BC, gelatin, dextran, alginate) and synthetic materials (e.g. PVA, PVP, poly(acrylic acid), AMPS) have been identified and employed to produce hydrogels suitable for wound dressing applications (**section 1.4.3** and **Table 1.4**). Moreover, being responsive to different stimuli such as pH, temperature or light, hydrogels could prove beneficial in chronic wound treatment [Guaresti *et al.,* 2018; Sood *et al.,* 2016]. Therefore, different homo and heteropolymeric composite hydrogels, with stimuli responsive release of the active

agents (hydrophilic and lipophilic) in a controlled manner, have attracted wide attention within the scientific community (**Figure 1.2**). High affinity for water makes the loading of hydrophilic active agents into the hydrogel base material relatively easy. Furthermore, the use of solubility enhancing carriers like cyclodextrins (**Figure 1.3**) enables the loading of lipophilic active agents as well in hydrogel matrix [Wathoni *et al.,* 2017; Paramera *et al.,* 2011; Mohan *et al.,* 2012].

Owing to the unique properties, BC has attracted wide research interest in biomedical sector. BC is a highly pure, biocompatible and non-pyrogenic polysaccharide polymer [Pandey *et al.,* 2017]. Although the molecular formula of BC is similar to plant cellulose, unlike plant cellulose, BC is free from biogenic compounds like pectin, hemicellulose, lignin and other constituents of lignocellulosic material which make it chemically pure and suitable for biomedical applications [Portela *et al.,* 2019] (**Table 2.1**). In addition, its thermal stability, hydrophilicity, transparency, high mechanical strength in the wet state and nanofibrillar morphology, allowing loading of a variety of healing agents, are further desirable properties for its consideration as a hydrogel matrix for wound dressings [Zmejkoski *et al.,* 2018; Moniri *et al.,* 2017]. The unique features of bacterial cellulose led to its applications in various biomedical sectors like orthopaedics (bone regeneration), cardiology (vascular conduits), dentistry (dental implants), dermatology (temporary skin substitute) and in wound management (wound dressings) (**Table 2.2**).

5.2. Production and Purification of BC hydrogels

The concept of moist healing [Winter, 1962] has revolutionised the field of wound management and led to an increased interest in the use of hydrogel-based

dressings. In the current study, BC was used as a hydrogel matrix for the production of antimicrobial hydrogels with wound dressing applications. *G. xylinus* produced BC hydrogel pellicles (**Figure 2.1**) at the air-liquid interface in HS medium, in 2 weeks under static conditions. During incubation, *G. xylinus* utilised the carbon source (in the medium) and produced three dimensional nanofibers of BC (**Figure 2.2)** and resulted in highly porous pellicles, as shown in **Figure 2.3**.

The BC pellicles after production were harvested and purified to get rid of entrapped bacterial cells and excess media (**Figure 4.1a**). The removal of bacteria and extraneous material on purification was confirmed in SEM photomicrographs (**Figure 4.3a&b**) and EDX results (**Figure 4.4a&b**). Once purified, the BC hydrogel pellicles become clear and transparent (**Figure 4.1b**).

5.3. Physicochemical characterisation of BC and antimicrobial-loaded hydrogels

The swelling ratio of a hydrogel indicates its ability to absorb fluid and is an important property for dressings, especially those used to manage heavily exudating wounds. Hydrogel wound dressings with high degrees of swelling can be applied to a wide variety of wound types, ranging from dry necrotic wounds to full thickness wounds that produce a high volume of exudate [Kokabi *et al*., 2007]. BC is insoluble in water and most organic solvents, but when immersed in aqueous media its fibrous structure imbibes large amounts of fluid (**Figure 2.4**) and it swells. In the current study, the swelling behaviour evaluation test results of the biosynthetic BC hydrogel reveal a high swelling capacity with a swelling ratio of 12.08 ± 0.96 after 24 h, which is in agreement with that reported by other groups [Nakayama *et al*., 2004; Maneerung *et al*., 2008; Wei *et al*., 2011]. The high swelling of BC results from the

development of hydrogen bonds with water molecules and the network-like structure of the biopolymer itself that allows BC to imbibe and hold onto those molecules (**Figure 2.4**) within the crosslinked polymer voids [Maneerung *et al*., 2008]. This high water absorptivity enables BC to maintain a moist environment at the wound site by donating or receiving fluids, thus maintaining an optimal environment in which healing can progress [Lin *et al*., 2013].

BC does not have inherent antimicrobial properties [Wu *et al.,* 2014]. BC has dense three dimensional interwoven cellulose ribbons, leading to a network structure with interspersed voids, which was evident in SEM images (**Figure 4.3b-d**). The unique nanofibrillar structure and reswelling properties of BC enables it to be loaded with antimicrobial and healing agents [Fu *et al*., 2013, Shah *et al*., 2013, Wu *et al*., 2014]. This morphological feature of BC attracted attention and several attempts have been made to load different antimicrobial agents in BC for wound dressing applications.

Ionic silver is a broad spectrum antimicrobial agent with activity against yeast, fungi and several antibiotic resistant bacteria, including methicillin resistant *S. aureus* (MRSA) and vancomycin resistant enterococci (VRE) [Murphy and Evans, 2012]. Of equal importance, Ag^+ has relatively low toxicity in human cells at concentrations that are antimicrobially active against pathogenic microbes [Copcia *et al*., 2011; Wilkinson *et al*., 2011]. Since the dawn of the antibiotic era, the use of Ag^+ has gradually decreased, but the upsurge in multidrug resistant microbial strains has led to a resurgence in interest [Chopra, 2007]. Ag^+ ions are highly reactive and can bind to multiple intra and extra cellular target sites, resulting in changes to microbial cellular functionality, structural integrity, permeability and transport systems [Chopra,

2007; Low *et al*., 2013; Maneerung *et al*., 2008; Martin *et al*., 2015]. Once transported into the bacterial cytoplasm, Ag^+ interact with essential intracellular enzymes and DNA, thus restricting the ability to maintain vital cell functions and impairing cell replication, that eventually lead to cell death [Castellano *et al*., 2007; Low *et al*.,, 2011; Low *et al*., 2013]. The multifaceted, broad spectrum mode of action of Ag^+ can be highly effective at controlling chronic wound infections even at parts per million concentrations [Brett, 2006]. Low and co-workers (2011) reported the minimum lethal concentration (MLC) of Ag^+ (from silver nitrate, $AgNO_3$) against *P. aeruginosa* and *S. aureus*, two most common wound colonising opportunistic pathogens, to be 1.59 x 10^{-3} % w/v (equivalent to 15.9 ppm) and 5.08 x 10^{-3} % w/v (equivalent to 50.8 ppm) respectively [Low *et al*., 2011]. There are several commercially available topical silver products including dressings (Acticoat®, Contreet-H®, Actisorb Silver 220®, Aquacel-Ag®, Ag Extra™), solutions (Sulfamylon®) and creams (Silvadene®, Flamazine™) [Martin *et al*., 2013]. The most commonly used products contain silver nitrate or silver sulfadiazine [Ip *et al*., 2006].

Zeolites are non-reactive, aluminosilicate microporous crystalline frameworks with anionic cavities occupied by cations or water molecules [Kwakye-Awuah *et al*, 2008]. The cations and water molecules have considerable freedom of movement, thus the charge balancing cations can be exchanged in aqueous medium with other cationic species, without affecting the structure of zeolites [Copcia *et al*., 2011]. Cationic Ag^+ interacts with the ionic zeolite framework to form silver zeolite (AgZ); the prolonged release of Ag^+ from the zeolite structure can be achieved by a controlled exchange of cations [Kwakye-Awuah *et al*, 2013].

Curcumin (diferuloylmethane) (CUR) is a naturally derived low molecular weight polyphenolic compound well known for its pharmacological benefits in wound healing, such as anti-inflammatory, anti-infective and anti-oxidant activities [Akbik *et al*., 2014]. However, the hydrophobic nature of CUR can limit its biomedical applications. This can be overcome by encapsulation into solubility enhancing carriers like cyclodextrin (CD). CDs are cyclic truncated-cone shaped oligosaccharides used as excipients in the pharmaceutical sector [Del Valle, 2004; Jambhekar and Breen 2016]. In the current study, water soluble inclusion complex of CUR was produced with HPβCD.

The emergence of nanotechnology enabling the production of silver nanoparticles has served a new therapeutic modality. Silver nanoparticles (AgNP) owing to their characteristic broad-spectrum antimicrobial properties have received increased focus in biomedical applications including for wound management [Parveen *et al*., 2018; Ravindran *et al*., 2019]. Among the several different approaches to synthesise AgNP, the use of natural substances like plant extracts has received wide research consideration due to the safe and eco-friendly procedure [Ravindran *et al*., 2019; Keshari *et al*., 2018; Alsammarraie *et al*., 2018].

In the current study, three different types of BC based antimicrobial hydrogel dressings were produced. Purified padded dry BC was loaded with:

1. An Ag^{+} donor, $AgNO_3$ or AgZ to produce silver-loaded BC hydrogels,
2. Curcumin to produce curcumin-loaded BC hydrogels
3. Curcumin reduced silver nanoparticles to produce cAgNP-loaded BC hydrogels

Loading of chosen antimicrobial agent was performed by immersion under static and agitated conditions for AgZ. Aqueous AgZ suspension tends to sediment under static conditions, hence the loading was not consistent (visual examination, **Figure 4.2a**). Abridged uptake of AgZ was further confirmed by reduced antimicrobial activity of AgZ-loaded BC (static) in the disc diffusion assay test results (**Figure 4.8**). Based on these findings, loading under agitated conditions was adopted as a standard protocol throughout this study.

The microporous structure, large surface area and moisture retention ability enables BC to absorb and retain large amount of active compounds [Portela *et al*., 2019]. When padded dry BC was immersed in a solution or a suspension, due to its structural properties, it imbibed the fluid and along with the fluid, the antimicrobial agents penetrated through the voids and got physically trapped in the fibre networks. This resulted in the production of silver-loaded BC**,** Cur:HPβCD-loaded BC and cAgNP-loaded BC. These results are in agreement with findings reported in literature where authors reported the incorporation of compounds in BC by immersion. Shao *et al*., (2016) reported the incorporation of tetracycline hydrochloride in BC by immersion technique to produce antibacterial membranes. In another study, BC based antimicrobial wound dressings have been proposed; the quaternary ammonium compound with antimicrobial property was produced using dilinoleic acid, ethylenediamine and tyrosine and impregnated in BC by immersion technique [Żywicka *et al*., 2018]. These dressings demonstrated strong antimicrobial activity against *S. aureus* and *S. epidermidis*.

Along with carbon and oxygen traces (elemental composition of BC), aluminium, silicon, calcium, sodium, magnesium and iron (elemental composition of zeolites), the traces for elemental silver could be found in EDX results of $AgNO_3$-loaded BC, AgZ-loaded BC and cAgNP-loaded BC, confirming the presence of silver in these hydrogels (**Figure 4.4c&d; Figure 4.27**). In addition to the EDX findings, the loading of antimicrobial agents ($AgNO_3$, AgZ, CUR:HPβCD and cAgNP) in BC was evident in SEM photomicrographs (**Figure 4.3g,h&j; Figure 4.15d; Figure 4.26**). SEM images confirmed that the antimicrobial agents got trapped in the BC fibres. Analysis of SEM images further revealed that, in addition to cAgNP, there was CUR:HPβCD trapped in cAgNP-loaded BC **(Figure 4.26**). Along with the reducing and capping properties of CUR in CUR:HPβCD in cAgNP synthesis, CUR:HPβCD has demonstrated other wound healing properties (e.g. antimicrobial and antioxidant activities, discussed later). Thus, the excess of CUR inclusion complex in cAgNP-loaded BC may deliver additional benefits contributing to wound healing.

CUR:HPβCD (yellow powder) was produced (**Scheme S5a-c** in the supporting information) from the CUR (dark yellow powder) and HPβCD (white powder) by solvent extraction method. These results in agreement with Yallapu *et al*., (2010) where the authors reported the formation of light yellow coloured fluffy power of CUR:CD using CUR and βCD by the solvent evaporation method.

The formation of the CUR:HPβCD inclusion complex was confirmed before loading in BC. The solubility test results (**Figure 4.14**) on an aqueous solution of the inclusion complex gave a strong absorbance peak at around 430 nm, corresponding to lambda max for CUR and confirmed the inclusion of CUR in HPβCD. These results correspond with previous studies reporting CUR has poor aqueous solubility

[Mohammadian *et al*., 2019], which could be enhanced by its inclusion in CD cavity [Mohan *et al*., 2012; Li *et al*., 2018].

CUR is a crystalline compound with a distinctive diffraction pattern, whereas HPβCD is amorphous in nature, which is evident in the XRD results (**Figure 4.17a&b**). Upon the inclusion of CUR in CD cavity, the diffraction peaks of CUR disappears [Aytac & Uyar 2017]. The loss of characteristic peaks of CUR upon inclusion in HPβCD, which was evident in the XRD test results (**Figure 4.17c**), further confirmed that CUR formed an inclusion complex with HPβCD. Similar findings are published by Mohan *et al*., (2012), where the authors reported the loss of well-defined crystalline peaks in the XRD results of CUR after its inclusion in hydroxypropyl-γ-cyclodextrin (HPγCD). In another study, the authors produced the inclusion complex of CUR with HPβCD by the solvent evaporation method; the characteristic diffraction peaks of CUR were reported to be absent in the XRD of the inclusion complex whereas some peaks were seen in the physical mixture of the parent compounds (CUR and HPβCD) [Radjaram *et al*., 2013]. Aytac and Uyar (2017) made an attempt of producing the core-shell nanofibers of CUR:HPβCD as a core and polylactic acid as a shell by electrospinning. The authors reported the loss of diffraction peaks of CUR in the nanofibers in the XRD results, suggesting the true inclusion complexation between CUR and HPβCD [Aytac & Uyar 2017]. Inclusion complex formation was also suggested in ^{1}H NMR results, with upfield shift in H^{3} and H^{5} protons of HPβCD upon inclusion of CUR in its cavity (**Figure S5&6).** ROESY NMR correlation between H5 of HPβCD and CUR aryl protons spectrum further confirmed these findings **(Figure 4.18**).

The thermokinetic data could be used to understand the thermal decomposition reaction and helps determine the storage conditions [Shamsipur *et al*., 2013]. The

comparison of TG curves of pure compounds, their physical mixture and the CUR:HPβCD inclusion complex could provide evidence of interactions between compounds and the formation of inclusion complex [Mura, 2015]. Thermal degradation data revealed that the thermal stability of the inclusion complex was higher as compared to its constituting moieties (**Figure 4.20**), but as the current study aims at the application of the product at the physiological temperature, so the decomposition at high temperatures (>300 °C) was not significant. It should be noted that, due to the inclusion of CUR in HPβCD cavity, the thermal behaviour of CUR was different from free CUR, which is in accordance with Ishiguro *et al*., (1995), where the authors observed the difference in the weight loss trend in TG curves of free CD (αCD), physical mixture (αCD and linoleic acid) and encapsulated linoleic acid in αCD. αCD and linoleic acid demonstrated a distinctive weight loss trend. The authors reported all significant weight losses from the parent moieties in both the physical mixture and the encapsulated complex, although the weight loss related to linoleic acid was less in the inclusion complex as compared to the physical mixture. This suggests that linoleic acid complexed with αCD resulting in its thermal stability after inclusion in CD cavity [Ishiguro *et al*., 1995]. In the current study, the melting endothermal peak for CUR was absent in the thermogram of the inclusion complex. This may be due to molecular interactions of inclusion of CUR in the HPβCD cavity (**Figure 4.20c**) thus indicating the formation of the inclusion complex.

The use of natural compounds in nanotechnology is attracting wide research interest. In the present study, a novel green chemistry approach using aqueous CUR:HPβCD to reduce $AgNO_3$ to produce cAgNP was developed. The change in colour from colourless to pale yellow to yellow brown with CUR:HPβCD dose increase during cAgNP production was observed. This could be due to the

excitation of surface plasmon vibrations in AgNPs, which is in accordance with findings reported by Alsammarraie *et al*., (2018). The authors used the aqueous extract of turmeric powder to synthesise AgNP by stirring overnight at room temperature. The colour of the mixture changed from yellow (at the start) to light brown, brown and finally brown-red (after 24 h) [Alsammarraie *et al*., 2018]. In another research, AgNP were produced using tubers of *Curcuma longa* (powder and aqueous extract). The authors observed the bioreduction of AgNP from $AgNO_3$ associated with the change in colour to pale yellow (after 2 h), which intensified with time and increased dose of *C. longa* powder or extract, due to excitation of surface plasmon vibrations in AgNP [Sathishkumar *et al*., 2010].

cAgNP produced in the current study were characterised for the size distribution and surface charge. TEM results revealed the average size of cAgNP in the range of 42.71 ± 17.97 nm with a homogenous thin layer of capping agent (**Figure 4.25a-c**). As the method employed in the current work only involved $AgNO_3$ and CUR:HPβCD, without the use of any organic solvents and additional capping agents, this suggests that CUR:HPβCD was acting both as a reducing and capping agent. These results are in agreement with the green synthesis of AgNP by Alsammarraie *et al*., (2018), where an aqueous extract of turmeric has been reported as both reducing and capping agent. The functional groups in turmeric have been proposed as potent reducing agents and the proteins as a capping agent to stabilise AgNP [Alsammarraie *et al*., 2018]. Similar findings are published by Song *et al*., (2019), where the authors fabricated AgNP using CUR by ultra-sonication for 30 min and reported the role of CUR as reducing and capping agent. Yang *et al*., (2016) undertook the synthesis of AgNP by two different methods and observed that AgNP produced using CUR were more stable than AgNP synthesised by citric acid. The

authors reported the role of CUR as reducing and capping agent in the synthesis route. Moreover, Khan *et al*., (2019) also reported the use of curcumin (in the form of curcumin oxide) as a reducing and capping agent in AgNP synthesis.

SEM photomicrographs also revealed the diameter of cAgNP (37.2-65.1 nm) (**Figure 4.26a&b**), which is in agreement with TEM results. DLS results identified nanoparticles with the hydrodynamic diameter of 182.10 ± 8.83 nm and PDI of 0.196 ± 0.009 (**Figure 4.25d**). These results indicate both the nucleation to form new nanoparticles and aggregation could be happening consecutively. These findings are consistent with studies reported by Sathishkumar *et al*., (2010), where the authors have shown that during the AgNP synthesis using *C. longa* (powder or extract), both nucleation to form new AgNP and aggregation to form larger particles occurred consecutively.

Low PDI value (0.196) indicates that the colloidal cAgNP was not very polydispersed. The zeta potential value is directly proportional to the stability of nanoparticle dispersion [Srivatsan *et al*., 2015]. Zeta potential value of -20.1 ± 0.702 mV recorded in the current study was in a close range to the previously reported values of -27.9 mV for AgNP bioreduced using curcumin [Song *et al*., 2019].

FTIR results (**Figure 4.5b; 4.16d**) confirmed that the purified biosynthetic BC hydrogel produced by *G. xylinus* closely resembles commercial cellulose. The broad, characteristic peak around 3328 cm^{-1} falls within the region of 3200–3550 cm^{-1}, which is attributed to the stretching of O–H bond [El-Shishtawy *et al*., 2011]. This may also be due to the stretching of the intramolecular hydrogen bond of 3O···H–O5 within the BC network, which has been reported to show a characteristic peak at 3348 cm^{-1} [Oh *et al*., 2005]. The narrow peak at 2900 cm^{-1} is due to C–H stretching of CH_2 and CH_3

group, whereas the peak at 1640 cm^{-1} is due to the O–H bending of water molecules [Barud *et al*., 2008]. The peak at 1375 cm^{-1} (C–H bending) provides an indication for the presence of crystalline regions within the BC structure [Castro *et al*., 2011]. Besides that, the peaks at 1159 cm^{-1} (asymmetrical C–O–C bridge stretching) and 1055 cm^{-1} (skeletal vibrations involving C–O stretching) can also be attributed to BC [Barud *et al*., 2008]. The encapsulation of $AgNO_3$ into the BC is confirmed by the occurrence of the specific peaks for Ag at 733 cm^{-1} and 803 cm^{-1} [Valverde-Aguilar *et al*., 2011]. The vibration bands within the region of 1350–1400 cm^{-1} are attributed to nitrate ions (NO^{3-}) [Salim and Malek, 2016]; hence the presence of a broad peak in the region of 1300 - 1400 cm^{-1}, indicates the availability of the nitrate group within $AgNO_3$-loaded BC. The peaks of AgZ-loaded BC at 980 cm^{-1} (asymmetric vibration of Si–O) suggest the presence of a three-dimensional silica phase within the zeolite structure and the peak at 665 cm^{-1} (symmetric stretch) may be attributed to the internal vibrations of the tetrahedral framework [Shameli *et al*., 2011]. FTIR spectra of zeolites reveal the occurrence of a large, intense band at around 986 cm^{-1}, corresponding to the vibration of the Si–O–Si [Hanim *et al*., 2016], whereas the peak at 676 cm^{-1} may be due to the bending of Al–O bonds within the zeolite structure [Shameli *et al*., 2011]. Additionally, peaks occurring within the region of 420–500 cm^{-1} may also indicate internal vibrations due to the bending of the T–O tetrahedra, e.g. 477 cm^{-1} corresponding to the internal vibration of (Si, Al)O_4 tetrahedra within the zeolite structure [Karimi-Shamshabadi and Nezamzadeh-Ejhieh, 2016]. The presence of silver within the AgZ-loaded BC network is confirmed by the peak at 553 cm^{-1}, that indicates the Ag–O stretching of AgO and Ag_2O within the 500–600 cm^{-1} region [Waterhouse *et al*., 2001; Kim *et al*., 2013].

Moreover, in case of FTIR results of CUR, the characteristic sharp peak at 3504 cm^{-1} and a broad peak at band regions of 3308 cm^{-1} suggested the presence of OH; 1619 cm^{-1} was assigned to C=C and C=O vibrations; 1591 cm^{-1} to the stretching vibrations of benzene ring and 1497 cm^{-1} to the C=C (**Figure 4.16a**). For HPβCD the characteristic broad peak at 3340 cm^{-1} was assigned to stretching vibrations of OH group; 2927 cm^{-1} to C-H stretching and other prominent peaks presented at 1156 cm^{-1} and 1084 cm^{-1} (C-H), 1024 cm^{-1} (C-O-C glucose units) (**Figure 4.16b**). In CUR:HPβCD, due to the encapsulation of CUR in HPβCD cavity, the peaks of CUR appeared to be masked or shifted. The prominent peaks at 3504 cm^{-1} and 1619 cm^{-1} appeared to be masked by HPβCD molecular vibrations in the inclusion complex (**Figure 4.16c**), which could be due to the inclusion of CUR in HPβCD cavity [Sun *et al*., 2014; Mohan *et al*., 2012; Li *et al*., 2018]. Furthermore, the characteristic peaks of the inclusion complex and BC were observed in the CUR:HPβCD-loaded BC spectrum (**Figure 4.16e**), thereby confirming the loading of the inclusion complex in the BC network.

The thermokinetic data did not show decomposition at normal working temperatures, suggesting that the production and storage of the inclusion complex at room temperature does not affect its thermal stability [**Figure 4.20**]. BC is thermally stable at the standard autoclaving temperatures [**Figure 4.19**]. The data from the current study suggests that the inclusion complex is also thermally stable at such temperatures. Since BC and the inclusion complex are both thermally stable at the standard autoclaving temperatures, the hydrogel dressings may be sterilised by autoclaving prior to the application on the wound site.

Wound dressings with high moisture content offer several benefits including, but not limited to, high malleability, easy and pain free removal of the dressing, cooling and

soothing effect resulting in a sensation of pain reduction with a capability of developing a moist microclimate that has been proven to enhance epithelialisation [Vowden and Vowden, 2017, Winter, 1962, Di *et al*., 2017, Tyeb *et al*., 2018]. BC (> 99.5 %) and other BC based hydrogels produced in the current study i.e. $AgNO_3$-loaded BC (99.16 ± 0.20 %), AgZ-loaded BC (98.06 ± 0.16 %), CUR:HPβCD-loaded-BC (97.63±0.057 %) and cAgNP-loaded BC (98.86 ± 0.04 %) demonstrated high moisture content. These findings indicate that the difference in the mass of neat hydrated BC and antimicrobial-loaded BC is contributed to by antimicrobial agents ($AgNO_3$, AgZ, CUR:HPβCD, cAgNP), which were physically trapped in the fibre network of BC during the loading process. Attributed to the high water content, these hydrogels can confer benefits (discussed above) like increased malleability, soft texture and can create a moist environment with increased dissolved oxygen to facilitate aerobic conditions at the wound-dressing interface. In addition, these hydrogels may ease removal of the dressing, reduce pain sensation and therefore, improve patient comfort and compliance. These features have been reported to facilitate the wound healing process [Jiji *et al*., 2019, Zmejkoski *et al*., 2018, Portela *et al*., 2019, Khalid *et al*., 2017] and therefore, BC and BC based hydrogels have attracted increased interest in the wound care sector.

Monitoring of wound healing process is vital from a clinical perspective [Flanagan *et al*., 2003, Kenworthy *et al*., 2018, Malone *et al*., 2020]. Routinely, this assessment is carried out by visual observation of the wound site by the removal of the dressing; however, this can disturb the granulating tissue and could cause trauma to the wound [Vowden and Vowden, 2017]. A dressing with the feature enabling non-invasive monitoring of the healing process without the need to remove the wound dressing has the potential to ensure effective management [Zhang *et al*., 2017]. This

would allow regular clinical assessment of the wound healing process, improve patient comfort and potentially lower the cost of treatment with less frequent dressing change.

Transparency is a property that measures the ability of the material to allow the light pass through without scattering [Shahbazi *et al*., 2019]. In the current study an attempt was made to produce the hydrogel dressings delivering this feature. BC demonstrated over 85 % transmission (%) and CUR:HPβCD-loaded BC demonstrated over 66 %, advocating their ability to deliver the clinical monitoring of the healing process through the hydrogel. The transparency assessment of the hydrogels was further extended by reading the text typed in different colours through hydrated BC and antimicrobial-loaded BC hydrogels. BC (**Figure 4.6a; Figure 21a; Figure 4.30a**), $AgNO_3$-loaded BC (**Figure 4.6b**), CUR:HPβCD-loaded BC (**Figure 4.21b**) and cAgNP-loaded (**Figure 4.30b**) demonstrated good transparency when text was read through these hydrogels. AgZ-loaded BC displayed limited transparency feature, as text was not fully readable through these hydrogels (**Figure 4.6c**). This could be attributed to the colour of the AgZ, which reduced the transparency levels of these hydrogels. A lower AgZ (<1 %) concentration may resolve this issue and could improve the transparency levels.

Several protocols have been reported in the literature to evaluate the transparency of hydrogels with wound dressing applications [Di *et al*., 2017, Tehrani *et al*., 2016]. The method designed and employed in the current study for transparency testing may not exactly mirror the real wound site; for that to be considered, this study could be extended to *in vivo* animal models. Nevertheless, this method has several advantages due to its simplicity and low cost.

Several methods have been reported for the determination of small molecule antimicrobial release from wound dressings (including metal ions) such as beaker, diffusion cell, paddle over disc and two compartment model [Maneerung *et al*., 2008; Wei *et al*., 2011; Jadhav *et al*., 2012; Peršin *et al*., 2014; Wu *et al*., 2014]. Each method has unique advantages and disadvantages, and hence no single, standard method has been adopted for the determination of silver release from dressings. In this study, a refined silver release method using 24-well tissue culture flat bottom plates and TSB as the release medium was developed for underpinning the release properties of silver compounds ($AgNO_3$ and AgZ) from BC. At the wound site, silver release from dressings is dependent on several factors, including the type of wound, classification and size of dressing and volume of exudate. The method designed and employed for the determination of silver release in the current study may not exactly mirror the real wound environment; for that to occur the presence of phagocytes, inflammatory mediators, hydrolytic enzymes, reactive oxygen species, bacteria and their associated by-products would need to be considered [Ovington, 2007; Martin *et al*., 2013]. Nevertheless, this method has several advantages due to its simplicity, low cost and biorelevant temperature conditions. Silver release, as quantified by ICP indicated that the Ag^+ zeolite-loaded hydrogels (AgZ-loaded BC) released more Ag^+ (137.60 ± 16.17 ppm) than their $AgNO_3$ (64.53 ± 6.47 ppm) counterparts ($AgNO_3$-loaded BC) (**Figure 4.7**). The microporous zeolite framework allows greater initial Ag^+ loading and a subsequent ion-exchange mediated release of biologically active Ag^+ into the surrounding medium [Kwakye-Awuah *et al*., 2008]. The results further confirmed that silver release from AgZ-loaded BC was steady and prolonged, which advocates the potential application of AgZ-loaded BC as an antimicrobial hydrogel

dressing for infected non-healing wounds. This feature would permit less frequent dressing change, which could bring the cost of wound management down.

Invasion of opportunistic microbes could impair wound healing, leading to chronic non-healing wounds [Williams *et al*. 2018, Nagoba and Davane, 2019]. Following the evaluation of release behaviour of these hydrogels, antimicrobial properties of silver-loaded BC hydrogels was evaluated using the disc diffusion assay. The antimicrobial test results revealed that BC loaded under conditions of constant agitation demonstrated greater antimicrobial activity, compared to the statically loaded hydrogels. This may be due to the more evenly distributed Ag^+ loading under agitated condition as compared to static incubation, which contributed to a more consistent release of Ag^+ (**Figure 4.8**).

The prolonged antimicrobial activity exhibited by AgZ-loaded BC against both *P. aeruginosa* and *S. aureus* (**Figure 4.9; Figure 4.10**) resulted from the controlled release of Ag^+ from the zeolite structure. Zeolites are crystalline aluminosilicate cages with cavities occupied by cations or water molecules. The AgZ acts as an inorganic reservoir and silver in the zeolite have considerable freedom of movements [Kwakye-Awuah *et al*., 2008]. Varied amount of Ag^+ can be stored in zeolites and the release profile of silver depends on the zeolite and the ionic strength of the medium. Therefore, AgZ serve as a unique platform for the controlled release of silver [Dutta and Wang, 2019]. In the current study, in addition to the ionic exchange-based release of Ag^+ encapsulated within the zeolite, BC matrix was able to provide a second layer of controlled release. In contrast, release of Ag^+ from $AgNO_3$-loaded

BC was only controlled by the BC matrix, hence Ag^+ release was less prolonged when compared to AgZ-loaded BC.

Results revealed that both AgZ-loaded BC and $AgNO_3$-loaded BC exhibited antimicrobial activity against the Gram positive and Gram negative strains tested, but that activity was stronger and more prolonged against *P. aeruginosa* compared to *S. aureus*. Ag^+ has strong bactericidal activity [Copcia *et al*., 2011], and Gram negative bacteria are more susceptible to Ag^+ than the Gram positive species [Ip *et al*., 2006; Waghmare *et al*., 2015] due to differences in their cell wall structure and composition. The Gram positive bacterial cell wall contains a thicker peptidoglycan layer than that of Gram negative strains. Gram positive bacterial cell walls typically lack an outer membrane and are mainly composed of a thick, negatively charged peptidoglycan layer and cytoplasmic phospholipid bilayer. Contrary to this, Gram negative microorganisms have a thin (≈2–3 nm) peptidoglycan layer between the outer membrane and the cytoplasmic phospholipid bilayer [Le *et al*., 2010]. The composition of the peptidoglycan layer, which contains teichoic acids, contributes to the overall anionic charge of the Gram positive cell surface [Neuhaus and Baddiley, 2003]; this greater net anionic charge may bind more Ag^+, thus reducing the amount that can reach the plasma membrane and intracellular targets to exert their antimicrobial activity. This finding is in agreement with Le *et al*. (2010) who reported that *E. coli* (Gram negative) was more sensitive to the effects of silver nanoparticles (versus *S. aureus*, a Gram positive) because of differences in the thickness of the peptidoglycan layer [Le *et al*., 2010]. Gram negative microorganisms are generally less sensitive to antibiotics and certain antimicrobial agents due to the selective permeability and protective mechanism of their outer membrane structure

[Bomberger *et al*., 2009; Sperandeo *et al*., 2009]. Nevertheless, Ag^{+} has shown its ability to exert microbiocidal activity against a variety of pathogenic microorganisms, including drug resistant strains. In addition, its multi-target antimicrobial activities are advantageous in limiting the potential development of resistant microbial strains [Brett, 2006; Radecka *et al*., 2015]. Hence, the development of a responsive, topical silver formulation would be extremely useful for the treatment of infected chronic wounds.

The release of CUR was also examined from CUR:HPβCD-loaded BC hydrogels. Results revealed that the maximum CUR release of 82.19 ± 4.75 % was achieved at 48 h (**Figure 4.23**) through these hydrogels. These findings confirmed high bioavailability of CUR at the wound site to control bacterial infection during the treatment period. The antimicrobial properties of CUR:HPβCD-loaded BC hydrogels against *S. aureus* was evaluated using the disc diffusion assay by measuring the zone of inhibition (**Figure 4.24**). CUR is well known for its antimicrobial properties against a broad range of microorganisms [Mun *et al*., 2013; Hu *et al*., 2013, Silva *et al*., 2018]. Its antimicrobial activity ensues due to its ability to interact with an essential prokaryotic cell division initiating protein (FtsZ) [Silva *et al*., 2018, Rai *et al*., 2008]. Moreover, it has been identified to possess an inhibitory effect against sortase A, a membrane-associated transpeptidase that plays a crucial role in modulating the ability of Gram-positive bacteria (including *S. aureus*) to adhere to the host tissue and cause infection [Hu *et al*., 2013]. The disc diffusion results confirmed that CUR maintained its antimicrobial feature even after encapsulation in the HPβCD cavity, demonstrating the potential use of CUR:HPβCD as an antimicrobial for wound management.

Silver nanoparticles have been intensively studied as antimicrobial agents [Alsammarraie *et al*., 2018, Lyu *et al*., 2020, Sathishkumar *et al*., 2010]. Different mechanisms of action of AgNPs have been proposed as their antibacterial and antifungal effect is not completely known [Guzman *et al*., 2012]. In bacteria, AgNPs have the ability to increase the permeability of the cell membrane, interfere with DNA replication, denaturation of bacterial proteins and release of silver ions inside the bacterial cell [Lyu *et al*., 2020, Guzman *et al*., 2012].

Like $AgNO_3$-loaded BC and AgZ-loaded BC, cAgNP-loaded BC demonstrated higher activity against *P. aeruginosa* as compared to *S. aureus* (Figure 4.29). This could be explained by the difference in the cell structure of Gram positive and Gram negative bacteria. AgNPs have been reported to have the ability to separate cytoplasm from bacterial cell wall (plasmolysis effect), leading to the cell death in *P. aeruginosa*. In *S. aureus*, AgNPs act differently and cause the bacterial cell death by inhibiting the cell wall synthesis [Lyu *et al*., 2020, Guzman *et al*., 2012, Song *et al*., 2006].

Normal skin has the ability to control the water loss by evaporation from the body, to prevent dehydration, which gets compromised when the integrity of the skin is affected by injury. Lamke *et al*., (1977) reported the evaporation water loss of 204±12 g/m^2/24 h from the normal skin, which could go up to 5138.4±201.6 g/m^2/24 h in case of a granulating wound.

An ideal wound dressing material must have a property to control the evaporative water loss from the wound [Hu *et al*., 2019]. High WVTR may lead to dehydration and scab formation, whereas very low WVTR may lead to the accumulation of

exudate, maceration of periwound skin and increased risk of infections [Tyeb *et al*., 2018]. Previous reported studies suggest that a WVTR level of 2000-2500 g/m^2/24 h would be sufficient to maintain an optimum moist environment at the wound site [Hu *et al*., 2019, Adeli *et al*., 2019]. The WVTR results in the present study revealed that the WVTR range of BC (2526.32-3137.68 g/m^2/24h) and CUR:HPβCD-loaded BC hydrogels (2258.53-2460.63 g/m^2/24h) were close to the recommended range, hence would be suitable for wound healing applications. Moreover, the results revealed that the loss of water from neat BC hydrogels was more than from the test hydrogels (CUR:HPβCD-loaded BC). We postulated this is due to the CUR-HPβCD loaded in the BC network structure reducing the void space in the hydrogels and controlling the transmission of water in CUR:HPβCD-loaded BC hydrogels compared to neat BC.

5.4. *In vivo* studies of hydrogels: haemocompatibility, cytocompatibility and antioxidant activity

Haemocompatibility is an important feature for a material to be considered for clinical application as a wound dressing. If not haemocompatible, a material may activate coagulation and adverse cellular response. With the aim of wound management applications, haemocompatiblity of BC and antimicrobial-loaded BC hydrogels was tested. The test results revealed that BC is a non-haemolytic material as % haemolysis caused by BC hydrogels when in contact with defibrinated horse blood was < 0.1 %. These results on the haemocompatible nature of BC are in accordance with findings of Leitão *et al*., (2013) who reported BC as haemocompatible, thus a safe and suitable material in cardiovascular applications for the development of vascular grafts. In another *in vitro* study, BC when maintained

in contact with human blood for 3 h at 37 ºC with gentle inversion every 30 min, demonstrated hemolytic index of 1.43 %, which confirmed its haemocompatible nature [Andrade *et al*., 2011]. Moreover, CUR:HPβCD-loaded BC prepared by dissolving CUR:HPβCD in NS and loaded in padded dry BC also demonstrated haemocompatible nature (<0.20 % percent haemolysis) for wound management applications. $AgNO_3$-loaded BC, AgZ-loaded BC and cAgNP-loaded BC demonstrated high haemolysis (%). The higher haemolysis (%) of the tested hydrogels could be attributed to the use of deionised water instead of the isotonic solution for the synthesis of solution of $AgNO_3$, suspension of AgZ and colloidal cAgNP for loading in padded dry BC. In the case of chronic wound, there could be necrotic tissue or slough at the wound bed, hence the haemolytic behaviour of these hydrogels may be minimal. However, further research on the production of silver-loaded BC and production of AgNP using CUR:HPβCD dissolved in isotonic solution for loading in BC may improve haemocompatibility of these hydrogels.

In addition to haemocompatibility, cytocompatibility is another vital property for a material with potential biomedical application. In the current study, cytocompatibility of BC was tested and the results revealed that BC in cytocompatible with HEK 293 cell line with the cell viability (%) of > 98.5 %. These results are in accordance with other findings where BC has been documented to be cytocompatible for biomedical applications. Jiji *et al*., (2019) developed thymol enriched BC hydrogels for third degree burn wound repair. The authors found these hydrogels to be biocompatible to mouse 3T3 fibroblast cells (*in vitro* study) and effective natural burn wound material in female albino Wistar rats (*in vivo* study). Pértile *et al*., (2012), conducted a BC long-term biocompatibility (up to 1 year) evaluating the biocompatibility of BC

subcutaneous implants and BC nanofibres (injected subcutaneously) in male BALB/c mice (*in vivo* model). The authors found no clinical signs of inflammation at the incision sites, with no foreign body reaction; signs of angiogenesis inside the BC implants were reported. No significant effect on leukocyte haematopoiesis was observed by BC nanofiber implants in the test animals as compared to the controls (with no BC nanofiber implants). Based on these findings, the authors confirmed that BC is an eligible material for biomedical applications [Pértile *et al*., 2012]. Di *et al*., (2017) fabricated transparent composite wound dressings of BC with poly(2-hydroxethyl methacrylate) with and without silver. The authors tested the biocompatibility of these hydrogels (*in vitro*) on the NIH-3T3 (mouse embryonic fibroblast cell line). Both composite hydrogels demonstrated good cell viability, but at each time point (24 h, 36 h and 48 h), BC hydrogels without silver showed slightly higher cell viability (78.5 %, 109 % and 104.5 % respectively) as compared to silver loaded composite hydrogels (72.8 %, 94.5 % and 90.6 % respectively) [Di *et al*., 2017]. These results further confirm the cytocompatible nature of BC. Cytocompability is one of the many intrinsic features of BC leading to its use in fabricating proprietary products like Dermafill™, Biofill®, XCell®, and Gengiflex® [Portela *et al*., 2019, Lee *et al*., 2014, Lopes *et al*., 2014, Moniri *et al*., 2017]. High bacterial burden at the wound site has a deleterious effect on the wound healing, hence the use of an antimicrobial becomes imperative. Since bacteriostatic and/or bactericidal agents may have a harmful effect on the host cells, therefore a benefit:risk ratio has to be evaluated for the selection of antimicrobial wound dressings [Hiro *et al*., 2012]. The use of proprietary silver dressings in chronic wound management to control the microbial bioburden is a good example where the benefit outweighs the risk of cytotoxic effect of silver [Hiro *et al*., 2012, Zou *et al*., 2012]. In

the current study, the MTT cytocompatibility study aims to find out how the antimicrobial agent (silver and CUR) release from the BC-based hydrogels affects the survival of mammalian cells. Different cell lines were used in this study and most of them (Panc 1, MSTO, U251 and A549) tolerated up to 2% CUR:HPβCD over 24hrs and showed very good survival rates (**Figure 4.22a-c**). Despite being very sensitive, the A549 cell line also showed around 60 % survival at the highest tested dose (2 % CUR:HPβCD). Although this will be a significant decrease in cell survival in comparison to control, this dose has not even reached the standard IC50/50 % cell death to define this as a highly toxic effect. Moreover, in patients, this will correspond to how much free CUR is being released from the material and get in the systemic circulation. It is very unlikely that this amount will cause the toxic effect to vital organs. When cell viability (%) was tested for free CUR:HPβCD and CUR:HPβCD-loaded in BC, the experimental results showed that there was no significant difference between the two forms (**Figure 4.22a-c**). Hence, it can be concluded that BC matrix used to deliver CUR:HPβCD inclusion complex does not affect the cell viability. These results are in accordance with other cytotoxicity studies reporting the cytocompatible nature of CUR and its conjugates for biomedical applications. Amirthalingam *et al*., (2015), reported the production of curcumin containing chitosan microcomplex particles and loading these in chitosan scaffold to fabricate antimicrobial wound dressings. The authors tested the cytotoxicity and the ability of these CUR containing chitosan scaffolds on Vero cells as a model for mammalian cells by *in vitro* MTT assay. The results showed that the material was non-toxic and supports cell proliferation (48 h incubation), thus hold the potential for wound management applications [Amirthalingam *et al*., 2015]. In another study, CUR containing nanofibrous scaffolds were found to be sufficiently cytocompatible with L-

929 fibroblasts to support cell growth over a period of 3 days [Kurniawan *et al*., 2017]. Liu *et al*., (2019), reported the synthesised of CUR containing chitosan:aloe membrane for skin regeneration. The biocompatibility tests were undertaken on NIH-3T3 cells (*in vitro*) and on male Wistar rats (*in vivo*) as implants in a full-thickness skin wounds. *In vitro* test results revealed that CUR stimulates proliferation as CUR containing film achieved 112.49 % cell viability (relative) among all the groups tested (Film1: chitosan:aloe vera; Film 2: chitosan:aloe vera-PLGA; Film 3: chitosan:aloe vera-CUR-loaded PLGA). Moreover, in the *in vivo* studies where gauze was used as a control, all the 3 composite films showed better and faster healing than the control group. Among all the composite films, film 3 with CUR showed fastest wound healing with smallest wound size on day 7 and 14. These findings further support the potential wound dressing applications of CUR:HPβCD-loaded BC hydrogels.

Cytocompatibility of $AgNO_3$-loaded BC, AgZ-loaded BC and cAgNP-loaded BC hydrogels was tested on Panc 1, U251 and MSTO cell lines. cAgNP-loaded BC hydrogels demonstrated good cell viability (%) with all the tested cell lines as determined by MTT assay (**Figure 4.28**). Panc 1, U251 and MSTO showed 84.08 ± 7.80 %, 95.4 ± 4.42 % and 95.58 ± 8.05 % cell viability (%) respectively. When the test was undertaken with the equivalent amount of free cAgNP, the viability (%) was highly reduced with Panc 1 (23.77 ± 5.05 %), U251 (33.58 ± 9.61 %) and MSTO (38.21 ± 12.31 %). These results suggest that BC controls the release of cAgNP, thus minimising the cytotoxic effect on the mammalian cells. These findings support the potential application of cAgNP-loaded BC for wound management as hydrogel dressings.

$AgNO_3$-loaded BC and AgZ-loaded BC have variable response with the tested cell lines (**Figure 4.11a&b**). $AgNO_3$-loaded BC displayed lower cytocompatibilty as compared to AgZ-loaded BC against all three cell lines (Panc 1 12.4 ± 1.86% vs 28.8 ± 9.38; U251 30.58 ± 12.47 vs 58.87 ± 4.1 and MSTO 58.01 ± 20.93 vs 73.39 ± 8.25 % for $AgNO_3$-loaded BC vs AgZ-loaded BC). When free $AgNO_3$ and AgZ were tested, the viability was highly reduced. These results further confirm that BC acts as a controlled release matrix, thus minimising the cytotoxic effects of strong antimicrobial agents like silver. The cytotoxicity of 0.55 % $AgNO_3$-loaded BC and 1 % AgZ-loaded BC could be improved by reducing the amount of silver content in the hydrogels. This could be decided based on the type and site of wound, dose requirement for controlling infection at the wound site and the risk to benefit ratio assessment, by the wound management team.

In addition to infection, oxidative stress has been identified, through preclinical and clinical studies, as one of the major causes of nonhealing in chronic wounds [Mohanty and Sahoo, 2017]. CUR is reported as a potent antioxidant due to its ability to reduce reactive oxygen species such as super oxide radicals, lipid peroxyl radicals and hydroxyl radicals [Akbik *et al*., 2014, Jena *et al*., 2011]. Its antioxidant activity arises due to its ability to undergo H-atom abstraction from its phenol groups, giving rise to a stable, delocalised radical species [Mohanty and Sahoo, 2017]. Several methods have been adopted to assess the free radical scavenging potential of anti-oxidant substance and the DPPH assay is still one of the routinely practiced method for this assessment. In the current study, along with $AgNO_3$, AgZ and HPβCD, the antioxidant activity of CUR:HPβCD was assessed by this assay. Moreover, the study was extended to test CUR:HPβCD reduced AgNP as well. The reaction of DPPH

radicals with antioxidant is a kinetic driven process, which varies for different antioxidants. In the current study, a fixed reaction time mode of 30 min was adopted for estimation of the antioxidant activity [Mishra *et al*., 2012].

The test results confirmed that HPβCD used as an aqueous solubility enhancing carrier for CUR does not have antioxidant activity. These results are in accordance with findings of Rakmai *et al*., (2018), who reported that antioxidant activity of essential oil from guava leaves gets more stable to sunlight exposure after encapsulation in HPβCD. Whilst determining the antioxidant activity of free guava leaf oil, encapsulated guava leaf oil in HPβCD and free HPβCD by the DPPH assay, the authors observed no antioxidant activity for free HPβCD [Rakmai *et al*., 2018]. Also, $AgNO_3$ and AgZ did not reveal free radical scavenging activity in the DPPH assay. Due to CUR, the inclusion complex of CUR:HPβCD demonstrated antioxidant activity with IC_{50} value of 1087.49 ± 6.47 µg/mL. These findings support the antioxidant potential of BC hydrogels loaded with CUR:HPβCD to reduce the oxidative stress at the impaired wound site. The results confirmed the preservation of antioxidant activity of CUR in the inclusion complex and are in accordance with Aytac & Uyar (2017). The authors reported time dependent antioxidant activity (*in vitro* DPPH assay) for CUR:HPβCD-polylactic acid electrospun nanofibers [Aytac & Uyar, 2017].

Wound dressing with antioxidant properties [Ahmed *et al*., 2018] along with antimicrobial activity may prove beneficial. Colloidal cAgNP aqueous medium produced using CUR:HPβCD also demonstrated antioxidant activity as determined by DPPH assay. When loaded in BC to produce cAgNP-loaded BC hydrogels, this could prove beneficial in wound healing process and reduce oxidative stress at the wound site, which may otherwise interfere with the healing process [Cano Sanchez

et al., 2018]. These test results support the wound management application of CUR:HPβCD-loaded BC and cAgNP-loaded BC as an antimicrobial and antioxidant hydrogel dressings.

Attributing to the unique properties, the hydrogels produced in the current study could be employed in the management of infected, heavily exudating wounds, as it allows the healing process to be monitored without removing the dressing, hence no damage to fragile underlying tissue.

Chapter 6
Conclusion

The results presented here confirm the excellent cytocompatibility and haemocompatibility of biosynthetic BC hydrogels *in vitro*. An analysis of the physicochemical properties also indicates that BC displays good thermal stability at physiological conditions. The moist and responsive nature of BC, along with superb water imbibing capabilities, make it an ideal biomaterial as a matrix for wound dressings, as all of these features are advantageous for modern wound dressing materials.

The present study demonstrates the production, physicochemical characterisation, *in vitro* biocompatibility and antimicrobial performance of biosynthetic BC based hydrogels for potential wound management applications. Different antimicrobial healing agents were loaded in BC to produce hydrogels and their potential application in wound management as hydrogel dressings was evaluated.

Silver-loaded BC hydrogels demonstrated broad-spectrum (against, Gram +ve and Gram –ve bacteria) antimicrobial activity for the management of chronic, infected wounds. AgZ-loaded BC hydrogels offered prolonged antimicrobial activity as compared to $AgNO_3$-loaded BC with an equivalent amount of elemental silver. Both these dressings did not display the capability of scavenging free radicals. Both silver-loaded BC hydrogels demonstrated higher cell viability (%) as compared to the equivalent free silver compounds, confirming that BC controls silver release in hydrogels, hence minimises the cytotoxicity to mammalian cell lines. The haemocompatibility of silver-loaded BC hydrogels needs further research attention, as the currently produced hydrogels displayed some haemolytic property. This problem could be resolved by replacing water with isotonic solvent for $AgNO_3$ and

AgZ and/or by reducing the concentration of the silver compound. Transparency of $AgNO_3$-loaded BC ensures monitoring of the healing process without the need of removing the dressing from the site. However, AgZ-loaded BC, due to the nature of zeolite component, had limited transparency but shows high moisture content, imparting malleability and strong antimicrobial properties. These features advocate the potential application of these silver-loaded BC hydrogels in infected chronic wound management as antimicrobial dressings. Moreover, AgZ-loaded BC offered an added advantage of a controlled and prolonged silver release, which could be beneficial in clinical practice.

The physicochemical characterisation confirmed the formation of IC of CUR:HPβCD with enhanced aqueous solubility compared to free CUR. Varying the solvent volume ratios during the solvent evaporation protocol, IC 75 emerged to be the best preparation method with the highest encapsulation efficacy. The CUR:HPβCD-loaded-BC hydrogels demonstrated high light transmission, a property that has a potential of clinical wound monitoring without the need to remove the dressing. Moreover, these hydrogels offer optimum WVTR that could help maintain the moist environment at the wound site. Their high moisture content, biocompatibility (cytocompatibility and haemocompatibility), antimicrobial and antioxidant properties advocates their potential application as hydrogel dressings for chronic, infected wound management. These findings suggest that biosynthetic CUR:HPβCD-loaded BC hydrogels could represent an alternative in the dressing landscape for wound management.

Moreover, the current study demonstrates the production, physicochemical and *in vitro* characterisation of cAgNP-loaded BC hydrogels. The results confirmed that cAgNPs were successfully synthesised, following the green chemistry approach using aqueous solution of CUR:HPβCD and loaded in BC to produce hydrogels with a potential wound dressing application. These hydrogels demonstrated broad-spectrum antimicrobial activity along with antioxidant properties. Moreover, the hydrogels showed cytocompatibility with the tested cell lines. The high moisture content and the good level of transparency further advocate their potential application in the management of chronic wounds with high microbial bioburden.

Future Work

Further research aims to extend the antimicrobial studies on a wider spectrum of pathogenic organisms, including common opportunistic fungi that pose a significant health risk to patients suffering from infected wounds and in particular, immunocompromised individuals which can result in candidiasis/candidemia and invasive aspergillosis.

Also, the current work would be extended to optimise the performance of BC hydrogels loaded with microencapsulated antimicrobial healing agents to provide a responsive, controlled release delivery platform, whilst minimising the toxicity associated with localised high concentrations of topical silver. The set objective would be approached by producing modified composite hydrogels of BC with polymers like poly-γ-glutamic acid (γ-PGA), chitosan and poly(sulfobetaine methacrylate) (SBMA). The preliminary work has already been started on the composite BC hydrogels with chitosan (in collaboration with University of Sumatera

Utara, Indonesia), BC composite hydrogels with (γ-PGA) (in collaboration with Silesian University of Technology, Gliwice, Poland) and BC-SBMA composite hydrogels (in collaboration with Sun Yat-sen University, Guangzhou, China).

Future work would also involve a series of *in vivo* systematic studies on animal models to better understand the healing properties of these hydrogels when in contact with wound fluid, blood and immune cells. The data obtained from these studies would allow evaluation and potential progressive translational research to the next stage of clinical trials.

Chapter 7
References

- Abdelrahman T. and Newton H. (2011). Wound dressings: principles and practice. *Surgery (Oxford) 29*, 491-495.
- Adeli, H., Khorasani, M. T. and Parvazinia, M. (2019) Wound dressing based on electrospun PVA/chitosan/starch nanofibrous mats: Fabrication, antibacterial and cytocompatibility evaluation and in vitro healing assay, *International Journal of Biological Macromolecules*, Netherlands, Elsevier B.V, **122**, pp. 238–254, [online] Available from: https://www.sciencedirect.com/science/article/pii/S0141813018337644.
- Aguiar, P., Amaral, C., Rodrigues, A. and de Souza, A. (2017) A diabetic foot ulcer treated with hydrogel and hyperbaric oxygen therapy: a case study, *Journal of Wound Care*, London, MA Healthcare, **26**(11), pp. 692–695, [online] Available from: https://www.ncbi.nlm.nih.gov/pubmed/29131751.
- Ahmad, S., Ahmad, M., Manzoor, K., Purwar, R. and Ikram, S. (2019) A review on latest innovations in natural gums based hydrogels: Preparations & applications, *International Journal of Biological Macromolecules*, [online] Available from: http://www.sciencedirect.com/science/article/pii/S0141813019304568.
- Ahmed, E. M. (2015) Hydrogel: Preparation, characterization, and applications: a review, *Journal of Advanced Research*, **6**, pp. 105-121.
- Ahmed, A. S., Mandal, U. K., Taher, M., Susanti, D. and Jaffri, J. M. (2017) PVA-PEG physically cross-linked hydrogel film as a wound dressing: experimental design and optimization, *Pharmaceutical Development and Technology*, England, Taylor & Francis, **23**(8), pp. 751–760, [online] Available from: http://www.tandfonline.com/doi/abs/10.1080/10837450.2017.1295067.
- Ahmed, O. M., Mohamed, T., Moustafa, H., Hamdy, H., Ahmed, R. R. and Aboud, E. (2018) Quercetin and low level laser therapy promote wound healing process in

diabetic rats via structural reorganization and modulatory effects on inflammation and oxidative stress, *Biomedicine & Pharmacotherapy*, [online] Available from: http://www.sciencedirect.com/science/article/pii/S0753332217360638.

- Akbik, D., Ghadiri, M., Chrzanowski, W. and Rohanizadeh, R. (2014) Curcumin as a wound healing agent, *Life Sciences*, Netherlands, Elsevier Inc, **116**(1), pp. 1–7, [online] Available from: https://www.sciencedirect.com/science/article/pii/S0024320514007036.
- Akhtar, M. F., Hanif, M. and Ranjha, N. M. (2016) Methods of synthesis of hydrogels … A review, *Saudi Pharmaceutical Journal*, Saudi Arabia, Elsevier B.V, **24**(5), pp. 554–559, [online] Available from: http://dx.doi.org/10.1016/j.jsps.2015.03.022.
- Alibolandi, M., Mohammadi, M., Taghdisi, S. M., Abnous, K. and Ramezani, M. (2017) Synthesis and preparation of biodegradable hybrid dextran hydrogel incorporated with biodegradable curcumin nanomicelles for full thickness wound healing, *International Journal of Pharmaceutics*, Netherlands, Elsevier B.V, **532**(1), pp. 466–477, [online] Available from: https://www.sciencedirect.com/science/article/pii/S0378517317309080.
- Almeida, M., Reis, R. L. and Silva, T. H. (2020) Marine invertebrates are a source of bioadhesives with biomimetic interest, *Materials Science & Engineering C*, Netherlands, Elsevier B.V, **108**, p. 110467, [online] Available from: http://dx.doi.org/10.1016/j.msec.2019.110467.
- Alsammarraie, F. K., Wang, W., Zhou, P., Mustapha, A. and Lin, M. (2018) Green synthesis of silver nanoparticles using turmeric extracts and investigation of their antibacterial activities, *Colloids and Surfaces B: Biointerfaces*, Netherlands, Elsevier B.V, **171**, pp. 398–405, [online] Available from: https://www.sciencedirect.com/science/article/pii/S0927776518305071.

- Amirthalingam, M., Kasinathan, N., Mutalik, S. and Udupa, N. (2015) In vitro biocompatibility and release of curcumin from curcumin microcomplex-loaded chitosan scaffold, *Journal of microencapsulation*, England, **32**(4), p. 364, [online] Available from: https://www.ncbi.nlm.nih.gov/pubmed/25893983.
- Andrade, F. K., Silva, J. P., Carvalho, M., Castanheira, E. M. S., Soares, R. and Gama, M. (2011) Studies on the hemocompatibility of bacterial cellulose, *Journal of Biomedical Materials Research Part A*, Hoboken, Wiley Subscription Services, Inc., A Wiley Company, (4), pp. 554–566, [online] Available from: https://onlinelibrary.wiley.com/doi/abs/10.1002/jbm.a.33148.
- Andreu, V., Mendoza, G., Arruebo, M. and Irusta, S. (2015) Smart Dressings Based on Nanostructured Fibers Containing Natural Origin Antimicrobial, Anti-Inflammatory, and Regenerative Compounds, *Materials (Basel, Switzerland)*, Switzerland, MDPI AG, **8**(8), pp. 5154–5193, [online] Available from: https://www.ncbi.nlm.nih.gov/pubmed/28793497.
- Archana, D., Singh, B. K., Dutta, J. and Dutta, P. (2013) In vivo evaluation of chitosan–PVP–titanium dioxide nanocomposite as wound dressing material, *Carbohydrate Polymers*, England, Elsevier Ltd, **95**(1), pp. 530–539, [online] Available from: https://www.sciencedirect.com/science/article/pii/S0144861713002725.
- Arroyo, A. A., Casanova, P. L., Soriano, J. V. and Torra i Bou, J. (2015) Open-label clinical trial comparing the clinical and economic effectiveness of using a polyurethane film surgical dressing with gauze surgical dressings in the care of post-operative surgical wounds, *International Wound Journal*, Oxford, UK, Blackwell Publishing Ltd, **12**(3), pp. 285–292, [online] Available from: https://onlinelibrary.wiley.com/doi/abs/10.1111/iwj.12099.

- ASTM E96 / E96M-16 (2016). Standard Test Methods for Water Vapor Transmission of Materials.
- ASTM F756-17 (2017). Standard Practice for Assessment of Hemolytic Properties of Materials.
- Aytac, Z. and Uyar, T. (2017) Core-shell nanofibers of curcumin/cyclodextrin inclusion complex and polylactic acid: Enhanced water solubility and slow release of curcumin, *International Journal of Pharmaceutics*, Netherlands, Elsevier B.V, **518**(1–2), pp. 177–184, [online] Available from: http://dx.doi.org/10.1016/j.ijpharm.2016.12.061.
- Azeredo, H. M. C., Barud, H., Farinas, C. S., Vasconcellos, V. M. and Claro, A. M. (2019) Bacterial Cellulose as a Raw Material for Food and Food Packaging Applications, *Frontiers in Sustainable Food Systems*, Frontiers Media S.A, **3**, [online] Available from: https://www.openaire.eu/search/publication?articleId=doajarticles::27a7dcb10dda2ab586da136aaeb8289d.
- Balakrishnan, B., Mohanty, M., Umashankar, P. and Jayakrishnan, A. (2005) Evaluation of an in situ forming hydrogel wound dressing based on oxidized alginate and gelatin, *Biomaterials*, Netherlands, Elsevier Ltd, **26**(32), pp. 6335–6342, [online] Available from: https://www.sciencedirect.com/science/article/pii/S0142961205003194.
- Balan, V. and Verestiuc, L. (2014) Strategies to improve chitosan hemocompatibility: A review, *European Polymer Journal*, Elsevier Ltd, **53**, pp. 171–188, [online] Available from: https://www.sciencedirect.com/science/article/pii/S0014305714000433.

- Bankoti, K., Rameshbabu, A. P., Datta, S., Datta, P., Maity, P. P., Goswami, P., Ghosh, S. K., Mitra, A. and Dhara, S. (2017) Accelerated healing of full thickness dermal wounds by macroporous waterborne polyurethane-chitosan hydrogel scaffolds, *Materials Science & Engineering C*, Netherlands, Elsevier B.V, **81**, pp. 133–143, [online] Available from: https://www.sciencedirect.com/science/article/pii/S092849311632848X.
- Barrientos, S., Stojadinovic, O., Golinko, M. S., Brem, H. and Tomic-Canic, M. (2008) PERSPECTIVE ARTICLE: Growth factors and cytokines in wound healing, *Wound Repair and Regeneration*, Malden, USA, Blackwell Publishing Inc, **16**(5), pp. 585–601, [online] Available from: https://onlinelibrary.wiley.com/doi/abs/10.1111/j.1524-475X.2008.00410.x.
- Barud, H., Assunção, R., Martines, M., Dexpert-Ghys, J., Marques, R., Messaddeq, Y. and Ribeiro, S. (2008) Bacterial cellulose–silica organic–inorganic hybrids, *Journal of Sol-Gel Science and Technology*, Boston, Springer US, **46**(3), pp. 363–367, [online] Available from: https://search.proquest.com/docview/2259559871.
- Behera, S. S., Das, U., Kumar, A., Bissoyi, A. and Singh, A. K. (2017) Chitosan/TiO2 composite membrane improves proliferation and survival of L929 fibroblast cells: Application in wound dressing and skin regeneration, *International Journal of Biological Macromolecules*, Elsevier B.V, **98**, pp. 329–340, [online] Available from: https://www.sciencedirect.com/science/article/pii/S0141813016324965.
- Boffito, M., Sirianni, P., Di Rienzo, A.M. and Chiono, V. (2014) Thermosensitive block copolymer hydrogels based on poly(ε-caprolactone) and polyethylene glycol for biomedical applications: State of the art and future perspectives, *Journal of Biomedical Materials Research: Part A*. **103**; pp. 1276–1290. doi:10.1002/jbm.a.35253.

- Bomberger, J. M., Maceachran, D. P., Coutermarsh, B. A., Ye, S., O'Toole, G. A. and Stanton, B. A. (2009) Long-Distance Delivery of Bacterial Virulence Factors by Pseudomonas aeruginosa Outer Membrane Vesicles, *PLoS pathogens*, United States, Public Library of Science, **5**(4), p. e1000382, [online] Available from: https://www.ncbi.nlm.nih.gov/pubmed/19360133.
- Boonkaew, B., Barber, P. M., Rengpipat, S., Supaphol, P., Kempf, M., He, J., John, V. T. and Cuttle, L. (2014) Development and Characterization of a Novel, Antimicrobial, Sterile Hydrogel Dressing for Burn Wounds: Single-Step Production with Gamma Irradiation Creates Silver Nanoparticles and Radical Polymerization, *Journal of Pharmaceutical Sciences*, United States, Elsevier Inc, **103**(10), pp. 3244–3253, [online] Available from: https://www.sciencedirect.com/science/article/pii/S0022354915303944.
- Boonkaew, B., Kempf, M., Kimble, R., Supaphol, P. and Cuttle, L. (2014a) Antimicrobial efficacy of a novel silver hydrogel dressing compared to two common silver burn wound dressings: Acticoat™ and PolyMem Silver, *Burns*, Netherlands, Elsevier Ltd, **40**(1), pp. 89–96, [online] Available from: https://www.clinicalkey.es/playcontent/1-s2.0-S0305417913001587.
- Brett, D. W. (2006) A discussion of silver as an antimicrobial agent: alleviating the confusion, *Ostomy/wound management*, United States, **52**(1), pp. 34–41, [online] Available from: https://www.ncbi.nlm.nih.gov/pubmed/16464989.
- Brölmann, F. E., Eskes, A. M., Goslings, J. C., Niessen, F. B., de Bree, R., Vahl, A. C., Pierik, E. G., Vermeulen, H. and Ubbink, D. T. (2013) Randomized clinical trial of donor-site wound dressings after split-skin grafting, *British journal of surgery*, England, Wiley Subscription Services, Inc, **100**(5), pp. 619–627, [online] Available from:

https://www.narcis.nl/publication/RecordID/oai:pure.amc.nl:publications%2F498b2a01-8306-4a43-8864-d0f91089226c.

- Caló, E. and Khutoryanskiy, V. V. (2015) Biomedical applications of hydrogels: A review of patents and commercial products, *European Polymer Journal*, Elsevier Ltd, **65**, pp. 252–267, [online] Available from: http://dx.doi.org/10.1016/j.eurpolymj.2014.11.024.
- Cano Sanchez, M., Lancel, S., Boulanger, E. and Neviere, R. (2018) Targeting Oxidative Stress and Mitochondrial Dysfunction in the Treatment of Impaired Wound Healing: A Systematic Review, *Antioxidants (Basel, Switzerland)*, Switzerland, MDPI AG, **7**(8), p. 98, [online] Available from: https://www.ncbi.nlm.nih.gov/pubmed/30042332.
- Cao, Y., Naseri, M., He, Y., Xu, C., Walsh, L. J. and Ziora, Z. M. (2019) Non-antibiotic Antimicrobial Agents to Combat Biofilm-forming Bacteria, *Journal of Global Antimicrobial Resistance*, Elsevier Ltd, [online] Available from: http://dx.doi.org/10.1016/j.jgar.2019.11.012.
- Capanema, N. S. ., Mansur, A. A. ., Mansur, H. S., de Jesus, A. C., Carvalho, S. M. and de Oliveira, L. C. (2018) Superabsorbent crosslinked carboxymethyl cellulose-PEG hydrogels for potential wound dressing applications, *International Journal of Biological Macromolecules*, Netherlands, Elsevier B.V, **106**, pp. 1218–1234, [online] Available from: https://www.sciencedirect.com/science/article/pii/S0141813017316756.
- Capella, V., Rivero, R. E., Liaudat, A. C., Ibarra, L. E., Roma, D. A., Alustiza, F., Mañas, F., Barbero, C. A., Bosch, P., Rivarola, C. R. and Rodriguez, N. (2019) Cytotoxicity and bioadhesive properties of poly-N-isopropylacrylamide

hydrogel, *Heliyon*, [online] Available from: http://www.sciencedirect.com/science/article/pii/S2405844018387383.

- Cappello, J., Crissman, J., Dorman, M., Mikolajczak, M., Textor, G., Marquet, M. and Ferrari, F. (1990) Genetic Engineering of Structural Protein Polymers, *Biotechnology Progress*, USA, American Chemical Society, **6**(3), pp. 198–202, [online] Available from: https://onlinelibrary.wiley.com/doi/abs/10.1021/bp00003a006.
- Castellano, J. J., Shafii, S. M., Ko, F., Donate, G., Wright, T. E., Mannari, R. J., Payne, W. G., Smith, D. J. and Robson, M. C. (2007) Comparative evaluation of silver-containing antimicrobial dressings and drugs, *International Wound Journal*, Oxford, UK, Blackwell Publishing Ltd, **4**(2), pp. 114–122, [online] Available from: https://onlinelibrary.wiley.com/doi/abs/10.1111/j.1742-481X.2007.00316.x.
- Castro, C., Zuluaga, R., Putaux, J.-L., Caro, G., Mondragon, I. and Gañán, P. (2011) Structural characterization of bacterial cellulose produced by Gluconacetobacter swingsii sp. from Colombian agroindustrial wastes, *Carbohydrate Polymers*, Elsevier Ltd, **84**(1), pp. 96–102, [online] Available from: http://dx.doi.org/10.1016/j.carbpol.2010.10.072.
- Catanzano, O., D'Esposito, V., Acierno, S., Ambrosio, M. ., De Caro, C., Avagliano, C., Russo, R., Russo, P., Miro, A., Ungaro, F., Calignano, A., Formisano, P. and Quaglia, F. (2015) Alginate–hyaluronan composite hydrogels accelerate wound healing process, *Carbohydrate Polymers*, England, Elsevier Ltd, **131**, pp. 407–414, [online] Available from: https://www.sciencedirect.com/science/article/pii/S0144861715005159.
- Cereceres, S., Touchet, T., Browning, M. B., Smith, C., Rivera, J., Höök, M., Whitfield-Cargile, C., Russell, B. and Cosgriff-Hernandez, E. (2015) Chronic Wound Dressings Based on Collagen-Mimetic Proteins, *Advances in Wound Care*, United

States, Mary Ann Liebert, Inc, **4**(8), pp. 444–456, [online] Available from: https://www.liebertpub.com/doi/abs/10.1089/wound.2014.0614.

- Champeau, M., Póvoa, V., Militão, L., Cabrini, F. M., Picheth, G. F., Meneau, F., Jara, C. P., de Araujo, E. P. and de Oliveira, M. G. (2018) Supramolecular poly(acrylic acid)/F127 hydrogel with hydration-controlled nitric oxide release for enhancing wound healing, *Acta Biomaterialia*, England, Elsevier Ltd, **74**, pp. 312–325, [online] Available from: https://www.sciencedirect.com/science/article/pii/S1742706118302940.
- Chan, C. K., Shin, J. and Jiang, S. X. K. (2018) Development of Tailor-Shaped Bacterial Cellulose Textile Cultivation Techniques for Zero-Waste Design, *Clothing and Textiles Research Journal*, Los Angeles, CA, SAGE Publications, **36**(1), pp. 33–44, [online] Available from: https://journals.sagepub.com/doi/full/10.1177/0887302X17737177.
- Chao, Y., Sugano, Y. and Shoda, M. (2001) Bacterial cellulose production under oxygen-enriched air at different fructose concentrations in a 50-liter, internal-loop airlift reactor, *Applied Microbiology and Biotechnology*, Berlin/Heidelberg, Springer-Verlag, **55**(6), pp. 673–679, [online] Available from: https://www.ncbi.nlm.nih.gov/pubmed/11525613.
- Chaturvedi, A., Bajpai, J., Bajpai, A. K. and K.Singh, S. (2016) Evaluation of poly (vinyl alcohol) based cryogel–zinc oxide nanocomposites for possible applications as wound dressing materials, *Materials Science & Engineering C*, Netherlands, Elsevier B.V, **65**, pp. 408–418, [online] Available from: https://www.sciencedirect.com/science/article/pii/S0928493116303526.
- Chawla, P. R., Bajaj, I. B., Survase, S. A. and Singhal, R. S. (2009) Microbial cellulose: fermentative production and applications, *Food Technology and*

Biotechnology, Sveuciliste U Zagrebu, **47**(2), pp. 107–124, [online] Available from: https://doaj.org/article/542393daf4c840128de74c1dc9e67123.

- Chen, H., Chen, Y., Xing, X., Tan, H., Jia, Y., Zhou, T., Ling, Z. and Hu, X. (2017) Covalently antibacterial alginate-chitosan hydrogel dressing integrated gelatin microspheres containing tetracycline hydrochloride for wound healing, *Materials Science & Engineering C*, Netherlands, Elsevier B.V, **70**(Pt 1), pp. 287–295, [online] Available from: https://www.sciencedirect.com/science/article/pii/S0928493116311018.
- Chen, L., Han, D. and Jiang, L. (2011) On improving blood compatibility: From bioinspired to synthetic design and fabrication of biointerfacial topography at micro/nano scales, *Colloids and Surfaces B: Biointerfaces*, Netherlands, Elsevier B.V, **85**(1), pp. 2–7, [online] Available from: https://www.sciencedirect.com/science/article/pii/S0927776510005990.
- Chen, S.-H., Tsao, C.-T., Chang, C.-H., Lai, Y.-T., Wu, M.-F., Chuang, C.-N., Chou, H.-C., Wang, C.-K. and Hsieh, K.-H. (2013) Assessment of reinforced poly(ethylene glycol) chitosan hydrogels as dressings in a mouse skin wound defect model, *Materials Science & Engineering C*, Netherlands, Elsevier B.V, **33**(5), pp. 2584–2594, [online] Available from: http://dx.doi.org/10.1016/j.msec.2013.02.031.
- Chen, Z., Bertin, R. and Froldi, G. (2013a) EC50 estimation of antioxidant activity in DPPH assay using several statistical programs, *Food Chemistry*, England, Elsevier Ltd, **138**(1), pp. 414–420, [online] Available from: http://dx.doi.org/10.1016/j.foodchem.2012.11.001.
- Chhatri, A., Bajpai, A. ., Bajpai, J., Sandhu, S., Jain, N. and Biswas, J. (2011) Cryogenic fabrication of savlon loaded macroporous blends of alginate and polyvinyl alcohol (PVA). Swelling, deswelling and antibacterial behaviors, *Carbohydrate*

Polymers, Elsevier Ltd, **83**(2), pp. 876–882, [online] Available from: https://www.sciencedirect.com/science/article/pii/S014486171000723X.

- Chopra, I. (2007) The increasing use of silver-based products as antimicrobial agents: a useful development or a cause for concern?, *Journal of Antimicrobial Chemotherapy*, **59**(4), pp. 587-590.
- Cirillo, G., Curcio, M., Spizzirri, U. G., Vittorio, O., Tucci, P., Picci, N., Iemma, F., Hampel, S. and Nicoletta, F. P. (2017) Carbon nanotubes hybrid hydrogels for electrically tunable release of Curcumin, *European Polymer Journal*, Elsevier Ltd, **90**, pp. 1–12, [online] Available from: https://www.sciencedirect.com/science/article/pii/S0014305716317219.
- Coates, A. and Hu, Y. (2015). *Conventional Antibiotics – Revitalized by New Agents*. In: Phoenix, D.A., Harris, F. and Dennison, S.R. (eds) Novel Antimicrobial Agents and Strategies, 1st ed., Wiley, Germany, pp. 17-33.
- Copcia, V., Luchian, C., Dunca, S., Bilba, N. and Hristodor, C. (2011) Antibacterial activity of silver-modified natural clinoptilolite, *Journal of Materials Science*, New York, Springer US, **46**(22), pp. 7121–7128, [online] Available from: https://search.proquest.com/docview/2259702055.
- Costa, A. F. S., Almeida, F. C. G., Vinhas, G. M. and Sarubbo, L. A. (2017) Production of Bacterial Cellulose by *Gluconacetobacter hansenii* Using Corn Steep Liquor As Nutrient Sources, *Frontiers in microbiology*, Switzerland, Frontiers Media S.A, **8**, p. 2027, [online] Available from: https://www.ncbi.nlm.nih.gov/pubmed/29089941.
- Costa, P. and Sousa Lobo, J. M. (2001) Modeling and comparison of dissolution profiles, *European Journal of Pharmaceutical Sciences*, Netherlands, Elsevier B.V, [online] Available from: http://dx.doi.org/10.1016/S0928-0987(01)00095-1.

- da Silva, L. P., Santos, T. C., Rodrigues, D. B., Pirraco, R. P., Cerqueira, M. T., Reis, R. L., Correlo, V. M. and Marques, A. P. (2017) Stem Cell-Containing Hyaluronic Acid-Based Spongy Hydrogels for Integrated Diabetic Wound Healing, *Journal of Investigative Dermatology*, United States, Elsevier Inc, **137**(7), pp. 1541–1551, [online] Available from: https://www.sciencedirect.com/science/article/pii/S0022202X17311612.
- Das, N. (2013). Preparation methods and properties of hydrogel: A Review, *International Journal of Pharmacy and Pharmaceutical Sciences*, **5**(3), pp. 112-117.
- Dash, S., Murthy, P. N., Nath, L. and Chowdhury, P. (2010) Kinetic modeling on drug release from controlled drug delivery systems, *Acta poloniae pharmaceutica*, Poland, **67**(3), p. 217, [online] Available from: https://www.ncbi.nlm.nih.gov/pubmed/20524422.
- Daunton, C., Kothari, S., Smith, L. and Steele, D. (2012) A history of materials and practices for wound management, *Wound Practice & Research: Journal of the Australian Wound Management Association*, **20**(4), pp. 174–186.
- de Oliveira Barud, H. G., da Silva, R. R., da Silva Barud, H., Tercjak, A., Gutierrez, J., Lustri, W. R., de Oliveira, O. B. and Ribeiro, S. J. . (2016) A multipurpose natural and renewable polymer in medical applications: Bacterial cellulose, *Carbohydrate Polymers*, England, Elsevier Ltd, **153**, pp. 406–420, [online] Available from: http://dx.doi.org/10.1016/j.carbpol.2016.07.059.
- Dealey, C. (2012) The Physiology of Wound Healing, in: the care of wounds: A Guide for Nurses, Wiley-Blackwell, U.K., pp. 1–14. doi:10.1002/9780470774946.ch1.
- Dealey, C. (2012a) General Principles of Wound Management, in: the care of wounds: A Guide for Nurses, Wiley-Blackwell, U.K., pp. 61–91. doi:10.1002/9780470774946.ch1.

- Del Valle, E. M. M. (2004) Cyclodextrins and their uses: a review, *Process Biochemistry*, Elsevier Ltd, [online] Available from: http://dx.doi.org/10.1016/S0032-9592(03)00258-9.
- Demidova-Rice, T. N., Hamblin, M. R. and Herman, I. M. (2012) Acute and impaired wound healing: pathophysiology and current methods for drug delivery, part 1: normal and chronic wounds: biology, causes, and approaches to care, *Advances in skin & wound care*, United States, **25**(7), pp. 304–314, [online] Available from: https://www.ncbi.nlm.nih.gov/pubmed/22713781.
- Dhivya, S., Padma, V. V. and Santhini, E. (2015) Wound dressings – a review, *BioMedicine*, Taichung, China Medical University, **5**(4), pp. 1–5, [online] Available from: https://www.ncbi.nlm.nih.gov/pubmed/26615539.
- Di, Z., Shi, Z., Ullah, M. W., Li, S. and Yang, G. (2017) A transparent wound dressing based on bacterial cellulose whisker and poly(2-hydroxyethyl methacrylate), *International Journal of Biological Macromolecules*, Netherlands, Elsevier B.V, **105**(Pt 1), pp. 638–644, [online] Available from: https://www.sciencedirect.com/science/article/pii/S0141813017316835.
- Dobre, T., Stoica, A., Parvulescu, O. C., Stroescu, M. and Iavorschi, G. (2008) Factors Influence on Bacterial Cellulose Growth in Static Reactors, *Revista de Chimie*, **59**(5).
- Du, L., and Liu, W. (2012) Occurrence, fate, and ecotoxicity of antibiotics in agro-ecosystems. A review, *Agronomy for Sustainable Development*, Paris, Springer-Verlag, **32**(2), pp. 309–327, [online] Available from: https://hal.archives-ouvertes.fr/hal-00930539.
- Dufour, G., Evrard, B. and de Tullio, P. (2015) Rapid quantification of 2-hydroxypropyl-β-cyclodextrin in liquid pharmaceutical formulations by 1H nuclear

magnetic resonance spectroscopy, *European Journal of Pharmaceutical Sciences*, Elsevier B.V, **73**, pp. 20–28, [online] Available from: http://dx.doi.org/10.1016/j.ejps.2015.03.005.

- Dutta, P. and Wang, B. (2019) Zeolite-supported silver as antimicrobial agents, *Coordination Chemistry Reviews*, Elsevier B.V, **383**, pp. 1–29, [online] Available from: http://dx.doi.org/10.1016/j.ccr.2018.12.014.
- El-Sherbiny, I. M. and Yacoub, M. H. (2013) Hydrogel scaffolds for tissue engineering: Progress and challenges, Bloomsbury Qatar Foundation Journals, [online] Available from: http://hdl.handle.net/10044/1/29584.
- El-Shishtawy, R., El-Shishtawy, R., Asiri, A., Asiri, A., Abdelwahed, N., Abdelwahed, N., Al-Otaibi, M. and Al-Otaibi, M. (2011) In situ production of silver nanoparticle on cotton fabric and its antimicrobial evaluation, *Cellulose*, Dordrecht, Springer Netherlands, **18**(1), pp. 75–82, [online] Available from: https://search.proquest.com/docview/2259903866.
- Embuscado, M. E., BeMiller, J. N. and Marks, J. S. (1996) Isolation and partial characterization of cellulose produced by Acetobacter xylinum, *Food Hydrocolloids*, Elsevier Ltd, **10**(1), pp. 75–82, [online] Available from: http://dx.doi.org/10.1016/S0268-005X(96)80057-9.
- Esa, F., Tasirin, S. M. and Rahman, N. A. (2014) Overview of Bacterial Cellulose Production and Application, *Agriculture and Agricultural Science Procedia*, Elsevier B.V, **2**, pp. 113–119, [online] Available from: http://dx.doi.org/10.1016/j.aaspro.2014.11.017.
- Fan, L., Yang, J., Yang, H., Peng, M. and Hu, J. (2016) Preparation and characterization of chitosan/gelatin/PVA hydrogel for wound dressings, *Carbohydrate Polymers*, England, Elsevier Ltd, **146**, pp. 427–434, [online]

Available from: https://www.sciencedirect.com/science/article/pii/S0144861716301771.

- Fernandes, M., Gama, M., Dourado, F. and Souto, A. P. (2019) Development of novel bacterial cellulose composites for the textile and shoe industry, *Microbial Biotechnology*, United States, Wiley Subscription Services, Inc, **12**(4), pp. 650–661, [online] Available from: https://onlinelibrary.wiley.com/doi/abs/10.1111/1751-7915.13387.
- Flanagan, M. (2003) Wound measurement: can it help us to monitor progression to healing?, *Journal of Wound Care*, London, MA Healthcare, **12**(5), pp. 189–194, [online] Available from: https://www.ncbi.nlm.nih.gov/pubmed/12784601.
- Flanagan, M. (2013) Wound Healing and Skin Integrity: Principles and Practice, first ed., Wiley-Blackwell, UK.
- Fleck, A., Cabral, P. F. G., Vieira, F. F. M., Pinheiro, D. A., Pereira, C. R., Santos, W. C. and Machado, T. B. (2016) Punica granatum L. Hydrogel for Wound Care Treatment: From Case Study to Phytomedicine Standardization, *Molecules (Basel, Switzerland)*, Switzerland, MDPI AG, **21**(8), p. 1059, [online] Available from: https://www.ncbi.nlm.nih.gov/pubmed/27556440.
- Fontana, J. D., de Souza, A. M., Fontana, C. K., Torriani, I. L., Moreschi, J. C., Gallotti, B. J., de Souza, S. J., Narcisco, G. P., Bichara, J. A. and Farah, L. F. (1990) Acetobacter cellulose pellicle as a temporary skin substitute, *Applied biochemistry and biotechnology*, United States, (1), pp. 253–264, [online] Available from: https://www.ncbi.nlm.nih.gov/pubmed/2353811.
- Fu, L., Zhang, J. and Yang, G. (2013) Present status and applications of bacterial cellulose-based materials for skin tissue repair, *Carbohydrate Polymers*, England,

Elsevier Ltd, **92**(2), pp. 1432–1442, [online] Available from: http://dx.doi.org/10.1016/j.carbpol.2012.10.071.

- Gao, W.-H., Chen, K.-F., Yang, R.-D., Yang, F. and Han, W.-J. (2011) Properties of bacterial cellulose and its influence on the physical properties of paper, *BioResources*, North Carolina State University, **6**(1), pp. 144–153, [online] Available from: https://doaj.org/article/d913ca7c07c24273ac1341630fe3fd9a.
- Gea, S., Reynolds, C. T., Roohpour, N., Wirjosentono, B., Soykeabkaew, N., Bilotti, E. and Peijs, T. (2011) Investigation into the structural, morphological, mechanical and thermal behaviour of bacterial cellulose after a two-step purification process, *Bioresource Technology*, England, Elsevier Ltd, **102**(19), pp. 9105–9110, [online] Available from: http://dx.doi.org/10.1016/j.biortech.2011.04.077.
- Ghadi, R., Jain, A., Khan, W. and Domb, A. (2016) *10 - Microparticulate polymers and hydrogels for wound healing*, *Wound Healing Biomaterials*, Elsevier Ltd, pp. 203–225, [online] Available from: http://dx.doi.org/10.1016/B978-1-78242-456-7.00010-6.
- Gharibi, R., Yeganeh, H. and Abdali, Z. (2018) Preparation of antimicrobial wound dressings via thiol–ene photopolymerization reaction, *Journal of Materials Science*, New York, Springer US, **53**(3), pp. 1581–1595, [online] Available from: https://search.proquest.com/docview/1963515333.
- Goh, M., Hwang, Y. and Tae, G. (2016) Epidermal growth factor loaded heparin-based hydrogel sheet for skin wound healing, *Carbohydrate Polymers*, England, Elsevier Ltd, **147**, pp. 251–260, [online] Available from: https://www.sciencedirect.com/science/article/pii/S0144861716303095.
- Gonzalez, J. S., Ludueña, L. N., Ponce, A. and Alvarez, V. A. (2014) Poly(vinyl alcohol)/cellulose nanowhiskers nanocomposite hydrogels for potential wound

dressings, *Materials Science & Engineering C*, Netherlands, Elsevier B.V, **34**, pp. 54–61, [online] Available from: https://www.sciencedirect.com/science/article/pii/S0928493113005742.

- Gopi, S., Balakrishnan, P., Chandradhara, D., Poovathankandy, D. and Thomas, S. (2019) General scenarios of cellulose and its use in the biomedical field, *Materials Today Chemistry*, Elsevier Ltd, **13**, pp. 59–78, [online] Available from: http://dx.doi.org/10.1016/j.mtchem.2019.04.012.
- Gorgieva and Trček (2019) Bacterial Cellulose: Production, Modification and Perspectives in Biomedical Applications, *Nanomaterials*, MDPI, **9**(10), p. 1352, [online] Available from: https://search.proquest.com/docview/2296659418.
- Gottlieb, H. E., Kotlyar, V. and Nudelman, A. (1997) NMR Chemical Shifts of Common Laboratory Solvents as Trace Impurities, *The Journal of organic chemistry*, United States, American Chemical Society, **62**(21), pp. 7512–7515, [online] Available from: https://www.ncbi.nlm.nih.gov/pubmed/11671879.
- Grip, J., Engstad, R. E., Skjæveland, I., Škalko-Basnet, N., Isaksson, J., Basnet, P. and Holsæter, A. M. (2018) Beta-glucan-loaded nanofiber dressing improves wound healing in diabetic mice, *European Journal of Pharmaceutical Sciences*, Netherlands, Elsevier B.V, **121**, pp. 269–280, [online] Available from: https://www.sciencedirect.com/science/article/pii/S0928098718302562.
- Guaresti, O., García–Astrain, C., Aguirresarobe, R. ., Eceiza, A. and Gabilondo, N. (2018) Synthesis of stimuli–responsive chitosan–based hydrogels by Diels–Alder cross–linking `click´ reaction as potential carriers for drug administration, *Carbohydrate Polymers*, England, Elsevier Ltd, **183**, pp. 278–286, [online] Available from: http://dx.doi.org/10.1016/j.carbpol.2017.12.034.

- Guest, J. F., Ayoub, N., McIlwraith, T., Uchegbu, I., Gerrish, A., Weidlich, D., Vowden, K. and Vowden, P. (2017) Health economic burden that different wound types impose on the UK's National Health Service, *International Wound Journal*, Oxford, UK, Blackwell Publishing Ltd, **14**(2), pp. 322–330, [online] Available from: https://onlinelibrary.wiley.com/doi/abs/10.1111/iwj.12603.
- Gulrez, S. K. H., Al-Assaf, S. and Phillips, G. O. (2011) Hydrogels: Methods of Preparation, Characterisation and Applications, InTech, [online] Available from: https://www.openaire.eu/search/publication?articleId=intech_____::33f9b5267eb9362bdb0543cefd4209cc.
- Guo, S. and DiPietro, L.A. (2010) Factors Affecting Wound Healing, *Journal of Dental Research*, **89**; pp. 219–229. doi:10.1177/0022034509359125.
- Gupta, B., Tummalapalli, M., Deopura, B. and Alam, M. (2014) Preparation and characterization of in-situ crosslinked pectin–gelatin hydrogels, *Carbohydrate Polymers*, England, Elsevier Ltd, **106**, pp. 312–318, [online] Available from: https://www.sciencedirect.com/science/article/pii/S0144861714001404.
- Guzman, M., Dille, J. and Godet, S. (2012) Synthesis and antibacterial activity of silver nanoparticles against gram-positive and gram-negative bacteria, *Nanomedicine: Nanotechnology, Biology and Medicine*, [online] Available from: http://www.sciencedirect.com/science/article/pii/S1549963411001791.
- Haas, S., Chen, Y., Fuchs, C., Handschuh, S., Steuber, M. and Schönherr, H. (2013) Amphiphilic Block Copolymer Vesicles for Active Wound Dressings: Synthesis of Model Systems and Studies of Encapsulation and Release, *Macromolecular Symposia*, **328**(1), pp. 73–79.
- Hadisi, Z., Nourmohammadi, J. and Nassiri, S. M. (2018) The antibacterial and anti-inflammatory investigation of Lawsonia Inermis-gelatin-starch nano-fibrous dressing

in burn wound, *International Journal of Biological Macromolecules*, Netherlands, Elsevier B.V, **107**(Pt B), pp. 2008–2019, [online] Available from: https://www.sciencedirect.com/science/article/pii/S0141813017318202.

- Häkkinen, L., Koivisto, L., Heino, J. and Larjava, H. (2015) Cell and Molecular Biology of Wound Healing, in: A. Vishwakarma, P. Sharpe, S. Shi, M. Ramalingam (Eds.), Stem Cell Biology and Tissue Engineering in Dental Sciences, Academic Press, U.K., pp. 669–690. doi:10.1016/b978-0-12-397157-9.00054-0.
- Han (2016) *Innovations and Advances in Wound Healing*, Berlin, Heidelberg, Springer, [online] Available from: https://ebookcentral.proquest.com/lib/[SITE_ID]/detail.action?docID=4178861.
- Hanim, S. A. M., Malek, N. A. N. N. and Ibrahim, Z. (2016) Amine-functionalized, silver-exchanged zeolite NaY: Preparation, characterization and antibacterial activity, *Applied Surface Science*, Elsevier B.V, **360**, pp. 121–130, [online] Available from: http://dx.doi.org/10.1016/j.apsusc.2015.11.010.
- Helenius, G., Bäckdahl, H., Bodin, A., Nannmark, U., Gatenholm, P. and Risberg, B. (2006) In vivo biocompatibility of bacterial cellulose, *Journal of Biomedical Materials Research Part A*, Hoboken, Wiley Subscription Services, Inc., A Wiley Company, (2), pp. 431–438, [online] Available from: https://onlinelibrary.wiley.com/doi/abs/10.1002/jbm.a.30570.
- Hennink, W. and van Nostrum, C. (2012) Novel crosslinking methods to design hydrogels, *Advanced Drug Delivery Reviews*, Elsevier B.V, **64**, pp. 223–236, [online] Available from: http://dx.doi.org/10.1016/j.addr.2012.09.009.
- Hestrin, S. and Schramm, M. (1954) Synthesis of cellulose by Acetobacter xylinum. II. Preparation of freeze-dried cells capable of polymerizing glucose to cellulose, *The*

Biochemical journal, England, **58**(2), p. 345, [online] Available from: https://www.ncbi.nlm.nih.gov/pubmed/13208601.

- Hiller, C. ., Hübner, U., Fajnorova, S., Schwartz, T. and Drewes, J. (2019) Antibiotic microbial resistance (AMR) removal efficiencies by conventional and advanced wastewater treatment processes: A review, *Science of the Total Environment*, Netherlands, Elsevier B.V, **685**, pp. 596–608, [online] Available from: http://dx.doi.org/10.1016/j.scitotenv.2019.05.315.
- Hiro, M. E., Pierpont, Y. N., Ko, F., Wright, T. E., Robson, M. C. and Payne, W. G. (2012) Comparative evaluation of silver-containing antimicrobial dressings on in vitro and in vivo processes of wound healing, *Eplasty*, United States, Open Science Company, LLC, **12**, p. e48, [online] Available from: https://www.ncbi.nlm.nih.gov/pubmed/23150745.
- Hoare, T. R. and Kohane, D. S. (2008) Hydrogels in drug delivery: Progress and challenges, *Polymer*, Elsevier Ltd, **49**(8), pp. 1993–2007, [online] Available from: https://www.sciencedirect.com/science/article/pii/S0032386108000487.
- Hoefer, D., Schnepf, J., Hammer, T., Fischer, M. and Marquardt, C. (2015) Biotechnologically produced microbial alginate dressings show enhanced gel forming capacity compared to commercial alginate dressings of marine origin, *Journal of Materials Science: Materials in Medicine*, New York, Springer US, **26**(4), pp. 1–9, [online] Available from: https://search.proquest.com/docview/1664401532.
- Holloway, J. L., Lowman, A. M. and Palmese, G. R. (2013) The role of crystallization and phase separation in the formation of physically cross-linked PVA hydrogels, *Soft Matter*, **9**(3), pp. 826–833.
- Hsu, C.-M., Yu, S.-C., Tsai, Y. and Tsai, F.-J. (2013) Enhancement of rhubarb extract solubility and bioactivity by 2-hydroxypropyl-β-cyclodextrin, *Carbohydrate*

Polymers, England, Elsevier Ltd, **98**(2), pp. 1422–1429, [online] Available from: https://www.sciencedirect.com/science/article/pii/S0144861713007133.

- Hu, P., Huang, P. and Chen, M. W. (2013) Curcumin reduces Streptococcus mutans biofilm formation by inhibiting sortase A activity, *Archives of Oral Biology*, England, Elsevier Ltd, **58**(10), pp. 1343–1348, [online] Available from: https://www.clinicalkey.es/playcontent/1-s2.0-S0003996913001714.
- Hu, S., Cai, X., Qu, X., Yu, B., Yan, C., Yang, J., Li, F., Zheng, Y. and Shi, X. (2019) Preparation of biocompatible wound dressings with long-term antimicrobial activity through covalent bonding of antibiotic agents to natural polymers, *International Journal of Biological Macromolecules*, Netherlands, Elsevier B.V, **123**, pp. 1320–1330, [online] Available from: https://www.sciencedirect.com/science/article/pii/S0141813018337784.
- Hwang, M.-R., Kim, Jong, Lee, J., Kim, Y., Kim, Jeong, Chang, S., Jin, S., Kim, Jung, Lyoo, W., Han, S., Ku, S., Yong, C. and Choi, H.-G. (2010) Gentamicin-Loaded Wound Dressing With Polyvinyl Alcohol/Dextran Hydrogel: Gel Characterization and In Vivo Healing Evaluation, *AAPS PharmSciTech*, Boston, Springer US, **11**(3), pp. 1092–1103, [online] Available from: https://www.ncbi.nlm.nih.gov/pubmed/20607628.
- Ian, S., Joanna|Sarker, Prodip|Rimmer, Stephen|Swanson, Linda|MacNeil, Sheila|Douglas, (2010) Hyperbranched poly(NIPAM) polymers modified with antibiotics for the reduction of bacterial burden in infected human tissue engineered skin, *Biomaterials*, Netherlands, Elsevier Ltd, **32**(1), pp. 258–267, [online] Available from: https://www.clinicalkey.es/playcontent/1-s2.0-S0142961210011221.
- Ijaz, Q. A., Abbas, N., Arshad, M. S., Hussain, A., Shahiq-uz-Zaman and Javaid, Z. (2018) Synthesis and evaluation of pH dependent polyethylene glycol-co-acrylic acid

hydrogels for controlled release of venlafaxine HCl, *Journal of Drug Delivery Science and Technology*, Elsevier B.V, **43**, pp. 221–232, [online] Available from: https://www.sciencedirect.com/science/article/pii/S1773224717304537.

- Ip, M., Lui, S. L., Poon, V. K. M., Lung, I. and Burd, A. (2006) Antimicrobial activities of silver dressings: an in vitro comparison, *Journal of Medical Microbiology*, England, Soc General Microbiol, **55**(1), pp. 59–63, [online] Available from: http://jmm.sgmjournals.org/cgi/content/abstract/55/1/59.
- Ishiguro, T., Adachi, S. and Matsuno, R. (1995) Thermogravimetric Analysis of Cyclodextrin-Fatty Acid Complex Formation and Its Use for Predicting Suppressed Autoxidation of Fatty Acids, *Bioscience, Biotechnology, and Biochemistry*, Taylor & Francis, **59**(1), pp. 51–54, [online] Available from: http://www.tandfonline.com/doi/abs/10.1271/bbb.59.51.
- Jadhav, H., Joshi, A., Misra, M. and Shahiwala, A. (2012) Effect of Various Formulation Parameters on the Properties of Hydrogel Wound Dressings, *Drug Delivery Letters*, Bentham Science Publishers Ltd, **2**(1), pp. 8–13, [online] Available from: http://www.eurekaselect.com/openurl/content.php?genre=article&issn=2210304x&volume=2&issue=1&spage=8.
- Jagannath, A., Raju, P. and Bawa, A. (2010) Comparative evaluation of bacterial cellulose (nata) as a cryoprotectant and carrier support during the freeze drying process of probiotic lactic acid bacteria, *LWT - Food Science and Technology*, Elsevier Ltd, **43**(8), pp. 1197–1203, [online] Available from: http://dx.doi.org/10.1016/j.lwt.2010.03.009.
- Jambhekar, S. S. and Breen, P. (2016) Cyclodextrins in pharmaceutical formulations I: structure and physicochemical properties, formation of complexes, and types of

complex, *Drug Discovery Today*, England, Elsevier Ltd, **21**(2), pp. 356–362, [online] Available from: http://dx.doi.org/10.1016/j.drudis.2015.11.017.

- Jankaew, R., Rodkate, N., Lamlertthon, S., Rutnakornpituk, M., Rutnakornpituk, B., Wichai, U. and Ross, G. (2015) 'Smart' carboxymethylchitosan hydrogels crosslinked with poly(N-isopropylacrylamide) and poly(acrylic acid) for controlled drug release, *Polymer Testing*, Elsevier Ltd, **42**, pp. 26–36, [online] Available from: https://www.sciencedirect.com/science/article/pii/S0142941814002700.
- Jantarat, C., Sirathanarun, P., Ratanapongsai, S., Watcharakan, P., Sunyapong, S. and Wadu, A. (2014) Curcumin-Hydroxypropyl-β-Cyclodextrin Inclusion Complex Preparation Methods: Effect of Common Solvent Evaporation, Freeze Drying, and pH Shift on Solubility and Stability of Curcumin, *Tropical Journal of Pharmaceutical Research*, **13**(8), p. 1215.
- Jayakumar, R., Prabaharan, M., Sudheesh Kumar, P. ., Nair, S. . and Tamura, H. (2011) Biomaterials based on chitin and chitosan in wound dressing applications, *Biotechnology Advances*, England, Elsevier Inc, **29**(3), pp. 322–337, [online] Available from: https://www.sciencedirect.com/science/article/pii/S0734975011000061.
- Jena, S., Anand, C., Chainy, G. and Dandapat, J. (2011) Induction of oxidative stress and inhibition of superoxide dismutase expression in rat cerebral cortex and cerebellum by PTU-induced hypothyroidism and its reversal by curcumin, *Neurological Sciences*, Milan, Springer Milan, **33**(4), pp. 869–873, [online] Available from: https://www.ncbi.nlm.nih.gov/pubmed/22076484.
- Jeong, D., Joo, S.-W., Shinde, V. V. and Jung, S. (2018) Triple-crosslinkedβ-cyclodextrin oligomer self-healing hydrogel showing high mechanical strength, enhanced stability and pH responsiveness, *Carbohydrate Polymers*, England,

Elsevier Ltd, **198**, pp. 563–574, [online] Available from: https://www.sciencedirect.com/science/article/pii/S0144861718307720.

- Jiang, S., Liu, S. and Feng, W. (2011) PVA hydrogel properties for biomedical application, *Journal of the Mechanical Behavior of Biomedical Materials*, Netherlands, Elsevier Ltd, **4**(7), pp. 1228–1233, [online] Available from: https://www.sciencedirect.com/science/article/pii/S1751616111000786.
- Jiang, T., Duan, Q., Zhu, J., Liu, H. and Yu, L. (2020) Starch-based biodegradable materials: Challenges and opportunities, *Advanced Industrial and Engineering Polymer Research*, [online] Available from: http://www.sciencedirect.com/science/article/pii/S254250481930051X.
- Jiji, S., Udhayakumar, S., Rose, C., Muralidharan, C. and Kadirvelu, K. (2019) Thymol enriched bacterial cellulose hydrogel as effective material for third degree burn wound repair, *International Journal of Biological Macromolecules*, Netherlands, Elsevier B.V, **122**, pp. 452–460, [online] Available from: http://dx.doi.org/10.1016/j.ijbiomac.2018.10.192.
- João De Masi, E. C. D., Campos, A. C. L., João De Masi, F. D., Ratti, M. A. S., Ike, I. S. and João De Masi, R. D. (2016) The influence of growth factors on skin wound healing in rats, *Brazilian Journal of Otorhinolaryngology*, Brazil, Elsevier Editora Ltda, **82**(5), pp. 512–521, [online] Available from: http://dx.doi.org/10.1016/j.bjorl.2015.09.011.
- Jones, V. J. (2006) The use of gauze: will it ever change?, *International Wound Journal*, Oxford, UK; Malden, USA, Blackwell Publishing Ltd, **3**(2), pp. 79–88, [online] Available from: https://onlinelibrary.wiley.com/doi/abs/10.1111/j.1742-4801.2006.00215.x.

- Juby, K. ., Dwivedi, C., Kumar, M., Kota, S., Misra, H. and Bajaj, P. (2012) Silver nanoparticle-loaded PVA/gum acacia hydrogel: Synthesis, characterization and antibacterial study, *Carbohydrate Polymers*, England, Elsevier Ltd, **89**(3), pp. 906–913, [online] Available from: https://www.sciencedirect.com/science/article/pii/S0144861712003736.
- Kaditi, E., Mountrichas, G. and Pispas, S. (2011) Amphiphilic block copolymers by a combination of anionic polymerization and selective post-polymerization functionalization, *European Polymer Journal*, Elsevier Ltd, **47**(4), pp. 415–434, [online] Available from: http://dx.doi.org/10.1016/j.eurpolymj.2010.09.012.
- Kaith, B. S., Sharma, R. and Kalia, S. (2015) Guar gum based biodegradable, antibacterial and electrically conductive hydrogels, *International Journal of Biological Macromolecules*, Netherlands, Elsevier B.V, **75**, pp. 266–275, [online] Available from: https://www.sciencedirect.com/science/article/pii/S0141813015000574.
- Kamoun, E. A. (2016) N-succinyl chitosan–dialdehyde starch hybrid hydrogels for biomedical applications, *Journal of Advanced Research*, Egypt, Elsevier B.V, **7**(1), pp. 69–77, [online] Available from: https://www.sciencedirect.com/science/article/pii/S2090123215000259.
- Kamoun, E. A., Kenawy, E.-R. S. and Chen, X. (2017) A review on polymeric hydrogel membranes for wound dressing applications: PVA-based hydrogel dressings, *Journal of Advanced Research*, Egypt, Elsevier B.V, **8**(3), pp. 217–233, [online] Available from: https://www.sciencedirect.com/science/article/pii/S2090123217300243.
- Kamoun, E. A., Kenawy, E.-R. S., Tamer, T. M., El-Meligy, M. A. and Mohy Eldin, M. S. (2015) Poly (vinyl alcohol)-alginate physically crosslinked hydrogel membranes for wound dressing applications: Characterization and bio-evaluation, *Arabian Journal of*

Chemistry, Elsevier B.V, **8**(1), pp. 38–47, [online] Available from: https://www.sciencedirect.com/science/article/pii/S1878535213004310.

- Karimi-Shamsabadi, M. and Nezamzadeh-Ejhieh, A. (2016) Comparative study on the increased photoactivity of coupled and supported manganese-silver oxides onto a natural zeolite nano-particles, *Journal of Molecular Catalysis. A, Chemical*, Elsevier B.V, pp. 103–114, [online] Available from: http://dx.doi.org/10.1016/j.molcata.2016.03.034.
- Kasuya, A. and Tokura, Y. (2014) Attempts to accelerate wound healing, *Journal of Dermatological Science*, Netherlands, Elsevier Ireland Ltd, **76**(3), pp. 169–172, [online] Available from: https://www.clinicalkey.es/playcontent/1-s2.0-S0923181114002540.
- Kateel, R., Bhat, G., Baliga, S., Augustine, A. J., Ullal, S. and Adhikari, P. (2018) Antibacterial action of Tropical honey on various bacteria obtained from diabetic foot ulcer, *Complementary Therapies in Clinical Practice*, England, Elsevier Ltd, **30**, pp. 29–32, [online] Available from: http://dx.doi.org/10.1016/j.ctcp.2017.11.001.
- Kenawy, E.-R., Kamoun, E.A., Mohy Eldin, M.S. and El-Meligy, M. (2014) Physically crosslinked poly(vinyl alcohol)-hydroxyethyl starch blend hydrogel membranes: Synthesis and characterization for biomedical applications, *Arabian Journal of Chemistry*, **7**(3); pp. 372-380. doi.org/10.1016/j.arabjc.2013.05.026.
- Kenworthy, P., Phillips, M., Grisbrook, T. L., Gibson, W., Wood, F. M. and Edgar, D. W. (2018) Monitoring wound healing in minor burns—A novel approach, *Burns*, [online] Available from: http://www.sciencedirect.com/science/article/pii/S0305417917303595.
- Keshari, A. K., Srivastava, R., Singh, P., Yadav, V. B. and Nath, G. (2018) Antioxidant and antibacterial activity of silver nanoparticles synthesized by Cestrum

nocturnum, *Journal of Ayurveda and Integrative Medicine*, United States, Elsevier B.V, **11**(1), pp. 37–44, [online] Available from: http://dx.doi.org/10.1016/j.jaim.2017.11.003.

- Keshk, S. and Sameshima, K. (2006) Influence of lignosulfonate on crystal structure and productivity of bacterial cellulose in a static culture, *Enzyme and Microbial Technology*, Elsevier Inc, **40**(1), pp. 4–8, [online] Available from: http://dx.doi.org/10.1016/j.enzmictec.2006.07.037.
- Keshk, S. M. (2014) Bacterial Cellulose Production and its Industrial Applications, *Journal of Bioprocessing & Biotechniques*, **4**(2).
- Khalid, A., Ullah, H., Ul-Islam, M., Khan, R., Khan, S., Ahmad, F., Khan, T. and Wahid, F. (2017) Bacterial cellulose-TiO2 nanocomposites promote healing and tissue regeneration in burn mice model, *RSC Adv*, **7**(75), pp. 47662–47668.
- Khan, M. J., Shameli, K., Sazili, A. Q., Selamat, J. and Kumari, S. (2019) Rapid Green Synthesis and Characterization of Silver Nanoparticles Arbitrated by Curcumin in an Alkaline Medium, *Molecules (Basel, Switzerland)*, Switzerland, MDPI AG, **24**(4), p. 719, [online] Available from: https://www.ncbi.nlm.nih.gov/pubmed/30781541.
- Khan, S. U., Anjum, S. I., Rahman, K., Ansari, M. J., Khan, W. U., Kamal, S., Khattak, B., Muhammad, A. and Khan, H. U. (2018) Honey: Single food stuff comprises many drugs, *Saudi Journal of Biological Sciences*, Saudi Arabia, Elsevier B.V, **25**(2), pp. 320–325, [online] Available from: http://dx.doi.org/10.1016/j.sjbs.2017.08.004.
- Kharkar, P. M., Rehmann, M. S., Skeens, K. M., Maverakis, E. and Kloxin, A. M. (2016) Thiol-ene click hydrogels for therapeutic delivery, *ACS biomaterials science &*

engineering, United States, **2**(2), pp. 165–179, [online] Available from: https://www.ncbi.nlm.nih.gov/pubmed/28361125.

- Kim, P. S., Kim, M. K., Cho, B. K., Nam, I.-S. and Oh, S. H. (2013) Effect of H2 on deNOx performance of HC-SCR over Ag/Al2O3: Morphological, chemical, and kinetic changes, *Journal of Catalysis*, Elsevier Inc, **301**, pp. 65–76, [online] Available from: http://dx.doi.org/10.1016/j.jcat.2013.01.026.
- King, B., Barrett, S. and Cutting, K. . (2017) Clinical evaluation of a bioactive beta-glucan gel in the treatment of 'hard-to-heal' wounds, *Journal of Wound Care*, London, MA Healthcare, **26**(2), pp. 58–63, [online] Available from: https://www.ncbi.nlm.nih.gov/pubmed/28182518.
- Kiritsi, D. and Nyström, A. (2018) The role of TGFβ in wound healing pathologies, *Mechanisms of Ageing and Development*, Ireland, Elsevier B.V, **172**, pp. 51–58, [online] Available from: http://dx.doi.org/10.1016/j.mad.2017.11.004.
- Klein, E. Y., Van Boeckel, T. P., Martinez, E. M., Pant, S., Gandra, S., Levin, S. A., Goossens, H. and Laxminarayan, R. (2018) Global increase and geographic convergence in antibiotic consumption between 2000 and 2015, *PNAS Plus*, United States, National Academy of Sciences, **115**(15), pp. E3463–E3470, [online] Available from: https://www.ncbi.nlm.nih.gov/pubmed/29581252.
- Klemm, D., Heublein, B., Fink, H. and Bohn, A. (2005) Cellulose: Fascinating Biopolymer and Sustainable Raw Material, *Angewandte Chemie International Edition*, Weinheim, WILEY-VCH Verlag, **44**(22), pp. 3358–3393, [online] Available from: https://onlinelibrary.wiley.com/doi/abs/10.1002/anie.200460587.
- Klemm, D., Schumann, D., Udhardt, U. and Marsch, S. (2001) Bacterial synthesized cellulose — artificial blood vessels for microsurgery, *Progress in Polymer Science*, Elsevier B.V, **26**(9), pp. 1561–1603.

- Koehler, J., Brandl, F. P. and Goepferich, A. M. (2018) Hydrogel wound dressings for bioactive treatment of acute and chronic wounds, *European Polymer Journal*, [online] Available from: http://www.sciencedirect.com/science/article/pii/S0014305717315033.
- Koehler, J., Wallmeyer, L., Hedtrich, S., Goepferich, A. M. and Brandl, F. P. (2017) pH-Modulating Poly(ethylene glycol)/Alginate Hydrogel Dressings for the Treatment of Chronic Wounds, *Macromolecular Bioscience*, Germany, Wiley Subscription Services, Inc, **17**(5), pp. 1600369-n/a, [online] Available from: https://onlinelibrary.wiley.com/doi/abs/10.1002/mabi.201600369.
- Koh, T. J. and DiPietro, L. A. (2011) Inflammation and wound healing: the role of the macrophage, *Expert Reviews in Molecular Medicine*, England, Cambridge University Press, **13**, p. e23, [online] Available from: http://journals.cambridge.org/abstract_S1462399411001943.
- Kokabi, M., Sirousazar, M. and Hassan, Z. M. (2007) PVA–clay nanocomposite hydrogels for wound dressing, *European Polymer Journal*, Elsevier Ltd, **43**(3), pp. 773–781, [online] Available from: http://dx.doi.org/10.1016/j.eurpolymj.2006.11.030.
- Kondaveeti, S., Bueno, P. V. de A., Carmona-Ribeiro, A. M., Esposito, F., Lincopan, N., Sierakowski, M. R. and Petri, D. F. S. (2018) Microbicidal gentamicin-alginate hydrogels, *Carbohydrate Polymers*, England, Elsevier Ltd, **186**, pp. 159–167, [online] Available from: https://www.sciencedirect.com/science/article/pii/S0144861718300626.
- Kongruang, S. (2008) Bacterial Cellulose Production by Acetobacter xylinum Strains from Agricultural Waste Products, *Applied Biochemistry and Biotechnology*, New York, Humana Press Inc, **148**(1), pp. 245–256, [online] Available from: https://www.ncbi.nlm.nih.gov/pubmed/18418756.

- Kono, H., Otaka, F. and Ozaki, M. (2014) Preparation and characterization of guar gum hydrogels as carrier materials for controlled protein drug delivery, *Carbohydrate Polymers*, England, Elsevier Ltd, **111**, pp. 830–840, [online] Available from: https://www.sciencedirect.com/science/article/pii/S0144861714005207.
- Koosehgol, S., Ebrahimian-Hosseinabadi, M., Alizadeh, M. and Zamanian, A. (2017) Preparation and characterization of in situ chitosan/polyethylene glycol fumarate/thymol hydrogel as an effective wound dressing, *Materials Science & Engineering C*, Netherlands, Elsevier B.V, **79**, pp. 66–75, [online] Available from: http://dx.doi.org/10.1016/j.msec.2017.05.001.
- Krystynowicz, A., Czaja, W., Wiktorowska-Jezierska, A., Gonçalves-Miśkiewicz, M., Turkiewicz, M. and Bielecki, S. (2002) Factors affecting the yield and properties of bacterial cellulose, *Journal of Industrial Microbiology & Biotechnology*, London, Nature Publishing Group, **29**(4), pp. 189–195, [online] Available from: https://www.ncbi.nlm.nih.gov/pubmed/12355318.
- Krzyszczyk, P., Schloss, R., Palmer, A. and Berthiaume, F. (2018) The Role of Macrophages in Acute and Chronic Wound Healing and Interventions to Promote Pro-wound Healing Phenotypes, *Frontiers in physiology*, Switzerland, Frontiers Research Foundation, **9**, p. 419, [online] Available from: https://www.ncbi.nlm.nih.gov/pubmed/29765329.
- Kumari, S., Kumar Annamareddy, S. H., Abanti, S. and Kumar Rath, P. (2017) Physicochemical properties and characterization of chitosan synthesized from fish scales, crab and shrimp shells, *International Journal of Biological Macromolecules*, Netherlands, Elsevier B.V, **104**(Pt B), pp. 1697–1705, [online] Available from: https://www.sciencedirect.com/science/article/pii/S0141813016326903.

- Kurczewska, J., Pecyna, P., Ratajczak, M., Gajęcka, M. and Schroeder, G. (2017) Halloysite nanotubes as carriers of vancomycin in alginate-based wound dressing, *Saudi Pharmaceutical Journal*, Saudi Arabia, Elsevier B.V, **25**(6), pp. 911–920, [online] Available from: https://www.sciencedirect.com/science/article/pii/S1319016417300282.
- Kurkov S. V. & Loftsson T. (2013). Cyclodextrins. *International Journal of Pharmaceutics,* **453**, pp.167-180.
- Kurniawan, A., Gunawan, F., Nugraha, A. T., Ismadji, S. and Wang, M.-J. (2017) Biocompatibility and drug release behavior of curcumin conjugated gold nanoparticles from aminosilane-functionalized electrospun poly(N-vinyl-2-pyrrolidone) fibers, *International Journal of Pharmaceutics*, Netherlands, Elsevier B.V, **516**(1–2), pp. 158–169, [online] Available from: https://www.sciencedirect.com/science/article/pii/S0378517316310353.
- Kurosumi, A., Sasaki, C., Yamashita, Y. and Nakamura, Y. (2009) Utilization of various fruit juices as carbon source for production of bacterial cellulose by Acetobacter xylinum NBRC 13693, *Carbohydrate Polymers*, Elsevier Ltd, **76**(2), pp. 333–335, [online] Available from: http://dx.doi.org/10.1016/j.carbpol.2008.11.009.
- Kwakye-Awuah, B., Wemegah, D. D., Nkrumah, I., Williams, C. and Radecka, I. (2013) Antimicrobial activity of silver-zeolite LTA on heavily-contaminated underground Ghanian waters, International Journal of Science and Research, 2(11), pp. 26-31.
- Kwakye-Awuah, B., Williams, C., Kenward, M. and Radecka, I. (2008) Antimicrobial action and efficiency of silver-loaded zeolite X, *Journal of Applied Microbiology*,

Oxford, UK, Blackwell Publishing Ltd, **104**(5), pp. 1516–1524, [online] Available from: https://onlinelibrary.wiley.com/doi/abs/10.1111/j.1365-2672.2007.03673.x.

- Lamke, L.-O., Nilsson, G. and Reithner, H. (1977) The evaporative water loss from burns and water vapour permeability of grafts and artificial membranes used in the treatment of burns, *Burns*.
- Le, A.-T., Tam, L. T., Tam, P. D., Huy, P. ., Huy, T. Q., Van Hieu, N., Kudrinskiy, A. A. and Krutyakov, Y. A. (2010) Synthesis of oleic acid-stabilized silver nanoparticles and analysis of their antibacterial activity, *Materials Science & Engineering C*, Elsevier B.V, **30**(6), pp. 910–916, [online] Available from: http://dx.doi.org/10.1016/j.msec.2010.04.009.
- Lee, K., Buldum, G., Mantalaris, A. and Bismarck, A. (2014) More Than Meets the Eye in Bacterial Cellulose: Biosynthesis, Bioprocessing, and Applications in Advanced Fiber Composites, *Macromolecular Bioscience*, Germany, Wiley Subscription Services, Inc, **14**(1), pp. 10–32, [online] Available from: https://onlinelibrary.wiley.com/doi/abs/10.1002/mabi.201300298.
- Lee, M. S., Seo, S. R. and Kim, J. -. (2012a) A β-cyclodextrin, polyethyleneimine and silk fibroin hydrogel containing Centella asiatica extract and hydrocortisone acetate: releasing properties and in vivo efficacy for healing of pressure sores, *Clinical and Experimental Dermatology*, Oxford, UK, Blackwell Publishing Ltd, **37**(7), pp. 762–771, [online] Available from: https://onlinelibrary.wiley.com/doi/abs/10.1111/j.1365-2230.2011.04331.x.
- Lee, Y.-H., Chang, J.-J., Yang, M.-C., Chien, C.-T. and Lai, W.-F. (2012) Acceleration of wound healing in diabetic rats by layered hydrogel dressing, *Carbohydrate Polymers*, Elsevier Ltd, **88**(3), pp. 809–819, [online]

Available from: https://www.sciencedirect.com/science/article/pii/S0144861712000483.

- Leitão, A. F., Gupta, S., Silva, J. P., Reviakine, I. and Gama, M. (2013) Hemocompatibility study of a bacterial cellulose/polyvinyl alcohol nanocomposite, *Colloids and Surfaces B: Biointerfaces*, Netherlands, Elsevier B.V, **111**, pp. 493–502, [online] Available from: http://dx.doi.org/10.1016/j.colsurfb.2013.06.031.
- Lestari, P., Elfrida, N., Suryani, A. and Suryadi, Y. (2014) Study on the Production of Bacterial Cellulose from Acetobacter Xylinum Using Agro - Waste, *Jordan Journal of Biological Sciences*, Az Zarqa' - Jordan, The Hashemite University : The Deanship of Scientific Research and Graduate Studies, **7**(1), pp. 75–80, [online] Available from: http://platform.almanhal.com/Summon/Preview/?id=2-56265.
- Li, H., Kong, N., Laver, B. and Liu, J. (2016) Hydrogels Constructed from Engineered Proteins, *Small*, Germany, Wiley Subscription Services, Inc, **12**(8), pp. 973–987, [online] Available from: https://onlinelibrary.wiley.com/doi/abs/10.1002/smll.201502429.
- Li, H., Yang, J., Hu, X., Liang, J., Fan, Y. and Zhang, X. (2011) Superabsorbent polysaccharide hydrogels based on pullulan derivate as antibacterial release wound dressing, *Journal of Biomedical Materials Research Part A*, Hoboken, Wiley Subscription Services, Inc., A Wiley Company, (1), pp. 31–39, [online] Available from: https://onlinelibrary.wiley.com/doi/abs/10.1002/jbm.a.33045.
- Li, J., Koh, J.-J., Liu, S., Lakshminarayanan, R., Verma, C. S. and Beuerman, R. W. (2017) Membrane Active Antimicrobial Peptides: Translating Mechanistic Insights to Design, *Frontiers in neuroscience*, Switzerland, Frontiers Research Foundation, **11**, p. 73, [online] Available from: https://www.ncbi.nlm.nih.gov/pubmed/28261050.

- Li, N., Wang, N., Wu, T., Qiu, C., Wang, X., Jiang, S., Zhang, Z., Liu, T., Wei, C. and Wang, T. (2018) Preparation of curcumin-hydroxypropyl-β-cyclodextrin inclusion complex by cosolvency-lyophilization procedure to enhance oral bioavailability of the drug, *Drug Development and Industrial Pharmacy*, **44**(12), pp. 1966–1974.
- Li, Z. and Tan, B. H. (2014) Towards the development of polycaprolactone based amphiphilic block copolymers: molecular design, self-assembly and biomedical applications, *Materials Science & Engineering C*, Netherlands, Elsevier B.V, **45**, pp. 620–634, [online] Available from: http://dx.doi.org/10.1016/j.msec.2014.06.003.
- Lin, K. W. and Lin, H. Y. (2004) Quality Characteristics of Chinese-style Meatball Containing Bacterial Cellulose (Nata), *Journal of Food Science*, Oxford, UK, Blackwell Publishing Ltd, **69**(3), pp. SNQ107–SNQ111, [online] Available from: https://onlinelibrary.wiley.com/doi/abs/10.1111/j.1365-2621.2004.tb13378.x.
- Lin, W.-C., Lien, C.-C., Yeh, H.-J., Yu, C.-M. and Hsu, S. (2013) Bacterial cellulose and bacterial cellulose–chitosan membranes for wound dressing applications, *Carbohydrate Polymers*, England, Elsevier Ltd, **94**(1), pp. 603–611, [online] Available from: http://dx.doi.org/10.1016/j.carbpol.2013.01.076.
- Liu, L., Gao, Q., Lu, X. and Zhou, H. (2016) In situ forming hydrogels based on chitosan for drug delivery and tissue regeneration, *Asian Journal of Pharmaceutical Sciences*, Elsevier B.V, **11**(6), pp. 673–683, [online] Available from: http://dx.doi.org/10.1016/j.ajps.2016.07.001.
- Liu, M., Liu, L., Jia, S., Li, S., Zou, Y. and Zhong, C. (2018) Complete genome analysis of Gluconacetobacter xylinus CGMCC 2955 for elucidating bacterial cellulose biosynthesis and metabolic regulation, *Scientific reports*, England, Nature Publishing Group, **8**(1), pp. 6266–10, [online] Available from: https://www.ncbi.nlm.nih.gov/pubmed/29674724.

- Liu, X., You, L., Tarafder, S., Zou, L., Fang, Z., Chen, J., Lee, C. H. and Zhang, Q. (2019) Curcumin-releasing chitosan/aloe membrane for skin regeneration, *Chemical Engineering Journal*, Elsevier B.V, **359**, pp. 1111–1119, [online] Available from: https://www.sciencedirect.com/science/article/pii/S1385894718323052.
- Loftsson, T., Jarho, P., Másson, M. and Järvinen, T. (2005). Cyclodextrins in drug delivery, *Expert Opinion. Drug Deliv*ery, **2**, pp. 335-351.
- Lopes, T. D., Riegel-Vidotti, I. C., Grein, A., Tischer, C. A. and Faria-Tischer, P. C. de S. (2014) Bacterial cellulose and hyaluronic acid hybrid membranes: Production and characterization, *International Journal of Biological Macromolecules*, Netherlands, Elsevier B.V, **67**, pp. 401–408, [online] Available from: https://www.sciencedirect.com/science/article/pii/S0141813014002190.
- Lou, W., Venkataraman, S., Zhong, G., Ding, B., Tan, J. P. ., Xu, L., Fan, W. and Yang, Y. Y. (2018) Antimicrobial polymers as therapeutics for treatment of multidrug-resistant Klebsiella pneumoniae lung infection, *Acta Biomaterialia*, England, Elsevier Ltd, **78**, pp. 78–88, [online] Available from: http://dx.doi.org/10.1016/j.actbio.2018.07.038.
- Low, W. L., Martin, C., Hill, D. J. and Kenward, M. A. (2011) Antimicrobial efficacy of silver ions in combination with tea tree oil against Pseudomonas aeruginosa , Staphylococcus aureus and Candida albicans, *International Journal of Antimicrobial Agents*, Netherlands, Elsevier B.V, **37**(2), pp. 162–165, [online] Available from: https://www.clinicalkey.es/playcontent/1-s2.0-S0924857910004760.
- Low, W., Martin, C., Hill, D. and Kenward, M. (2013) Antimicrobial efficacy of liposome-encapsulated silver ions and tea tree oil against *Pseudomonas aeruginosa*, *Staphylococcus aureus* and *Candida albicans*, *Letters in Applied Microbiology*,

England, Wiley Subscription Services, Inc, **57**(1), pp. 33–39, [online] Available from: https://onlinelibrary.wiley.com/doi/abs/10.1111/lam.12082.

- Lucas, T., Waisman, A., Ranjan, R., Roes, J., Krieg, T., Muller, W., Roers, A. and Eming, S. A. (2010) Differential Roles of Macrophages in Diverse Phases of Skin Repair, *The Journal of Immunology*, United States, Am Assoc Immnol, **184**(7), pp. 3964–3977, [online] Available from: http://www.jimmunol.org/cgi/content/abstract/184/7/3964.
- Luo, P., Liu, L., Xu, W., Fan, L. and Nie, M. (2018) Preparation and characterization of aminated hyaluronic acid/oxidized hydroxyethyl cellulose hydrogel, *Carbohydrate Polymers*, Elsevier Ltd, **199**, pp. 170–177, [online] Available from: https://www.sciencedirect.com/science/article/pii/S0144861718307197.
- Lyu, Y., Yu, M., Liu, Q., Zhang, Q., Liu, Z., Tian, Y., Li, D. and Changdao, M. (2020) Synthesis of silver nanoparticles using oxidized amylose and combination with curcumin for enhanced antibacterial activity, *Carbohydrate Polymers*, [online] Available from: http://www.sciencedirect.com/science/article/pii/S014486171931241X.
- Madaghiele, M., Demitri, C., Sannino, A. and Ambrosio, L. (2014) Polymeric hydrogels for burn wound care: Advanced skin wound dressings and regenerative templates, *Burns & trauma*, England, Medknow, **2**(4), pp. 153–161, [online] Available from: https://www.ncbi.nlm.nih.gov/pubmed/27602378.
- Maitra, J. and Shukla, V.K. (2014) Cross-linking in Hydrogels- A Review, *American Journal of Polymer Science*, **4**, pp. 25-31. doi:10.5923/j.ajps.20140402.01.
- Malagurski, I., Levic, S., Mitric, M., Pavlovic, V. and Dimitrijevic-Brankovic, S. (2018) Bimetallic alginate nanocomposites: New antimicrobial biomaterials for biomedical

application, *Materials Letters*, Elsevier B.V, **212**, pp. 32–36, [online] Available from: https://www.sciencedirect.com/science/article/pii/S0167577X17315227.

- Malone, M., Schwarzer, S., Walsh, A., Xuan, W., Al Gannass, A., Dickson, H. G. and Bowling, F. L. (2020) Monitoring wound progression to healing in diabetic foot ulcers using three-dimensional wound imaging, *Journal of Diabetes and its Complications*, [online] Available from: http://www.sciencedirect.com/science/article/pii/S1056872719310050.
- Maneerung, T., Tokura, S. and Rujiravanit, R. (2008) Impregnation of silver nanoparticles into bacterial cellulose for antimicrobial wound dressing, *Carbohydrate Polymers*, Elsevier Ltd, **72**(1), pp. 43–51, [online] Available from: http://dx.doi.org/10.1016/j.carbpol.2007.07.025.
- Manna, B. and Morrison, C. A. (2020) Wound Debridement. In: StatPearls [Internet]. Treasure Island (FL): StatPearls Publishing, [online] Available from: https://www.ncbi.nlm.nih.gov/books/NBK507882/
- Manolova, Y., Deneva, V., Antonov, L., Drakalska, E., Momekova, D. and Lambov, N. (2014) The effect of the water on the curcumin tautomerism: A quantitative approach, *Spectrochimica Acta Part A: Molecular and Biomolecular Spectroscopy*, Elsevier B.V, **132**, pp. 815–820, [online] Available from: https://www.sciencedirect.com/science/article/pii/S1386142514008889.
- Marcolino, V. A., Zanin, G. M., Durrant, L. R., Benassi, M. D. T. and Matioli, G. (2011) Interaction of Curcumin and Bixin with β-Cyclodextrin: Complexation Methods, Stability, and Applications in Food, *Journal of Agricultural and Food Chemistry*, United States, American Chemical Society, **59**(7), pp. 3348–3357, [online] Available from: http://dx.doi.org/10.1021/jf104223k.

- Martin, C., Low, W. L., Amin, M. C. I. M., Radecka, I., Raj, P. and Kenward, K. (2013) Current trends in the development of wound dressings, biomaterials and devices, *Pharmaceutical patent analyst*, England, **2**(3), pp. 341–359, [online] Available from: https://www.ncbi.nlm.nih.gov/pubmed/24237061.
- Martin, C., Low, W. L., Gupta, A., Amin, M. C. I. M., Radecka, I., Britland, S. T., Raj, P. and Kenward, K. (MA) (2015) Strategies for Antimicrobial Drug Delivery to Biofilm, *Current Pharmaceutical Design*, United Arab Emirates, Bentham Science Publishers Ltd, **21**(1), pp. 43–66, [online] Available from: http://www.eurekaselect.com/openurl/content.php?genre=article&issn=1381-6128&volume=21&issue=1&spage=43.
- Martin, F. T., O'Sullivan, J. B., Regan, P. J., McCann, J. and Kelly, J. L. (2010) Hydrocolloid dressing in pediatric burns may decrease operative intervention rates, *Journal of Pediatric Surgery*, United States, Elsevier Inc, **45**(3), pp. 600–605, [online] Available from: https://www.clinicalkey.es/playcontent/1-s2.0-S0022346809007787.
- Martin, M (2013a) Physiology of Wound Healing, in: Flanagan (ed.), Wound Healing and Skin Integrity: Principles and Practice, John Wiley & Sons, Ltd., U.K., pp. 33-51.
- Martínez Ávila, H., Schwarz, S., Feldmann, E.-M., Mantas, A., von Bomhard, A., Gatenholm, P. and Rotter, N. (2014) Biocompatibility evaluation of densified bacterial nanocellulose hydrogel as an implant material for auricular cartilage regeneration, *Applied Microbiology and Biotechnology*, Berlin/Heidelberg, Springer Berlin Heidelberg, **98**(17), pp. 7423–7435, [online] Available from: https://www.ncbi.nlm.nih.gov/pubmed/24866945.
- Masaoka, S., Ohe, T. and Sakota, N. (1993) Production of cellulose from glucose by Acetobacter xylinum, *Journal of Fermentation and Bioengineering*, Elsevier

B.V, **75**(1), pp. 18–22, [online] Available from: http://dx.doi.org/10.1016/0922-338X(93)90171-4.

- Matica, M. A., Aachmann, F. L., Tøndervik, A., Sletta, H. and Ostafe, V. (2019) Chitosan as a Wound Dressing Starting Material: Antimicrobial Properties and Mode of Action, *International journal of molecular sciences*, Switzerland, MDPI, **20**(23), p. 5889, [online] Available from: https://www.ncbi.nlm.nih.gov/pubmed/31771245.
- Miguel, S. P., Ribeiro, M. P., Brancal, H., Coutinho, P. and Correia, I. J. (2014) Thermoresponsive chitosan–agarose hydrogel for skin regeneration, *Carbohydrate Polymers*, England, Elsevier Ltd, **111**, pp. 366–373, [online] Available from: https://www.sciencedirect.com/science/article/pii/S0144861714004573.
- Mishra, K., Ojha, H. and Chaudhury, N. K. (2012) Estimation of antiradical properties of antioxidants using DPPH assay: A critical review and results, *Food Chemistry*, Elsevier Ltd, **130**(4), pp. 1036–1043, [online] Available from: https://www.sciencedirect.com/science/article/pii/S0308814611011058.
- Mohamad, N., Buang, F., Mat Lazim, A., Ahmad, N., Martin, C. and Mohd Amin, M. C. I. (2016) Characterization and biocompatibility evaluation of bacterial cellulose-based wound dressing hydrogel: effect of electron beam irradiation doses and concentration of acrylic acid, *Journal of Biomedical Materials Research Part B: Applied Biomaterials*, **105**(8), pp. 2553–2564.
- Mohammadian, M., Salami, M., Momen, S., Alavi, F., Emam-Djomeh, Z. and Moosavi-Movahedi, A. A. (2019) Enhancing the aqueous solubility of curcumin at acidic condition through the complexation with whey protein nanofibrils, *Food Hydrocolloids*, Elsevier Ltd, **87**, pp. 902–914, [online] Available from: http://dx.doi.org/10.1016/j.foodhyd.2018.09.001.

- Mohammadinejad, R., Maleki, H., Larrañeta, E., Fajardo, A. R., Nik, A. B., Shavandi, A., Sheikhi, A., Ghorbanpour, M., Farokhi, M., Govindh, P., Cabane, E., Azizi, S., Aref, A. R., Mozafari, M., Mehrali, M., Thomas, S., Mano, J. F., Mishra, Y. K. and Thakur, V. K. (2019) Status and future scope of plant-based green hydrogels in biomedical engineering, *Applied Materials Today*, Elsevier Ltd, **16**, pp. 213–246, [online] Available from: https://www.sciencedirect.com/science/article/pii/S2352940719300332.
- Mohammadkazemi, F., Azin, M. and Ashori, A. (2015) Production of bacterial cellulose using different carbon sources and culture media, *Carbohydrate Polymers*, England, Elsevier Ltd, **117**, pp. 518–523, [online] Available from: http://dx.doi.org/10.1016/j.carbpol.2014.10.008.
- Mohan, P. R. K., Sreelakshmi, G., Muraleedharan, C. and Joseph, R. (2012) Water soluble complexes of curcumin with cyclodextrins: Characterization by FT-Raman spectroscopy, *Vibrational Spectroscopy*, Elsevier B.V, **62**, pp. 77–84, [online] Available from: https://www.sciencedirect.com/science/article/pii/S092420311200118X.
- Mohanty, C. and Sahoo, S. K. (2017) Curcumin and its topical formulations for wound healing applications, *Drug Discovery Today*, England, Elsevier Ltd, **22**(10), pp. 1582–1592, [online] Available from: https://www.sciencedirect.com/science/article/pii/S1359644616304378.
- Moniri, M., Boroumand Moghaddam, A., Azizi, S., Abdul Rahim, R., Bin Ariff, A., Zuhainis Saad, W., Navaderi, M. and Mohamad, R. (2017) Production and Status of Bacterial Cellulose in Biomedical Engineering, *Nanomaterials*, Basel, MDPI AG, **7**(9), p. 257, [online] Available from: https://search.proquest.com/docview/1952055255.

- Morgado, P. I., Aguiar-Ricardo, A. and Correia, I. J. (2015) Asymmetric membranes as ideal wound dressings: An overview on production methods, structure, properties and performance relationship, *Journal of Membrane Science*, Elsevier B.V, **490**, pp. 139–151, [online] Available from: http://dx.doi.org/10.1016/j.memsci.2015.04.064.
- Morgado, P. I., Lisboa, P. F., Ribeiro, M. P., Miguel, S. P., Simões, P. C., Correia, I. J. and Aguiar-Ricardo, A. (2014) Poly(vinyl alcohol)/chitosan asymmetrical membranes: Highly controlled morphology toward the ideal wound dressing, *Journal of Membrane Science*, Elsevier B.V, **469**, pp. 262–271, [online] Available from: https://www.sciencedirect.com/science/article/pii/S0376738814004864.
- Morton, L.M. and Phillips, T.J. (2016) Wound healing and treating wounds, *Journal of the American Academy of Dermatology*. **74**; pp. 589–605. doi:10.1016/j.jaad.2015.08.068.
- Moura, L. I. ., Dias, A. M. ., Carvalho, E. and de Sousa, H. C. (2013) Recent advances on the development of wound dressings for diabetic foot ulcer treatment—A review, *Acta Biomaterialia*, England, Elsevier Ltd, **9**(7), pp. 7093–7114, [online] Available from: http://dx.doi.org/10.1016/j.actbio.2013.03.033.
- Moura, L. I. ., Dias, A. M. ., Suesca, E., Casadiegos, S., Leal, E. C., Fontanilla, M. R., Carvalho, E., Carvalho, L. and de Sousa, H. C. (2014) Neurotensin-loaded collagen dressings reduce inflammation and improve wound healing in diabetic mice, *BBA - Molecular Basis of Disease*, Elsevier B.V, **1842**(1), pp. 32–43, [online] Available from: https://www.sciencedirect.com/science/article/pii/S0925443913003049.
- Mousavi, S., Khoshfetrat, A. B., Khatami, N., Ahmadian, M. and Rahbarghazi, R. (2019) Comparative study of collagen and gelatin in chitosan-based hydrogels for effective wound dressing: Physical properties and fibroblastic cell

behavior, *Biochemical and Biophysical Research Communications*, [online] Available from: http://www.sciencedirect.com/science/article/pii/S0006291X19316250.

- Mozalewska, W., Czechowska-Biskup, R., Olejnik, A. K., Wach, R. A., Ulański, P. and Rosiak, J. M. (2017) Chitosan-containing hydrogel wound dressings prepared by radiation technique, *Radiation Physics and Chemistry*, Elsevier Ltd, **134**, pp. 1–7, [online] Available from: http://dx.doi.org/10.1016/j.radphyschem.2017.01.003.
- Mukherjee, D., Azamthulla, M., Santhosh, S., Dath, G., Ghosh, A., Natholia, R., Anbu, J., Teja, B. V. and Muzammil, K. M. (2018) Development and characterization of chitosan-based hydrogels as wound dressing materials, *Journal of Drug Delivery Science and Technology*, Elsevier B.V, **46**, pp. 498–510, [online] Available from: http://dx.doi.org/10.1016/j.jddst.2018.06.008.
- Mun, S.-H., Joung, D.-K., Kim, Y.-S., Kim, Y.-C., Kim, S.-B., Kang, O.-H., Seo, Y.-S., Lee, D.-S., Shin, D.-W., Kweon, K.-T. and Kwon, D.-Y. (2013) Synergistic antibacterial effect of curcumin against methicillin-resistant Staphylococcus aureus, *Phytomedicine*, Germany, Elsevier GmbH, **20**(8–9), pp. 714–718, [online] Available from: https://www.sciencedirect.com/science/article/pii/S0944711313000780.
- Mura, P. (2015) Analytical techniques for characterization of cyclodextrin complexes in the solid state: A review, *Journal of Pharmaceutical and Biomedical Analysis*, England, Elsevier B.V, **113**, pp. 226–238, [online] Available from: https://www.sciencedirect.com/science/article/pii/S0731708515000977.
- Murphy, P. S. and Evans, G. R. D. (2012). Advances in wound healing: A review of current wound healing products. *Plastic Surgery International*, Available from: https://doi.org/10.1155/2012/190436.

- Nagoba, B. and Davane, M. (2019) Studies on wound healing potential of topical herbal formulations- do we need to strengthen study protocol?, *Journal of Ayurveda and Integrative Medicine*, [online] Available from: http://www.sciencedirect.com/science/article/pii/S0975947618307344.
- Nakayama, A., Kakugo, A., Gong, J. P., Osada, Y., Takai, M., Erata, T. and Kawano, S. (2004) High Mechanical Strength Double-Network Hydrogel with Bacterial Cellulose, *Advanced Functional Materials*, Weinheim, WILEY-VCH Verlag, **14**(11), pp. 1124–1128, [online] Available from: https://onlinelibrary.wiley.com/doi/abs/10.1002/adfm.200305197.
- Nalampang, K., Panjakha, R., Molloy, R. and Tighe, B. J. (2013) Structural effects in photopolymerized sodium AMPS hydrogels crosslinked with poly(ethylene glycol) diacrylate for use as burn dressings, *Journal of biomaterials science. Polymer edition*, England, **24**(11), pp. 1291–1304, [online] Available from: https://www.ncbi.nlm.nih.gov/pubmed/23796031.
- Naseri-Nosar, M. and Ziora, Z. M. (2018) Wound dressings from naturally-occurring polymers: A review on homopolysaccharide-based composites, *Carbohydrate Polymers*, England, Elsevier Ltd, **189**, pp. 379–398, [online] Available from: https://www.sciencedirect.com/science/article/pii/S0144861718301413.
- Neuhaus, F. C. and Baddiley, J. (2003) A Continuum of Anionic Charge: Structures and Functions of d-Alanyl-Teichoic Acids in Gram-Positive Bacteria, *Microbiology and Molecular Biology Reviews*, United States, American Society for Microbiology, **67**(4), pp. 686–723, [online] Available from: http://mmbr.asm.org/content/67/4/686.abstract.
- Nimeskern, L., Martínez Ávila, H., Sundberg, J., Gatenholm, P., Müller, R. and Stok, K. S. (2013) Mechanical evaluation of bacterial nanocellulose as an implant material

for ear cartilage replacement, *Journal of the Mechanical Behavior of Biomedical Materials*, Netherlands, Elsevier Ltd, **22**, pp. 12–21, [online] Available from: http://dx.doi.org/10.1016/j.jmbbm.2013.03.005.

- Nishi, Y., Uryu, M., Yamanaka, S., Watanabe, K., Kitamura, N., Iguchi, M. and Mitsuhashi, S. (1990) The structure and mechanical properties of sheets prepared from bacterial cellulose, *Journal of Materials Science*, **25**(6), pp. 2997–3001.
- Nistor, M.-T., Chiriac, A. P., Vasile, C., Verestiuc, L. and Nita, L. E. (2011) Synthesis of hydrogels based on poly(NIPAM) inserted into collagen sponge, *Colloids and Surfaces B: Biointerfaces*, Netherlands, Elsevier B.V, **87**(2), pp. 382–390, [online] Available from: http://dx.doi.org/10.1016/j.colsurfb.2011.05.046.
- Novaes Jr, A. B. and Novaes, A. B. (1993) Bone formation over a TiAl6V4(IMZ) implant placed into an extraction socket in association with membrane therapy (Gengiflex), *Clinical Oral Implants Research*, Copenhagen, Munksgaard International Publishers, **4**(2), pp. 106–110, [online] Available from: https://onlinelibrary.wiley.com/doi/abs/10.1034/j.1600-0501.1993.040207.x.
- Oh, S. Y., Yoo, D. I., Shin, Y., Kim, H. C., Kim, H. Y., Chung, Y. S., Park, W. H. and Youk, J. H. (2005) Crystalline structure analysis of cellulose treated with sodium hydroxide and carbon dioxide by means of X-ray diffraction and FTIR spectroscopy, *Carbohydrate Research*, Netherlands, Elsevier Ltd, **340**(15), pp. 2376–2391, [online] Available from: http://dx.doi.org/10.1016/j.carres.2005.08.007.
- Oikawa, T., Morino, T. and Ameyama, M. (1995) Production of Cellulose from D-Arabitol by Acetobacter xylinum KU-1, *Bioscience, Biotechnology, and Biochemistry*, Taylor & Francis, **59**(8), pp. 1564–1565, [online] Available from: http://www.tandfonline.com/doi/abs/10.1271/bbb.59.1564.

- Okur, M. E., Karantas, I. D., Şenyiğit, Z., Okur, N. Ü. and Siafaka, P. I. (2020) Recent trends on wound management; new therapeutic choices based on polymeric carriers, *Asian Journal of Pharmaceutical Sciences*, [online] Available from: http://www.sciencedirect.com/science/article/pii/S1818087619311808.
- Oliveira, R. N., McGuinness, G. B., Ramos, M. E. T., Kajiyama, C. E. and Thiré, R. M. S. M. (2016) Properties of PVA Hydrogel Wound-Care Dressings Containing UK Propolis, *Macromolecular Symposia*, Wiley Subscription Services, Inc, **368**(1), pp. 122–127, [online] Available from: https://onlinelibrary.wiley.com/doi/abs/10.1002/masy.201500149.
- Oryan, A., Jalili, M., Kamali, A. and Nikahval, B. (2018) The concurrent use of probiotic microorganism and collagen hydrogel/scaffold enhances burn wound healing: An in vivo evaluation, *Burns*, Netherlands, Elsevier Ltd, [online] Available from: https://www.sciencedirect.com/science/article/pii/S0305417918304042.
- Ovington, L. G. (2007) Advances in wound dressings, *Clinics in Dermatology*, [online] Available from: http://www.sciencedirect.com/science/article/pii/S0738081X06001349.
- Pacelli, S., Paolicelli, P., Dreesen, I., Kobayashi, S., Vitalone, A. and Casadei, M. A. (2015) Injectable and photocross-linkable gels based on gellan gum methacrylate: A new tool for biomedical application, *International Journal of Biological Macromolecules*, Netherlands, Elsevier B.V, **72**, pp. 1335–1342, [online] Available from: https://www.sciencedirect.com/science/article/pii/S0141813014007223.
- Padil, V. V. ., Wacławek, S., Černík, M. and Varma, R. S. (2018) Tree gum-based renewable materials: Sustainable applications in nanotechnology, biomedical and environmental fields, *Biotechnology Advances*, England, Elsevier Inc, **36**(7), pp.

1984–2016, [online] Available from: https://www.sciencedirect.com/science/article/pii/S0734975018301460.

- Pal, A., Goswami, D., Cuellar, H., Castro, B., Kuang, S. and Martinez, V. (2018) Early detection and monitoring of chronic wounds using low-cost, omniphobic paper-based smart bandages, Biosensors and Bioelectronics, 117, pp. 696-705.
- Pal, K., Banthia, A. K. and Majumdar, D. K. (2009) Polymeric Hydrogels: Characterization and Biomedical Applications, *Designed Monomers and Polymers*, Taylor & Francis Group, **12**(3), pp. 197–220, [online] Available from: http://www.tandfonline.com/doi/abs/10.1163/156855509X436030.
- Pal, K., Banthia, A.K. and Majumdar, D.K. (2006) Starch based hydrogel with potential biomedical application as artificial skin, *African Journal of Biomedical Research,* **9**: pp. 23-29. doi:10.4314/ajbr.v9i1.48769.
- Pan, H., Fan, D., Duan, Z., Zhu, C., Fu, R. and Li, X. (2019) Non-stick hemostasis hydrogels as dressings with bacterial barrier activity for cutaneous wound healing, *Materials Science & Engineering C*, Elsevier B.V, **105**, p. 110118, [online] Available from: https://www.sciencedirect.com/science/article/pii/S092849311832335X.
- Pandey, M., Mohamad, N., Low, W.-L., Martin, C. and Mohd Amin, M. (2017) Microwaved bacterial cellulose-based hydrogel microparticles for the healing of partial thickness burn wounds, *Drug Delivery and Translational Research*, New York, Springer US, **7**(1), pp. 89–99.
- Pang, M., Huang, Y., Meng, F., Zhuang, Y., Liu, H., Du, M., Ma, Q., Wang, Q., Chen, Z., Chen, L., Cai, T. and Cai, Y. (2020) Application of bacterial cellulose in skin and bone tissue engineering, *European Polymer Journal*, Elsevier Ltd, **122**, p. 109365, [online] Available from: http://dx.doi.org/10.1016/j.eurpolymj.2019.109365.

- Paramera, E. I., Konteles, S. J. and Karathanos, V. T. (2011) Stability and release properties of curcumin encapsulated in Saccharomyces cerevisiae, β-cyclodextrin and modified starch, *Food Chemistry*, Elsevier Ltd, **125**(3), pp. 913–922, [online] Available from: https://www.sciencedirect.com/science/article/pii/S0308814610011702.
- Park, J.-S., An, S.-J., Jeong, S.-I., Gwon, H.-J., Lim, Y.-M. and Nho, Y.-C. (2017) Chestnut Honey Impregnated Carboxymethyl Cellulose Hydrogel for Diabetic Ulcer Healing, *Polymers*, Switzerland, MDPI, **9**(7), p. 248, [online] Available from: https://www.ncbi.nlm.nih.gov/pubmed/30970925.
- Park, J.-S., Lim, Y.-M., Baik, J., Jeong, J.-O., Jeong, S.-I., An, S.-J., Gwon, H.-J. and Khil, M.-S. (2018) Preparation and evaluation of β-glucan hydrogel prepared by the radiation technique for drug carrier applications, *International Journal of Biological Macromolecules*, Netherlands, Elsevier B.V, **118**(Pt A), pp. 333–339, [online] Available from: https://www.sciencedirect.com/science/article/pii/S0141813017333482.
- Parveen, A., Kulkarni, N., Yalagatti, M., Abbaraju, V. and Deshpande, R. (2018) In vivo efficacy of biocompatible silver nanoparticles cream for empirical wound healing, *Journal of Tissue Viability*, England, Elsevier Ltd, **27**(4), pp. 257–261, [online] Available from: http://dx.doi.org/10.1016/j.jtv.2018.08.007.
- Patel, J. P. and Parsania, P. H. (2018) 3 - Characterization, testing, and reinforcing materials of biodegradable composites, *Biodegradable and Biocompatible Polymer Composites*, Shimpi, N. G. (ed.), Woodhead Publishing, [online] Available from: http://www.sciencedirect.com/science/article/pii/B9780081009703000031.
- Paul, W. and Sharma, C.P. (2015) *The Role of Growth Factors, Cytokines, Nutrition and Matrix Metalloproteinases, in Wound Healing*, In: Advances in Wound Healing

Materials: Science and Skin Engineering, Smithers Group Company, Shropshire, U.K., pp. 61-80.

- Pereira, R., Carvalho, A., Vaz, D. C., Gil, M. ., Mendes, A. and Bártolo, P. (2013) Development of novel alginate based hydrogel films for wound healing applications, *International Journal of Biological Macromolecules*, Netherlands, Elsevier B.V, **52**, pp. 221–230, [online] Available from: http://dx.doi.org/10.1016/j.ijbiomac.2012.09.031.
- Peršin, Z., Maver, U., Pivec, T., Maver, T., Vesel, A., Mozetič, M. and Stana-Kleinschek, K. (2014) Novel cellulose based materials for safe and efficient wound treatment, *Carbohydrate Polymers*, England, Elsevier Ltd, **100**, pp. 55–64, [online] Available from: http://dx.doi.org/10.1016/j.carbpol.2013.03.082.
- Pértile, R. A. ., Moreira, S., Gil da Costa, R. M., Correia, A., Guãrdao, L., Gartner, F., Vilanova, M. and Gama, M. (2012) Bacterial Cellulose: Long-Term Biocompatibility Studies, *Journal of Biomaterials Science, Polymer Edition*, England, Routledge, **23**(10), pp. 1339–1354, [online] Available from: http://www.tandfonline.com/doi/abs/10.1163/092050611X581516.
- Pinho, E., Grootveld, M., Soares, G. and Henriques, M. (2014) Cyclodextrin-based hydrogels toward improved wound dressings, *Critical Reviews in Biotechnology*, England, Informa Healthcare USA, Inc, **34**(4), pp. 328–337, [online] Available from: https://www.ncbi.nlm.nih.gov/pubmed/23919239.
- Plungpongpan, K., Koyanukkul, K., Kaewvilai, A., Nootsuwan, N., Kewsuwan, P. and Laobuthee, A. (2013) Preparation of PVP/MHEC Blended Hydrogels via Gamma Irradiation and their Calcium ion Uptaking and Releasing Ability, *Energy Procedia*, Elsevier Ltd, **34**, pp. 775–781, [online] Available from: https://www.sciencedirect.com/science/article/pii/S1876610213010564.

- Portela, R., Leal, C. R., Almeida, P. L. and Sobral, R. G. (2019) Bacterial cellulose: a versatile biopolymer for wound dressing applications, *Microbial Biotechnology*, United States, Wiley Subscription Services, Inc, **12**(4), pp. 586–610, [online] Available from: https://onlinelibrary.wiley.com/doi/abs/10.1111/1751-7915.13392.
- Powers, J. G., Higham, C., Broussard, K. and Phillips, T. J. (2016) Wound healing and treating wounds: Chronic wound care and management, *Journal of the American Academy of Dermatology*, United States, **74**(4), p. 607, [online] Available from: https://www.ncbi.nlm.nih.gov/pubmed/26979353.
- Powers, J. G., Morton, L. M. and Phillips, T. J. (2013) Dressings for chronic wounds, *Dermatologic Therapy*, **26**(3), pp. 197–206.
- Qing, C. (2017) The molecular biology in wound healing & non-healing wound, *Chinese journal of traumatology = Zhonghua chuang shang za zhi*, China, Elsevier B.V, **20**(4), pp. 189–193, [online] Available from: https://www.ncbi.nlm.nih.gov/pubmed/28712679.
- Queen, D., Gaylor, J. D. ., Evans, J. ., Courtney, J. and Reid, W. (1987) The preclinical evaluation of the water vapour transmission rate through burn wound dressings, *Biomaterials*, Netherlands, Elsevier Ltd, **8**(5), pp. 367–371, [online] Available from: https://www.sciencedirect.com/science/article/pii/014296128790007X.
- R. Rebelo, A., Archer, A. J., Chen, X., Liu, C., Yang, G. and Liu, Y. (2018) Dehydration of bacterial cellulose and the water content effects on its viscoelastic and electrochemical properties, *Science and Technology of Advanced Materials*, United States, Taylor & Francis, **19**(1), pp. 203–211, [online] Available from: http://www.tandfonline.com/doi/abs/10.1080/14686996.2018.1430981.

- Raafat, A. I., Eid, M. and El-Arnaouty, M. B. (2012) Radiation synthesis of superabsorbent CMC based hydrogels for agriculture applications, *Nuclear Inst. and Methods in Physics Research, B*, Elsevier B.V, **283**, pp. 71–76, [online] Available from: https://www.sciencedirect.com/science/article/pii/S0168583X12002194.
- Radecka, I., Martin, C. and Hill, D. (2015). *The Problem of Microbial Drug Resistance*. In: Phoenix D.A, Harris F, Dennison S.R (eds). Novel antimicrobial agents and strategies. Wiley, Germany, pp. 1-16.
- Radjaram, A., Hafid, A.F. & Setyawan, D. (2013). Dissolution enhancement of curcumin by hydroxypropyl-β-cyclodextrin complexation. *International Journal of Pharmacy and Pharmaceutical Sciences,* **5**, pp. 401-405.
- Raghunathan, D. (2013). Production of Microbial Cellulose from the New Bacterial Strain Isolated From Temple Wash Waters. *International Journal of Current Microbiology and Applied Sciences* **2**(12), pp. 275-290.
- Rai, D., Singh, J. K., Roy, N. and Panda, D. (2008) Curcumin inhibits FtsZ assembly: an attractive mechanism for its antibacterial activity, *The Biochemical journal*, England, [online] Available from: https://www.ncbi.nlm.nih.gov/pubmed/17953519.
- Rakhshaei, R. and Namazi, H. (2017) A potential bioactive wound dressing based on carboxymethyl cellulose/ZnO impregnated MCM-41 nanocomposite hydrogel, *Materials Science & Engineering C*, Netherlands, Elsevier B.V, **73**, pp. 456–464, [online] Available from: http://dx.doi.org/10.1016/j.msec.2016.12.097.
- Rakmai, J., Cheirsilp, B., Mejuto, J. C., Simal-Gándara, J. and Torrado-Agrasar, A. (2018) Antioxidant and antimicrobial properties of encapsulated guava leaf oil in hydroxypropyl-beta-cyclodextrin, *Industrial Crops & Products*, Elsevier B.V, **111**, pp.

219–225, [online] Available from: https://www.sciencedirect.com/science/article/pii/S0926669017307124.

- Rakmai, J., Cheirsilp, B., Torrado-Agrasar, A., Simal-Gándara, J. and Mejuto, J. C. (2017) Encapsulation of yarrow essential oil in hydroxypropyl-beta-cyclodextrin: physiochemical characterization and evaluation of bio-efficacies, *CYTA: Journal of Food*, Abingdon, Taylor & Francis Ltd, **15**(3), p. 409, [online] Available from: https://search.proquest.com/docview/1933955020.
- Ram, M., Singh, V., Kumawat, S., Kumar, Dinesh, Kumar, Dhirendra, Lingaraju, M. C., Uttam Singh, T., Rahal, A. and Kumar Tandan, S. (2015) Deferoxamine modulates cytokines and growth factors to accelerate cutaneous wound healing in diabetic rats, *European Journal of Pharmacology*, Netherlands, Elsevier B.V, **764**, pp. 9–21, [online] Available from: https://www.sciencedirect.com/science/article/pii/S0014299915300923.
- Ramanathan, G., Muthukumar, T. and Tirichurapalli Sivagnanam, U. (2017) In vivo efficiency of the collagen coated nanofibrous scaffold and their effect on growth factors and pro-inflammatory cytokines in wound healing, *European Journal of Pharmacology*, Netherlands, Elsevier B.V, **814**, pp. 45–55, [online] Available from: https://www.sciencedirect.com/science/article/pii/S0014299917305071.
- Ravindran, J., Arumugasamy, V. and Baskaran, A. (2019) Wound healing effect of silver nanoparticles from Tridax procumbens leaf extracts on Pangasius hypophthalmus, *Wound Medicine*, Elsevier GmbH, **27**(1), p. 100170, [online] Available from: http://dx.doi.org/10.1016/j.wndm.2019.100170.
- Reeves, R., Ribeiro, A., Lombardo, L., Boyer, R. and Leach, J. B. (2010) Synthesis and Characterization of Carboxymethylcellulose-Methacrylate Hydrogel Cell

Scaffolds, *Polymers*, Switzerland, MDPI AG, **2**(3), pp. 252–264, [online] Available from: https://www.ncbi.nlm.nih.gov/pubmed/22708058.

- Rezvanian, M., Ahmad, N., Mohd Amin, M. C. I. and Ng, S.-F. (2017) Optimization, characterization, and in vitro assessment of alginate-pectin ionic cross-linked hydrogel film for wound dressing applications, *International Journal of Biological Macromolecules*, Netherlands, Elsevier B.V, **97**, pp. 131–140, [online] Available from: https://www.sciencedirect.com/science/article/pii/S0141813016317780.

- Roquette 2006, Kleptose® Betacyclodextrins and hydroxypropyl betacyclodextrins. Available from: https://www.roquette.com/Pharma-and-Nutraceuticals-Hydroxypropyl-Beta-cyclodextrin.

- Ruddaraju, L. K., Pammi, S. V. N., Guntuku, G. sankar, Padavala, V. S. and Kolapalli, V. R. M. (2019) A review on anti-bacterials to combat resistance: From ancient era of plants and metals to present and future perspectives of green nano technological combinations, *Asian Journal of Pharmaceutical Sciences*, Netherlands, Elsevier B.V, **15**(1), pp. 42–59, [online] Available from: http://dx.doi.org/10.1016/j.ajps.2019.03.002.

- Saarai, A., Sedlacek, T., Kasparkova, V., Kitano, T. and Saha, P. (2012) On the characterization of sodium alginate/gelatine-based hydrogels for wound dressing, *Journal of Applied Polymer Science*, Hoboken, Wiley Subscription Services, Inc., A Wiley Company, **126**(S1), pp. E79–E88, [online] Available from: https://onlinelibrary.wiley.com/doi/abs/10.1002/app.36590.

- Saghazadeh, S., Rinoldi, C., Schot, M., Kashaf, S. S., Sharifi, F., Jalilian, E., Nuutila, K., Giatsidis, G., Mostafalu, P., Derakhshandeh, H., Yue, K., Swieszkowski, W., Memic, A., Tamayol, A. and Khademhosseini, A. (2018) Drug delivery systems and

materials for wound healing applications, *Advanced Drug Delivery Reviews*, Netherlands, Elsevier B.V, **127**, pp. 138–166, [online] Available from: http://dx.doi.org/10.1016/j.addr.2018.04.008.

- Saito, A., Miyazaki, H., Fujie, T., Ohtsubo, S., Kinoshita, M., Saitoh, D. and Takeoka, S. (2012) Therapeutic efficacy of an antibiotic-loaded nanosheet in a murine burn-wound infection model, *Acta Biomaterialia*, England, Elsevier Ltd, **8**(8), pp. 2932–2940, [online] Available from: https://www.sciencedirect.com/science/article/pii/S1742706112001663.
- Salim, M. M. and Malek, N. A. N. N. (2016) Characterization and antibacterial activity of silver exchanged regenerated NaY zeolite from surfactant-modified NaY zeolite, *Materials Science & Engineering C*, Netherlands, Elsevier B.V, **59**, pp. 70–77, [online] Available from: http://dx.doi.org/10.1016/j.msec.2015.09.099.
- Salton, M.R.J., and Kim K.S., (1996), *Structure*. In Baron, S (ed) Medical Microbiology", 4th ed., University of Taxas Medical Branch, USA.
- Santamaria, N., Gerdtz, M., Sage, S., McCann, J., Freeman, A., Vassiliou, T., De Vincentis, S., Ng, A. W., Manias, E., Liu, W. and Knott, J. (2013) A randomised controlled trial of the effectiveness of soft silicone multi-layered foam dressings in the prevention of sacral and heel pressure ulcers in trauma and critically ill patients: the border trial, *International Wound Journal*, Oxford, UK, Blackwell Publishing Ltd, **12**(3), pp. 302–308, [online] Available from: https://onlinelibrary.wiley.com/doi/abs/10.1111/iwj.12101.
- Sathishkumar, M., Sneha, K. and Yun, Y.-S. (2010) Immobilization of silver nanoparticles synthesized using Curcuma longa tuber powder and extract on cotton cloth for bactericidal activity, *Bioresource Technology*, England, Elsevier

Ltd, **101**(20), pp. 7958–7965, [online] Available from: https://www.sciencedirect.com/science/article/pii/S0960852410009077.

- Schreml, S., Szeimies, R.M., Prantl, L., Landthaler, M. and Babilas, P. (2010) Wound healing in the 21st century, *Journal of the American Academy of Dermatology*. **63**(5); pp. 866–881. doi:10.1016/j.jaad.2009.10.048.
- Schulz, L. T., Kim, S. Y., Hartsell, A. and Rose, W. E. (2019) Antimicrobial stewardship during a time of rapid antimicrobial development: Potential impact on industry for future investment, *Diagnostic Microbiology & Infectious Disease*, United States, Elsevier Inc, **95**(3), p. 114857, [online] Available from: http://dx.doi.org/10.1016/j.diagmicrobio.2019.06.009.
- Schumann, D. A., Wippermann, J., Klemm, D. O., Kramer, F., Koth, D., Kosmehl, H., Wahlers, T. and Salehi-Gelani, S. (2009) Artificial vascular implants from bacterial cellulose: preliminary results of small arterial substitutes, *Cellulose*, Dordrecht, Springer, **16**(5), pp. 877–885, [online] Available from: https://search.proquest.com/docview/2259906057.
- Selig, H. F., Lumenta, D. B., Giretzlehner, M., Jeschke, M. G., Upton, D. and Kamolz, L. P. (2012) The properties of an 'ideal' burn wound dressing--what do we need in daily clinical practice? Results of a worldwide online survey among burn care specialists, *Burns : journal of the International Society for Burn Injuries*, Netherlands, Elsevier B.V, **38**(7), p. 960, [online] Available from: https://www.ncbi.nlm.nih.gov/pubmed/22571855.
- Shah, N., Ul-Islam, M., Khattak, W. A. and Park, J. K. (2013) Overview of bacterial cellulose composites: A multipurpose advanced material, *Carbohydrate Polymers*, England, Elsevier Ltd, **98**(2), pp. 1585–1598, [online] Available from: http://dx.doi.org/10.1016/j.carbpol.2013.08.018.

- Shahbazi, H., Tataei, M., Enayati, M. ., Shafeiey, A. and Malekabadi, M. A. (2019) Structure-transmittance relationship in transparent ceramics, *Journal of Alloys and Compounds*, Elsevier B.V, **785**, pp. 260–285, [online] Available from: https://www.sciencedirect.com/science/article/pii/S092583881930132X.
- Shameli, K., Ahmad, M. B., Zargar, M., Yunus, W. M. Z. W. and Ibrahim, N. A. (2011) Fabrication of silver nanoparticles doped in the zeolite framework and antibacterial activity, *International journal of nanomedicine*, New Zealand, Dove Press, **6**, pp. 331–341, [online] Available from: https://www.ncbi.nlm.nih.gov/pubmed/21383858.
- Shamsipur, M., Pourmortazavi, S., Beigi, A., Heydari, R. and Khatibi, M. (2013) Thermal Stability and Decomposition Kinetic Studies of Acyclovir and Zidovudine Drug Compounds, *AAPS PharmSciTech*, Boston, Springer US, **14**(1), pp. 287–293, [online] Available from: https://www.ncbi.nlm.nih.gov/pubmed/23299688.
- Shao, W., Liu, H., Wang, S., Wu, J., Huang, M., Min, H. and Liu, X. (2016) Controlled release and antibacterial activity of tetracycline hydrochloride-loaded bacterial cellulose composite membranes, *Carbohydrate Polymers*, England, Elsevier Ltd, **145**, pp. 114–120, [online] Available from: http://dx.doi.org/10.1016/j.carbpol.2016.02.065.
- Sharma, A., Thakur, M., Bhattacharya, M., Mandal, T. and Goswami, S. (2019) Commercial application of cellulose nano-composites – A review, *Biotechnology Reports*, Netherlands, Elsevier B.V, **21**, p. e00316, [online] Available from: http://dx.doi.org/10.1016/j.btre.2019.e00316.
- Shepherd, J., Sarker, P., Rimmer, S., Swanson, L., MacNeil, S. and Douglas, I. (2011) Hyperbranched poly(NIPAM) polymers modified with antibiotics for the

reduction of bacterial burden in infected human tissue engineered skin, *Biomaterials*. **32**(1): pp. 258-267. doi:10.1016/j.biomaterials.2010.08.084.

- Shi, Z., Zhang, Y., Phillips, G. O. and Yang, G. (2014) Utilization of bacterial cellulose in food, *Food Hydrocolloids*, Elsevier Ltd, **35**, pp. 539–545, [online] Available from: http://dx.doi.org/10.1016/j.foodhyd.2013.07.012.
- Silva, A. C. da, Santos, P. D. de F., Silva, J. T. do P., Leimann, F. V., Bracht, L. and Gonçalves, O. H. (2018) Impact of curcumin nanoformulation on its antimicrobial activity, *Trends in Food Science & Technology*, Elsevier Ltd, **72**, pp. 74–82, [online] Available from: http://dx.doi.org/10.1016/j.tifs.2017.12.004.
- Silveira, F.C.A., Pinto, F.C.M., Neto, S.S.C., Leal, M.C., Cesário, J. and Aguiar, J.L.A. (2016). Treatment of tympanic membrane perforation using bacterial cellulose: a randomized controlled trial. *Brazilian Journal of Otorhinolaryngol*; 82(2), pp. 203-208.
- Singh, B. and Dhiman, A. (2015) Designing bio-mimetic moxifloxacin loaded hydrogel wound dressing to improve antioxidant and pharmacology properties, **5**(55), pp. 44666–44678.
- Singh, B. and Dhiman, A. (2016) Evaluation of network parameters and drug release behavior of gum acacia-crosslinked-carbopol hydrogel wound dressings, *Polymer Science Series A*, Moscow, Pleiades Publishing, **58**(5), pp. 754–764.
- Singh, B. and Pal, L. (2011) Radiation crosslinking polymerization of sterculia polysaccharide–PVA–PVP for making hydrogel wound dressings, *International Journal of Biological Macromolecules*, Netherlands, Elsevier B.V, **48**(3), pp. 501–510, [online] Available from: https://www.sciencedirect.com/science/article/pii/S0141813011000195.

- Singh, B., Varshney, L., Francis, S. and Rajneesh (2017) Synthesis and characterization of tragacanth gum based hydrogels by radiation method for use in wound dressing application, *Radiation Physics and Chemistry*, [online] Available from: http://www.sciencedirect.com/science/article/pii/S0969806X16304005.
- Singh, R. and Singh, D. (2012) Radiation synthesis of PVP/alginate hydrogel containing nanosilver as wound dressing, *Journal of Materials Science: Materials in Medicine*, Boston, Springer US, **23**(11), pp. 2649–2658, [online] Available from: https://www.ncbi.nlm.nih.gov/pubmed/22886579.
- Singh, S., Young, A. and McNaught, C.-E. (2017a) The physiology of wound healing, *Surgery (Oxford)*, Elsevier Ltd, **35**(9), pp. 473–477, [online] Available from: http://dx.doi.org/10.1016/j.mpsur.2017.06.004.
- Singh, V. K., Banerjee, I., Agarwal, T., Pramanik, K., Bhattacharya, M. K. and Pal, K. (2014) Guar gum and sesame oil based novel bigels for controlled drug delivery, *Colloids and Surfaces B: Biointerfaces*, Netherlands, Elsevier B.V, **123**, pp. 582–592, [online] Available from: https://www.sciencedirect.com/science/article/pii/S092777651400527X.
- Skórkowska-Telichowska, K., Czemplik, M., Kulma, A. and Szopa, J. (2013) The local treatment and available dressings designed for chronic wounds, *Journal of American Academy of Dermatology*. **68**: pp. e117-e126. doi:10.1016/j.jaad.2011.06.028.
- Smith & Nephew. (2020) Flexigel◊ Sheet [online]. Available from: https://www.smith-nephew.com/professional/products/advanced-wound-management/other-wound-care-products/flexigel-sheet/#. Accessed on 7th July 2020.
- Solway, D. R., Consalter, M. and Levinson, D. J. (2010) Microbial cellulose wound dressing in the treatment of skin tears in the frail elderly, *Wounds : a compendium of*

clinical research and practice, United States, **22**(1), p. 17, [online] Available from: https://www.ncbi.nlm.nih.gov/pubmed/25901459.

- Song, E.-H., Song, J., Jeong, S.-H., Park, J.-U., Kim, S. and Kim, H.-E. (2017) Polyurethane-silica hybrid foams from a one-step foaming reaction, coupled with a sol-gel process, for enhanced wound healing, *Materials Science & Engineering C*, Netherlands, Elsevier B.V, **79**, pp. 866–874, [online] Available from: https://www.sciencedirect.com/science/article/pii/S0928493116322858.
- Song, H.Y., Ko, K.K.., Oh, I.H. and Lee, B.T. (2006) Fabrication of silver nanoparticles and their antimicrobial mechanisms. *European Cells and Materials, **11***, pp.58-59.
- Song, Z., Wu, Y., Wang, H. and Han, H. (2019) Synergistic antibacterial effects of curcumin modified silver nanoparticles through ROS-mediated pathways, *Materials Science & Engineering C*, Netherlands, Elsevier B.V, **99**, pp. 255–263, [online] Available from: https://www.sciencedirect.com/science/article/pii/S0928493117344247.
- Sood, N., Bhardwaj, A., Mehta, S. and Mehta, A. (2016) Stimuli-responsive hydrogels in drug delivery and tissue engineering, *Drug Delivery*, England, Taylor & Francis, **23**(3), pp. 748–770, [online] Available from: http://www.tandfonline.com/doi/abs/10.3109/10717544.2014.940091.
- Sperandeo, P., Dehò, G. and Polissi, A. (2009) The lipopolysaccharide transport system of Gram-negative bacteria, *BBA - Molecular and Cell Biology of Lipids*, Elsevier B.V, **1791**(7), pp. 594–602, [online] Available from: http://dx.doi.org/10.1016/j.bbalip.2009.01.011.
- Srivatsan, K. V., Duraipandy, N., Begum, S., Lakra, R., Ramamurthy, U., Korrapati, P. S. and Kiran, M. S. (2015) Effect of curcumin caged silver nanoparticle on collagen stabilization for biomedical applications, *International Journal of Biological*

Macromolecules, Netherlands, Elsevier B.V, **75**, pp. 306–315, [online] Available from: https://www.sciencedirect.com/science/article/pii/S0141813015000616.

- Sulaeva, I., Henniges, U., Rosenau, T. and Potthast, A. (2015) Bacterial cellulose as a material for wound treatment: Properties and modifications. A review, *Biotechnology Advances*, England, Elsevier Inc, **33**(8), pp. 1547–1571, [online] Available from: http://dx.doi.org/10.1016/j.biotechadv.2015.07.009.
- Sulaeva, I., Hettegger, H., Bergen, A., Rohrer, C., Kostic, M., Konnerth, J., Rosenau, T. and Potthast, A. (2020) Fabrication of bacterial cellulose-based wound dressings with improved performance by impregnation with alginate, *Materials Science & Engineering C*, Netherlands, Elsevier B.V, **110**, p. 110619, [online] Available from: http://dx.doi.org/10.1016/j.msec.2019.110619.
- Sun, G., Zhang, X., Shen, Y.-I., Sebastian, R., Dickinson, L. E., Fox-Talbot, K., Reinblatt, M., Steenbergen, C., Harmon, J. W. and Gerecht, S. (2011) Dextran hydrogel scaffolds enhance angiogenic responses and promote complete skin regeneration during burn wound healing, *Proceedings of the National Academy of Sciences of the United States of America*, United States, National Academy of Sciences, **108**(52), pp. 20976–20981, [online] Available from: https://www.jstor.org/stable/23077172.
- Sun, Y., Du, L., Liu, Y., Li, M., Li, X., Jin, Y. and Qian, X. (2014) Transdermal delivery of the in situ hydrogels of curcumin and its inclusion complexes of hydroxypropyl-β-cyclodextrin for melanoma treatment, *International Journal of Pharmaceutics*, Netherlands, Elsevier B.V, **469**(1), pp. 31–39, [online] Available from: https://www.sciencedirect.com/science/article/pii/S0378517314002671.
- Takao, T., Kitatani, F., Watanabe, N., Yagi, A. and Sakata, K. (1994) A Simple Screening Method for Antioxidants and Isolation of Several Antioxidants Produced

by Marine Bacteria from Fish and Shellfish, *Bioscience, Biotechnology, and Biochemistry*, Taylor & Francis, **58**(10), pp. 1780–1783, [online] Available from: http://www.tandfonline.com/doi/abs/10.1271/bbb.58.1780.

- Tehrani, Z., Nordli, H. R., Pukstad, B., Gethin, D. T. and Chinga-Carrasco, G. (2016) Translucent and ductile nanocellulose-PEG bionanocomposites—A novel substrate with potential to be functionalized by printing for wound dressing applications, *Industrial Crops & Products*, Elsevier B.V, **93**, pp. 193–202, [online] Available from: https://www.sciencedirect.com/science/article/pii/S0926669016300930.
- Tejiram, S., Kavalukas, S.L., Shupp, J.W. and Barbul, A (2016) Fundamentals and strategies for wound healing, in: M. Agren (ed.), Wound Healing Biomaterials-Volume 1: Therapies and Regeration, WP Woodhead Publishing, U.K., pp. 3–39. doi:10.1016/b978-1-78242-455-0.00001-x.
- Tirrell, D. A., Fournier, M. J. and Mason, T. L. (1991) Protein engineering for materials applications, *Current Opinion in Structural Biology*, Elsevier Ltd, **1**(4), pp. 638–641, [online] Available from: http://dx.doi.org/10.1016/S0959-440X(05)80089-2.
- Tort, S., Demiröz, F. T., Coşkun Cevher, Ş., Sarıbaş, S., Özoğul, C. and Acartürk, F. (2019) The effect of a new wound dressing on wound healing: Biochemical and histopathological evaluation, *Burns*, [online] Available from: http://www.sciencedirect.com/science/article/pii/S0305417918309768.
- Tsai, Y.-C., Li, S., Hu, S.-G., Chang, W.-C., Jeng, U.-S. and Hsu, S. (2015) Synthesis of Thermoresponsive Amphiphilic Polyurethane Gel as a New Cell Printing Material near Body Temperature, *ACS Applied Materials & Interfaces*, United States, American Chemical Society, **7**(50), pp. 27613–27623, [online] Available from: http://dx.doi.org/10.1021/acsami.5b10697.

- Tyeb, S., Kumar, A., Kumar, N. and Verma, V. (2018) Flexible agar-sericin hydrogel film dressing for chronic wounds, *Carbohydrate Polymers*, England, Elsevier Ltd, **200**, pp. 572–582, [online] Available from: https://www.sciencedirect.com/science/article/pii/S0144861718309287.
- Tymen, S. D., Rojas, I. G., Zhou, X., Fang, Z. J., Zhao, Y. and Marucha, P. T. (2013) Restraint stress alters neutrophil and macrophage phenotypes during wound healing, *Brain, Behavior, and Immunity*, Netherlands, Elsevier Inc, **28**, pp. 207–217, [online] Available from: https://www.clinicalkey.es/playcontent/1-s2.0-S0889159112001961.
- Ul-Islam, M., Khan, S., Khattak, W.A., Ullah, M.W. and Park, U.K. (2015) Synthesis, Chemistry, and Medical Applications of Bacterial Cellulose Nanocomposites, In: Advanced Structured Materials- Eco-friendly Polymer Nanocomposites, Springer, pp, 399-437. Doi: 10.1007/978-81-322-2473-0_13
- Ullah H, and Ali S. (2017) Classification of Anti-Bacterial Agents and Their Functions 2017. Antimicrobial agents, pp. 1-16. DOI: 10.5772/intechopen.68695 accessed on 28Mar 2020
- Ullah, F., Othman, M. B. H., Javed, F., Ahmad, Z. and Akil, H. M. (2015) Classification, processing and application of hydrogels: A review, *Materials Science & Engineering C*, Netherlands, Elsevier B.V, **57**, pp. 414–433, [online] Available from: http://dx.doi.org/10.1016/j.msec.2015.07.053.
- Ullah, M. W., Manan, S., Kiprono, S. J., Ul-Islam, M. and Yang, G. (2019) *Synthesis, Structure, and Properties of Bacterial Cellulose*, *Nanocellulose*, Weinheim, Germany, Wiley-VCH Verlag GmbH & Co. KGaA, pp. 81–113, [online] Available from: https://onlinelibrary.wiley.com/doi/abs/10.1002/9783527807437.ch4.

- Valverde-Aguilar, G., Garcia-Macedo, J. A., Renteria-Tapia, V. M., Gomez, R. W. and Quintana-Garcia, M. (2011) Modelling of optical absorption of silver NP's produced by UV radiation embedded in mesostructured silica films, *Journal of Nanoparticle Research: An Interdisciplinary Forum for Nanoscale Science and Technology*, Dordrecht, Springer, **13**(10), pp. 4613–4622, [online] Available from: https://search.proquest.com/docview/1111850969.
- Varghese, S. and Jamora, C. (2012) Hydrogels: a versatile tool with a myriad of biomedical and research applications for the skin, *Expert Review of Dermatology*, London, Informa Healthcare, **7**(4), pp. 315–317, [online] Available from: http://www.tandfonline.com/doi/abs/10.1586/edm.12.28.
- Velnar, T., Bailey, T. and Smrkolj, V. (2009) The Wound Healing Process: An Overview of the Cellular and Molecular Mechanisms, *Journal of International Medical Research*. **37**; pp. 1528–1542. doi:10.1177/147323000903700531.
- Verma, A. and Mehata, M. S. (2016) Controllable synthesis of silver nanoparticles using Neem leaves and their antimicrobial activity, *Journal of Radiation Research and Applied Sciences*, Elsevier B.V, **9**(1), pp. 109–115, [online] Available from: http://dx.doi.org/10.1016/j.jrras.2015.11.001.
- Vowden, P. and Vowden, K. (2017) Wound dressings: principles and practice, *Surgery (Oxford)*, Elsevier Ltd, **35**(9), pp. 489–494, [online] Available from: https://www.sciencedirect.com/science/article/pii/S0263931917301370.
- Waghmare, S., Waghmare, S., Mulla, M., Mulla, M., Marathe, S., Marathe, S., Sonawane, K. and Sonawane, K. (2015) Ecofriendly production of silver nanoparticles using Candida utilis and its mechanistic action against pathogenic microorganisms, *3 Biotech*, Berlin/Heidelberg, Springer Berlin Heidelberg, **5**(1), pp. 33–38, [online] Available from: https://www.ncbi.nlm.nih.gov/pubmed/28324356.

- Wang, J. and Wei, J. (2017) Interpenetrating network hydrogels with high strength and transparency for potential use as external dressings, *Materials Science & Engineering C*, Netherlands, Elsevier B.V, **80**, pp. 460–467, [online] Available from: https://www.sciencedirect.com/science/article/pii/S0928493117316594.
- Wang, J., Tavakoli, J. and Tang, Y. (2019) Bacterial cellulose production, properties and applications with different culture methods – A review, *Carbohydrate Polymers*, England, Elsevier Ltd, **219**, pp. 63–76, [online] Available from: http://dx.doi.org/10.1016/j.carbpol.2019.05.008.
- Wang, M., Xu, L., Hu, H., Zhai, M., Peng, J., Nho, Y., Li, J. and Wei, G. (2007) Radiation synthesis of PVP/CMC hydrogels as wound dressing, *Nuclear Inst. and Methods in Physics Research, B*, Elsevier B.V, **265**(1), pp. 385–389, [online] Available from: http://dx.doi.org/10.1016/j.nimb.2007.09.009.
- Wang, P.H., Huang, B.S., Horng, H.C., Yeh, C.C. and Chen, Y.J. (2018) Wound healing, *Journal of the Chinese Medical Association*, **81**; pp. 94-101. doi.org/10.1016/j.jcma.2017.11.002.
- Wang, T., Zhu, X.-K., Xue, X.-T. and Wu, D.-Y. (2012) Hydrogel sheets of chitosan, honey and gelatin as burn wound dressings, *Carbohydrate Polymers*, Elsevier Ltd, **88**(1), pp. 75–83, [online] Available from: http://dx.doi.org/10.1016/j.carbpol.2011.11.069.
- Wang, W., Yu, L. J., Zhang, S. M., Fu, L. N. and Yang, G. (2009) Fabrication of Novel Cellulose/Chitosan Artificial Skin Composite, *Materials Science Forum*, pp. 1034–1038, [online] Available from: https://www.scientific.net/MSF.610-613.1034.
- Waterhouse, G. I. N., Bowmaker, G. A. and Metson, J. B. (2001) The thermal decomposition of silver (I, III) oxide: A combined XRD, FT-IR and Raman spectroscopic study, *Physical Chemistry Chemical Physics*, **3**(17), pp. 3838–3845.

- Wathoni, N., Motoyama, K., Higashi, T., Okajima, M., Kaneko, T. and Arima, H. (2017) Enhancement of curcumin wound healing ability by complexation with 2-hydroxypropyl-γ-cyclodextrin in sacran hydrogel film, *International Journal of Biological Macromolecules*, Netherlands, Elsevier B.V, **98**, pp. 268–276, [online] Available from: http://dx.doi.org/10.1016/j.ijbiomac.2017.01.144.
- Wathoni, N., Motoyama, K., Higashi, T., Okajima, M., Kaneko, T. and Arima, H. (2016) Physically crosslinked-sacran hydrogel films for wound dressing application, *International Journal of Biological Macromolecules*, Netherlands, Elsevier B.V, **89**, pp. 465–470, [online] Available from: http://dx.doi.org/10.1016/j.ijbiomac.2016.05.006.
- Wei, B., Yang, G. and Hong, F. (2011) Preparation and evaluation of a kind of bacterial cellulose dry films with antibacterial properties, *Carbohydrate Polymers*, Elsevier Ltd, **84**(1), pp. 533–538, [online] Available from: http://dx.doi.org/10.1016/j.carbpol.2010.12.017.
- Wei, H., Ping|Huang, Ping Chen, Min (2013) Curcumin reduces Streptococcus mutans biofilm formation by inhibiting sortase A activity, *Archives of Oral Biology*, England, Elsevier Ltd, **58**(10), pp. 1343–1348, [online] Available from: https://www.clinicalkey.es/playcontent/1-s2.0-S0003996913001714.
- Wilkinson, L. ., White, R. and Chipman, J. . (2011) Silver and nanoparticles of silver in wound dressings: a review of efficacy and safety, *Journal of Wound Care*, London, MA Healthcare, **20**(11), pp. 543–549, [online] Available from: https://www.ncbi.nlm.nih.gov/pubmed/22240850.
- Williams D. F. (1986). Definitions in Biomaterials, in Proceedings of a Consensus Conference of the European Society for Biomaterials (Chester: Elsevier).

- Williams, H., Campbell, L., Crompton, R. A., Singh, G., McHugh, B. J., Davidson, D. J., McBain, A. J., Cruickshank, S. M. and Hardman, M. J. (2018) Microbial Host Interactions and Impaired Wound Healing in Mice and Humans: Defining a Role for BD14 and NOD2, *Journal of Investigative Dermatology*, [online] Available from: http://www.sciencedirect.com/science/article/pii/S0022202X18318931.
- Winter, G. D. (1962) Formation of the Scab and the Rate of Epithelization of Superficial Wounds in the Skin of the Young Domestic Pig, *Nature*, England, **193**(4812), pp. 293–294, [online] Available from: http://dx.doi.org/10.1038/193293a0.
- Witthayaprapakorn, C. (2011) Design and Preparation of Synthetic Hydrogels Via Photopolymerisation for Biomedical Use as Wound Dressings, *Procedia Engineering*, Elsevier Ltd, **8**, pp. 286–291, [online] Available from: https://www.sciencedirect.com/science/article/pii/S1877705811000671.
- Witthayaprapakorn, C. and Molloy, R. (2012) Design and Preparation of Synthetic Hydrogels by Redox Initiation via Free Radical Polymerisation for Biomedical Use as Wound Dressings, *Advanced Materials Research*, **506**, pp. 315–318, [online] Available from: https://www.scientific.net/AMR.506.315.
- Wong, W. R., Oliver, A. G. and Linington, R. G. (2012) Development of Antibiotic Activity Profile Screening for the Classification and Discovery of Natural Product Antibiotics, *Chemistry & Biology*, United States, Elsevier Ltd, **19**(11), pp. 1483–1495, [online] Available from: http://dx.doi.org/10.1016/j.chembiol.2012.09.014.
- Wound Care (2020). Intrasite Conformable dressings [online]. Available from: https://www.wound-care.co.uk/intrasite-conforming-dressings.html. [Accessed on 7th July 2020].

- Wu, D.-Q., Zhu, J., Han, H., Zhang, J.-Z., Wu, F.-F., Qin, X.-H. and Yu, J.-Y. (2018) Synthesis and characterization of arginine-NIPAAm hybrid hydrogel as wound dressing: In vitro and in vivo study, *Acta Biomaterialia*, England, Elsevier Ltd, **65**, pp. 305–316, [online] Available from: http://dx.doi.org/10.1016/j.actbio.2017.08.048.
- Wu, J., Zheng, Y., Song, W., Luan, J., Wen, X., Wu, Z., Chen, X., Wang, Q. and Guo, S. (2014) In situ synthesis of silver-nanoparticles/bacterial cellulose composites for slow-released antimicrobial wound dressing, *Carbohydrate Polymers*, [online] Available from: http://www.sciencedirect.com/science/article/pii/S0144861713011223.
- Wu, T., Huang, J., Jiang, Y., Hu, Y., Ye, X., Liu, D. and Chen, J. (2018a) Formation of hydrogels based on chitosan/alginate for the delivery of lysozyme and their antibacterial activity, *Food Chemistry*, England, Elsevier Ltd, **240**, pp. 361–369, [online] Available from: https://www.sciencedirect.com/science/article/pii/S0308814617311962.
- Xie, H., Chen, W., Chen, X., Shen, X., He, Y., Luo, Q., Ge, W., Yuan, W., Tang, X., Hou, D., Jiang, D., Wang, Q., Liu, Q., Liu, Y. and Li, K. (2018) Preparation of chitosan-collagen-alginate composite dressing and its promoting effects on wound healing, *International Journal of Biological Macromolecules*, Netherlands, Elsevier B.V, **107**(Pt A), pp. 93–104, [online] Available from: https://www.sciencedirect.com/science/article/pii/S0141813017306438.
- Xu, K., Cantu, D. A., Fu, Y., Kim, J., Zheng, X., Hematti, P. and Kao, W. J. (2013) Thiol-ene Michael-type formation of gelatin/poly(ethylene glycol) biomatrices for three-dimensional mesenchymal stromal/stem cell administration to cutaneous wounds, *Acta Biomaterialia*, England, Elsevier Ltd, **9**(11), pp. 8802–8814, [online]

Available from: https://www.sciencedirect.com/science/article/pii/S174270611300305X.

- Xu, Q., A, S., Gao, Y., Guo, L., Creagh-Flynn, J., Zhou, D., Greiser, U., Dong, Y., Wang, F., Wang, Wei, Wang, Wenxin, Tai, H. and Liu, W. (2018) A hybrid injectable hydrogel from hyperbranched PEG macromer as a stem cell delivery and retention platform for diabetic wound healing, *Acta Biomaterialia*, England, Elsevier Ltd, **75**, pp. 63–74, [online] Available from: https://www.sciencedirect.com/science/article/pii/S1742706118303155.
- Yallapu, M. M., Jaggi, M. and Chauhan, S. C. (2010) β-Cyclodextrin-curcumin self-assembly enhances curcumin delivery in prostate cancer cells, *Colloids and Surfaces B: Biointerfaces*, Netherlands, Elsevier B.V, **79**(1), pp. 113–125, [online] Available from: https://www.sciencedirect.com/science/article/pii/S0927776510001876.
- Yang, D. H., Seo, D. I., Lee, D.-W., Bhang, S. H., Park, K., Jang, G., Kim, C. H. and Chun, H. J. (2017) Preparation and evaluation of visible-light cured glycol chitosan hydrogel dressing containing dual growth factors for accelerated wound healing, *Journal of Industrial and Engineering Chemistry*, Elsevier B.V, **53**, pp. 360–370, [online] Available from: http://dx.doi.org/10.1016/j.jiec.2017.05.007.
- Yang, X. X., Li, C. M. and Huang, C. Z. (2016) Curcumin modified silver nanoparticles for highly efficient inhibition of respiratory syncytial virus infection, *Nanoscale*, England, **8**(5), pp. 3040–3048, [online] Available from: https://www.ncbi.nlm.nih.gov/pubmed/26781043.
- Yoo, Y., Hyun, H., Yoon, S.-J., Kim, S. Y., Lee, D.-W., Um, S., Hong, S. O. and Yang, D. H. (2018) Visible light-cured glycol chitosan hydrogel dressing containing endothelial growth factor and basic fibroblast growth factor accelerates wound

healing in vivo, *Journal of Industrial and Engineering Chemistry*, Elsevier B.V, **67**, pp. 365–372, [online] Available from: http://dx.doi.org/10.1016/j.jiec.2018.07.009.

- Yoon, D. S., Lee, Y., Lee, J. W., Lee, M., Lee, K.-M., Ryu, H. A., Jang, Y., Choi, Y., Choi, W. J., Park, K. M. and Park, K. D. (2016) Cell recruiting chemokine-loaded sprayable gelatin hydrogel dressings for diabetic wound healing, *Acta Biomaterialia*, England, Elsevier Ltd, **38**, pp. 59–68, [online] Available from: https://www.sciencedirect.com/science/article/pii/S1742706116301921.
- Yoshino, T., Asakura, T. and Toda, K. (1996) Cellulose production by Acetobacter pasteurianus on silicone membrane, *Journal of Fermentation and Bioengineering*, Elsevier B.V, **81**(1), pp. 32–36, [online] Available from: http://dx.doi.org/10.1016/0922-338X(96)83116-3.
- Zahan, K. A., Nordin, K., Mustapha, M. and Mohd Zairi, M. N. (2015) Effect of Incubation Temperature on Growth of Acetobacter xylinum 0416 and Bacterial Cellulose Production, *Applied Mechanics and Materials*, Zurich, Trans Tech Publications Ltd, **815**, pp. 3–8, [online] Available from: https://www.scientific.net/AMM.815.3.
- Zahan, K., Pa'e, N. and Muhamad, I. (2015a) Monitoring the Effect of pH on Bacterial Cellulose Production and Acetobacter xylinum 0416 Growth in a Rotary Discs Reactor, *Arabian Journal for Science and Engineering*, Berlin/Heidelberg, Springer Berlin Heidelberg, **40**(7), pp. 1881–1885.
- Zakaria, J. and Nazeri, M.A. (2012). Optimization of Bacterial Cellulose Production from Pineapple Waste: Effect of Temperature, pH and Concentration. 5th Engineering Conference, "Engineering Towards Change - Empowering Green Solutions.

- Zhang and Galo, (2016). Antimicrobial peptides. In *Current Biology 26*, R14–R19, Elsevier Ltd, doi: 10.1016/j.cub.2015.11.017.
- Zhang, F., Zhang, H. and Wu, J. (2013) Physically crosslinked hydrogels from polysaccharides prepared by freeze–thaw technique, *Reactive and Functional Polymers*, Elsevier B.V, **73**(7), pp. 923–928, [online] Available from: https://www.sciencedirect.com/science/article/pii/S1381514813000047.
- Zhang, H., Luo, X., Tang, H., Zheng, M. and Huang, F. (2017) A novel candidate for wound dressing: Transparent porous maghemite/cellulose nanocomposite membranes with controlled release of doxorubicin from a simple approach, *Materials science & engineering. C, Materials for biological applications*, Netherlands, [online] Available from: https://www.ncbi.nlm.nih.gov/pubmed/28629087.
- Zhang, X., Zhang, Z., Zhong, Z. and Zhuo, R. (2012) Amphiphilic Block-Graft Copolymers Poly(ethylene glycol)-b-(polycarbonates-g-palmitate) Prepared via the Combination of Ring-Opening Polymerization and Click Chemistry, *Journal of Polymer Science: Part A Polymer Chemistry,* **50**, pp. 2687–2696. doi:10.1002/pola.26051.
- Zhao, L., Gwon, H.-J., Lim, Y.-M., Nho, Y.-C. and Kim, S. Y. (2015) Gamma ray-induced synthesis of hyaluronic acid/chondroitin sulfate-based hydrogels for biomedical applications, *Radiation Physics and Chemistry*, Elsevier Ltd, **106**, pp. 404–412, [online] Available from: https://www.sciencedirect.com/science/article/pii/S0969806X14003624.
- Zhao, L., Kang, L., Chen, Y., Li, G., Wang, L., Hu, C. and Yang, P. (2018) Spectral study on conformation switchable cationic calix[4]carbazole serving as curcumin container, stabilizer and sustained-delivery carrier, *Spectrochimica Acta Part A:*

Molecular and Biomolecular Spectroscopy, Elsevier B.V, **193**, pp. 276–282, [online] Available from: http://dx.doi.org/10.1016/j.saa.2017.12.037.

- Zhou, Y., Zhao, Y., Wang, L., Xu, L., Zhai, M. and Wei, S. (2012) Radiation synthesis and characterization of nanosilver/gelatin/carboxymethyl chitosan hydrogel, *Radiation Physics and Chemistry*, Elsevier Ltd, **81**(5), pp. 553–560, [online] Available from: https://www.sciencedirect.com/science/article/pii/S0969806X12000199.
- Zhu, C., Li, F., Zhou, X., Lin, L. and Zhang, T. (2014) Kombucha-synthesized bacterial cellulose: Preparation, characterization, and biocompatibility evaluation, *Journal of Biomedical Materials Research Part A*, United States, Wiley Subscription Services, Inc, **102**(5), pp. 1548–1557, [online] Available from: https://onlinelibrary.wiley.com/doi/abs/10.1002/jbm.a.34796.
- Zhu, L. and Bratlie, K. M. (2018) pH sensitive methacrylated chitosan hydrogels with tunable physical and chemical properties, *Biochemical Engineering Journal*, Elsevier B.V, **132**, pp. 38–46, [online] Available from: http://dx.doi.org/10.1016/j.bej.2017.12.012.
- Zmejkoski, D., Spasojević, D., Orlovska, I., Kozyrovska, N., Soković, M., Glamočlija, J., Dmitrović, S., Matović, B., Tasić, N., Maksimović, V., Sosnin, M. and Radotić, K. (2018) Bacterial cellulose-lignin composite hydrogel as a promising agent in chronic wound healing, *International Journal of Biological Macromolecules*, Netherlands, Elsevier B.V, **118**(Pt A), pp. 494–503, [online] Available from: http://dx.doi.org/10.1016/j.ijbiomac.2018.06.067.
- Zoellner, P., Kapp, H. and Smola, H. (2007) Clinical performance of a hydrogel dressing in chronic wounds: a prospective observational study, *Journal of Wound*

Care, London, MA Healthcare, **16**(3), pp. 133–136, [online] Available from: https://www.ncbi.nlm.nih.gov/pubmed/17385591.

- Zou, S., Yoon, W., Han, S., Jeong, S., Cui, Z. and Kim, W. (2012) Cytotoxicity of silver dressings on diabetic fibroblasts, *International Wound Journal*, Oxford, UK, Blackwell Publishing Ltd, **10**(3), pp. 306–312, [online] Available from: https://onlinelibrary.wiley.com/doi/abs/10.1111/j.1742-481X.2012.00977.x.
- Zubik, K., Singhsa, P., Wang, Y., Manuspiya, H. and Narain, R. (2017) Thermo-Responsive Poly(N-Isopropylacrylamide)-Cellulose Nanocrystals Hybrid Hydrogels for Wound Dressing, *Polymers*. **9**(4): 119. doi:10.3390/polym9040119.
- Żywicka, A., Fijałkowski, K., Junka, A. F., Grzesiak, J. and El Fray, M. (2018) Modification of Bacterial Cellulose with Quaternary Ammonium Compounds Based on Fatty Acids and Amino Acids and the Effect on Antimicrobial Activity, *Biomacromolecules*, United States, American Chemical Society, **19**(5), pp. 1528–1538, [online] Available from: http://dx.doi.org/10.1021/acs.biomac.8b00183.

Appendix 1

Supporting information

Table T1: Silver release kinetic equations:

Kinetic model	Equation
Zero order	$Q_t = Q_0 + K_0 t$
First order	$log\ Q_t = log\ Q_0 + \frac{K_1 t}{2.303}$
Higuichi	$Q_t = K_H t^{1/2}$
Korsmeyer-Peppas	$\frac{M_t}{M_\alpha} = at^n$

where: Q_o= Initial amount of drug release or dissolved at time "t" (usually, t=0), Q_t= Amount of drug released or dissolved in time "t", K_0 = Zero order release constant, K_1= First order release constant, K_H = Higuchi dissolution constant, $\frac{M_t}{M_\alpha}$ = Fractional release of drug and n = Release exponent.

NMR analysis of inclusion complex

Figure S1: ^{1}H NMR of the CUR:HPβCD inclusion complex in D_2O

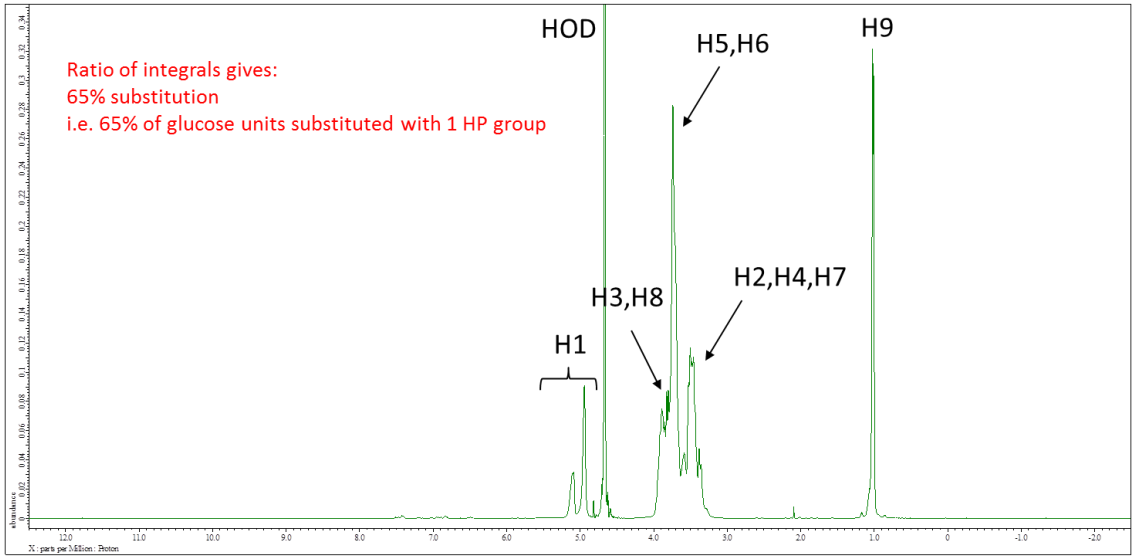

Figure S2: Expansion of ^{1}H NMR of the CUR:HPβCD inclusion complex in D_2O

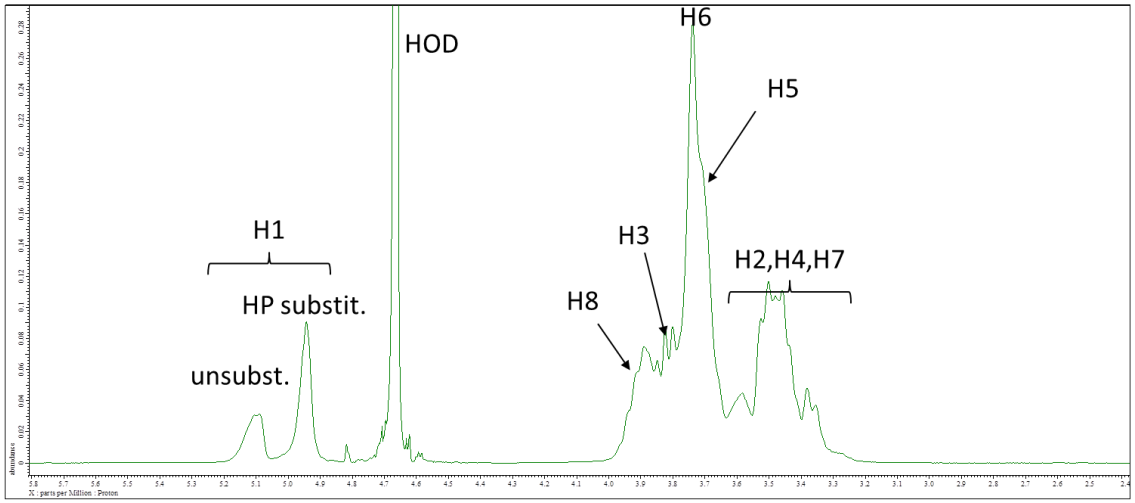

Figure S3: ^{13}C NMR of the CUR:HPβCD inclusion complex in D_2O.

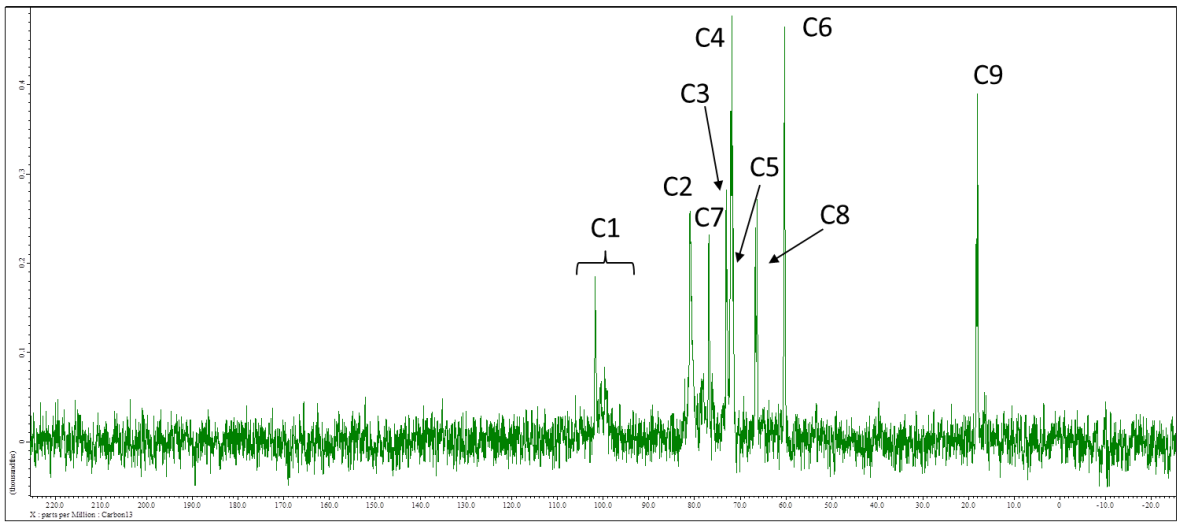

Assignments from HSQC and HMBC

Figure S4: Expansion of ^{13}C NMR of the CUR:HPβCD inclusion complex in D_2O.

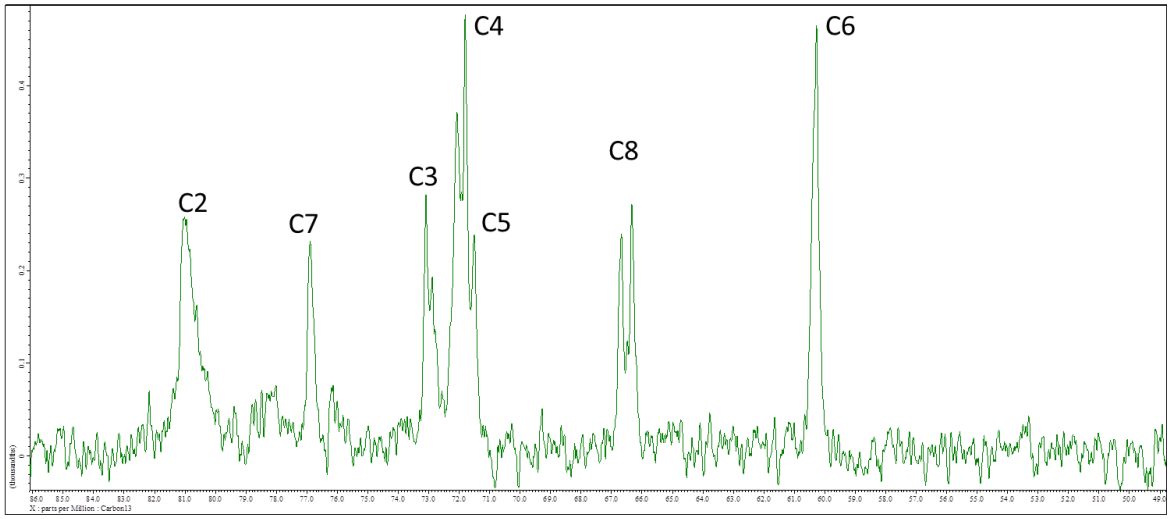

NB: Some peaks "doubled" due to 65% substitution of HP groups

Scheme S5: Structural assignment

S5 a: The schematic representation of curcumin (CUR).

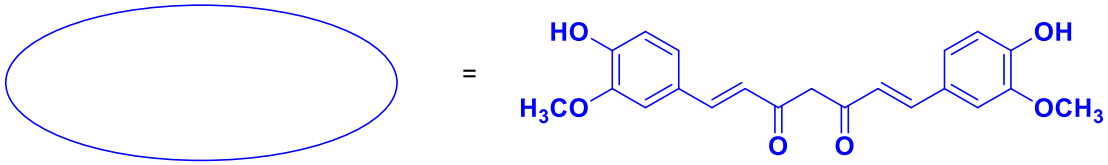

S5 b: The schematic representation of hydroxylpropyl-β-cyclodextrin (HPβCD).

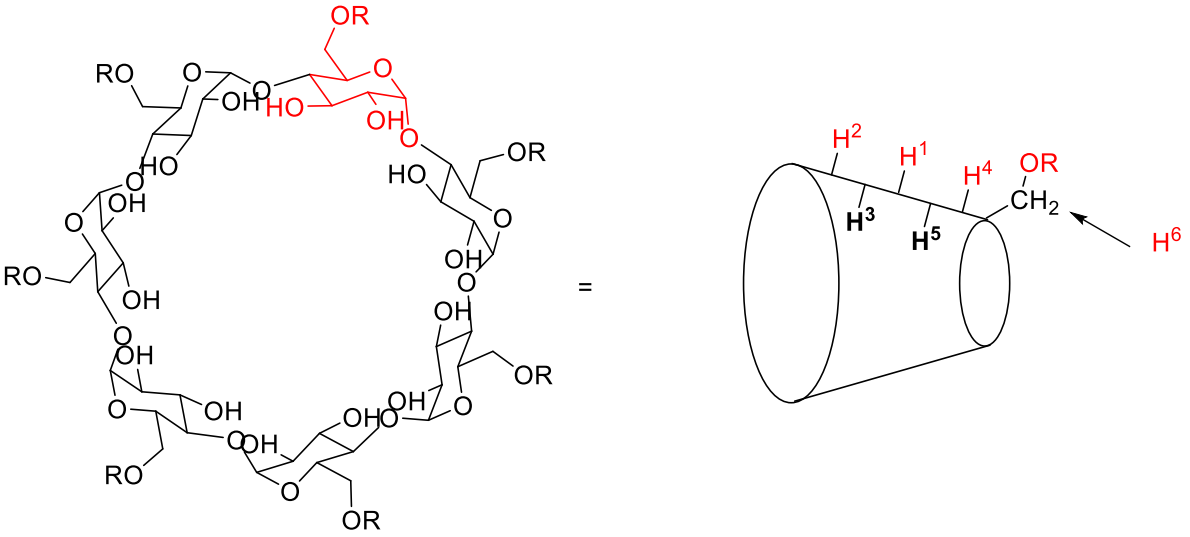

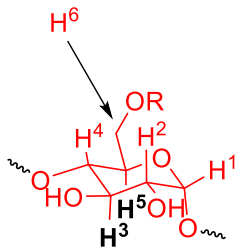

R = $CH_2CH(CH_3)OH$ or H

S5 c: The schematic representation of CUR:HPβCD inclusion complex

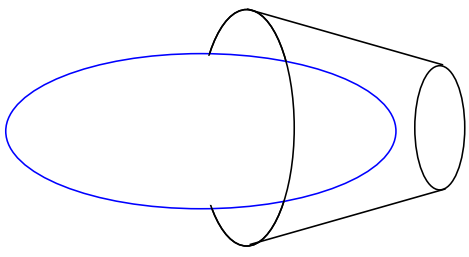

Appendix 2

Papers Published

- Kwiecień, I., Niewolik, D., Ekere, A. I., **Gupta, A**. and Radecka, I., 2020. Synthesis of hydrogels made of poly-γ-glutamic acid (γ-PGA) for potential applications as probiotic delivery vehicles. *Applied Sciences*, **10**(8), https://doi.org/10.3390/app10082787.

- **Gupta, A**., Briffa, S.M., Swingler, S., Gibson, H., Kannapan,V., Adamus, G., Kowalczuk, M., Martin, C. and Radecka, I., 2020. Synthesis of Silver Nanoparticles Using Curcumin-Cyclodextrins Loaded into Bacterial Cellulose-Based Hydrogels for Wound Dressing Applications. *BioMacromolecules*, https://doi.org/10.1021/acs.biomac.9b01724.

- **Gupta, A**., Keddie, D.J., Kannappan, V., Gibson, H., Khalil, I.R., Kowlaczuk, M., Martin, C., Shuai, X. and Radecka, I., 2019. Production and characterisation of bacterial cellulose hydrogels loaded with curcumin encapsulated in Cyclodextrins as wound dressings. *European Polymer Journal*, **118,** pp. 437-450.

- **Gupta, A**., Kowlaczuk, M., Heaselgrave, W., Britland, S.T., Martin, C. and Radecka, I., 2019. The production and application of hydrogels for wound management- A review. *European Polymer Journal*, **111**, pp.134-151.

- Khalil, I.R., Khechara, M.P., Kurusamy, S., Armesilla, A.L., **Gupta, A**., Mendrek, B., Khalaf, T., Scandola, M., Focarete, M.L., Kowalczuk. And Radecka, I., 2018. Poly-Gamma-Glutamic Acid (γ-PGA)-Based Encapsulation of Adenovirus to Evade Neutralizing Antibodies. Molecules, **23**(10), doi: 10.3390/molecules23102565.

- **Gupta, A**., Low, W.L., Britland, S.T., Radecka, I., and Martin, C., 2017. Physicochemical characterisation of biosynthetic bacterial cellulose as a potential wound dressing material. *British Journal of Pharmacy*, **2**(2), pp. S37-38.

- **Gupta, A**., Low, W.L., Radecka, I., Britland, S.T., Amin, M.C. and Martin, C., 2016. Characterisation and in vitro antimicrobial activity of biosynthetic silver-loaded bacterial cellulose hydrogels. *Journal of Microencapsulation*, **33**(8), pp. 725-734.

Oral Presentations

- Gupta, A., et al. **"A novel approach of silver nanoparticles synthesis using curcumin-cyclodextrins as reducing agent and loading in bacterial cellulose to produce hydrogel wound dressings"** in *6th European Conference on Cyclodextrins*, Santiago de Compostela, Spain, 2nd-4th October 2019.

- Gupta, A., *et al. "***Production and characterisation of bacterial cellulose hydrogels loaded with silver nanoparticles produced using curcumin-cyclodextrin as a reducing agent"** in *10th Asian Cyclodextrin Conference*, in Chengdu, China, 29th August-1st September 2019.

- Gupta, A., *et al. "***Production and characterisation of biosynthetic silver-loaded-bacterial cellulose hydrogels for wound management**" in *The Royal Society of Chemistry Anti-bacterial metal meeting*, Wolverhampton, UK, 15th April 2019.

- Gupta, A., *et al.* "**Fabrication and characterisation of bacterial cellulose hydrogels of curcumin encapsulated in cyclodextrins for wound dressing applications**" in *Biomaterials Symposium*, Lancaster, UK, 11-12th Feb 2019.

- Gupta, A., *et al*. "**Development and characterisation of novel antimicrobial cellulose based hydrogels loaded with curcumin-cyclodextrins inclusion complex as potential wound dressings**" in *6th International Conference on Natural Polymers and Workshop on Natural Polymers*, Kottayam, India, 7-9th December 2018.

- Gupta, A., *et al.* "**Biosynthetic cellulose based hydrogels of curcumin encapsulated in Cyclodextrins as wound dressings**" in ISBPPB, Krakow, Poland, 15-18th July 2018.

- Gupta, A., *et al.* "**The production of biosynthetic hydrogels containing curcumin encapsulated in cyclodextrins for wound management applications**" in *Career in Polymer X Conference*, Prague, Czeck Republic, 22-23rd June 2018.

- Gupta, A., *et al.* "**Physicochemical characterisation of biosynthetic bacterial cellulose as a potential wound dressing material**" in *8th APS International PharmSci Conference*, Hertfordshire, UK, 6th September 2017.

- Gupta, A., *et al.* "**The application of silver zeolite-loaded biosynthetic hydrogels for enhanced wound management"** in *6th APS International PharmSci Conference*, Nottingham, UK, 9th September 2015.

Poster Presentation

- Gupta, A., *et al*. "**Synthesis and characterisation of biosynthetic hydrogels with antibacterial properties as wound dressings**" presented in *Annual Research Conference 2020* [online]**,** University of Wolverhampton, UK, 16th June 2020.

- Gupta, A., *et al*. "**Synthesis and characterisation of biosynthetic hydrogels with antibacterial and antifungal properties as wound dressings"** presented in *Wound Care Conference Today 2020**,*** Marshall Arena, Milton Keynes, UK, 26-27th February 2020

- Gupta, A., et al. **"A novel approach of silver nanoparticles synthesis using curcumin-cyclodextrins as reducing agent and loading in bacterial cellulose to produce hydrogel wound dressings"** presented in *6th European Conference on Cyclodextrins*, Santiago de Compostela, Spain, 2nd-4th October 2019.

- Gupta, A., *et al. "***Production and characterisation of bacterial cellulose hydrogels loaded with silver nanoparticles produced using curcumin-cyclodextrin as a reducing agent"** presented in *10th Asian Cyclodextrin Conference,* Chengdu, China, 29th August-1st September 2019.

- Gupta, A., *et al*. "**Production and** c**haracterisation of curcumin-loaded biosynthetic hydrogels as wound dressings**" presented in *Annual Research Conference**,*** University of Wolverhampton*,* UK, 18th June 2019.

- Gupta, A., *et al*. "**Curcumin-loaded biosynthetic hydrogekls in wound management: synthesis, characterisation and *in vitro* antimicrobial activity**" presented in *6th International Conference on Natural Polymers and Workshop on Natural Polymers,* Kottayam, India, 7-9th December 2018.

- Gupta, A., *et al*. "**Biosynthetic hydrogels of curcumin encapsulated in Cyclodextrins for potential wound management applications**" presented in *Annual Research Conference*, University of Wolverhampton, UK, 12th June 2018.

- Gupta, A., *et al*. "**Physicochemical characterisation of biosynthetic bacterail cellulose as a potential wound dressing material**" presented in 8*th APS International PharmSci Conference*, University of Hertfordshire, UK, 5th-7th September 2017.

- Gupta, A., et al., "**Silver-loaded biosynthetic hydrogels in wound management: synthesis, characterisation and *in vitro* antimicrobial activity"** presented in *EAP 2017- The Theroy of Everything*, Kettering, UK, 12th-14th May 2017.

- Gupta, A., *et al*. "**Characterisation of biosynthetic bacterial cellulose as a potential wound dressing material**" presented in *Annual Research Conference,* University of Wolverhampton, UK, 19th June 2017.

- Gupta, A., *et al*. "**Antimicrobial silver nanoparticle-loaded bacterial cellulose hydrogels- Wound management applications** " presented in *Chemistry: The Science around us*, Sheffield, UK, 9th September 2016.

- Gupta, A., *et al*. "**Improved antimicrobial activity of silver nanoparticle-loaded bacterial cellulose hydrogels**" presented in *7th APS International PharmSci Conference*, Glasgow, UK, 5th-7th September 2016.

- Gupta, A., *et al*. "**Synthesis and study of silver nanoparticles loaded biosynthetic hydrogel as a potential antimicrobial wound dressing"** presented in *Annual Research Conference,* University of Wolverhampton, UK, 21st June 2016.

- Gupta, A., *et al*. "***In vitro,* quantitative study of the antimicrobial activity of nanoparticulate silver encapsulated in biosynthetic bacterial cellulose hydrogels**" presented in *Emerging Analytical Professionals 2016 Conference*, Hampshire, UK, 13th-15th May 2016.

- Gupta, A., *et al*. "**The application of silver zeolite-loaded biosynthetic hydrogels for enhanced wound management**" presented in *6th APS International PharmSci Conference*, Nottingham, UK, 9th September 2015.

- Gupta, A., *et al*. "**The application of silver zeolite-loaded biosynthetic hydrogels for enhanced wound management**" presented in *Controlled Release Society Annual Meeting*, Edinburgh, UK, 25th -29th July 2015.

- Gupta, A., *et al*. "**Antibacterial properties of Silver zeolite loaded biosynthetic hydrogels and its potential wound management applications**" presented in *Annual Research Conference,* University of Wolverhampton, UK, 16th June 2015.

- Gupta, A., *et al.* "**The antibacterial properties of Silver zeolite loaded biosynthetic hydrogels and its potential wound management applications**" presented in *2nd International Seminar on Biodegradable Polymer*, University of Wolverhampton, UK, 22nd April 2015.

Awards

- Awarded "**Second Best Poster**" in *Annual Research Conference 2020* [online], University of Wolverhampton, UK, 16th June 2020.

- Awarded "**Second Best Oral Presentation**" *10th Asian Cyclodextrin Conference*, in Chengdu, China, 29th August-1st September 2019.

- Awarded "**Best Oral Presentation**" in *6th International Conference on Natural Polymers and Workshop on Natural Polymers*, Kottayam, India, 7-9th December 2018.

- Awarded "**Best Poster**" in *6th International Conference on Natural Polymers and Workshop on Natural Polymers*, Kottayam, India, 7-9th December 2018.

- Awarded "**Best Oral Presentation**" in *Career in Polymer X Conference*, Prague, 22-23rd June 2018.

- Awarded "**Winner of the poster prize 2017"** in *8th APS International PharmSci Conference*, University of Hertfordshire, UK, 5th -7th September 2017.

- **Scholarship** awarded by the Royal Society of Chemistry to attend *Emerging Analytical Professionals 2017- The Theroy of Everything*, Kettering, UK, 12th-14th May 2017.

- **Scholarship Winner** in *III International Summer School on Cyclodextrins*, Polo Universitario Asti Studi Superiori –Piazza Fabrizio de Andre' Asti, Italy, 29th June-1st July 2016.

- Awarded **Winner of the poster competition 2016** in *Annual Research Conference 2016*, University of Wolverhampton, UK, 21st June 2016.

- **Scholarship** awarded by the Royal Society of Chemistry to attend *Emerging Analytical Professionals 2016 Conference*, Hampshire, UK, 13th-15th May 2016.

- Awarded **Winner of the poster prize 2015** sponsored by GSK in *6th APS International PharmSci Conference*, East Midlands Conference Centre, Nottingham, UK, 9th September 2015.

- Awarded **Winner in the category of clarity of message as voted by competition attendees** in *Annual Research Conference 2015,* University of Wolverhampton, UK, 16th June 2015.

- Awarded **Winner of the poster competition 2015** in *Annual Research Conference 2015*, University of Wolverhampton, UK, 16th June 2015.